



722
2018

Berichte

zur Polar- und Meeresforschung

Reports on Polar and Marine Research

The Expedition PS112 of the Research Vessel POLARSTERN to the Antarctic Peninsula Region in 2018

Edited by

Bettina Meyer and Wiebke Weßels

with contributions of the participants

Die Berichte zur Polar- und Meeresforschung werden vom Alfred-Wegener-Institut, Helmholtz-Zentrum für Polar- und Meeresforschung (AWI) in Bremerhaven, Deutschland, in Fortsetzung der vormaligen Berichte zur Polarforschung herausgegeben. Sie erscheinen in unregelmäßiger Abfolge.

Die Berichte zur Polar- und Meeresforschung enthalten Darstellungen und Ergebnisse der vom AWI selbst oder mit seiner Unterstützung durchgeführten Forschungsarbeiten in den Polargebieten und in den Meeren.

Die Publikationen umfassen Expeditionsberichte der vom AWI betriebenen Schiffe, Flugzeuge und Stationen, Forschungsergebnisse (inkl. Dissertationen) des Instituts und des Archivs für deutsche Polarforschung, sowie Abstracts und Proceedings von nationalen und internationalen Tagungen und Workshops des AWI.

Die Beiträge geben nicht notwendigerweise die Auffassung des AWI wider.

Herausgeber

Dr. Horst Bornemann

Redaktionelle Bearbeitung und Layout

Birgit Reimann

Alfred-Wegener-Institut
Helmholtz-Zentrum für Polar- und Meeresforschung
Am Handelshafen 12
27570 Bremerhaven
Germany

www.awi.de

www.reports.awi.de

Der Erstautor bzw. herausgebende Autor eines Bandes der Berichte zur Polar- und Meeresforschung versichert, dass er über alle Rechte am Werk verfügt und überträgt sämtliche Rechte auch im Namen seiner Koautoren an das AWI. Ein einfaches Nutzungsrecht verbleibt, wenn nicht anders angegeben, beim Autor (bei den Autoren). Das AWI beansprucht die Publikation der eingereichten Manuskripte über sein Repositorium ePIC (electronic Publication Information Center, s. Innenseite am Rückdeckel) mit optionalem print-on-demand.

The Reports on Polar and Marine Research are issued by the Alfred Wegener Institute, Helmholtz Centre for Polar and Marine Research (AWI) in Bremerhaven, Germany, succeeding the former Reports on Polar Research. They are published at irregular intervals.

The Reports on Polar and Marine Research contain presentations and results of research activities in polar regions and in the seas either carried out by the AWI or with its support.

Publications comprise expedition reports of the ships, aircrafts, and stations operated by the AWI, research results (incl. dissertations) of the Institute and the Archiv für deutsche Polarforschung, as well as abstracts and proceedings of national and international conferences and workshops of the AWI.

The papers contained in the Reports do not necessarily reflect the opinion of the AWI.

Editor

Dr. Horst Bornemann

Editorial editing and layout

Birgit Reimann

Alfred-Wegener-Institut
Helmholtz-Zentrum für Polar- und Meeresforschung
Am Handelshafen 12
27570 Bremerhaven
Germany

www.awi.de

www.reports.awi.de

The first or editing author of an issue of Reports on Polar and Marine Research ensures that he possesses all rights of the opus, and transfers all rights to the AWI, including those associated with the co-authors. The non-exclusive right of use (einfaches Nutzungsrecht) remains with the author unless stated otherwise. The AWI reserves the right to publish the submitted articles in its repository ePIC (electronic Publication Information Center, see inside page of verso) with the option to "print-on-demand".

Titel: In-situ-Aufnahme durch das von SEAPUMP entwickelte In Situ Camera System (ICS) einer Salpe (Salpa thompsoni) in 100 m Tiefe vor Elephant Island (Foto: Christian Konrad and Morten Iversen).

Cover: In situ photo of salp (Salpa thompsoni) taken off Elephant Island at 100 m depth by the In Situ Camera System (ICS) developed by SEAPUMP (Photo: Christian Konrad and Morten Iversen).

The Expedition PS112 of the Research Vessel POLARSTERN to the Antarctic Peninsula Region in 2018

**Edited by
Bettina Meyer and Wiebke Weßels
with contributions of the participants**

Please cite or link this publication using the identifiers

**<http://hdl.handle.net/10013/epic.817381f9-3e34-45ee-81ab-28632d043e61> and
https://doi.org/10.2312/BzPM_0722_2018**

ISSN 1866-3192

PS112

18 March 2018 - 5 May 2018

Punta Arenas – Punta Arenas

**Chief scientist
Bettina Meyer**

**Coordinator
Rainer Knust**

Contents

1.	Überblick und Fahrtverlauf	3
	Summary and Itinerary	5
2.	Weather Conditions during PS112	7
3.	Microbial Food Web	11
4.	How will a Population Shift from Krill to Salps Impact the Export and Recycling of Organic Matter in the Southern Ocean?	15
4.1	Drifting sediment traps	15
4.2	Direct observation of feeding and swimming behaviour of <i>Salpa thompsoni</i> and <i>Euphausia superba</i> using video recording and particle image velocimetry	17
4.3	Production and composition of fecal pellets from krill and salps: Fecal pellet production, gut passage time, and settling velocities of aggregates in the Western Atlantic sector of the Southern Ocean	19
4.4	Vertical profiles with the In-Situ Camera and driftcam system	23
5.	Biology of the Pelagic Tunicate, <i>Salpa Thompsoni</i> , in the Western Atlantic Sector of the Southern Ocean during March-May 2018	28
6.	KRILLBIS	34
7.	The Performance of Krill vs. Salps to Withstand in a Warming Southern Ocean (Pekris)	40
8.	Microzooplankton	47
9.	Climate Sensitivity in Various Fishes from the Antarctic Peninsula: Molecular Ecology and Cellular Mechanisms	51
10.	Fin Whale Abundance	61
11.	Trace Metal Biogeochemistry	65

12.	Physical Oceanography and Bio-Optical Parameters	72
13.	Sampling and Observation of <i>Salpa Thompsoni</i> and Larval Krill by Scientific Divers	78
APPENDIX		
A.1	Teilnehmende Institute / Participating Institutions	80
A.2	Fahrtteilnehmer / Cruise Participants	83
15.	Schiffsbesatzung / Ship's Crew	85
A.4	Stationsliste / Station List	86

1. ÜBERBLICK UND FAHRTVERLAUF

Bettina Meyer

AWI

Die Expedition PS112 mit FS *Polarstern* startete am 18. März 2018 und endete am 05. Mai mit 50 Wissenschaftlern/innen und Technikern aus 11 Nationen in Punta Arenas, Chile, und wurde von drei Drittmittelprojekten beherrscht (Abb. 1.1). Das KrillBIS-Projekt (KrillBestandsforschung Im Südpolarmeer) gab die Untersuchungsregion vor. Es stellt den deutschen Forschungsbeitrag im Rahmen von CCAMLR (Kommission zum Schutze der marinen lebenden Ressourcen) dar. Die Zielregionen, in denen Krill- und Salpenabundanzen mittels Netzfängen und akustischen Messverfahren aufgenommen wurden, waren das östliche und westliche Gebiet der Brainsfield Strait, das Gebiet nördlich der South Shetland Islands und King George Island, das Gebiet um Elephant Island sowie östlich der antarktischen Halbinsel Erebus und Terror Gulf mit dem Antarctic Sound (cf. Abb. 6.1). Vier Prozess-Studien in diesem Gebiet (eine um Deception Island, zwei nördlich von Elephant Island sowie eine in Erebus und Terror Gulf), die sich auf die zwei weiteren Drittmittelprojekte bezogen, ergänzten das Krill/Salpen Bestandsforschungsprojekt KrillBIS. Bei den Drittmittelprojekten handelte es sich zum einen, um das vom Niedersächsischen Ministerium für Wissenschaft und Kultur (MWK) finanzierte Projekt POSER (POPulation Shift and Ecosystem Response – Krill vs. Salps) und zum anderen um das vom BMBF geförderte Projekt PEKRIS (PERformance of KRill vs. Salps to withstand in a warming Southern Ocean). Das POSER-Projekt beschäftigt sich mit der Interaktion zwischen Krill und Salpen und dessen Einfluss auf die biologische Kohlenstoffpumpe sowie der Phytoplanktongemeinschaft und dem Recycling des Spurenmetalls Eisen, welches für das Phytoplanktonwachstum essentiell ist. Das PEKRIS-Projekt hingegen untersucht die Plastizität von Krill und Salpen gegenüber ansteigenden Meerwassertemperaturen.

Unsere Arbeiten starteten in Admiralty Bay, King George Island, mit der Kalibrierung des Fischecholots EK60, um mit diesem Gerät die Biomasse von Krill und Salpen auf dem CCAMLR-Transekt zu bestimmen. Nach der Kalibrierung folgte der erste Abschnitt des CCAMLR-Transekts, in der Brainsfield Strait, der für eine dreitägige Prozessstudie um Deception Island unterbrochen wurde. Auf den CCAMLR-Stationen wurde das IKMT Netz nach dem CCAMLR-Protokoll eingesetzt sowie Chl a und POC Proben in den obersten 200 Metern der Wassersäule bestimmt. Weiter ging es auf den zweiten Abschnitt des CCAMLR-Transekts, nördlich der South Shetland Inseln bis nördlich von Elephant Island, wo die zweite Prozessstudie durchgeführt wurde. Anschließend bewegten wir uns auf den CCAMLR-Transekt Richtung Süden (Erebus und Terror Gulf), wo die dritte Prozessstudie unsere CCAMLR-Arbeiten unterbrach. Dieses Gebiet unterscheidet sich von den vorangegangenen insoweit, dass es ein Krill dominiertes System darstellt, wo kaum Salpen vorhanden sind. Im Rahmen der dort stattfindenden Prozessstudien haben wir untersucht, inwieweit die zahlreich vorhandenen Meeresberge die Zirkulation und die Krillbiomasse beeinflussen. Unsere letzte Prozessstudie führte uns über den Antarctic Sound auf unseren nördlich gerichteten und letzten CCAMLR Transekt wieder in das Gebiet nördlich von Elephant Island. Durch die Anwendung gleicher Untersuchungsmethoden, jedoch zeitlich versetzt, erhielten wir einen Einblick in die Dynamik der Krill- und Salpenabundanz um Elephant Island. Ein Akustiktransekt zur Bestimmung der Verteilung der Krill- und Salpen-Biomasse mit CTD- sowie ADCP-Profilen rundete das Forschungsprogramm ab.

PS112 ist ein Baustein in einer Reihe von Forschungsprojekten, die zusammen eine umfassende Einschätzung der möglichen Konsequenzen des Klimawandels auf Krill und die Krill-assoziierten Ökosysteme liefern (Abb. 1.1). Die Ergebnisse aller drei Studien werden in die Entwicklung eines „individual-based model“ (IBM) für Krill einfließen, welches helfen soll, Änderungen des Krillbestandes in Reaktion auf verschiedene Klima-Szenarien im atlantischen Sektor des Südozeans zu prognostizieren.

Der Zeitplan für PS112 ist aus zwei alternierenden Phasen zusammengesetzt: Das KrillBIS-Grid diente zur Erfassung akustischer Krillbiomasse und dem Sammeln von Populationsparametern von Salpen und Krill. Es befindet sich in CCAMLR Subarea 48.1 und stellt eine Replikation des US.AMLR-Grids dar (US Antarctic Marine Living Resources = AMLR) dar. Das AMLR-Grid wurde konzipiert, um das Beprobieren verschiedener Krillhabitats in der Nähe von Prädatorenkolonien zu ermöglichen. In Zusammenarbeit mit dem US Amerikanischen Antarktis Programm wurde während PS112 (Herbst) das AMLR-Grid repliziert, um saisonale Unterschiede in Krillbiomasse und Populationsparametern mit früheren AMLR Ausfahrten aus dem Sommer und Winter zu untersuchen. Zur Bearbeitung der Zielrichtungen im POSER- und PEKRIS-Projekt wurde das AMLR-Grid vierteljährlich unterbrochen, um die geplanten Prozessstudien mit Krill und Salpen über einen Zeitraum von 3-7 Zagen durchzuführen. Des Weiteren wurde im Rahmen der Probennahme von Krill und Salpen in den genannten Projekten Unterproben entnommen, mit denen der Mageninhalt dieser beiden Organismen auf das Vorhandensein von Mikroplastik untersucht werden soll. Dies ist Teil des Drittmittelantrags (SYNEGIA) von Prof. Dr. Patricia Holm, Universität Basel, Schweiz.

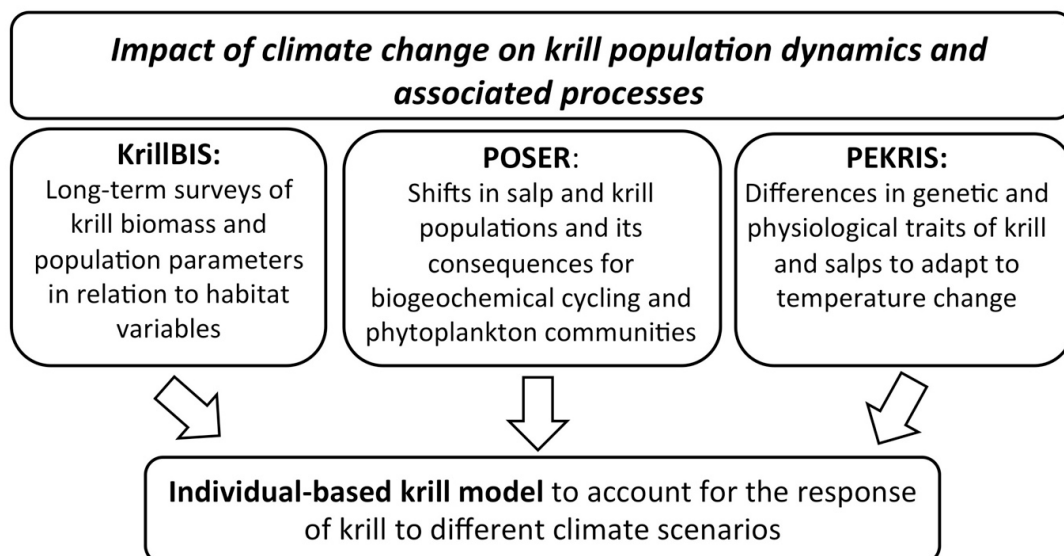


Abb. 1.1: Übersicht der Forschungsprojekte während PS112
Fig. 1: Overview of research projects conducted during PS112

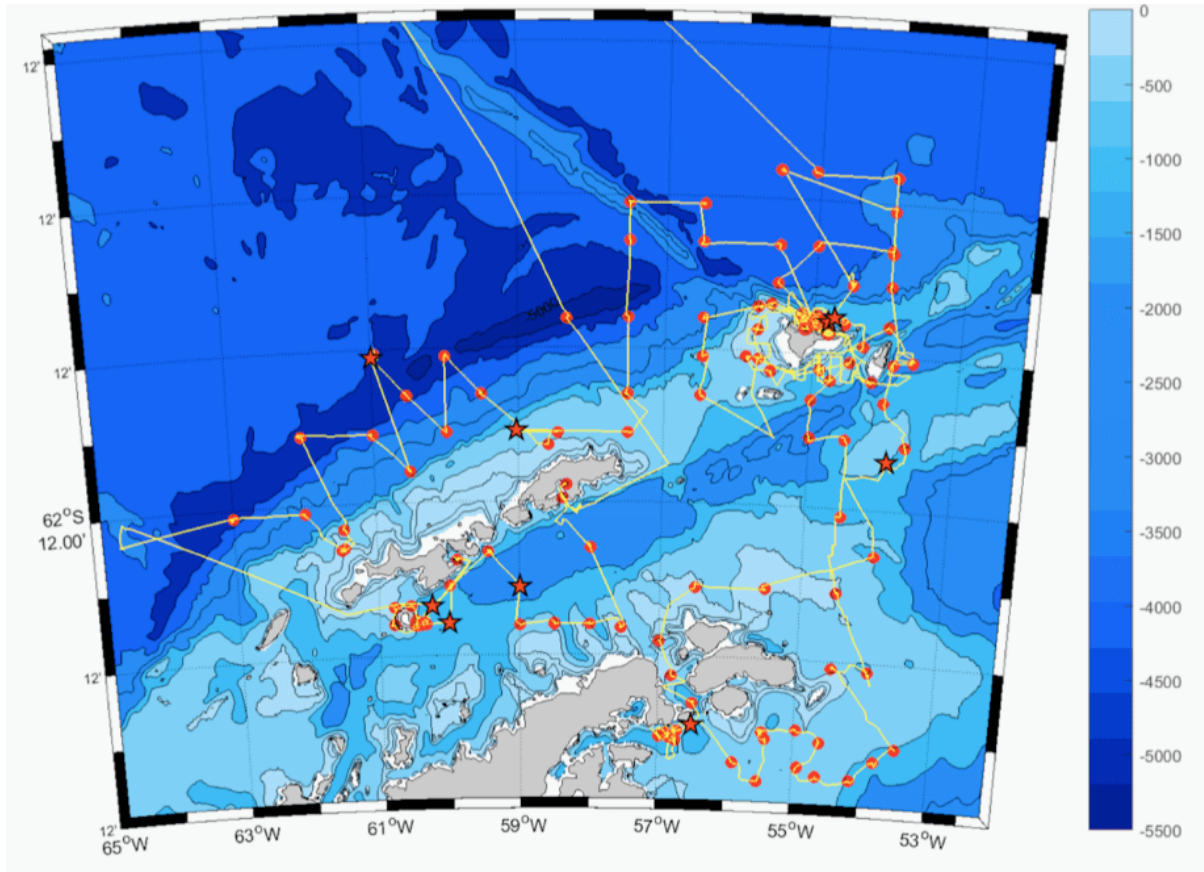


Abb. 1.2: Übersicht der Fahrtroute PS112.

Siehe <https://doi.pangaea.de/10.1594/PANGAEA.891424> für eine Darstellung des master tracks in Verbindung mit der Stationsliste für PS112.

Fig. 1.2: Overview of the cruise track PS112.

See <https://doi.pangaea.de/10.1594/PANGAEA.891424> to display the master track in conjunction with the list of stations for PS112.

SUMMARY AND ITINERARY

The expedition PS112 with RV *Polarstern* started in Punta Arenas, Chile, on 18 March and ended on 5 May with 50 scientists and technicians on board. Three third-party-funded projects dominated the expedition (Fig. 1.1): The KrillBIS project (Krill abundance research in the Southern Polar Ocean) determined the study region representing the German research contribution to CCAMLR (Commission for the Conservation of Antarctic Living Resources). This target region, where krill and salp abundances were investigated using net tows and hydro acoustic techniques, was the East and West Bransfield Strait, the area North of the South Shetland Islands, the area around Elephant Island, and the area East of the Antarctic Peninsula, Erebus and Terror Gulf as well as the Antarctic Sound (cf. Fig. 6.1). Four process

studies in this region (one around Deception Island, two around Elephant Island and one in the Erebus and Terror Gulf) focussing on the other two third-party funded projects completed the krill/salp directed research programme. One project is the POSER (Population Shift and Ecosystem Response) project funded by the Lower Saxony Ministry of Science and Culture (MWK). The third project is the PEKRIS (the performance of Krill vs. Salps to withstand in a warming ocean) project supported by the Federal Ministry for Education and Research (BMBF). POSER deals with the interaction between salps and krill and their influence on the biological carbon pump, as well as the phytoplankton community and the recycling of the trace metal iron, which is essential for phytoplankton growth. The PEKRIS project on the other hand investigates the plasticity of krill and salps under increasing ocean temperatures.

Our work started in Admiralty Bay, King George Island, with the calibration of the EK60 echo sounder, as this instrument was used for abundance estimates of krill and salps along the CCAMLR transect. The calibration was followed by the first leg of the transect in the Bransfield Strait, intersected by three days of process studies around Deception Island. At the CCAMLR stations the IKMT net was used according to the CCAMLR protocol and Chl a and POC samples were taken in the upper 200 m of the water column. The transect work continued on the second leg North of the South Shetland Islands to North of Elephant Island, where the second set of process studies was carried out. Subsequently we headed South along the CCAMLR transect to the Erebus and Terror Gulf to carry out the third set of process studies. This area differed from the previous ones as it is a krill dominated system, where few salps are present. In this area we investigated the influence of the numerous sea mounts present in this area on the ocean currents and the krill biomass. Our last process study took us back to Elephant Island through the Antarctic Sound after the last CCAMLR transect in northerly direction was completed. By conducting a similar set of experiments in an area that we studied earlier we got an insight into the temporal dynamics of the krill and salp abundance around Elephant Island. An acoustic transect to determine the distribution of the krill and salp abundances together with CTD and ADCP profiling concluded the research programme.

The PS112 cruise is a vital component in a set of research projects (outlined above) that were conducted to combine the project related scientific tasks and unite them in one overarching, synoptic assessment of the effect of climate change on krill and associated ecosystem processes (Fig. 1.2). The results of all three projects will feed into the development of an "individual based model" (IBM) for krill, which will provide information how the krill stock might change due to various climate scenarios in the Atlantic sector of the Southern Ocean.

The itinerary of PS112 consisted of two parts: One part was the CCAMLR grid in CCAMLR Subarea 48.1 replicating the US.AMLR (US Antarctic Marine Living Resources, hereafter "AMLR") survey grid. The AMLR survey grid was originally designed to provide repeated transects over a range of krill habitats and in close proximity to predator colonies. In a collaborative effort between Germany and the US Antarctic programme, we replicated the AMLR survey grid in order to compare seasonal differences in krill biomass and population parameters collected during PS112 (autumn) with previous AMLR summer and winter cruises. The research conducted here feeds into KRILBIS. The other part based on four process-oriented studies, outlined above, which will feed into the projects POSER and PEKRIS. In the frame of the sampling program of krill and salps with the outlined projects above. Subsamples of both samples were taken to investigate the presence of microplastic in the stomach content of both species. This is part of the third-party project application (SYNEGIA) headed by Prof. Dr. Patricia Holm, University Basel, Switzerland.

2. WEATHER CONDITIONS DURING PS112

Max Miller¹, Juliane Hempelt¹

¹DWD

Late Sunday evening, March 18, 2018, 22:00 pm, *Polarstern* left Punta Arenas for the campaign PS112. Moderate to fresh south-westerly winds, 5 °C and clear skies were observed.

Over Drake Passage strong south-westerly to westerly winds were prevailing. On Monday (Mar. 19) we still sailed inside the shelter of Tierra del Fuego. Entering Drake Passage on Tuesday the south-westerly winds increased up to 8 Bft with some peaks 9 Bft. The sea state grew to 5 m. On Wednesday (Mar. 21) winds remained stormy but veered northwest and became a tail wind.

On Thursday (Mar. 22) we reached the south side of King George Island and entered its lee with breaking clouds. North-westerly winds abated clearly. Until Saturday (we lied at anchor inside Admiralty Bay) wind often changed its strengths between 3 and 7 Bft, depending on the lee of surrounding mountains.

On Sunday (Mar. 25) a storm headed from west towards Antarctic Peninsula. Over Bransfield Strait it caused north-westerly winds 7 to 8 Bft, peaking temporarily at 9 Bft on Sunday evening. At the south side of the Strait a sea state up to 4 m was forced while it remained below 2 m at the north side due to shelter by the South Shetland Islands. Also on Monday we observed large differences of wind force between 5 and 9 Bft due to lee behind or jet effects between islands. On Tuesday (Mar. 27) a new storm followed. We measured westerly winds up to 11 Bft and a maximum gust of 78 knots. But *Polarstern* had entered the shelter of Half Moon Island early enough.

During the following days *Polarstern* operated at the east side of lows over Amundsen and Bellingshausen Sea. Until Easter Saturday (Mar. 31) winds from west to north didn't exceed 6 Bft.

On Easter Sunday (Apr. 01) we steamed towards the north side of the South Sandwich Islands. At the same time a low over Amundsen Sea and another one over Weddell Sea caused strong westerly winds over our area. On Sunday evening winds freshened up to 8 Bft forcing a sea state of 4 m. Already on Easter Monday winds abated, but a strong swell remained at first.

During the upcoming days troughs and ridges crossed our area. Winds switched from north to west and back at 4 to 6 Bft. On Sunday (Apr. 08) light and variable winds were prevailing off Elephant Island at a swell of only 1 m. But from west another storm approached. During the night to Monday winds veered northeast and peaked at 8 Bft on Monday, forcing a sea state of 3 to 4 m. On Tuesday the centre of the low crossed *Polarstern* and winds calmed for short times. Afterwards winds veered southeast at 7 Bft and precipitation switched into snow.

On Friday (Apr. 13) we got at the east side of a low over Bellingshausen Sea again. North-westerly winds increased up to 7 Bft. From Saturday on we operated south of Joinville Island. Its orographic influence caused sudden changes of wind force between 3 and 11 Bft! Considerable sea state could not build because of the shelter of the island and existing ice floes. On Sunday morning (Apr. 15) we crossed a Foehn area (Fig. 2.1) inside the lee of Joinville Islands. At a wind force 10 Bft temperature jumped up to 11 °C and relative humidity dropped to only

50 %. On Sunday evening a secondary low formed over Larsen Ice Shelf and headed towards Weddell Sea. Therefore winds veered southwest and within only a few minutes temperature dropped around 10 degrees.

On Monday (Apr. 16) a new complex low formed over Amundsen and Bellingshausen Sea. Again, northerly winds changed their force rapidly. Crossing the Antarctic Sound jet effects caused temporarily 9 Bft.

From Thursday (Apr. 19) on we operated at Bransfield Strait again. South of Falkland Islands a low formed, moved southeast and passed east of *Polarstern*. From Thursday evening until Friday evening winds veered clockwise from northwest to south and back to northwest and peaked at 8 Bft on Friday morning. Two further lows approached from Drake Passage and crossed *Polarstern* with their centres. Saturday evening (Apr. 21) and noon on Sunday winds became light and variable, otherwise we observed northerly winds around 7 Bft. Meanwhile we operated near Elephant Island again. Depending on our position and the orographic conditions wind force changed often.

From Monday (Apr. 23) on we were only at the north side of Elephant Island. Weak lows and ridges crossed our area. Due to the east-west-orientation of the north coast of the island we observed lee effects on the one hand and acceleration of westerly winds (for short times 9 Bft) on the other hand. But the sea state didn't exceed 3 m.

On Monday (Apr. 30) we left Elephant Island and started to round-up Clarence Island. During the night to Tuesday (May 01) a secondary low formed over Larsen Ice Shelf. It deepened to a storm and headed to Weddell Sea. On Tuesday morning it caused westerly winds at 10 to 11 Bft for short times. But we steamed inside the shelter along the east side of Clarence Island.



Fig. 2.1: Foehn area inside the lee of Joinville Island

Over Drake Passage strong westerly winds were prevailing. Heading to Punta Arenas we observed wind forces around 7 Bft and the sea state peaked at 4 m.

On Saturday morning, May 5, 2018, *Polarstern* reached Punta Arenas at temporarily strong and gusty westerly winds.

For further statistics see attached files (Fig. 2.2 – Fig. 2.7).

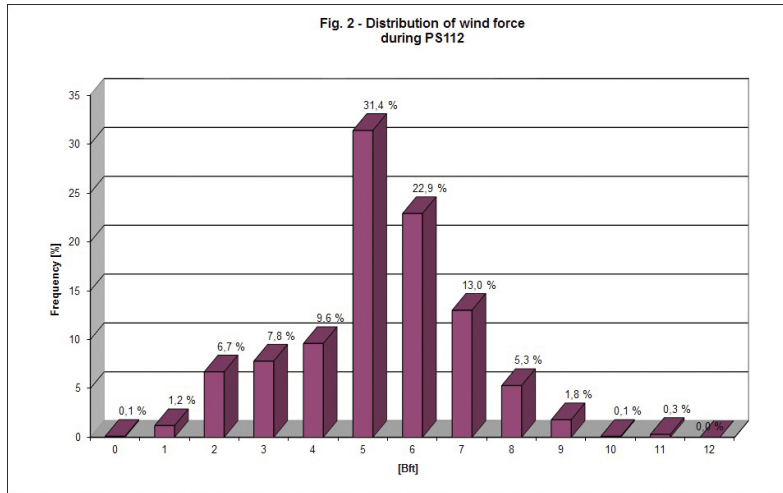


Fig. 2.2: Distribution of wind forces during PS112

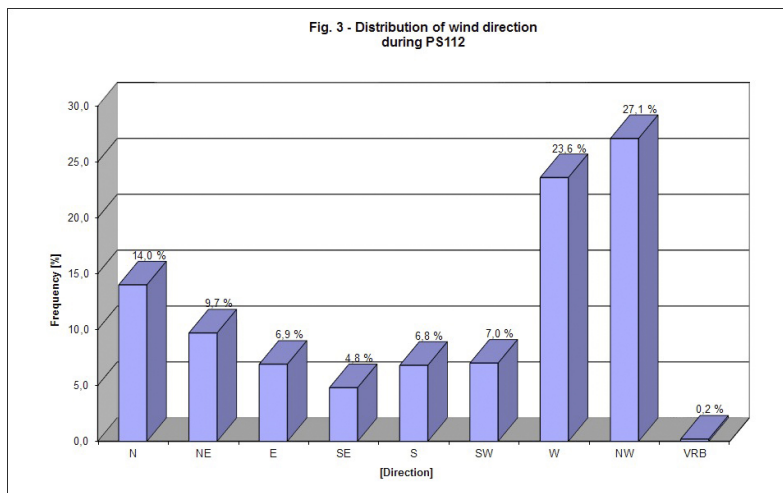


Fig. 2.3: Distribution of wind direction during PS112

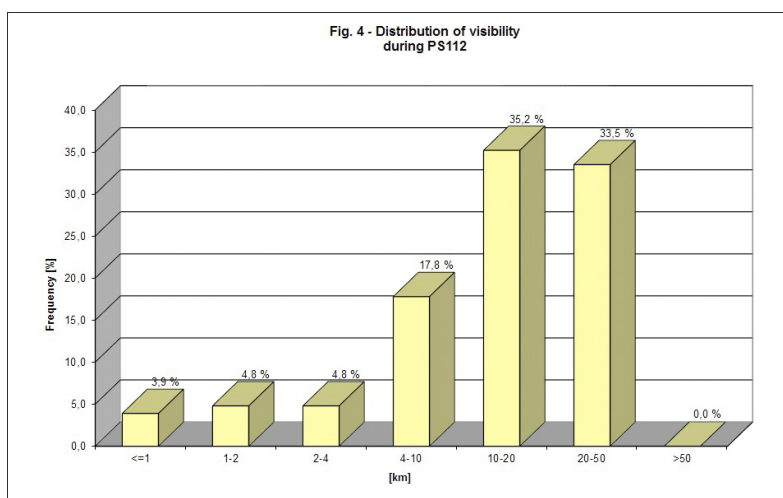


Fig. 2.4: Distribution of visibility during PS112

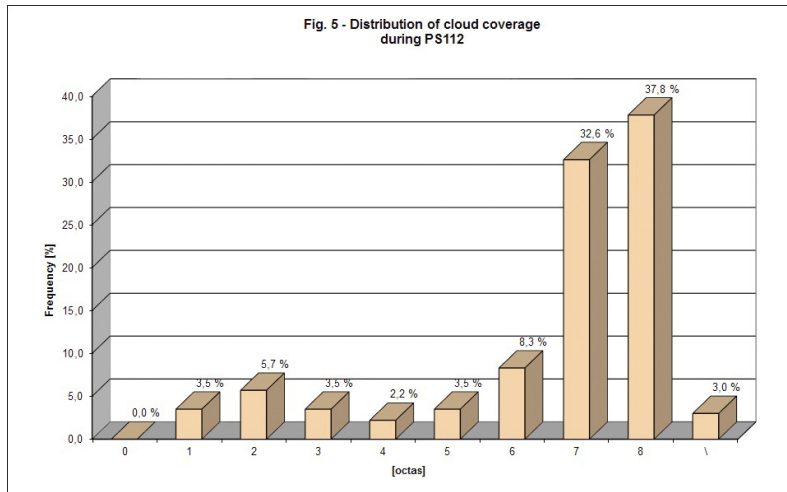


Fig. 2.5: Distribution of cloud coverage during PS112

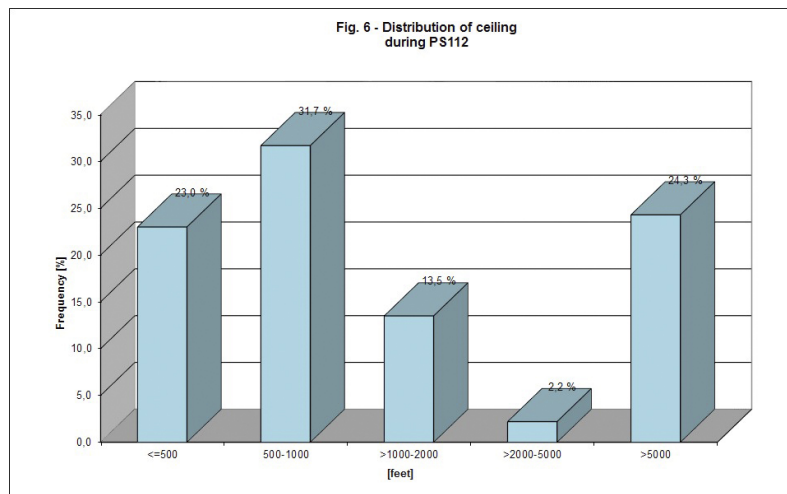


Fig. 2.6: Distribution of ceiling during PS112

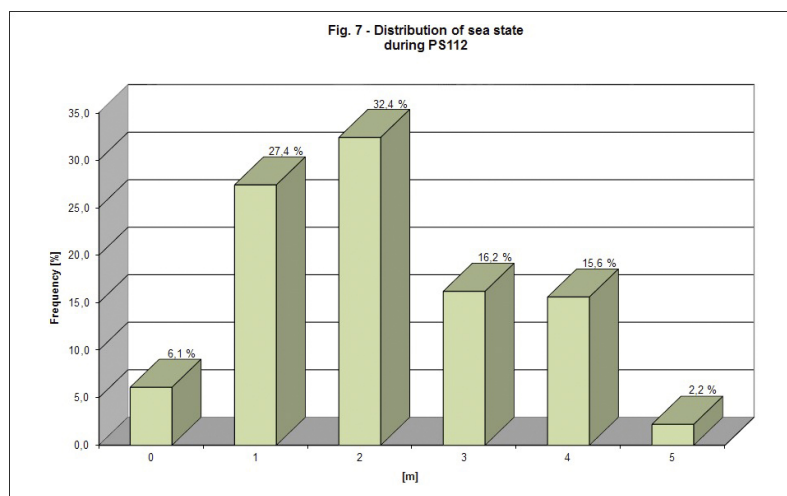


Fig. 2.7: Distribution of sea state during PS112

3. MICROBIAL FOOD WEB

Stefanie Moorthi, Christoph Plum,
Philipp Wenta, Dominik Bahlburg

ICBM, Uni Oldenburg

Grant-No. AWI_PS112_00

Objectives

In the western Antarctic Peninsula (WAP) and the Scotia Sea, krill and salps are the most important macrozooplankton grazers (Bernard et al., 2012; Pakhomov et al. 2002). However, krill and salp species occupy different ecological and spatial niches in the Southern Ocean, differing, e.g. in their reliance on sea ice, their life cycles, their mode of feeding and reproduction, and in the way they affect the lower food web by organic matter release (Bernard et al. 2012; Condon et al. 2011; Loeb et al. 1997). Recent observations have indicated that in some areas along the WAP, salps have replaced krill as major grazers in the pelagial (Ross et al. 2008). This observed shift has partly been attributed to shifts in phytoplankton composition towards small-sized cells and flagellates rather than large diatoms due to warming at the WAP (Moline et al. 2004). This might foster salp blooms in contrast to krill, as the latter cannot efficiently graze on small phytoplankton. While the autecology of these major grazers has been investigated before (especially of krill), not much is known about the ecosystem consequences of this regime shift.

In our project POSER (POpulation Shift and Ecosystem Response – Krill vs. Salps), we aim at understanding the consequences of such a shift for plankton community structure, biodiversity and biogeochemical cycles. To achieve this aim, we investigated the functional role of krill and salps in controlling phytoplankton and microbial food web composition and trophic interactions, productivity (through the (re)cycling of macronutrients), as well as nutrient fluxes and stoichiometry. In this context we wanted to determine 1) direct effects of salps and krill on plankton community structure through selective grazing, affecting net community production, and 2) indirect effects of these grazers on the stoichiometry of dissolved nutrients, primary production and phytoplankton food quality by modifying macronutrient concentrations and ratios due to altered nutrient recycling.

We pursued these research questions by combining field sampling with on-board experiments, where we manipulated the presence or absence of salps and krill, allowing us to investigate numerous factors that control plankton and nutrient dynamics in patches with high krill or salp abundances.

Work at sea

We took water samples from 4 depths (surface, deep chlorophyll maximum, 100 m, 200 m) at 10 different onshore and offshore locations to characterize natural plankton biomass and community structure, as well as the biochemistry of the water. We will analyze plankton biomass and community structure in different size fractions via microscopy (Lugol's and formaldehyde/glutardialdehyde samples), flow-cytometry, pigment analyses and ribosomal DNA-analyses (16S and 18S rDNA, the latter in different size fractions: $>0.4 \mu\text{m}$, $> 3 \mu\text{m}$, $> 10 \mu\text{m}$). At all stations, we also determined active bacterivorous nanoflagellates, including mixotrophic

phytoflagellates, via 24h grazing assays using fluorescent beads (0.5 μm) as food surrogates for bacteria. Furthermore, we will analyze seston particulate organic nutrients (carbon, nitrogen, phosphorus) and fatty acids, dissolved inorganic nutrients (nitrogen, phosphorus, silicate), as well as dissolved organic matter (DOM). In addition, we took Bongo net tows at all stations to collect and characterize mesozooplankton. All of these data will be related to krill and salp abundances in the water column determined by net tows, as well as to hydrographic conditions.

Secondly, we focused on experimental manipulations with krill and salps collected at our process study sites at the coasts of Deception and Elephant Island, where these two major grazers co-occurred. We conducted two full on-board grazing experiments, where we incubated krill and salps alone and in mixture (50 % of the abundances of krill and salps in monoculture, respectively) with a natural plankton community in cylindrical aquaria (70 L), as well as a plankton control without these consumers (4 replicates per treatment). In the first experimental period, we investigated direct grazing effects on plankton biomass and community structure. After 2 days, we added concentrated phytoplankton (via 10 μm net tows) to feed and maintain the grazers for a longer period of time in order to determine their effects on nutrient recycling and carbon export. After another 2-3 days, we terminated the first experimental phase and collected plankton, krill and salps and their fecal pellets for further analyses (Fig. 3.1, for analyses see below).

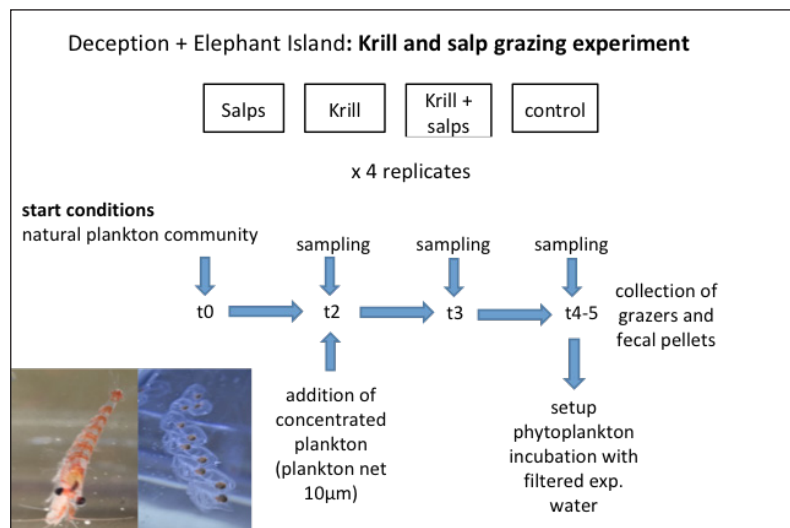


Fig. 3.1: Experimental design of the two full experiments conducted with krill and salps collected off the coasts of Deception Island and Elephant Island

Salps and krill presumably recycle nutrients in different amounts and ratios, which may indirectly affect phytoplankton biomass and community structure. Therefore, we filtered the remaining water preconditioned by krill and salps through nutrient recycling during the grazing experiment using a 0.2 μm filter cartridge to remove all organisms and incubated a fresh phytoplankton assemblage. In this subsequent incubation, running for 4-7 days, we investigated indirect effects of krill and salps on the plankton community via nutrient recycling (Fig. 3.1). At the beginning and the end of each experimental phase (grazing period, subsequent phytoplankton incubation), we also determined active bacterivores, including mixotrophs, via 24h uptake experiments with fluorescent beads (see above).

We conducted a similar experiment only with krill (and a control) at Admiralty Bay, where no salps occurred, and an additional grazing assay in the dark over 24h with krill and salps

collected off the coast of Elephant Island with a higher sampling resolution (every 6h) to get a better estimate on grazing rates excluding phytoplankton growth. At last, we conducted a grazing assay with solitary salps versus salps from aggregates to compare the grazing rates of the two different forms in the reproductive cycle of *Salpa thompsoni* and their effects on a plankton community over 24h. In all experiments, we measured chlorophyll fluorescence on a daily base, while every 2nd/3rd day we took samples for phytoplankton biomass and composition (Lugol preserved samples for microscopy), microzooplankton (formalin preserved samples for microscopy), nano- and picoplankton (flow cytometry), genetic diversity (16S and 18S rDNA for bacteria and eukaryotes), particulate and dissolved nutrients, pigments and fatty acids (FA), dissolved organic carbon, grazer stoichiometry (carbon, nitrogen, phosphorus) and FA, as well as fecal pellet stoichiometry (C, N, P), composition (phytoplankton) and FA. These samples will be analyzed in our laboratory at the ICBM, Univ. of Oldenburg, and in collaboration with the AWI.

Preliminary results

In most of our experiments, krill and salps showed a very clear grazing effect on phytoplankton, as indicated by decreasing chlorophyll a fluorescence in the grazer treatments compared to the control (Fig. 3.2). Here, salps alone had the strongest grazing impact on phytoplankton, while krill and the mixture of krill and salps were similar in their grazing impact. After feeding krill and salps with concentrated plankton and before filtering the water from different grazer treatments to set up the subsequent incubation with fresh plankton, we measured dissolved phosphorus and nitrate to monitor potential differences in nutrient recycling and to chose the right time point for setting up the plankton incubation. Especially for phosphate, we saw clear differences in nutrient recycling, as indicated by different dissolved phosphate concentrations, e.g. in the 2nd full grazing experiment conducted with organisms from the coast of Elephant Island. After a grazer incubation time of 4 days, phosphate concentrations were lowest in the control without grazers, only slightly higher in the salp incubation, while much higher in the krill incubation (Fig. 3.2). Phosphate concentrations in the mixed treatment (krill + salps) were intermediate, indicating the mixed recycling effects of krill and salps.

Even though it is not possible for us yet to draw any conclusions regarding effects of krill and salps on plankton composition or stoichiometry, first results indicate that we were able to capture direct effects on the plankton community through krill and salp grazing. We also observed that krill and salps differed in the amount (and presumably also in the ratio) of nutrients they recycled, as phosphate concentrations differed clearly, while nitrate concentrations did not (data not shown). The treatment combining krill and salps will enable us to study interactive effects of these two major grazers, which co-occurred in the natural habitats sampled at Deception and Elephant Island. In comparison to observed large-scale patterns in the field, our experiments allow us to disentangle direct and indirect consequences of potential grazer shifts from krill to salps for the plankton community structure and process rates within the food web.

Data management

We will fulfill all requirements of a good scientific practice laid out e.g. by the German Science Foundation (DFG). Results of our project will be published in peer-reviewed journals, if possible under the open access policy. Data will be provided to publisher databases such as Dryad. In addition, we will share all original data with the mathematical modelers within the project in order to allow for modeling and synthetic analyses.

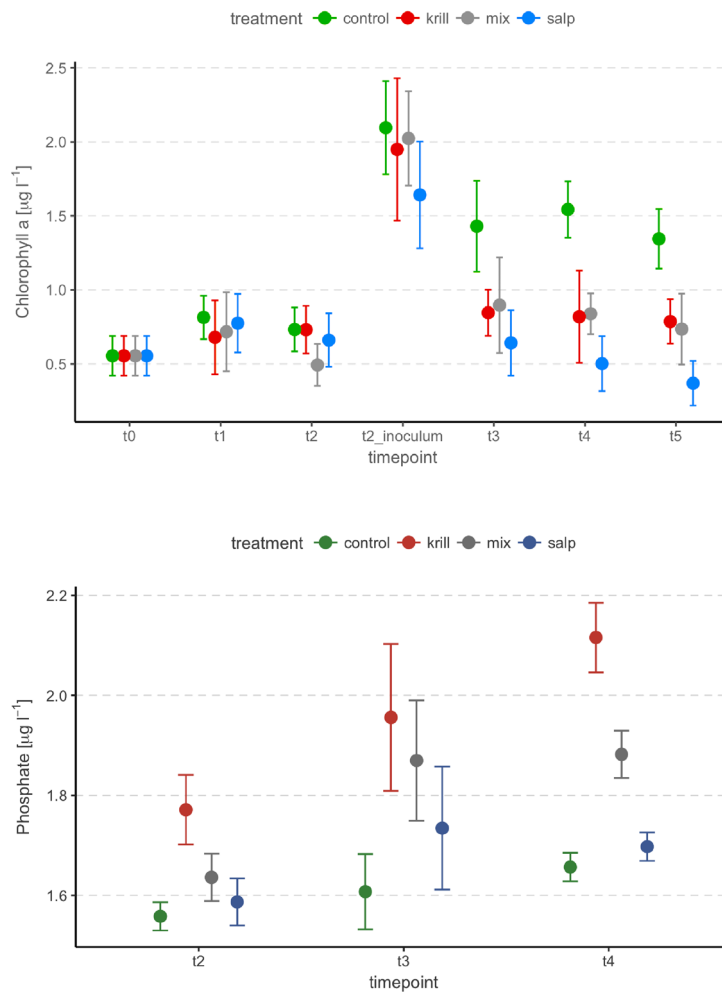


Fig. 3.2: Chlorophyll a concentrations (top) and phosphate concentrations (bottom) in different grazer treatments over the course of the experiment conducted with krill and salps collected off the coast of Elephant Island.

References

- Bernard KS, Steinberg DK, Schofield OME (2012) Summertime grazing impact of the dominant macrozooplankton off the Western Antarctic Peninsula. *Deep Sea Research I*, 62, 111–122.
- Condon RH, Steinberg DK, del Giorgio PA, Bouvier TC, Bronk DA, Graham WM, Ducklow HW (2011) Jellyfish blooms result in a major microbial respiratory sink of carbon in marine systems. *PNAS*, 108, 10225–10230.
- Loeb V, Siegel V, Holm-Hansen O, Hewitt R, Fraserk W, Trivelpiecek W, Trivelpiecek S (1997) Effects of sea-ice extent and krill or salp dominance on the Antarctic food web. *Nature*, 387, 897–900.
- Moline MA, Claustre H, Frazer TK, Schofield O, Vernet M (2004). Alteration of the food web along the Antarctic Peninsula in response to a regional warming trend. *Global Change Biology*, 10, 1973–1980.
- Pakhomov EA, Froneman PW, Perissinotto R (2002) Salp/krill interactions in the Southern Ocean: spatial segregation and implications for the carbon flux. *Deep Sea Research II*, 49, 1881–1907.
- Ross RM, Quetina LB, Martinson DG, Iannuzzi RA, Stammerjohn SE, Smith RC (2008) Palmer LTER: Patterns of distribution of five dominant zooplankton species in the epipelagic zone west of the Antarctic Peninsula, 1993–2004. *Deep Sea Research II*, 55, 2086–2105.

4. HOW WILL A POPULATION SHIFT FROM KRILL TO SALPS IMPACT THE EXPORT AND RECYCLING OF ORGANIC MATTER IN THE SOUTHERN OCEAN?

Morten H. Iversen^{1,2}, Clara M. Flintrop^{1,2}, Nora-Charlotte Pauli^{1,3}, Christian Konrad^{2,3}, Evgeny A. Pakhomov⁴, Larisa G. Pakhomova⁴

¹AWI

²MARUM, Uni Bremen

³ICBM, Uni Oldenburg

⁴UBC

Grant-No. AWI_PS112_00

4.1 Drifting sediment traps

Objectives

We used an array of free-drifting sediment traps to measure the export fluxes at 100 m, 200 m, and 300 m depth (Fig. 4.1, Table 4.1). Each collection depth had a trap station that consisted of four cylindrical collection tubes with a gyroscopical attachment (Fig. 4.1). Three of the four collection cylinders at each depth were used to collect samples for biogeochemical measurements of total dry weight, particulate organic carbon, particulate organic nitrogen, particulate inorganic carbon, and silica. The fourth trap cylinder at each depth was equipped with a viscous gel that preserved the structure, shape and size of the fragile settling particles (Fig. 4.2). After recovery of the drifting trap, the samples for bulk fluxes were frozen for later analysis in the home laboratory. The particles collected in the gel traps were photographed with a digital camera on board and frozen for further detailed investigations in the home laboratory. The image analyses of the gel traps will be used to determine the composition, abundance and size distribution of the sinking particles.

Work at sea

We deployed the drifting trap ten times during the PS112 cruise. The drifting array consisted of a surface buoy equipped with an Iridium satellite unit that provided trap positions every 10 minutes with a resolution of two minutes, we used two benthos floats for buoyancy and 14 small buoyancy balls were placed between the surface buoy and the two benthos floats to act as wave breakers and thereby reducing the hydrodynamic effects on the sediment traps. The trap cylinders were mounted to a sediment station with gimbal mounts ensuring that they were maintaining a vertical position in the water column. Each cylinder was 1 m tall and had a diameter 10.4 cm, which resulted in a collection area of 84.95 cm².



Fig. 4.1: Free-drifting sediment trap during deployment in front of Elephant Island with one of the trap stations with the four sediment trap cylinders.

4.1 Drifting sediment traps

Tab. 4.1: Deployments of the free-drifting sediment trap with information about station name, date of deployment, time for deployment and recovery, as well as latitude and longitude for deployment and recovery (see comments). The recovery of FDF10 did not get any ship's station number.

Station name	Date	Time [UTC]	Latitude	Longitude	Comments
PS112_25_44	2018-03-31	13:36	62°59,536'S	060°25,997'W	Deployment DF01
PS112_25_53	2018-04-01	14:30	62°52,214'S	060°12,030'W	Recovery DF01
PS112_54_01	2018-04-08	14:07	61°02.049'S	054°46.790'W	Deployment DF02
PS112_55_23	2018-04-09	13:10	61°03.013'S	054°52.575'W	Recovery DF02
PS112_90_03	2018-04-16	14:21	63°43.977'S	056°50.681'W	Deployment DF03
PS112_97_01	2018-04-17	11:22	63°38.792'S	056°28.785'W	Recovery DF03
PS112_98_01	2018-04-17	15:38	63°38.803'S	056°28.755'W	Deployment DF04
PS112_98_15	2018-04-18	14:16	63°36.986'S	056°25.424'W	Recovery DF04
PS112_106_03	2018-04-20	13:36	61°55.353'S	053°55.505'W	Deployment DF05
PS112_106_13	2018-04-21	14:06	61°48.694'S	053°38.838'W	Recovery DF05
PS112_118_01	2018-04-25	18:53	60°59.116'S	054°57.422'W	Deployment DF06
PS112_118_08	2018-04-26	10:54	60°55.622'S	055°09.133'W	Recovery DF06
PS112_119_01	2018-04-26	15:25	60°59.765'S	054°37.844'W	Deployment DF07
PS112_119_15	2018-04-27	12:02	60°55.899'S	054°43.898'W	Recovery DF07
PS112_120_01	2018-04-27	14:06	60°56.780'S	054°45.349'W	Deployment DF08
PS112_120_18	2018-04-28	10:55	60°57,450'S	054°52,048'W	Recovery DF08
PS112_121_01	2018-04-28	13:02	60°58,114'S	054°53,030'W	Deployment DF09
PS112_121_13	2018-04-29	11:00	60°58.948'S	054°55.870'W	Recovery DF09
PS112_122_01	2018-04-29	13:03	60°59.285'S	054°57.118'W	Deployment DF10
PS112_122_12	2018-04-30	11:00	60°57.406'S	054°58.179'W	Recovery DF10

Preliminary results

We deployed one trap off Deception Island, six traps off Elephant Island, two traps in the Weddell Sea off the entrance to the Antarctic Sound, and one trap in the eastern Bransfield Strait. All trap deployments were equipped with gel traps. We collected three types of aggregates during the cruise, krill fecal pellets, salp fecal pellets, and aggregates of heavily degraded biogenic material. We generally observed a decrease in numbers and sizes of krill fecal pellets with increasing water depth.

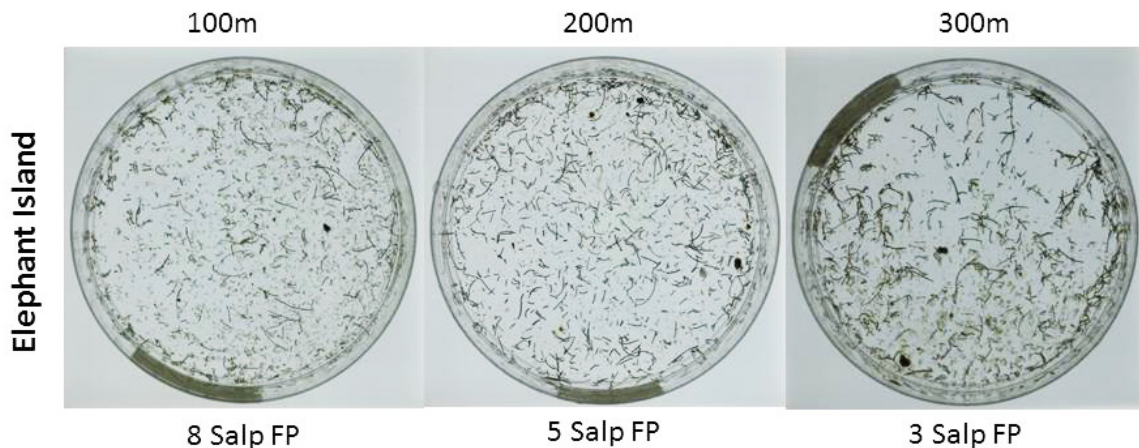


Fig. 4.2: Examples of the particles collected in the gel traps at 100 m, 200 m, and 300 m the Elephant Island

The gel trap collections showed that the composition of sinking particles were different at the four collection regions. At Deception Island, the Weddell Sea, and the eastern Bransfield Strait we mainly had krill fecal pellets in the traps collected from all depths. Off Elephant Island we observed many heavily degraded aggregates and salp fecal pellets. There were generally small salp fecal pellets in the traps that collected at 100 m, while the salp pellets collected at 200 and 300 meter depth were large, likely from solitary salps. We observed a decrease in salp pellets abundance with increasing depth, suggesting that there was a strong attenuation in salp pellet fluxes with increasing depth.

We will perform detailed image analyses of the gel traps back in the home laboratory. We will also make biogeochemical analyses to determine mass fluxes of dry material, organic carbon, organic nitrogen, inorganic carbon, silicate, and lithogenic material.

4.2 Direct observation of feeding and swimming behaviour of *Salpa thompsoni* and *Euphausia superba* using video recording and particle image velocimetry

Objectives

Because of changing seawater temperatures in the Southern Ocean, the tunicate *Salpa thompsoni* (from now on also referred to as “salp(s)”) is expanding its range further south towards the Antarctic continent, intruding into regions previously dominated exclusively by the Antarctic krill *Euphausia superba* (from now on also referred to as “krill”) (Atkinson et al. 2004; Pakhomov et al. 2002). Interactions between krill and salps are scarcely studied, but observations include krill feeding on salps (Kawaguchi and Takahashi 1996) and salps secreting a metabolite or chemokine that repels krill (Pakhomov 2018, pers. comm.).

Displacement of krill by salps in previously krill-dominated regions (Atkinson et al. 2004) influence large-scale changes in food-web structure as salps have low nutritional value and are not preferentially preyed upon by marine mammals (e.g. cetaceans). Furthermore, differences in grazing behaviour (size-selective grazing by krill vs. indiscriminate grazing by salps) can lead to changes in particle-size distribution in the water column. Yet, little is known about grazing rates, filtration volume, and swimming patterns of *S. thompsoni* compared to temperate salp species. Lastly, differences in the settling velocity and composition of salp and krill pellets can

affect export fluxes. Despite high settling velocities measured for fresh, intact fecal pellets of *S. thompsoni*, they have been observed to be significantly recycled in the upper water column (Iversen et al. 2016). Reasons for high turnover of salp fecal pellets in the euphotic zone are not yet known, with one hypothesis being that they are readily fragmented or (partially or completely) ingested by krill.

The three main objectives of video recording were to document

- I. The behaviour of krill and salps on their own and when together
- II. The behaviour of krill and salps when encountering their own or each other's faecal pellets
- III. The swimming and filtration patterns of *S. thompsoni* using food colouring and Particle Image Velocimetry (PIV)

Work at sea

A 60 L "Kreisel" (a circular aquarium fitted with air inlets for water circulation) was fitted with infrared illumination either from the back or from the side. To record, a minimum of 10 individuals of *E. superba* and/or *S. thompsoni* were added to the Kreisel filled with chl a-maximum water, where they were left to acclimatise for at least 24 h. Animals were recorded for 30-60 min using an exposure time of 900 milliseconds and a digital shift of 2. The camera was attached to a mount that allowed movement and recording in all directions. Swimming and feeding behaviour was recorded by following individual animals moving freely in the water column, with intermittent stationary shots to measure swimming speed. Reaction to settling fecal pellets was recorded by adding pellets to the Kreisel using a wide-mouth bore pipette and following them with the camera until they reached the bottom of the Kreisel. Qualitative recordings of krill and salps were done using visible light illumination. A portable LED (LEDZILLA-BiColor, Dedo Weigert, Germany) was mounted on a tripod to illuminate the Kreisel from above, and a SLR camera (Canon Rebel) was used to film krill and/or salp swimming and grazing behaviour.

To record filtration and wake patterns of swimming salps, individual salps were added to a ca. 50 L rectangular aquarium filled with chl a-maximum water. Red food colouring was gently ejected into or directly in front of the oral siphon with a pasteur pipette and the passage of the dye through the body and the ejection and wake patterns were recorded using a SLR camera (Canon Rebel). To determine the volumetric pumping rate and swimming pattern of *S. thompsoni* with PIV, a ca. 2 L rectangular aquarium was seeded with 5 µm polyamide particles to follow the magnitude and direction of the water stream pumped through and ejected by the salp. An infrared light source with a Fresnel lens in front created a light sheet in which particles were fully illuminated. Particle movement was recorded using a camera positioned perpendicular to the light sheet.

Preliminary results

Krill swimming behaviour could be divided into i) hovering, i.e. remaining suspended in one spot through leg-beating, ii) directional swimming, where leg-beating was used to swim upward, downward or forward, and iii) falling, where ceasing of leg-beating caused the krill to settle down in the water column. This behaviour in combination with adjustment of the tail was also observed to change the alignment of the body axis and thus to effect a change in the swimming direction. Fast downward swimming could be observed after sudden light incidence. However, swimming behaviour reversed to normal after acclimatization to changed light levels. It appeared that krill exhibited two different grazing mechanisms: (i) generating a water current past the mandibles through beating of the filter legs (thoracopods), and (ii) opening and closing the feeding basket. However, the basket was only deployed sporadically and there was no

obvious correlation to particle abundance and size, although a quantitative analysis is needed to verify this observation.

Salp swimming and grazing behaviour could be divided into (i) pumping and (ii) resting phases. Pumping resulted in propulsion of the salp and directional swimming (both forward and backward). Backward swimming was observed when salps encountered a solid obstacle (e.g. the Kreisel or aquarium wall) or when encountering an unknown taste/smell, such as the food colouring.

When kept together, salps and krill exhibited all of the behaviours described above, and overall did not seem to behave differently because of the presence of the other animal. However, on at least three occasions, individual krill were observed to latch onto large salp aggregates or chains, or completely engulfed smaller aggregates using their feeding basket, and remained attached for up to 5 minutes. Another salp was found to have a hole of approx. 1 cm diameter in its tunic after 2 days of being kept in the Kreisel together with krill which could have been inflicted by krill feeding on the salp.

Reactions of salps or krill when offered fecal pellets were difficult to assess because the high settling velocity of pellets prevented them from remaining suspended in the water column. This limited the time that animals could react to pellets in the water column, and animals were often not within detection distance of settling pellets. At first glance, neither attraction nor avoidance behaviour towards pellets was observed but further analysis of the recordings will be necessary to confirm this observation.

Food colouring visualized the jet wake structure of swimming salps, although backward-swimming to eject the food colour or temporarily ceasing to pump was sometimes observed when salps encountered the dye. The jet wake structure consisted of spherical vortex rings with small trailing jets, similar to those observed by Sutherland and Madin (2010). The PIV set-up was successfully used to record wake and filtration patterns. Three of the recorded specimens (one single aggregate and two aggregates which were part of a four-aggregate chain) had their feeding net deployed, allowing comparison to filtration and wake patterns of individuals with and without deployed net. Processing these recordings will enable us to analyse both the magnitude and direction of the “injected” and ejected water flow.

4.3 Production and composition of fecal pellets from krill and salps: Fecal pellet production, gut passage time, and settling velocities of aggregates in the Western Atlantic sector of the Southern Ocean

Objectives

Antarctic krill (*Euphausia superba*) and salps (*Salpa thompsoni*) both contribute to the biological carbon pump in the Southern Ocean by the production of fast sinking fecal pellets, which are rich in organic matter. In recent years, salp abundances have been increasing, shifting their distributional range beyond 60° south. This seems to lead to a dominance shift from krill to salps as major grazers in the Western Atlantic sector of the Southern Ocean. This dominance shift will also affect the biological carbon pump, however, detailed aspects of krill and salp contribution to carbon flux and carbon export to the deep sea remain unclear. To assess the impact of krill and salp fecal pellets to the biological carbon pump we used a combination of *in-situ* and laboratory analyses. Krill and salps were incubated to measure fecal pellet production rates. Subsequently, pellets were used to investigate size-specific sinking velocities in a vertical flow chamber. In addition, pellets were collected for later analysis of particulate organic carbon as well as molecular analysis of pellet composition.

Work at sea

We deployed a Marine Snow Catcher (MSC) at eleven stations to collect *in-situ* settling aggregates. Each MSC was deployed 10 m below the depth of fluorescence maximum. The MSC collects 100 L when closed with a drop weight. After retrieval, the snow catcher was left on deck for six to twelve hours to allow the captured particles to settle in the bottom part of the MSC. The particles were sinking very slowly and we therefore needed a long settling time on deck to ensure that all settling aggregates reach the bottom part of the MSC. Hereafter, we gently drained the upper part of the MSC and the particles in the bottom part were brought to the laboratory. We measured the size-specific settling velocities and microbial respiration of the aggregates in a flow chamber and made microscope images to determine their composition, as well as prepared the aggregates for determination of particulate organic carbon and nitrogen.

Antarctic Krill (*Euphausia superba*) was collected by IKMT net hauls at five stations covering our study regions (Stations number 13, 25, 55, 111). We incubated freshly caught *E. superba* to determine their *in-situ* fecal pellet production rate. Individual krill were incubated for six to ten hours with a replicate quantity of ten in 4.5 L buckets filled with ambient water from the fluorescent maximum zone at 0°-1°C in a temperature-controlled laboratory. A mesh (2 mm mesh size) was placed on the bottom of the buckets to prevent the krill from interacting with the freshly produced pellets. After the incubations we collected the pellets and measured their size, sinking velocity, microbial respiration, and prepared samples for particulate organic carbon and nitrogen, as well as samples for lipid and DNA analyses. In addition, water samples for DOC and dissolved nutrients were taken from each replicate at the start and end of the krill fecal pellet production incubations.

Salps were collected by IKMT net hauls and by scuba divers. During the voyage, in total 34 fecal pellet production experiments were conducted on both aggregate and solitary forms of *Salpa thompsoni* ranging in OA length between 8 and 61 mm. Freshly caught salp specimens were collected during day- and nighttime at the process studies near Deception and Elephant Islands. Individuals or short chains (3 to 8 individuals) of salps were placed in 25-20 l containers filled with the surface water and incubated in the temperature-controlled room (0-1 °C) for at least 8 hours (occasionally up to 24 hours). Containers were checked every two hours, pellets counted and after 4 or 8 hours collected for subsequent pigment, DNA, C/N analyses, and for size measurements as well as microbial respiration and sinking rates measurements. After each experiment, salps were measured, sexed, staged and frozen in -80 °C for further analyses at the home laboratory.

Krill and salp pellets produced in the FPP experiments were used to measure size and settling velocity in a flow chamber. In addition, pellets were pooled and filtered for POC (pre-combusted GF-F filters), DNA (polycarbonate filters), and lipids (GF-F filters).

To assess the different sinking speed of krill vs. salp pellets, size-specific sinking velocity of the on-board produced pellets was measured using a flow chamber. A vertical flow was applied so that the pellets were floating a diameter above the bottom of the chamber. The flow rate of the flow chamber was then used to calculate sinking velocity of the individual pellets. Measurements in the flow chamber were conducted with GF/F filtered *in-situ* seawater at ambient temperature and salinity. In addition, other aggregates collected by the marine snow catcher were measured for comparison. Measured pellets were individually frozen in Eppendorf tubes for size-specific POC analysis back home. In addition to the size-specific sinking velocity, microbial respiration of the pellet associated microbes was measured using a microsensor set-up.

Preliminary results

Size-specific sinking velocity of krill and salp pellets differed markedly with a mean sinking velocity of krill pellets of 233.38 m d^{-1} ($\text{sd} \pm 3.8$, Fig. 4.3), and 595.1 m d^{-1} ($\text{sd} \pm 26.41$) for salp pellets (Fig. 4.4). In contrast to krill pellets, salp pellet size was significantly correlated to sinking velocity ($p = 0.01$).

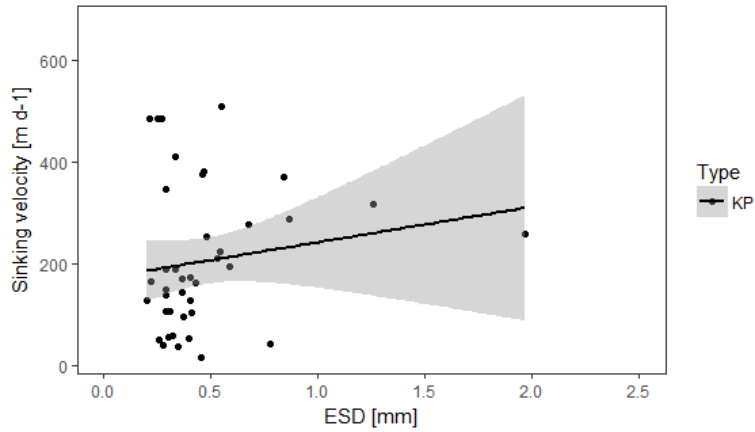


Fig. 4.3: Size vs. settling of krill pellets measured in a vertical flow chamber. Pellet volume is given as equivalent spherical diameter (ESD) in mm on the x-axis, sinking velocity in m d^{-1} is depicted on the y-axis.

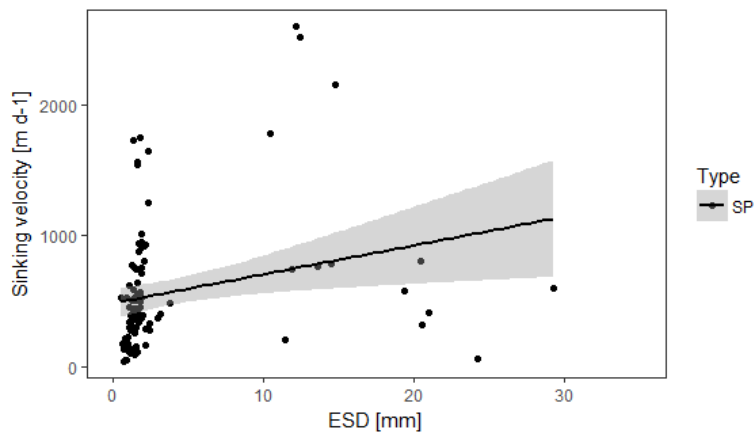


Fig. 4.4: Size vs. settling of salp pellets measured in a vertical flow chamber. Pellet volume is given as equivalent spherical diameter (ESD) in mm on the x-axis, sinking velocity in m d^{-1} is depicted on the y-axis.

Salp FPP was similar in both areas and ranged from 0.16 to 0.92 fecal pellets.ind.⁻¹h⁻¹ with the mean FPP rate of 0.4 ± 0.2 fecal pellets.ind.⁻¹h⁻¹ (Fig. 4.5). These rates are within previously reported values (Pakhomov et al. 2002; Phillips et al. 2009; Iversen et al. 2016). It was observed that mean FPP rates were nearly constant within the size 8-61 mm (Fig. 4.5).

4.3 Production and composition of fecal pellets from krill and salps

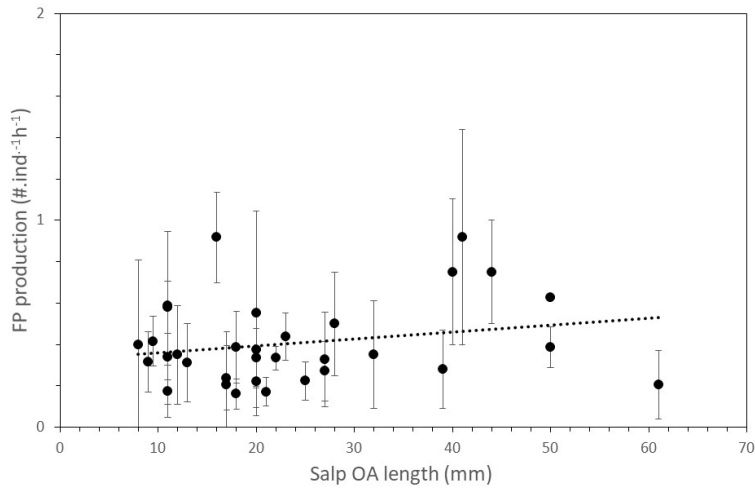


Fig 4.5: Mean fecal pellet production rates of *Salpa thompsoni* during the summer (March-April) 2018

During the FPP experiments, preliminary gut passage time measurements were conducted. It was assumed that gut passage time would be equal to time when about 90 % of food is evacuated from the salp stomach. Gut passage time was different for solitaries and aggregates (Fig. 4.6). Solitaries were represented by developing (stages 2-3) and actively feeding individuals and their gut passage times were substantially faster compared to aggregates of the similar size (Fig. 4.6). Gut passage time of aggregates was strongly size dependent and ranged from 5 hours to nearly 30 hours for 10 mm and 50 mm aggregates, respectively (Fig. 4.6).

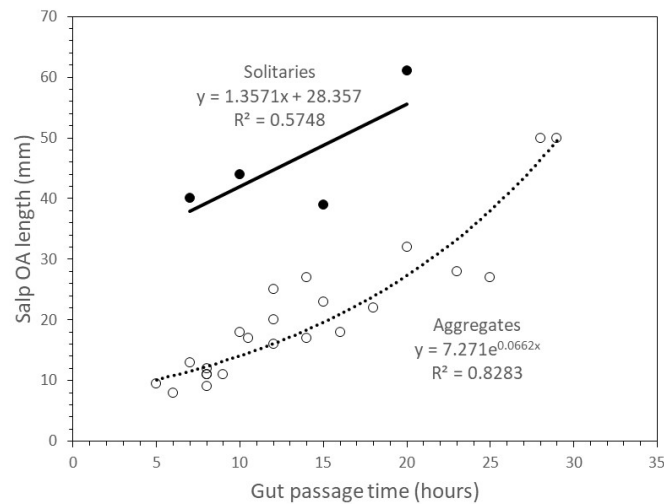


Fig. 4.6: Preliminary gut passage times for *Salpa thompsoni* aggregates and solitaries during summer (March-April) 2018

In total, approximately 930 guts of *Salpa thompsoni* were dissected out and frozen in -80°C for the subsequent gut pigment, DNA, diet composition and C/N analyses. After the lab analyses will be completed, pigment and C/N values will be used to calculate salp ingestions rates as well as grazing impacts.

4.4 Vertical profiles with the In-Situ Camera and driftcam system

Objectives and system description

The In Situ Camera (ISC) consisted of an industrial camera with removed infrared filter (from Basler) with backend electronics for timing, image acquisition and storage of data and a fixed focal length lens (16 mm Edmund Optics). Furthermore, a DSPL battery (24V, 38Ah) was used to power the system (Fig. 4.7).

A single board computer was both used as the operating system for the infrared camera and to acquire the images from the camera and send them to a SSD hard drive where they were stored. The illumination was provided by a custom made light source that consisted of infrared LEDs which were placed in an array in front of the camera. The choice of the infrared illumination was done to avoid disturbing the zooplankton that potentially would feed on the settling particles. With this geometrical arrangement of the camera and the light source we obtained shadow images of particles through the water column. We captured 2 images per second and lowered the ISC with 0.3 meters per second (lowest possible speed of winch).

The DriftCam consists of a Canon EOS 600D DSLR (18 Megapixel resolution) with an EF 50.2 macro-lens connected to a Canon Speedlight 430 EX II flash. Camera and flash were installed each in a POM pressure housing with a depth rating of 500 m. The camera could be programmed by using a Delamax LCD Timer, which allows time-lapse exposures at given intervals. The flash was mounted perpendicular to the optical axis of the camera at a distance of app. 30 cm.

Both camera systems were mounted on the same platform together with a Seabird SBE19 CTD equipped with an oxygen sensor, a turbidity sensor, and a fluorescence sensor (Fig. 4.7). However, we had some issues with the flash housing and the DriftCam was therefore not mounted during all deployments of the camera platform.

Work at sea

We made 70 vertical profiles with the camera platform (Table 4.1). All profiles were equipped with the ISC and the Seabird SBE19 CTD to get correlations of depth and images. During the whole cruise both instruments were used in standalone mode and data was then afterwards correlated with Matlab. Only a few of the profiles had the DriftCam mounted due to technical issues with the flash pressure housing. With that we got 69 successful profiles. An overview of all measured profiles can be found in Table 4.2.

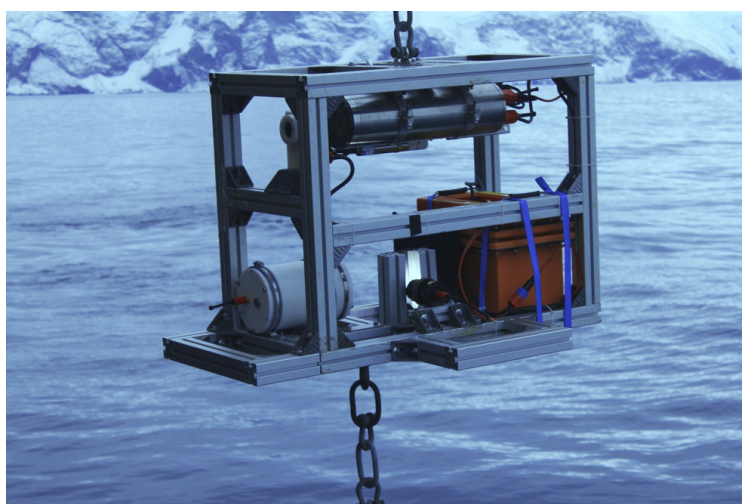


Fig. 4.7: Deployment of the camera system platform off Elephant Island. The platform was equipped with the In Situ Camera (ISC), the DriftCam, and a Seabird SBE19 CTD.

4.3 Production and composition of fecal pellets from krill and salps

Tab. 4.2: List of stations where the In Situ Camera (ISC) was deployed in the profiling mode

Profile No.	Station No	Date	Start Time	Latitude	Longitude	Profile depth [m]
1	PS112_08_05	2018-03-24	03:08:03	- 62.0902	- 58.3353	60
2	PS112_12_02	2018-03-25	04:43:20	- 63.0000	- 57.5000	500
3	PS112_17_03	2018-03-26	04:49:12	- 62.7664	- 59.0116	500
4	PS112_20_04	2018-03-26	20:44:20	- 63.0002	- 60.0010	500
5	PS112_24_06	2018-03-28	02:53:38	- 62.5815	- 59.8826	160
6	PS112_24_18	2018-03-29	00:16:15	- 62.5779	- 59.8792	360
7	PS112_25_09	2018-03-29	22:14:21	- 62.9736	- 60.4778	120
8	cancelled	cancelled	cancelled	cancelled	cancelled	cancelled
9	PS112_25_45	2018-03-31	22:14:54	- 62.9589	- 60.4333	500
10	PS112_25_52	2018-04-01	12:40:50	- 62.8865	- 60.2402	500
11	PS112_31_03	2018-04-03	23:38:47	- 61.7515	- 60.0086	50
12	PS112_34_02	2018-04-04	14:47:55	- 61.2341	- 60.9705	500
13	PS112_41_02	2018-04-05	21:39:34	- 61.7494	- 59.0007	300
14	PS112_47_02	2018-04-07	00:28:36	- 60.2505	- 56.5079	500
15	PS112_55_02	2018-04-08	14:52:55	- 61.0342	- 54.7798	500
16	PS112_55_11	2018-04-08	21:53:47	- 61.0143	- 54.8304	500
17	PS112_55_15	2018-04-09	02:46:47	- 61.0154	- 54.8507	500
18	PS112_55_18	2018-04-09	08:07:40	- 61.0079	- 54.9705	440
19	PS112_55_24	2018-04-09	14:38:06	- 61.0502	- 54.8763	230
20	PS112_90_01	2018-04-09	11:44:08	- 63.7351	- 56.8475	500
21	PS112_97_03	2018-04-17	13:31:12	- 63.6895	- 56.7118	270
22	PS112_98_02	2018-04-17	16:20:09	- 63.6495	- 56.4877	420
23	PS112_98_10	2018-04-17	21:35:24	- 63.6534	- 56.4852	500
24	PS112_98_11	2018-04-18	03:04:27	- 63.6432	- 56.4219	500
25	PS112_98_12	2018-04-18	09:04:26	- 63.6729	- 56.4620	500
26	PS112_98_16	2018-04-18	15:15:43	- 63.6164	- 56.4217	500
27	PS112_106_04	2018-04-20	14:22:35	- 61.9120	- 53.8958	500
28	PS112_106_10	2018-04-20	20:09:28	- 61.8956	- 53.9956	360
29	PS112_106_11	2018-04-21	02:04:30	- 61.9136	- 53.9187	500
30	PS112_106_12	2018-04-21	08:01:27	- 61.9103	- 53.7646	500
31	PS112_106_14	2018-04-21	15:09:23	- 61.8078	- 53.6535	500
32	PS112_118_02	2018-04-25	19:47:09	- 60.9804	- 54.9623	500
33	PS112_118_04	2018-04-26	00:06:09	- 60.9766	- 55.0232	450
34	PS112_118_05	2018-04-26	02:03:41	- 60.9901	- 55.0206	400
35	PS112_118_06	2018-04-26	04:02:29	- 60.9825	- 55.0214	460
36	PS112_118_07	2018-04-26	08:02:25	- 60.9392	- 55.0711	460

4. How will Population Shift from Krill to Salps Impact Organic Matter in the Southern Ocean?

Profile No.	Station No	Date	Start Time	Latitude	Longitude	Profile depth [m]
37	PS112_118_09	2018-04-26	11:41:22	- 60.9312	- 55.1617	340
38	PS112_119_02	2018-04-26	15:37:47	- 60.9978	- 54.6088	500
39	PS112_119_05	2018-04-26	19:10:43	- 60.9841	- 54.5528	500
40	PS112_119_06	2018-04-26	22:04:13	- 60.96257	- 54.5623	500
41	PS112_119_08	2018-04-27	00:22:45	- 60.96492	- 54.6229	500
42	PS112_119_08	2018-04-27	03:03:05	- 60.97025	- 54.6111	500
43	PS112_119_11	2018-04-27	06:04:10	- 60.95242	- 54.6303	500
44	PS112_119_12	2018-04-27	08:00:58	- 60.93875	- 54.6544	500
45	PS112_119_13	2018-04-27	10:01:26	- 60.93375	- 54.6837	500
46	PS112_119_06	2018-04-27	12:42:20	- 60.93528	- 54.7316	500
47	PS112_120_11	2018-04-27	20:06:18	- 60.95855	- 54.7553	500
48	PS112_120_12	2018-04-28	00:05:00	- 60.93465	- 54.7690	500
49	PS112_120_13	2018-04-28	02:01:12	- 60.94320	- 54.7807	500
50	PS112_120_14	2018-04-28	04:04:00	- 60.96165	- 54.7669	500
51	PS112_120_15	2018-04-28	05:58:17	- 60.96067	- 54.7666	500
52	PS112_120_16	2018-04-28	07:57:25	- 60.96077	- 54.8178	500
53	PS112_120_17	2018-04-28	09:51:27	- 60.95743	- 54.8675	500
54	PS112_120_19	2018-04-28	11:35:39	- 60.96212	- 54.8764	500
55	PS112_121_05	2018-04-28	16:46:22	- 60.96888	- 54.8769	500
56	PS112_121_06	2018-04-28	21:59:00	- 60.98027	- 54.9071	500
57	PS112_121_07	2018-04-29	00:00:50	- 60.98140	- 54.9153	500
58	PS112_121_09	2018-04-29	03:00:50	- 60.98130	- 54.9228	500
59	PS112_121_10	2018-04-29	04:58:55	- 60.98503	- 54.9031	500
60	PS112_121_11	3028-04-29	07:00:36	- 60.98830	- 54.8837	500
61	PS112_121_12	2018-04-29	09:02:31	- 60.98002	- 54.9087	500
62	PS112_121_14	2018-04-29	11:39:48	- 60.98437	- 54.9375	500
63	PS112_122_05	2018-04-29	21:03:09	- 60.96768	- 54.961	500
64	PS112_122_06	2018-04-29	23:03:28	- 60.96767	- 54.9878	500
65	PS112_122_07	2018-04-30	01:01:27	- 60.97360	- 55.0132	480
66	PS112_122_08	2018-04-30	03:01:20	- 60.97287	- 55.0283	500
67	PS112_122_09	2018-04-30	04:59:20	- 60.97413	- 55.0061	500
68	PS112_122_10	2018-04-30	07:09:09	- 60.96278	- 54.9911	500
69	PS112_122_11	2018-04-30	09:02:23	- 60.96418	- 54.9705	500
70	PS112_122_13	2018-04-30	11:41:04	- 60.95763	- 54.9716	500

Preliminary Results

We obtained vertical profiles of particle abundance and size-distribution through the water column. We still need to analyse the images, but the first glance at the images showed several large aggregates in the surface water, while the deeper water seemed to mainly have small and compact aggregates. We made several vertical profiles with the camera platform during the deployment of the drifting traps in order to follow the settling of salp and krill fecal pellets in relation to their vertical migration (Fig. 4.8).

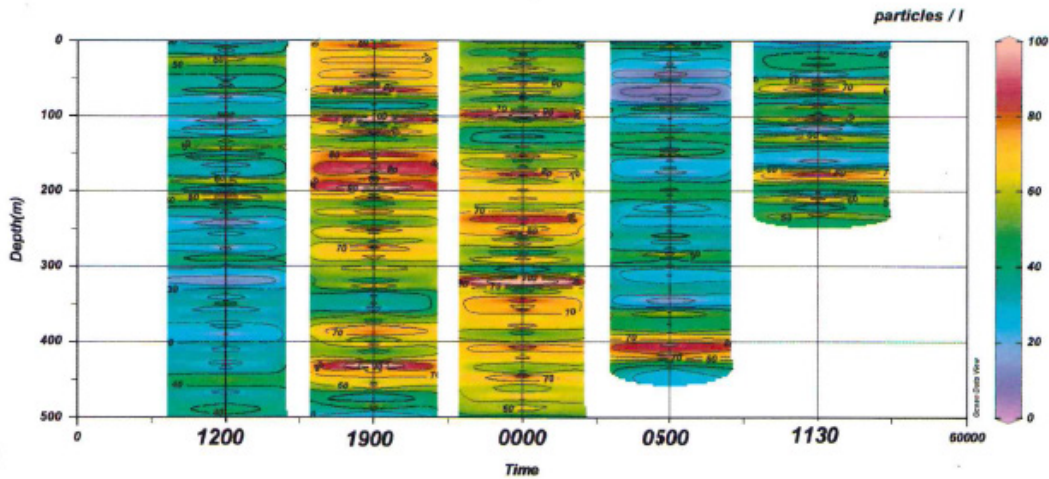


Fig. 4.8: Example of five vertical camera profiles in the upper 500 m of the water column during a free-drifting sediment trap deployment

The camera profiles further allow identifications of different particle types at specific depths and times. As an example, we show the vertical distribution of krill fecal pellets during five profiles captured over 24 hours next a deployed sediment trap (Fig. 4.9).

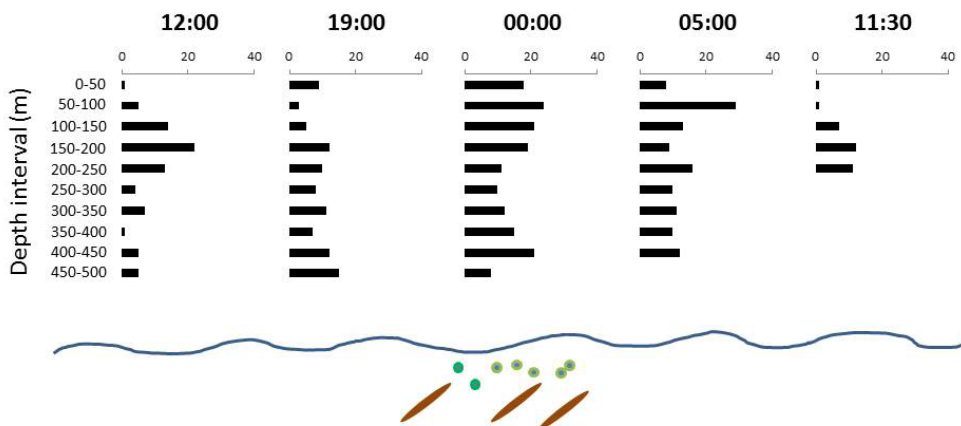


Fig. 4.9: Vertical distribution of krill fecal pellets from five vertical camera profiles captured over 24 hours next a free-drifting sediment trap

Data management

The final processed data will be submitted to the PANGAEA data library.

References

- Atkinson A, Schmidt K, Fielding S, Kawaguchi S, Geissler PA (2012) Variable food absorption by Antarctic krill: Relationships between diet, egestion rate and the composition and sinking rates of their fecal pellets. *Deep-Sea Research II*, 59-60, 147-158.
- Iversen MH, Pakhomov E, Hunt BPV, van der Jagt H, Wolf-Gladrow D, Klaas C (2016) Sinkers or floaters? Contribution from salp fecal pellets to the export flux during a large bloom event in the Southern Ocean. *Deep sea Research II*, 138, 116-125.
- Kawaguchi S, Takahashi Y (1996) Antarctic krill (*Euphausia superba* Dana) eat salps. *Polar Biology*, 16, 479-481.
- Pakhomov EA, Froneman PW, Perissinotto R (2002) Salp/krill interactions in the Southern Ocean: spatial segregation and implications for the carbon flux. *Deep Sea Research II*, 49, 1881–1907.
- Phillips B, Kremer P, Madin LP (2009) Defecation by *Salpa thompsoni* and its contribution to vertical flux in the Southern Ocean. *Marine Biology*, 156, 455-467.
- Sutherland KR, Madin LP (2010) Comparative jet wake structure and swimming performance of salps. *Journal of Experimental Biology*, 213, 2967-2975.

5. BIOLOGY OF THE PELAGIC TUNICATE, *SALPA THOMPSONI*, IN THE WESTERN ATLANTIC SECTOR OF THE SOUTHERN OCEAN DURING MARCH-MAY 2018

Evgeny A. Pakhomov¹, Larisa G. Pakhomova¹,
Morten H. Iversen^{2,3}, Clara M. Flintrop^{2,3}, Nora-
Charlotte Pauli^{2,4}, Christian Konrad^{3,4}

¹UBC

²AWI

³MARUM, Uni Bremen

⁴ICBM, Uni Oldenburg

Grant-No. AWI_PS112_00

Objectives

Metazoan plankton is recognized to be a cornerstone of the biological pump occupying an important intermediate position between primary producers and secondary consumers as well as critical “gatekeepers” for the carbon leaving the euphotic zone into the mesopelagic realm. Processes associated with aggregation of particles, grazing and active vertical migrations of metazoan zooplankton play significant role in the dynamics of the organic matter vertical flux in the ocean.

Pelagic tunicates (*Salpa thompsoni*) and Antarctic krill (*Euphausia superba*) are two most abundant large metazoans that contribute significantly but differently to the Southern Ocean biological pump. Moreover, their contribution to carbon flux may be altered due to climate change. Krill and salp interactions have received some attention in the past (Perissinotto and Pakhomov, 1998; Pakhomov et al. 2002; Atkinson et al., 2004). Nevertheless, their coexistence abilities/opportunities have seldom been researched.

One of the main objectives of the ANT 33-3 voyage was to investigate the population dynamics of *S. thompsoni* in the Atlantic sector of the Southern Ocean. While ecophysiology of *S. thompsoni* will be presented elsewhere, this contribution will focus on the general biology of *S. thompsoni* aiming to provide information about: (1) salp horizontal and vertical distribution, (2) general population structure of salps, and (3) variability in developmental stage composition of salps during austral summer 2018 in the vicinity of the Antarctic Peninsula.

Work at sea

Salps were collected at 106 stations using mainly the 2.5 m² Isaacs-Kidd Midwater Trawl equipped with the 0.5 mm mesh (Fig. 5.1). Samples were collected during the double oblique tows down to 170 m (AMLR protocol) at the speed of 2-2.5 knots. On two occasions near the Elephant Island, vertical distribution of salps was studied using the multi-RMT 1+8 trawl in the top 320 m layer during the day- and nighttime. In all catches, if present, salps were counted, measured (oral-atrial length to the nearest mm), sexed and staged. All solitaries as well as large aggregates were picket from the whole sample. Remaining sample was subsampled (1/4 to 1/40) to obtain min 150-350 small aggregates for detailed biological analysis. The grazing studies were undertaken during two process-studies near the Deception and Elephant Islands when salps were collected every 4-6 hours during 24-h cycle. Salp stomachs were dissected out and immediately frozen at -80 °C for a subsequent gut fluorescence analysis in

the laboratory (see Pauli et al., this volume) Healthy animals were used for gut evacuation rate measurements as well as for fecal pellet production experiments (results presented in Iversen et al., this volume).

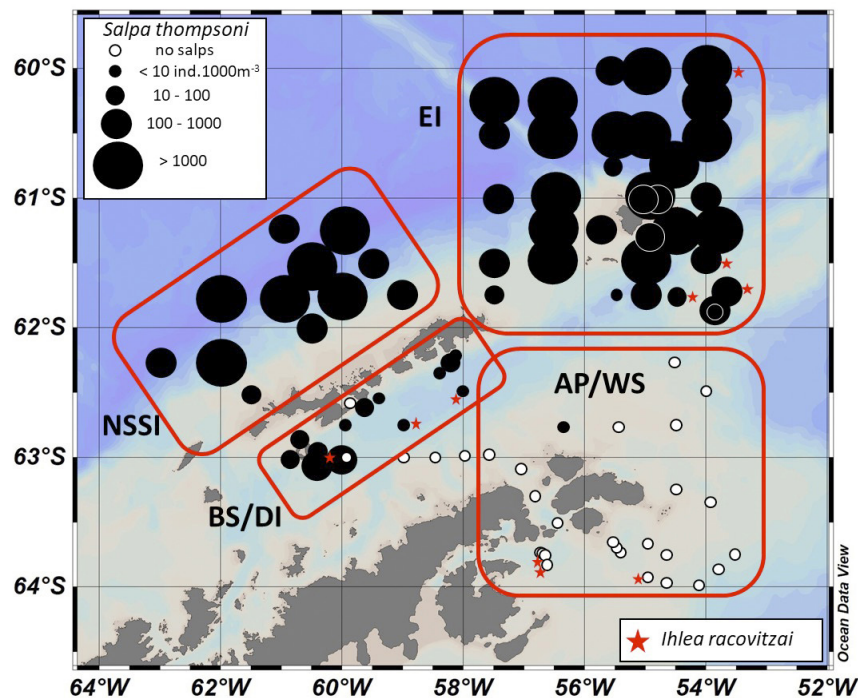


Fig. 5.1: Spatial distribution of *Salpa thompsoni* and *Ihlea racovitzai* in the western Atlantic Sector of the Southern Ocean during March-May 2018. BS/DI – Bransfield Strait and Deception Island region; NSSI – north of South Shetland Islands region; EI – Elephant Island region; and AP/WS – Antarctic Peninsula region affected by the Weddell Sea waters.

Preliminary results

Salp spatial distribution and abundance

Two species of salps, *Salpa thompsoni* and *Ihlea racovitzai*, were encountered in the area of investigation. *S. thompsoni* was by far the most abundant and frequently found species (Table 5.1, Fig. 5.1). *I. racovitzai* was only caught at 10 stations at very low ($\ll 10 \text{ ind.}1,000 \text{ m}^{-3}$) densities and was not found north of the South Shetland Islands (Table 5.1, Fig. 5.1). *S. thompsoni* was caught at every station in the regions north of the South Shetlands Islands as well as in the vicinity of the Elephant Island, with average densities 1,018 and 984 $\text{ind.}1,000 \text{ m}^{-3}$, respectively (Table 5.1). The maximum abundance reached 3,000-3,500 $\text{ind.}1,000 \text{ m}^{-3}$ (Table 5.1, Fig. 5.1). While *S. thompsoni* was found at 84 % stations in the Bransfield Strait, its average abundance was two orders of magnitude lower ($\sim 36 \text{ ind.}1,000 \text{ m}^{-3}$) compared to previous regions. Finally, the lowest density of *S. thompsoni* was found in the waters influenced by the Weddell Sea near the Antarctic Peninsula where salps were only caught at one station (Table 5.1, Fig. 5.1).

Tab. 5.1: Pelagic tunicate density during March-May 2018 near the Antarctic Peninsula

Region/Species	<i>Salpa thompsoni</i> (ind.1000 m ⁻³)			<i>Ihlea racovitzai</i>
	mean \pm 1SD	range	FO (%)	presence/absence
Bransfield Strait/ Deception Island (BS/DI)	35.8 \pm 49.5	0 – 187.1	83.8	+
North of South Shetland Islands (NSSI)	1018.9 \pm 897.8	39.8 – 3012.4	100.0	–
Elephant Island vicinity (EL)	984 \pm 886.0	2.4 – 3447.7	100.0	+
Antarctic Peninsula/ Weddell Sea (AP/WS)	0.3 \pm 1.6	0 – 8.1	4.2	+

Salp vertical migrations

In both regions, near Deception and Elephant Islands, the salp density in the top 170 m water layer during the daytime and nighttime was significantly different pointing to the active vertical migrations of *S. thompsoni* (Fig. 5.2). This difference was higher at the Deception Island (nearly 4.5-fold) compared to Elephant Island (2.5-fold). Depth stratified sampling showed that salps generally migrated within the top 320 m water layer concentration in the top 100 m during the nighttime and 200-300 m during the daytime (Fig. 5.3).

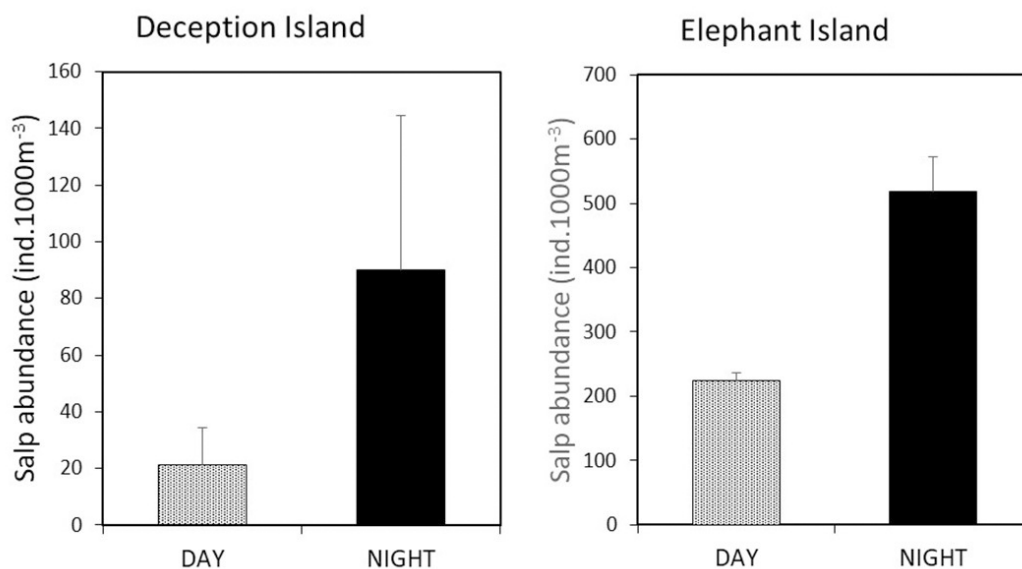


Fig. 5.2: Diel differences in average salp abundance in the near the Deception and Elephant Islands in the 0-170 m layer. Bars present one standard deviation of the mean.

5. Biology of the Pelagic Tunicate in the Western Atlantic Sector of the Southern Ocean

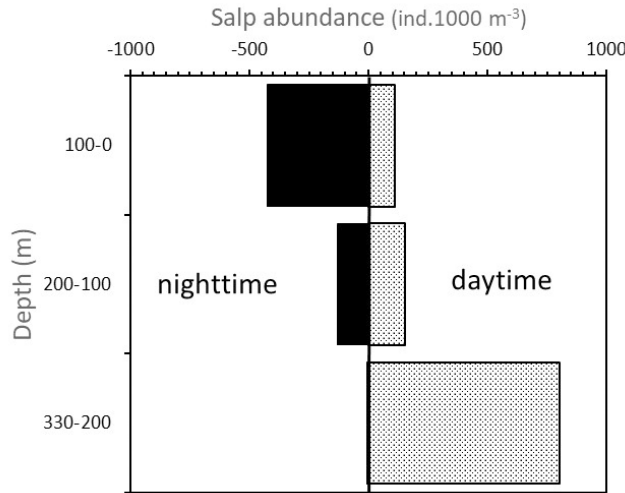


Fig. 5.3: *Salpa thompsoni* diel vertical migration in the vicinity of the Elephant Island

Salp biology

In total, 13,960 salps were measured and staged during the expedition. Length frequency distributions of aggregates were similar in three major salp regions (Fig. 5.4). Numerically, salps with OA length < 20 mm, e.g. recently released aggregate chains, dominated in all regions. Prevalence of small sized aggregates was reflected in dominance of early (0-1) developmental stages. Larger cohorts were not numerous but often distinct (Fig. 5.4). They consisted mostly of functional males (Fig. 5.4). It was noted for the first time, that functional females (stages 3 and 4) often had functional testes already developed (Fig. 5.5). Overall, males comprised generally < 5 % of total aggregate abundance (Fig. 5.4).

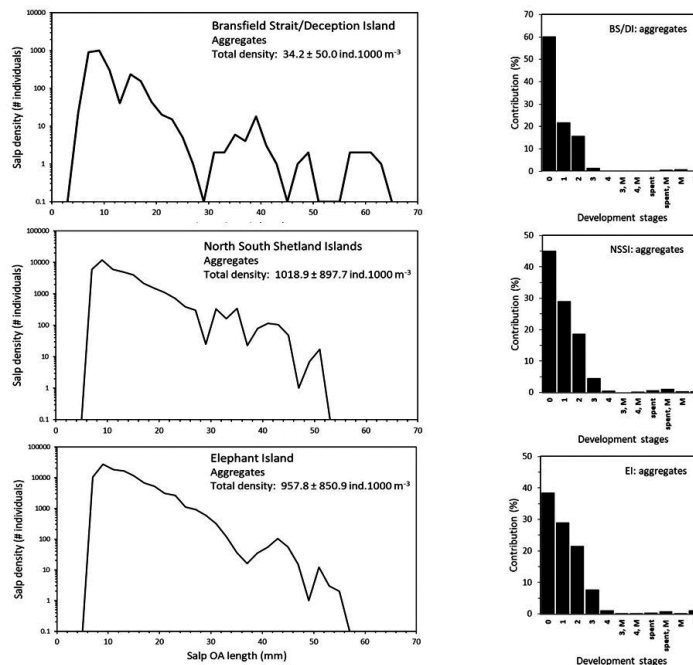


Fig. 5.4: Length frequency distribution and developmental stage composition of *Salpa thompsoni* aggregates in the western Atlantic Sector of the Southern Ocean during March-May 2018. BS/DI – Bransfield Strait and Deception Island region; NSSI – north of South Shetland Islands region; EI – Elephant Island region.



Fig. 5.5: Example of the stage 4 aggregate female with the fully developed male testes

Aggregate to solitary ratios varied widely between 50 and 370 and were generally higher (>100) north of the South Shetland Islands and near the Elephant Island. In all three regions, 110-130 mm solitary cohort was the most prominent feature in length frequency distributions (Fig. 5.6). In the Bransfield Strait region and, to a smaller degree near the Elephant Island, smaller cohorts between 20 and 100 mm were visible but less prominent (Fig. 5.6). This was reflected in the stage composition of solitaires. While in all regions solitaires that recently released chains (stages 5A/6A) numerically dominated, in the Bransfield Strait

contribution of recently released embryos and developing solitaires was significant. It appears that the *S. thompsoni* populations were actively reproducing at the time of our observations.

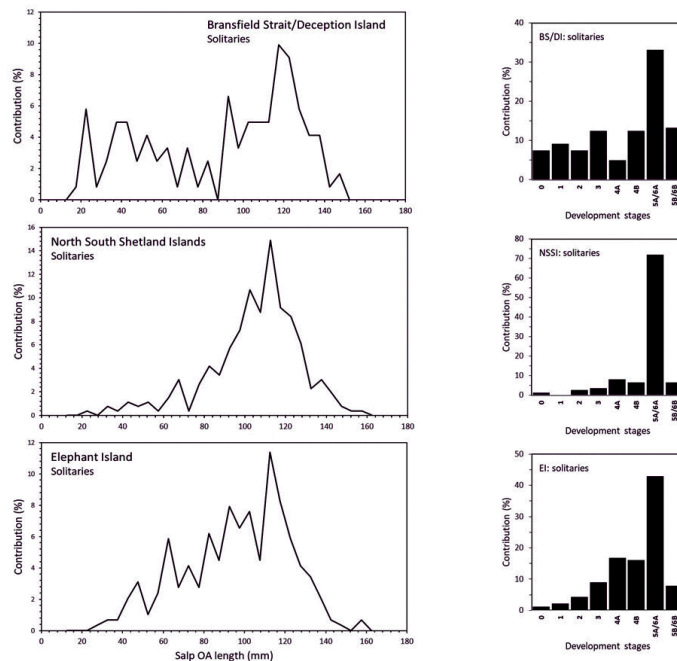


Fig. 5.6: Length frequency distribution and developmental stage composition of *Salpa thompsoni* solitaires in the western Atlantic Sector of the Southern Ocean during March-May 2018. BS/DI – Bransfield Strait and Deception Island region; NSSI – north of South Shetland Islands region; EL – Elephant Island region.

Preliminary conclusions

1. Fall 2018 appeared to be the “salp year” with the highest densities of salps exceeding 1000 ind.1000 m⁻³ observed in the regions most influenced by the ACC north of the South Shetland Islands and in the vicinity of the Elephant Island;
2. During fall 2018, *S. thompsoni* population was still actively reproducing, which was reflected in the size structure of aggregates and the stage composition of solitaires;

3. Salps were undergoing strong diel vertical migrations within top 300 m water layer;
4. Regions influenced by cold Weddell Sea water masses were devoid of *S. thompsoni*.

Data management

Salp biology data require verification and cleaning. The frozen samples, after delivered to the AWI, will be analyzed during 2018. As soon as data will be processed, and verified, data sets will be uploaded to the databases PANGAEA and/or SCAR-MarBIN.

Acknowledgments

We would like to acknowledge an invaluable contribution of the KRILBIS sampling team, namely Ryan Driscoll, Martina Vorkamp, Matteo Bernasconi, Anna Panasiuk and Justyna Wawrzynek, for assisting of sampling salps during the voyage.

References

- Atkinson A, Siegel V, Pakhomov EA. and Rothery P (2004) Long-term decline in krill stock and increase in salps within the Southern Ocean. *Nature*, 432, 100-103.
- Pakhomov EA, Froneman PW and Perissinotto R (2002) Salp/krill interactions in the Southern Ocean: spatial segregation and implications for the carbon flux. *Deep-Sea Research II*, 49, 1881-1907.
- Perissinotto R and Pakhomov EA (1998) The trophic role of the tunicate *Salpa thompsoni* in the Antarctic marine ecosystem. *Journal of Marine Systems*, 17, 361-374.

6. KRILLBIS

Ryan Driscoll², Evgeny Pakhomov⁶, Martina Vorkamp¹, Matteo Bernasconi³, Anna Panasiuk⁴, Larysa Pakhomova⁶, Natasha Waller⁵, Justyna Wawrzynek⁴, Bettina Meyer^{1,7}

¹AWI

²UCSC

³Uni St. Andrews

⁴Uni Gdansk

⁵AAD

⁶UBC

⁷ICBM, Uni Oldenburg

Grant-No. AWI_PS112_00

Objectives

Member states of the Convention for the Conservation of Antarctic Marine Living Resources (CCAMLR) are responsible for regular biomass surveys of *Euphausia superba* (Antarctic Krill). These surveys enable us to monitor both natural variability and climate change induced variations in Antarctic Krill abundance. Monitoring the Antarctic Krill population is critical to CCAMLR's ecosystem-based approach to fishery management, which requires that fishery regulations on target species (Antarctic krill) are sustainable and ensure the health of the krill dependent ecosystem. Past studies have indicated that salps may increase in abundance in response to recent warming trends. This may lead to potential resource competition with Antarctic krill. Salps and Antarctic krill co-occur around Antarctic Peninsula, one of the fastest warming regions on the planet. As part of the German contribution to CCAMLR, the PS112 continued a long-running time series of acoustic and net-based surveys in the Antarctic Peninsula region in relation to the bio-geophysical environment in compliance with CCAMLR goals. In addition to the CCAMLR survey, the KRILLBIS group's secondary goal was to collect krill and salp specimens for shipboard experiments under the umbrella groups POSER and PEKRIS.

The aim of the CCAMLR survey was to quantify aspects of krill, salp and other zooplankton biology and consisted of two complimentary parts. One was a series of systematic net tows interspersed along the acoustic transects. The net tows provided quantitative data on krill and salp demography (size, age and maturity) and population dynamics (spawning time, recruitment and larval development). The other was a series of acoustic transects using a multi-frequency SIMRAD EK60 echosounder for the estimation of the biomass and distribution of Antarctic krill in addition to other identifiable acoustic targets in accordance with CCAMLR protocol. The demographic data from the net tows will be used in the estimation of biomass from the acoustics.

Work at sea

The CCAMLR survey was broken into 4 areas around the South Shetland Island; Bransfield Strait, the north side South Shetland Islands, Elephant Island, and Joinville Island. Over the course of the cruise, 88 quantitative net tows were conducted between the CCAMLR survey and process studies (See Fig. 6.1, Table 6.1). The historical CCAMLR survey contained 108 stations of which 61 were completed. Transects were designed to follow previous surveys when possible or modified, for logistical reasons, to run across the shelf slope transition. An additional 27 quantitative tows were conducted in accordance with the goals of various process studies. Over 94 target trawls were conducted for the collection of live specimens for experiments.

The area south of Joinville Island and through the Antarctic Sound was purported to be a potential spawning ground for Antarctic krill (Marr 1962) but the area has rarely been surveyed. In addition, a recent study found that the Danger Islands' penguin colonies contain 55 % of all Adelie penguins in the region suggesting a large food source nearby. To investigate the area as a possible spawning ground for Antarctic krill, an exploratory survey was conducted in the region consisting of transects and stations that continued the layout of the northern CCAMLR stations. Several times during the survey planned transects had to be modified due to the presences of several large icebergs.

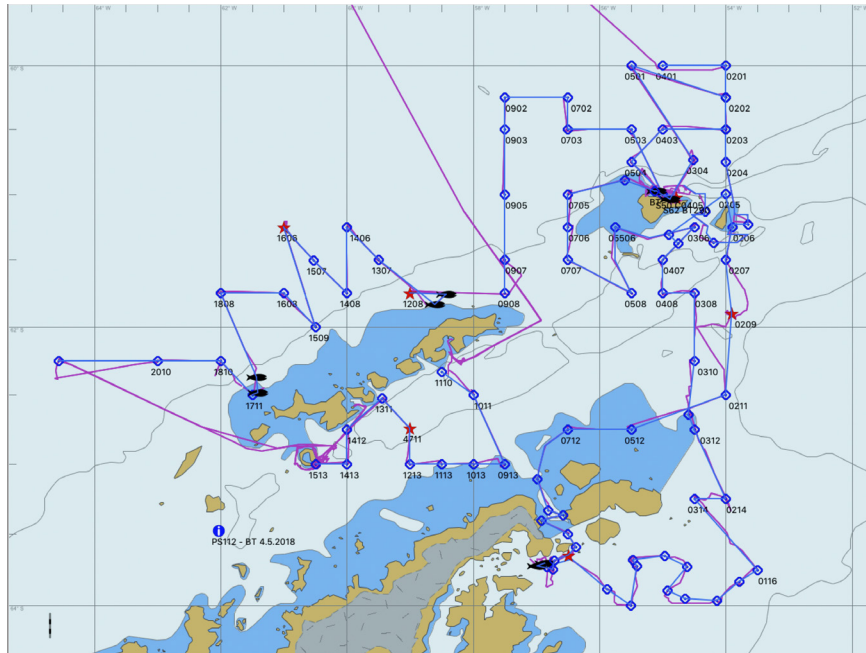


Fig. 6.1: CCAMLR survey transects and stations (blue squares). CCAMLR stations are numbered according to the schema from the USAMLR program. Stars represent „super stations“ where additional instruments were deployed for process studies. The transects and stations south of Joinville and in the Antarctic sound were exploratory CCAMLR survey stations and most do not have historical antecedents.

In order to properly compare data between areas during a single survey, and between years and areas from multiple surveys, it was necessary to adhere to the same sampling methodology throughout the cruise. Therefore, a single sampling protocol was established at the start of the CCAMLR survey for all net tows where the aim was to quantify the catch. A 1.8 m² IKMT net with a 505 µm mesh. The IKMT is one of the standard nets (along with the RMT 8 +1 net) used in past surveys in the area and it has the ability to collect both salps and krill in good condition. The net was towed obliquely to 170 m, or 20 m from the bottom, at a speed of 2 kts through the water. The net was fitted with a real time depth sensor to monitor fishing depth and a General Oceanics flowmeter to measure the volume of water filtered. The average volume of water filtered was 3,240 m³.

Samples were processed immediately following the tow. Euphausiids, salps and fish were enumerated to species. If the tow was larger than 2 L then random subsamples were taken until at least 200 of the target species (euphausiids and salps) were obtained. Sorted species and remaining zooplankton were preserved separately in 4 % buffered formalin or ethanol. Demographic data (length, sex and maturity) was collected on euphausiids and salps either before preservation or at least 2 days later. Due to logistical restraints, not all samples were

completed during the cruise. Remaining samples will be processed at the AWI. Length was measured from the tip of the rostrum to the tip of the uropod according to Mauchline (1980) and maturity stages were classified according to Makarov and Denys (1981).

The biomass estimate for Antarctic krill will be done using the SIMRAD EK60. Calibration of the 4 frequency EK 60 (38, 70, 120 and 200 KHz) occurred in Admiralty Bay and at Half Moon Island at the start of the cruise. A total of 2,077 nm of acoustic data was recorded over the course of the cruise. This includes data collected during CCAMLR transects, process studies, and small-scale surveys. The transect data will be separated into data clusters for biomass estimation post cruise.

The standard net used in past surveys by the USAMLR program is the IKMT. However, the RMT 8 +1 is often the standard net used in by other CCAMLR members. This net is fitted with an 8 m² net with a 2 cm mesh under a 1 m² net with a 200 µm mesh and is towed obliquely to slightly deeper depth (200 m). The different nets and sampling methodologies have different size and abundance-based selectivity for euphausiids and salps. Therefore, a methodological comparison was made between the 2 nets during the cruise by towing one net, immediately followed by the other, along the same track line alternating between the RMT and IKMT being towed first. Both nets were towed according to standard practice for that net. A total of 7 comparison tows were made. Samples were processed as above. The number of individuals per m³ and the length frequencies will be used to compare how the nets differ in their catch.

Preliminary results

All euphausiids, salps and fish were enumerated to species for every quantitative tow. The data will undergo final quality control checks at the AWI. Abundances and length frequencies for all enumerated species will be adjusted for the volume of water filtered. Demographic data for *Salpa thompsoni* was collected by Evgeny Pakhomov and Larisa Pakhomova at each station and will be incorporated into the KRILLBIS database.

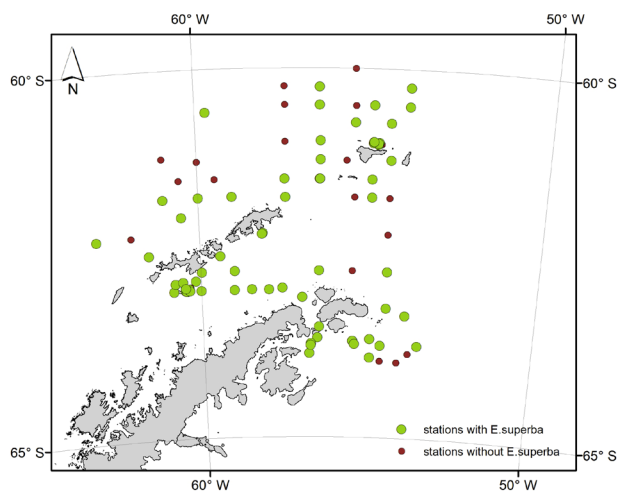


Fig. 6.2: Preliminary presence/absence data for *Euphausia superba* for all quantitative tows (N=88)

Although abundance and length frequency data are still undergoing processing some conclusions can be drawn from presence/absence data. *E. superba* showed a wide distribution throughout the survey area and was found in all areas though notably more in the inshore stations (see Fig. 6.2). *Salpa thompsoni* were also widespread from the north side of the Bransfield Strait to the northern stations and co-occurred with *E. superba* (see Fig. 6.3). However, it was not found in the colder water southerly stations. Small euphausiids occurred though out the survey area according to each species known habitat preferences. *E. crystallophias* was found in neritic stations in the Bransfield Strait and Weddell Sea but was absent in pelagic ACC influenced stations (see Fig. 6.4). Contrary to *E. crystallophias*, *E.*

frigida was found in the pelagic ACC influenced stations. *Thysanoessa macrura*, a ubiquitous Southern Ocean species, was found in all areas.

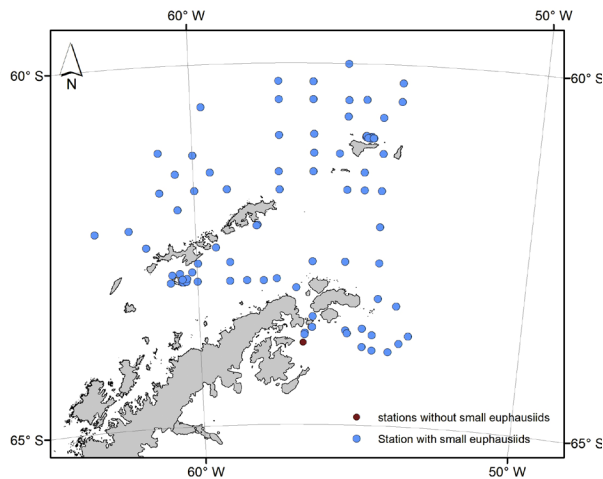
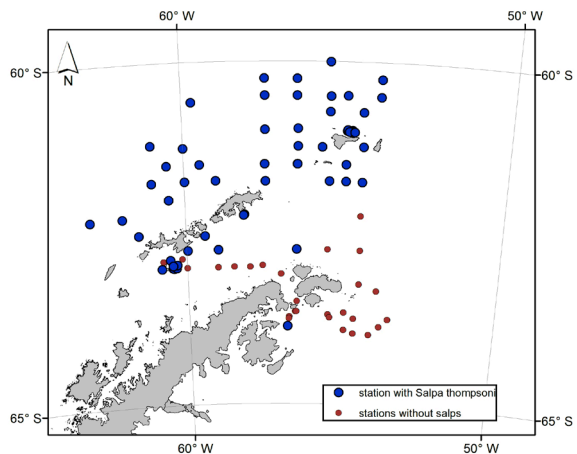


Fig. 6.3: Preliminary presence/absence data for small euphausiids (*E. frigida*, *E. crystallorophias*, *T. macrura*) for all quantitative tows ($N=88$)

Fig. 6.4: Preliminary presence/absence data for *Salpa thompsoni* for all quantitative tows ($N=88$)



Data management

Samples from the survey were stored in 4 % buffered formalin or ethanol and will be stored at the AWI in Bremerhaven. Data is stored in a Microsoft Access database for final quality control checks and processing. A copy of the survey data will be provided to CCAMLR in Hobart, Tasmania.

Tab. 5.1: Summary list of all quantitative tows including CCAMLR and process study tows

STATION	GEAR	START LAT	START LONG	FILTERED VOLUME [m ³]
PS112_59-2	IKMT	-60.2503	-53.9994	3978.278
PS112_58-2	IKMT	-60.5094	-54.0072	3979.222
PS112_77-3	IKMT	-63.3403	-53.9191	3189.974
PS112_61-2	IKMT	-60.7400	-54.5081	3987.586
PS112_70-2	IKMT	-61.2400	-54.4861	4030.148
PS112_73-2	IKMT	-61.7555	-54.4907	3881.687
PS112_74-2	IKMT	-62.2544	-54.5086	2415.971
PS112_76-4	IKMT	-62.7554	-54.4904	2143.332
PS112_57-2	IKMT	-60.4982	-54.9927	4323.628
PS112_50-2	IKMT	-61.0120	-54.9951	3435.429

STATION	GEAR	START LAT	START LONG	FILTERED VOLUME [m ³]
PS112_72-2	IKMT	-61.7499	-54.9962	3049.743
PS112_60-5	IKMT	-60.0036	-55.5322	3500.722
PS112_49-2	IKMT	-60.5080	-55.4996	3850.660
PS112_56-2	IKMT	-60.7345	-55.5114	3724.661
PS112_104-2	IKMT	-62.7466	-55.5196	2337.929
PS112_47-3	IKMT	-60.2539	-56.5167	3680.413
PS112_103-2	IKMT	-62.7467	-56.5028	3706.584
PS112_48-2	IKMT	-60.4995	-56.5132	3180.936
PS112_65-2	IKMT	-60.9829	-56.4859	4043.503
PS112_66-2	IKMT	-61.2416	-56.4780	4175.640
PS112_67-2	IKMT	-61.5011	-56.5017	4048.629
PS112_67-3	RMT	-61.5014	-56.4933	26745.756
PS112_46-2	IKMT	-60.2478	-57.5023	3098.510
PS112_44-4	IKMT	-60.9979	-57.4916	4382.041
PS112_43-2	IKMT	-61.5018	-57.5046	3333.780
PS112_42-2	IKMT	-61.7514	-57.4892	3405.549
PS112_16-2	IKMT	-63.0022	-59.0098	4430.336
PS112_38-2	IKMT	-61.4980	-59.5064	2421.636
PS112_36-2	IKMT	-61.7448	-59.9871	4765.096
PS112_20-7	IKMT	-62.9992	-60.0051	2667.631
PS112_35-2	IKMT	-61.5034	-60.5273	2845.635
PS112_33-2	IKMT	-61.9989	-60.5013	3594.210
PS112_34-10	IKMT	-61.1998	-60.9854	3681.087
PS112_32-2	IKMT	-61.7527	-61.0083	3303.157
PS112_29-2	IKMT	-62.5002	-61.5031	42495.33
PS112_28-2	IKMT	-62.2498	-61.9874	3416.745
PS112_23-1	IKMT	-60.5870	-59.6978	3091.63
PS112_37-2	IKMT	-61.2532	-59.9946	2460.623
PS112_13-3	IKMT	-62.9800	-57.5857	2087.753
PS112_14-3	IKMT	-63.0021	-57.9903	2758.016
PS112_18-2	IKMT	-62.5370	-59.4049	3633.399
PS112_21-2	IKMT	-62.9984	-60.4209	3290.207
PS112_25-1	IKMT	-63.0006	-60.4147	3619.369
PS112_25-28	IKMT	-62.9968	-60.4714	
PS112_25-31	IKMT	-63.0032	-60.8184	
PS112_25-33	IKMT	-62.8965	-60.7654	1077.265
PS112_25-35	IKMT	-62.8790	-60.5350	1380.391
PS112_25-37	IKMT	-62.9990	-60.4464	4821.621
PS112_25-40	IKMT	-62.9952	-60.3449	2789.988
PS112_25-47	IKMT	-62.9510	-60.3216	1951.433
PS112_25-49	IKMT	-62.9611	-60.4594	4443.017
PS112_25-60	IKMT	-62.8670	-60.1573	3224.712
PS112_27-2	IKMT	-62.2608	-63.0021	3600.550

STATION	GEAR	START LAT	START LONG	FILTERED VOLUME [m ³]
PS112_41-6	IKMT	-61.7368	-59.0241	3475.361
PS112_45-3	IKMT	-60.4998	-57.4885	3079.826
PS112_55-2	IKMT	-61.0298	-54.7657	3576.470
PS112_55-4	RMT	-61.0289	-54.7715	24199.698
PS112_55-12	RMT	-61.0089	-54.8407	24869.159
PS112_55-13	IKMT	-61.0058	-54.8333	3381.266
PS112_55-16	IKMT	-61.0317	-54.8517	3623.012
PS112_55-17	RMT	-61.0177	-54.8512	22276.234
PS112_55-19	RMT	-60.9986	-54.9871	17924.953
PS112_55-20	IKMT	-60.9971	-54.9811	2987.688
PS112_55-26	IKMT	-61.0253	-54.9316	6357.149
PS112_69-2	IKMT	-61.2500	-55.7421	2505.883
PS112_79-2	IKMT	-63.7468	-53.5035	3697.073
PS112_80-1	IKMT	-63.8567	-53.7866	3761.691
PS112_81-1	IKMT	-63.9775	-54.1177	3798.452
PS112_82-1	IKMT	-63.9636	-54.6333	3375.465
PS112_83-1	IKMT	-63.9174	-54.9423	3988.463
PS112_84-1	IKMT	-63.7511	-54.6365	4068.527
PS112_85-1	IKMT	-63.6651	-54.9540	3227.005
PS112_86-3	RMT	-63.6965	-55.4716	23431.99
PS112_86-1	IKMT	-63.6964	-55.4753	3490.065
PS112_87-1	IKMT	-63.7361	-55.4206	3914.738
PS112_93-1	IKMT	-63.6530	-56.5351	1686.552
PS112_94-1	IKMT	-63.7327	-56.7312	2356.748
PS112_95-1	IKMT	-63.8674	-56.7803	1898.080
PS112_96-1	IKMT	-63.7558	-56.7434	2251.794
PS112_98-9	IKMT	-63.6532	-56.5071	3221.136
PS112_99-2	IKMT	-63.5066	-56.4919	3037.601
PS112_102-2	IKMT	-63.1065	-56.9954	3536.404
PS112_105-3	IKMT	-62.5017	-53.9928	2492.258
PS112_106-17	IKMT	-61.7648	-53.6795	3767.088
PS112_106-6	IKMT	-61.8890	-53.9205	4307.845

References

- Makarov RR, Denys CJ (1981) Stages of sexual maturity of *Euphausia superba* Dana. BIOMASS Handbook, 11, 1-13.
- Marr JWS (1962) The natural history and geography of the Antarctic krill (*Euphausia superba* Dana). Discovery Reports, 32, 33-464.
- Mauchline J (1980) Measurement of body length of *Euphausia superba* Dana. BIOMASS Handbook 4.

7. THE PERFORMANCE OF KRILL VS. SALPS TO WITHSTAND IN A WARMING SOUTHERN OCEAN (PEKRIS)

Wiebke Wessels¹, Lutz Auerswald², Evgeny Pakhomov³, Larysa Pakhomova³, Bettina Meyer^{1,4}
K. Michael¹ (not on board)

¹ICBM, Uni Oldenburg
²DAFF
³UBC, Vancouver
⁴AWI

Grant-No. AWI_PS112_00

Objectives

The Western Antarctic Peninsula (WAP) ecosystem is facing severe alterations due to climate change, including rising temperatures, a decline in sea-ice and shifts in phytoplankton composition (Montes-Hugo et al. 2009). As a highly adapted cold-water species, the Antarctic krill is believed to be sensitive to rapid changes of its habitat (Flores et al. 2012). Long-running time series already provide some indication of a biological response to recent warming trends and its effects, such as a decline in krill abundance and an increase in salp numbers, which in turn, affect food quality and quantity of dependent predator species (Atkinson et al., 2004, Reid et al. 2005, Trivelpiece et al. 2011). PEKRIS examines the differences in genetic and physiological traits of krill versus salps to study their distinct potential to adapt to warming temperatures. Results will feed into a newly developed individual-based model for krill to predict its response to different climate change scenarios and provide new insights into potential consequences for krill-dependent ecosystem components. In addition, PEKRIS will provide further insights into the possibility of a proposed ecosystem shift from krill to salp-centered, based on the potentially higher capacity of salps to deal with increasing temperatures and changes in phytoplankton community.

Aims

- Investigate the physiological capacities of krill versus salps to cope with increasing temperatures
- Collect krill and salp samples for molecular analysis of temperature adaptation at the genetic level

Work at sea

At sea salps were collected at three locations (Deception Island (Station PS112_25), Elephant Island (Stations PS112_50/51, PS112_111) by vertical as well as oblique IKMT hauls. The EK60 signal was used to. Salps in good conditions (still pumping and swimming around) were immediately transferred into circular jellyfish tanks to recover from sampling stress. The aquaria were set up in a flow through system allowing constant water exchange with a flow rate of approximately 20L/h. Surrounding ocean water was supplied through the ship's pump and passed through a 5µm filter before being pumped into the Kreisel tanks. Due to the process of the water being pumped through the ship before arriving at the laboratory container, the water temperature increased by about 1°C compared to the local water temperature.

7. The Performance of Krill vs. Salps to Withstand in a Warming Southern Ocean (PEKRIS)

After recovery from sampling stress, animals were transferred into experimental tanks or respiration experiments. A description of the different experiments and number of replicates is given in Table 7.1.

Tab. 7.1: Description of the experimental work conducted on board

Experiment	Description
Temperature stress	Exposure of salps to 5°C (+3°C from control) for 48h. Temperature was increased by 1°C/12h. Sampling after 24h at 5°C and 48h at 5°C. N=8-10 per time point for control and treatment. Experiment was conducted 3 times with individual aggregate specimen.
Baseline respiration	Baseline respiration at control temperature (2 – 2.5°C) was determine for 24h. N=12 individual aggregate specimen, N=16 solitary specimen.
Respiration under acute temperature stress	Oxygen consumption was measured during acute temperature stress. Water temperature was increased by 2.5°C over 1.5h and determination of oxygen consumption for 1.5 – 2h at each of the following temperature steps (5°C, 7.5°C, 10°C, 12.5°C), N=6 individual aggregate specimen, N=10 solitary specimen
Respiration under prolonged temperature stress	Baseline respiration was recorded for 24h after animals were acclimated to a water temperature of 5°C for 48h. After 24h temperature in the water bath was increased by 2.5°C over 1.5h and oxygen consumption measured for 2h at each temperature step (7.5°C, 10°C, 12.5°C), N=10 individual aggregate specimen
Chain growth rates, released in aquaria	Daily size measurement of a few specimen from a newly released chain to determine growth rates, N=8
Chain growth rates, caught in the field	Size determination upon collection and after culturing the remaining specimen of the chain for 5 days in jellyfish tank, N=17.
Chain growth experiments, field observations	A multi-day station was conducted near the Deception Island between March 27 th and April 1 st and size structure was analysed for each net.
Respiration rates of chains	Determination of oxygen consumption of newly released chains, N=10, as well as small (OAL) collected from the field.
Salinity stress	Exposure of salps to low salinity conditions, 32.5 PSU (2 PSU below control), for 24h and 48h, N=10 per time point, experiment conducted only with individual aggregate specimen.
Respiration under salinity stress	Step-wise transfer of salps to 32 PSU, determination of oxygen consumption under low salinity stress for 24h, N=10 individual aggregate specimen.

Preliminary results

*Oxygen consumption rates in *Salpa thompsoni* under control conditions and acute temperature stress*

To determine oxygen consumption rates as a measure for metabolic activity, salps were transferred into respirometry chambers (2L Schott bottles filled with 0.2 μm filtered seawater). Oxygen concentrations in mg/L were measured using PreSens technology; a sensor spot on the inside of the bottle and a fiber optic cable on the outside. The measurements were controlled through the PreSens Measurement Studio 2 software interface. Baseline measurements of oxygen consumption were assessed over 24h in a water bath at control temperature (2°C). Preliminary analyses of the different respiration measurements show that overall, solitary salps have a significantly lower oxygen consumption ($p < 0.01$) than individual aggregate specimen (Fig. 7.1).

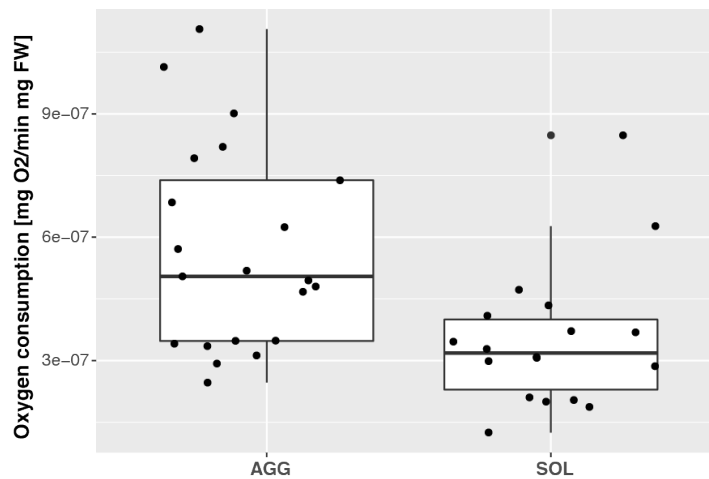


Fig. 7.1: Baseline oxygen consumption rates in mg O₂ per min and mg FW (calculated based on salp size) of individual aggregate specimen (AGG) and solitary specimen (SOL) at 2°C. Oxygen consumption was recorded over 24h for each experiment.

To assess the effect of acute temperature stress on oxygen consumption, the temperature in the water bath was increased by 2.5°C over 1.5h. Once a temperature step has been met, oxygen consumption as measured for 1.5-2h. For individual aggregate specimen, oxygen consumption was stable until 7.5°C and then doubled and tripled at 10°C and 12.5°C, respectively (Fig. 7.2)

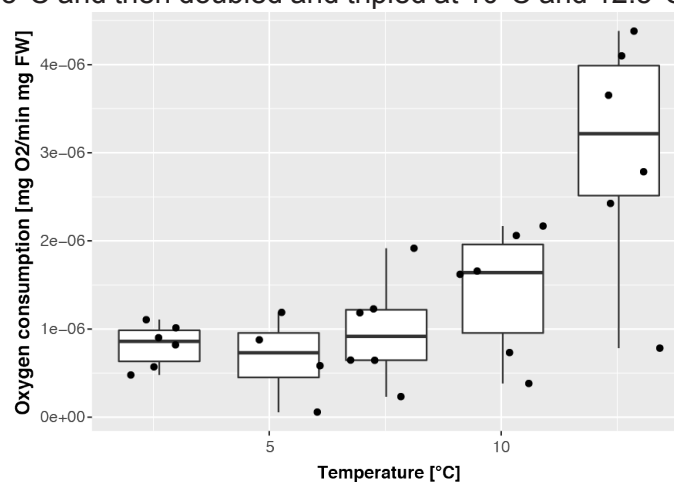


Fig. 7.2: Oxygen consumption rates in mg O₂ per min and mg FW (calculated based on salp size) under acute temperatures stress in individual aggregate specimens ranging from 2.5°C (control) to 12.5°C. Water temperature was increased by 2.5°C over a 1.5h increment. Oxygen consumption was measured at each temperature step for 2h.

Temperature stress experiment

For the first temperature stress experiment, 37 individual aggregate specimens were randomly placed in either of the treatment or control Kreisel. The temperature was slowly increased by 1°C per day from 2°C to 5°C. Reaching 4°C, we noticed the formation of small bubbles outside the tunic, inhibiting the salps to swim but kept them trapped the surface. The bubbles probably formed due to degassing of oxygen from the saturated cold water and increased when the water temperature reached 5°C (Fig. 7.3). After 24h at 5°C the first samples were taken from both treatment and control tanks, measured and staged, snap frozen in liquid nitrogen and preserved at -80°C until further analyses at AWI. Due to the fact that the salps were trapped at the water surface, which limited their feeding abilities (reduced formation of fecal pellets compared to control conditions) we this we stopped this first experiment after 72h°C. All remaining specimen from the temperature treatment were snap frozen in liquid nitrogen. Five specimen of each control tank were sampled.

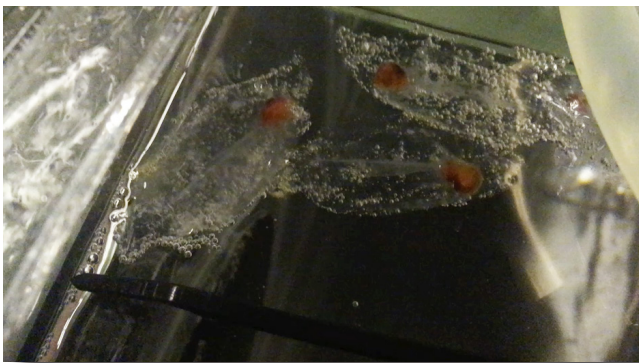


Fig. 7.3: Salpa thompsoni with bubbles trapped on/in the tunic and hence floating at the water surface

The remaining specimen of the control conditions were distributed between treatment and control tanks prior to starting the next experiment, resulting in 11 specimens per tank. For the second temperature experiment, the temperature was increased rapidly by 1°C/12h from 0.5°C to 3.5°C with lower rates of bubble formation. After 48h all salps were sampled from the tanks, size measured and staged prior to snap freezing in liquid nitrogen.

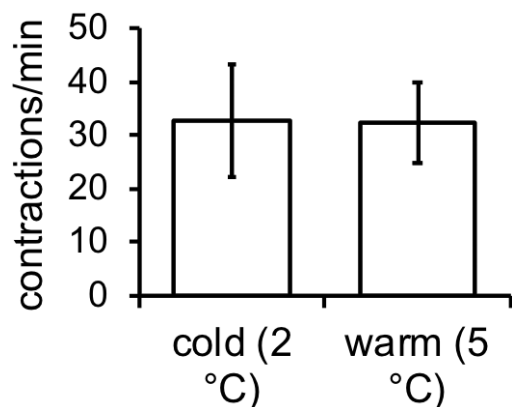


Fig 7.4: Pump rates as contractions per min of individual aggregate specimen kept at 2°C and 5°C for 48h prior to assessment

After returning to Elephant Island on April 23 freshly caught animals were transferred to Kreisel for acclimation and recovering from sampling stress. After 24h 15 animals were randomly placed in control and treatment tanks and allowed to recover from repeated handling stress for 12h. Salps in treatment tanks were subjected to a drastic temperature increase of 1°C/12h from 2°C to 5°C, which repeated bubble formation on/in the tunic. In order to assess the

impact of temperature on their swimming and/or feeding activity, we calculated pumping rates by filming salps under treatment and control conditions for a set period (30sec to 1min) and then counting the number of contractions. The pumping rates were calculated as number of contractions per minute. Salps under control conditions showed similar pump rates as salps acclimated to 5°C for 48h, 32.5 and 32.3 contractions per min, respectively (Fig. 7.4).

To determine whether the bubble formation was due to degassing of oxygen or bacterial respiration triggered by increased water temperatures, 3 specimens of each control and each treatment tank were fixed in 4% formaldehyde solution after 48h at 5°C for microscopy and potential DAPI staining at AWI. In addition, 5 specimens of each of the treatment tanks were used to establish baseline respiration rates at higher temperatures. To reduce any bias linked to the bubbles outside the salps, the bubbles were gently rubbed off prior to transfer into the Schott bottles used for respiration experiments. The remaining animals as well as 5 specimens of each of the control tank were measured and snap frozen in liquid nitrogen.

Oxygen consumption rates of specimens acclimated to 5°C for 48h did not differ from oxygen consumption rates of specimen at 2°C (Fig. 7.5).

Salpa thompsoni in aquaria and in-situ growth assessment

The IKMT was successful in catching salps, both intact aggregate chains and solitary specimen, in good conditions and the kreisel tanks allowed us to keep the animals healthy for up to 4 weeks. During the culturing process, several solitary specimens, stage 4B and 5B, released aggregate chains, which gave us the opportunity to study *in-aquaria* growth rates and link those to *in-situ* growth rates. In order to keep track of each chain individually, chains were removed from big aquaria and transferred to small 3L tanks for the study. To determine the daily growth rates, a few specimens were clipped off of each chain, measured under the microscope and frozen for later analyses at AWI.

The specimen size upon release varied between 4-6 mm and was potentially dependant on the fact that some chains might have been released prematurely due to sampling stress. However, chains not released prematurely were observed to start swimming and feeding within the first day. Over the first few days, the specimen within in the chains were increasing in size. Nevertheless, after about 6 days, the growth stopped and chains started to die (Fig. 7.6). Over the first days, chains grew on average 0.2 mm.day⁻¹, ranging from 0.13-0.35 mm.day⁻¹.

A multi-day station was conducted near the Deception Island between March 27 and April 1. Salps were collected using the IKMT trawl in the top 170 m layer. Size structure was dominated by salps 7-10 mm aggregates, although a second cohort (mode 14-16 mm) was clearly notable in the nighttime catches (Fig. 7.7). Continuous chain release was a characteristic of the area and preliminary cohort analysis suggested a rapid growth of recently released aggregates from ≈8 mm to ≈10 mm (Fig. 1). This would be equal to the daily growth of 0.4 mm.day⁻¹ for 8 mm aggregates.

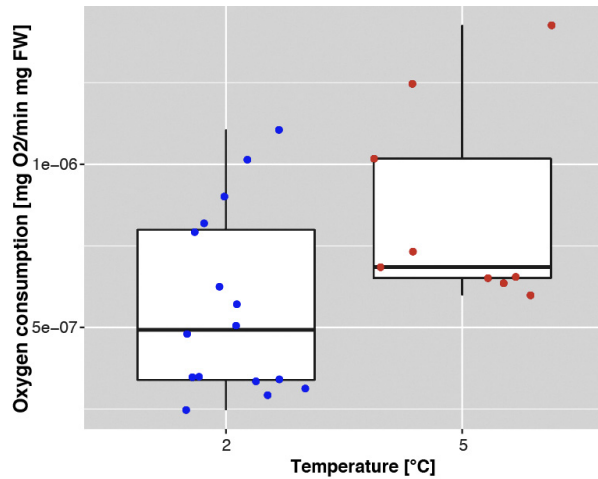


Fig. 7.5: Baseline oxygen consumption rates in mg O₂ per min and mg FW (calculated based on salp size) of individual aggregate specimen at 2°C (control) and 5°C (temperature treatment)

7. The Performance of Krill vs. Salps to Withstand in a Warming Southern Ocean (PEKRIS)

These very preliminary calculations for *in aquaria* and *in-situ* growth rates suggest a daily growth rate of about 5 % of body length per day. These estimates are on the higher end of growth estimates for *Salpa thompsoni* published by Loeb and Santora (2012) and well within the range rates reported by Pakhomov and Hunt (2017).

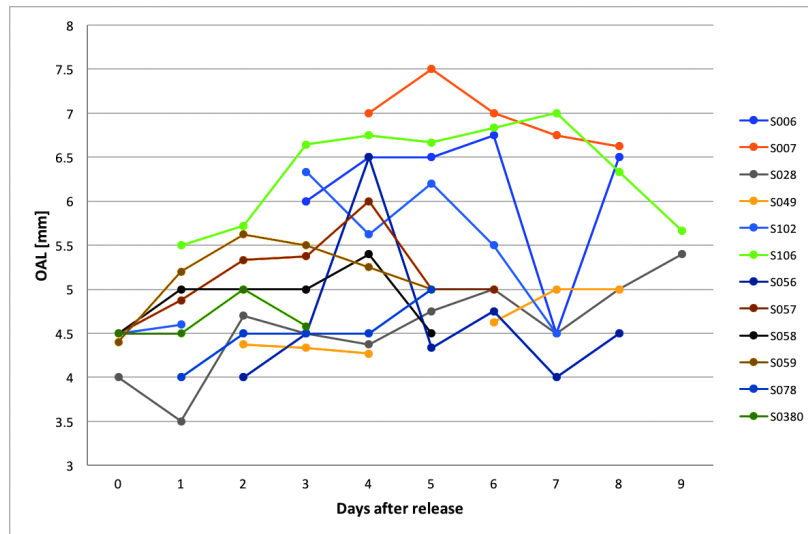


Fig 7.6: Daily oral-atrial length (OAL) measurements of freshly released aggregate chains in Kreisel tanks

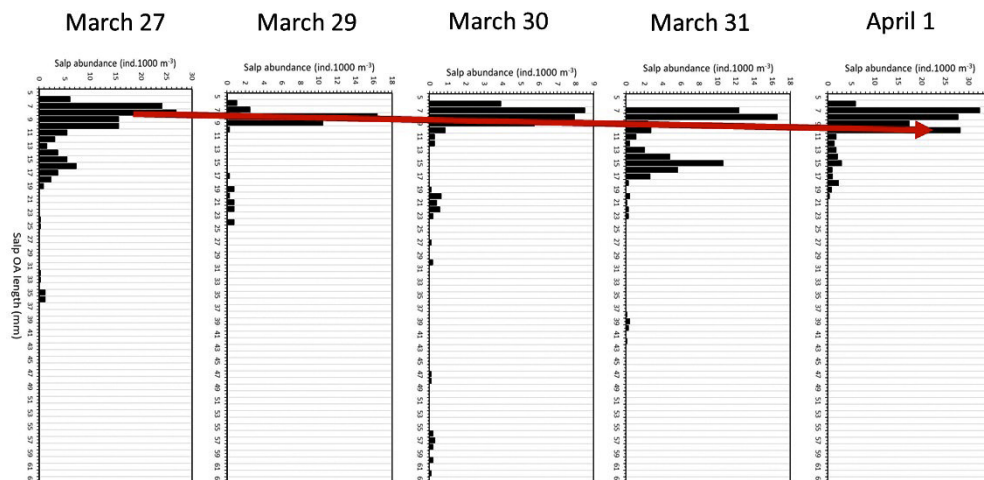


Fig. 7.7: Length frequency distribution of *Salpa thompsoni* near the Deception Island between March 27 and April 1, 2018. The red arrow shows proposed growth of the freshly released aggregate cohort.

Data management

Results from the PS112 (ANTXXXIII/3) expedition will be published in peer-reviewed journals by the participating scientists in co-operation with other colleagues. Citations will be available through the German National Library of Science and Technology portal. Sequence data obtained throughout the project will be submitted to the GenBank database. Raw DNA and RNA sequence data will be deposited in the National Center for Biotechnology Information (NCBI) Sequence Read Archive (SRA). Transcriptomic data referred to in scientific publications will be made available as supplementary electronic file to the respective publications.

References

- Atkinson A, Siegel V, Pakhomov E, Rothery P (2004) Long-term decline in krill stocks and increase in salps within the Southern Ocean. *Nature*, 432, 100-103.
- Flores H, Atkinson A, Kawaguchi S, Krafft BA, Milinevsky G, Nicol S, Reiss C, Tarling GA, Werner R, Bravo Rebolledo E, Cirelli V, Cuzin-Roudy J, Fielding S, van Franeker JA, Groeneveld J, Haraldsson M, Lombana A, Marschoff E, Meyer B, Pakhomov EA, Van de Putte AP, Rombolá E, Schmidt K, Siegel V, Teschke M, Tonkes H, Toullec JY, Trathan PN, Tremblay N, Werner T (2012) Impact of climate change on Antarctic krill. *Marine Ecology Progress Series*, 458, 1–19.
- Loeb VJ, Santora JA (2012) Population dynamics of *Salpa thompsoni* near the Antarctic Peninsula: growth rates and interannual variations in reproductive activity (1993-2009). *Progress in Oceanography*, 96, 93-107.
- Montes-Hugo M, Doney SC, Ducklow HW, Fraser W, Martinson D, Stammerjohn SE, Schofield O (2009) Recent changes in phytoplankton communities associated with rapid regional climate change along the western Antarctic Peninsula. *Science*, 323, 1470–1473.
- Pakhomov EA, Hunt BPV (2017) Trans-Atlantic variability in ecology of the pelagic tunicate *Salpa thompsoni* near the Antarctic Polar Front. *Deep-Sea Research II*, 138, 126-140.
- Reid K, Croxall JP, Briggs DR, Murphy EJ (2005) Antarctic ecosystem monitoring: quantifying the response of ecosystem indicators to variability in Antarctic krill. *ICES Journal of Marine Science. Journal du Conseil*, 62, 366–373.
- Trivelpiece WZ, Hinke JT, Miller AK, Reiss CS, Trivelpiece SG, Watters GM (2011) Variability in krill biomass links harvesting and climate warming to penguin population changes in Antarctica. *Proceedings of the National Academy of Sciences of the United States of America*, 108, 7625–7628.

8. MICROZOOPLANKTON

Marina Monti-Birkenmeier¹, Tommaso Diociaiuti¹,
not on board: A. Sabbatini², C. Morigi³, A.
Pallavicini⁴, A. Bartolini⁵

¹OGS-Trieste
²Uni Pol. Marche
³Uni Pisa
⁴Uni Trieste
⁵MNHN-Paris

Grant-No. AWI_PS112_00

Objectives

Microzooplankton organisms are considered one of the first links of the trophic system in consumer terms and play a key role in the transfer of nutrients and energy through planktonic food webs (Calbet & Saiz 2005). In Antarctica, they are an important food source for krill and salps. A modification in their composition and quantity might trigger a cascade of short- and long-term changes in ecosystem structure and function, affecting both biodiversity and biogeochemical cycles in the pelagic system. Integrating the data we already have from the sea-ice (previous winter cruise) with the data obtained in the last cruise we will assess the importance of microzooplankton as food source for krill and salps in two different seasons.

During the cruise we collected samples for microzooplankton qualitative analyses. Particular attention was paid to ciliates and foraminifers, ubiquitous components of the microzooplankton community in all the marine systems.

Between ciliates, tintinnids form a highly diverse group, currently accommodating 15 families, 69 genera, and over 1,500 morphospecies (Lynn 2008). Historically, tintinnids were considered to be a well-defined monophyletic assemblage and the taxonomy and systematics of this group were based on the lorica identification. Due to the frequent intraspecific variability and interspecific similarity, since 2002, tintinnid ciliates have been investigated using molecular approaches based on small subunit ribosomal DNA (SSU rDNA). Recently, the internal transcribed spacer (ITS) regions of the rDNA, which are less conserved than the SSU rDNA, and the use of large subunit ribosomal DNA (LSU rDNA) have been used to study tintinnid phylogeny (Xu et al. 2013).

Foraminifers were one of the most abundant groups present in the sea-ice during the previous winter cruise. Foraminifera is the only group among microzooplankton capable to secrete a calcareous test and they can be used as proxy for both past changes and surface ocean variations of sea-water conditions. In particular the study of foraminiferal biomass will be associated to the analyses of shell isotopic ($d^{18}O$, $d^{44}Ca$) and trace elements (Mg/Ca) to understand if the various environmental factors (namely $[CO_3^{2-}]$, temperature) passing from seasonal variations and ice to ice-free water, could affect foraminiferal biomineralization (and consequently biomass) (Kunioka et al. 2006).

In Antarctica, microplankton that is not grazed in the ice, or at the ice water interface, is released into the water column, where it can be exploited by pelagic grazers or potentially seed the following microplankton growth. Although all the material incorporated in the ice matrix will ultimately be released into the water column during ice melt as an important part of Antarctic

biomass, little is known about its fate. Samples from sediment traps will be analysed to assess the possible fate of sympagic organisms.

Work at sea

During the cruise PS112 (ANT-XXIX/10) samples from Rosette water sampler and from Net were collected in 19 stations (Table 7.1).

Tab. 8.1: Stations date, coordinates and activities

Station	Date	Time UTC	Lat	Lon	Rosette sampler	Bongo net	Phytoplankton net
PS112_17-2	26/3/2018	3:56	62° 45.599' S	059° 00.431' W	X		
PS112_20-2	26/3/2018	19:41	63° 00.008' S	060° 00.008' W	X	X	
PS112_24-1	27/3/2018	21:47	62° 35.006' S	059° 52.738' W		X	X
PS112_25-51	1/4/2018	11:49	62° 53.016' S	060° 14.037' W	X	X	X
PS112_34-1	4/4/2018	13:57	61° 15.333' S	060° 59.452' W	X	X	X
PS112_41-1	5/4/2018	20:47	61° 44.962' S	059° 00.008' W	X	X	X
PS112_55-6	8/4/2018	19:15	61° 01.345' S	054° 47.170' W	X	X	X
PS112_81-2	14/4/2018	16:59	63° 57.798' S	054° 08.383' W	X		
PS112_87-2	15/4/2018	11:20	63° 43.383' S	055° 24.619' W	X		
PS112_90-2	16/4/2018	12:52	63° 43.712' S	056° 50.379' W	X		
PS112_98-4	17/4/2018	18:09	63° 38.776' S	056° 29.579' W	X	X	X
PS112_101-1	18/4/2018	22:26	63° 19.779' S	056° 48.487' W	X	X	
PS112_104-1	19/4/2018	11:07	62° 44.931' S	055° 30.157' W	X		
PS112_106-5	20/4/2018	15:21	61° 53.935' S	053° 54.598' W	X	X	
PS112_118-3	25/4/2018	21:30	60° 58.578' S	054° 58.920' W	X		
PS112_119-3	26/4/2018	16:45	60° 59,998' S	054 ° 35,694' W	X		
PS112_120-4	27/4/2018	15:30	60° 57,675' S	054 ° 44,713' W	X	X	
PS112_121-2	28/4/2018	13:20	60° 58,103' S	054 ° 52,255' W	X		
PS112_122-2	29/4/2018	13:29	60° 58,965' S	054 ° 55,673' W	X		

Rosette water sampler

At each stations, 79 microzooplankton (MCZ) samples (Table 8.2) were collected at 5 depths (surface, DMC, 100, 200/300 and 500 m). 20 liters of seawater at every depth were immediately filtered on a 10 µm mesh to reduce them to a volume of 250 ml and preserved with 4 % formaldehyde solution buffered with CaCO₃. Samples will be analysed in a settling chamber, after sedimentation, using an inverted microscope. For each taxon, biomasses will be estimated by measuring the linear dimension of each organism with an eyepiece scale and equating shapes to standard geometric figures. Cell volumes will be converted to carbon values using appropriate formulae or conversion factors.

For an estimation of the dissolved inorganic carbon (DIC) present in the water column, 48 samples (Table 8.2) were collected in 40 ml glass vials, added with HgCl₂ and stored at 4°C. These data will be interpreted for the study of foraminifers test.

Bongo and phytoplankton nets

For tintinnids molecular and morphological analyses, 30 samples (Table 8.2) were collected using Bongo (100 µm) and phytoplankton (10 µm) nets.

Part of the sample was fixed in 80 % ethanol at 4°C and part in in 2 % Lugol solution until further processing for molecular analysis. The remainder of the sample was fixed in formaldehyde 4 % for subsequent morphological studies.

For foraminifers analyses, 47 samples were collected (Table 8.2) and filtered on board through a 40 µm mesh. Subsamples were stored at -20°C and part fixed in 4% formaldehyde solution buffered with CaCO₃.

Sediment trap samples were provided by the Carbon flux group (M. Iversen group). 26 samples (Table 8.2) were collected by using cylindrical 10 cm traps free drifting. The samples, preserved with formaldehyde, will be processed following the microzooplankton procedure.

In collaboration with the Microbial food web group (S. Moorthi group) we collected 168 microzooplankton samples (Table 8. 2) for the grazing experiments. At different time and experimental treatments, the samples were concentrated following the same procedure used for sea water microzooplankton samples.

The diving group (U. Freier group) provided two ice samples (Table 8.2). The ice was melted in a temperature constant room at 0°C in the dark by adding 0.2 µm filtered seawater in the proportion 1:3 to avoid osmotic stress. After 36 h, when the sea ice was melted, the volume was determined and 5 liters were concentrated following the same procedure used for sea water microzooplankton. The samples will be analysed at OGS.

Tab. 8.2.: Number of samples for the different parameters

	N° SAMPLES
MCZ DISTRIBUTION	79
TINTINNIDS	30
FORAMINIFERS	47
DIC	48
GRAZING EXPERIMENTS	168
SEDIMENT TRAPS	26
ICE	2

Preliminary results

Since microzooplankton analyses have to be done in a standardised way in the laboratory, no preliminary results are available.

The expected results will implement the knowledge of microzooplankton distribution and their trophic role in the polar food webs.

Tintinnids molecular and morphological analyses will clarify the synonymy and phylogeny of some Antarctic species. In particular is expected to compare the different morphotypes of the genus *Cymatocylis*. This genus is endemic to the Antarctic Ocean and is often the dominant genus present. Despite this, and the fact that this genus has been known since 1907, identification at the species level remains problematic.

Foraminifers data will assess the biological and chemical origin of proxy signals related to sea-ice (winter cruise) and ice free sea water (summer cruise).

The comparison between the microplankton assemblages from the sediment traps with the one found in the ice and in the ice-free seawater will let us to assess the possible fate of sympagic organisms.

All the samples will be back in the participating institutions and data will be obtained through laboratory analyses after the cruise.

Qualitative and quantitative analysis of microzooplankton in the seawater, sea ice and sediment traps will be conducted at OGS, Trieste. Dissolved inorganic carbon analyses will be carried out in the chemical laboratory of OGS, Trieste. Tintinnids morphological and molecular data will be conducted at OGS and at the Univ. of Trieste. The analyses on the calcitic test of the selected planktonic foraminifera, intratest oxygen isotope and Mg/Ca variations will be measured at the

Univ. of Pisa, Univ. of Pol. Marche and MNHN Paris. Microzooplankton samples of the grazing experiments will be analysed at the Univ. of Oldenburg, ICBM.

Data management

The results will be published in international peer-reviewed journals. All the data generated from these activities will be likely submitted to the NODC - National Oceanographic Data Center, following the data restriction of the Italian Antarctic Programme PNRA (*Programma Nazionale di Ricerca in Antartide*).

References

- Calbet A, Saiz E (2005) The ciliate–copepod link in marine ecosystems. *Aquatic Microbial Ecology*, 38, 57-167.
- Kunioka D, Shirai K, Takahata N, Sano Y, Toyofuku T, Ujiie Y (2006) Microdistribution of Mg/Ca, Sr/Ca, and Ba/Ca ratios in *Pulleniatina obliquiloculata* test by using a NanoSIMS : Implication for the vital effect mechanism. *Geochem. Geophys. Geosyst.*, 7 (12). Q12P20, doi:10.1029/2006GC001280.
- Lynn DH (2008) *The ciliated protozoa: characterization, classification and guide to the literature*, 3rd ed. Springer, Dordrecht.
- Xu D, Sun P, Warren A, Noh JH, Choi DL, Shin MK, Kim YO (2013) Phylogenetic investigations on ten genera of tintinnid ciliates (Ciliophora: Spirotrichea: Tintinnida), based on small subunit ribosomal RNA gene sequences. *Journal of Eukaryotic Microbiology* 2013, 60, 192–202.

9. CLIMATE SENSITIVITY IN VARIOUS FISHES FROM THE ANTARCTIC PENINSULA: MOLECULAR ECOLOGY AND CELLULAR MECHANISMS

Magnus Lucassen¹, Chiara Papetti², Nils Koschnick¹
not on board: Gisela Lannig-Bock¹, Felix Mark¹,
Christian Bock¹

¹AWI
²Uni Padova

Grant-No. AWI_PS112_00

Objectives

The ongoing release of the greenhouse gas CO₂ into the atmosphere is believed to cause both, global warming and ocean acidification. The changes largely differ between regions, and the Antarctic Peninsula is one area of the globe that is currently experiencing rapid warming. As solubility of CO₂ is enhanced in cold waters, the impact of climate change might be severed by the combination of both climate factors especially in the study area of our current expedition.

Temperature as a main abiotic factor comprises every aspect of the biochemistry and physiology of ectothermal organisms putatively culminating in shifting geographical distribution on a larger scale. Although limits may become manifested at the whole organism first, all levels of organization from the genetic basement to functional physiological levels are involved. For an understanding of climate-driven evolution and response to ongoing change the integration of molecules into functional units and networks up to the whole animal, must therefore be taken into account.

To continue our comprehensive physiological and molecular genetic studies of high and low Antarctic fish species and populations, live fish in the most pristine condition possible is indispensable for our physiological work. Especially the Antarctic eelpout (*Pachycara brachycephalum*) became an ideal model for our research resulting in a reasonable number of comparative studies during the past (*cf.* Windisch et al. 2014). Moreover, endemic Notothenioids were included more recently to expand our evidences to different fish groups. During PS112 we have caught fish from several fish orders and kept them alive to bring them to the home institute for physiological analyses and genetic profiling. There, we aim to (i) estimate acclimatory capacities/sensitivity towards combined treatments of warming, hypoxia and hypercapnia, (ii) determine the level of cold adaptation, and (iii) compare those laboratory-treated samples to *in-situ* samples from the field. The analyses comprise global (RNA-Seq) and targeted (qPCR) gene expression techniques considering the genetic background and population structure, assessment of cellular energy budgets and allocation, as well as metabolic profiling (by means of untargeted nuclear magnetic resonance spectroscopy, NMR).

The response of a species to changing environmental conditions largely depends on the genetic variation within populations. The pressure of these factors on natural populations at the edges of their distribution window may affect the population structure and variance. Using transcriptomic approaches, new candidate genes, which are under selective pressure and

are adaptive for cold adaptation, can be isolated. However, their selective nature can only be validated on the background of neutral genetic markers. Thus, population genetic structure and dynamic are being assessed alongside our functional genomic approaches in all species under study (Papetti et al. 2016a, 2012; Angostini et al. 2015).

At the cellular level temperature-dependent metabolic adjustments are key to maintain energetic homeostasis and thus functioning and survival of the animal at various temperatures. In the past, we examined the effect of acute warming on cellular energy metabolism in primary cell cultures of different Antarctic fish species (Mark et al. 2005). In line with the species' geographical distribution and environmental temperature exposure temperature-induced changes in cell metabolism in particular in cellular energy expenditure for protein synthesis differed between species thereby paralleling the degree of cold adaptation (Lannig et al. unpublished). According to the findings that thermal sensitivity of cell metabolism mirrors organism temperature tolerance another aim of the present project is to unravel the metabolic pathways and molecular mechanisms underlying cellular response to warming. Therefore, several fish species have been used to isolate cells for establishing permanent cell lines for later use at the home institute.

Work at sea

To investigate the sensitivity, resilience and capacity for acclima(tisa)tion of fish species from the coldest regions of our planet, the collection of good fish in the most pristine condition possible was one main target of our group.

- a) Using baited traps, we caught unharmed and quite unstressed specimens of the Antarctic eelpout. The baited traps were deployed for about 52 hours at Admiralty Bay, King-George-Island.
- b) For catching notothenioid species a commercially-sized 140' bottom trawl has been used alongside the cruise plot given by the CCAMLR project (see chapter 6, Fig. 6.1). As catching by net causes usually more physical stress to the animals trawling was limited to 15 minutes at ground and a fish lift was used. A fish lift is a device that is connected to the cod end of a typical trawl net and allows sorting fish from unwanted larger items (eg. sponges in the Antarctic case). It reduces the physical pressure on the catch by moving it out of the water flow thereby keeping the fish constantly in water during recovery of the net on the deck (Holst & McDonald 2000) (Fig. 9.1).
- c) Each haul from the bottom trawls was entirely analysed for basic ecological parameters (species composition, biomass, length and weight distribution, etc.). First, fish were sorted out from the epibenthic fauna. Fish of good quality were placed directly into the aquarium systems and kept alive. All other fish were sorted by species and processed. In case of large amounts of specimens subsampling of those species were performed. Ecological sampling of fish included the following parameters: Total and gutted weight, total and standard length, sex, gonad state and weight, liver weight. For population genetics fin-clips were taken and conserved in ethanol. Gonads were preserved in formol (10 % formaldehyde in seawater) for analyses of reproductive traits, and otoliths were taken for age determination. Furthermore, we collected samples of intestine and stomach (preserved in ethanol) for all *Trematomus* species, for the icefish *Chaenodraco wilsoni* and for *Notothenia rossii* in the framework of a collaboration with Patricia Holm (University of Basel, Switzerland) and Henrik Christiansen (KU Leuven, Belgium) to test for microplastic accumulation in their digestive apparatus and to characterize the microbiome population of notothenioids, respectively.
- d) The epibenthic by-catch of each haul was sorted entirely into operational taxonomic groups (OTU). In case of the last two hauls subsampling was performed. The weight and number

of specimens per OTU was determined, and all samples were photographed for later validation of the classification. Sponges were sampled in collaboration with Sven Rohde (ICBM, University of Oldenburg) and conserved for later analyses at the home institute. All cephalopods were collected and frozen. Further samples e.g. from certain crustaceans were conserved in ethanol for genetic analyses.

- e) For *in-situ* profiling of gene expression and physiological parameters undamaged fish have been sampled directly after short recovery in aquaria (transcriptomic sampling). This included –alongside with all parameters for ecological sampling (see above) the following: blood, blood serum, blood cells, liver, heart ventricle and atrium, spleen, gills, brain, kidney, head kidney, white muscle and red muscle taken from the pectoral fin. Tissue samples were excised, flash-frozen in liquid nitrogen (or, after its wastage, in an ethanol ice slurry of about -60°C) and stored at -80°C for transportation to Bremerhaven. These samples will serve as reference group for laboratory-treated fish and for the long-term molecular genetic and physiological sample archive of our working group started in 2003 including samples from the Eastern Weddell Sea and the Antarctic Peninsula. The analyses of samples collected over several years will allow the detection of spatio-temporal shifts in species composition, abundance and genetic variability in various areas of the Antarctic realm.
- f) After recovery, some fish were sampled for isolation of cell cultures. Cell cultures have been isolated from liver, spleen, kidney and head kidney from available species following standard protocols (Stapp et al. 2015), but with buffers and culture media adjusted to the specific osmolality of the species and temperature-corrected pH according to alpha-stat. For low-Antarctic species an osmolality of 410-430 mOsm/kg, for high Antarctic fish 520-540 mOsm/kg was used. The primary cultures were kept alive at 0°C . Culture media were exchanged regularly on demand after checking the viability with trypan blue staining under the microscope. The cell growth will be further monitored and cultured on the following cruise leg (PS113) until Bremerhaven. Subsamples should be frozen alongside to test for cell specificity.



Fig. 9.1: Fish lift (metal box in front) attached to bottom trawl net

Preliminary results

Catching alive fish by baited fish traps:

At King-George Island 2 baited traps have been deployed at about 450 m water depths in the opening of the Admiralty Bay, where the highest abundance could be expected due to former cruises (Fig. 9.2). After about 52 hours both traps were recovered. The traps were highly specific for the Antarctic eelpout *Pachycara brachycephalum* (Table 9.1). Indeed, in total about 1,000 eelpouts were caught. At the end of the cruise (about six weeks after the catch) more than 99,5 % of all fish survived. These specimens will be transported to Bremerhaven on the following cruise leg (PS113) and serve as excellent basis for future in-depth genetic and ecophysiological studies about the impact of climate factors on cold-adapted fish.

Tab. 9.1: Number of individuals of *P. brachycephalum* caught in the baited traps

Station	Date	Depth (m)	Specimens (n)
PS112_3-1	2018-03-22	434	~400
PS112_4-1	2018-03-22	457	~600

The composition, abundance and biology of the demersal fish fauna at the South Shetland Islands and the Antarctic Peninsula:

Bottom trawls were performed to characterize the demersal fish fauna and to collect genetic and physiological samples for further in-depth studies at the home institutes. A total of nine trawls have been performed during PS112 (Fig. 9.2), from which one was invalid due to a net failure. At each location two hauls were carried on at different depths. The positions for the trawls at the South Shetland Islands were in accordance with the CCAMLR survey from 2012 (Lucassen 2012; Kock and Jones 2013) on the upper shelf at water depths of 130 to 350 m. The two trawls at the Southern mouth of the Antarctic Sound (Eastern Antarctic Peninsula) were done at water depths of 440 and 630 m, respectively, and chosen after careful assessment of the bathymetry to avoid the complex sponge communities usually dominating on the upper shelf.



Fig. 9.2: Overview about fishing positions. Valid bottom trawls are shown as black squares with their respective station numbers, invalid hauls as red squares. Fish traps are depicted as blue diamonds.

9. Climate Sensitivity in Various Fishes from the Antarctic Peninsula

Overall, the total biomass of most hauls was dominated by fish in comparison to the by-catch. At station 40-1, by-catch was barely present, trawl 64-1 was the largest haul with about 620 kg fish, with *N. rossii* as most abundant species (594 kg). Only the last two hauls at the Southern mouth of the Antarctic sound (91-1 and 92-1) contained a rich community of epibenthic macro fauna (see below) accompanied by the highest fish species diversity and large amounts of *Pleuragramma antarcticus*. In total, more than 500 specimens according to the ecological and about 40 specimens according to the transcriptomic sampling procedure were taken (Table 9.2).

Trawling at the South Shetland Islands and Elephant Island revealed similar patterns of species distribution with the presence of several individuals of the genus *Lepidonotothen* and of the icefish family. *Notothenia rossii* was the dominant species at Elephant Island. The relative high abundance of *Champsocephalus gunnari* at Elephant Island, as it was expected according to Kock and Jones (2013) could not be confirmed on this survey. The species composition changed at the Eastern Antarctic Peninsula and became dominated by several *Trematomus* species, indicating a complex community structure at this location. However, given the limited numbers of individuals collected by our short trawls, further analyses are required to perform a comparison between previous surveys and our data.

A fish lift (Fig. 9.1) was attached close to the cod end of the net for retrieving alive fish under the most pristine condition possible. In general, the fish lift helped to improve the quality of the fish. Most sensitive species like *Pleuragramma antarcticus* and *Gymnoscopelus nicholsi* have been caught in significantly better shape. At station 29-3 reasonable amounts of juveniles were retrieved. Furthermore, krill (*Euphausia superba*) was abundant at several stations together with other non-sessile by-catch. Overall, only a small proportion of fish escaped from the cod end. This may be attributed to the strict benthic and/or sluggish life-style of most fish species present.

Tab. 9.2: List of fish species caught in the course of the bottom trawl survey

The biomass/number of a species is given as: (+) present; (++) common; (+++) highly abundant. In brackets the first number denotes the specimens, which have been processed ecologically, the second number gives the specimens additionally processed for transcriptomics (full range of tissues preserved at -80°C).

Species by Family	Station							
	29-3	30-1	39-1	40-1	63-1	64-1	91-1	92-1
Nototheniidae								
<i>Aethotaxis mitopteryx</i>								++ (10)
<i>Dissostichus mawsoni</i>	+ (1)			+ (5/4)	+ (1/1)			
<i>Gobionotothen gibberifrons</i>	+ (2)			+++ (35/4)				+ (7)
<i>Lepidonotothen larseni</i>	+++ (32)	++ (13)		++ (20)	+ (8)	+ (1)		
<i>Lepidonotothen nudifrons</i>	++ (12)			+ (2)				
<i>Notothenia coriiceps</i>	+ (2)		+ (5)	++ (19)		+ (8)		
<i>Notothenia rossii</i>				+ (10/5)		+++ (20)		
<i>Pleuragramma antarctica</i>		+ (1)					+++	+++ (2)
<i>Trematomus bernacchii</i>							+ (8/6)	+ (1/1)
<i>Trematomus eulepidotus</i>							+ (1)	

Species by Family	Station							
	29-3	30-1	39-1	40-1	63-1	64-1	91-1	92-1
<i>Trematomus hansonii</i>					+ (2/2)		+ (3)	++ (11/6)
<i>Trematomus lepidorhinus</i>							+ (6)	
<i>Trematomus loennbergii</i>							+ (3/3)	+ (3)
<i>Trematomus newnesi</i>							+ (4/2)	+ (8)
<i>Trematomus nicholai</i>							+ (7)	+ (2/1)
<i>Trematomus pennellii</i>							+ (1)	
<i>Trematomus scotti</i>							+ (4)	+ (6)
Bathdraconidae								
<i>Gymnodraco acuticeps</i>							+ (1)	+ (2)
<i>Parachaenichthys charcoti</i>	+ (3)							
Channichthyidae								
<i>Chaenocephalus aceratus</i>			+ (6)	++ (14)		+ (2)		
<i>Chaenodraco wilsoni</i>							++ (17)	+ (8)
<i>Champscephalus gunnari</i>	+ (2)			+ (2)	++ (11)	+++ (12)		
<i>Chionodraco rastrospinosus</i>				++ (15)	++ (17)	+ (2)	+ (5)	+ (6)
<i>Cryodraco antarcticus</i>	+++ (21)	+ (1)		+ (3)	+ (4)			
<i>Dacodraco hunteri</i>							+ (1)	+ (1)
<i>Pagetopsis macropterus</i>								+ (1)
<i>Pseudochaenichthys georgianus</i>	+ (2)			+ (1)				
Myctophidae								
<i>Electrona sp.</i>		+ (5)						
<i>Gymnoscopelus nicholsi</i>		+++ (9)		+ (2)				
Liparidae								
<i>Paraliparis antarcticus</i>							+ (2)	++ (15)
Unclassified								+ (2)
Sum of sampled specimens:	77	29	11	128/13	43/3	45	63/11	85/8

The gonado-somatic index ((GSI, gonads weight/total weight*100) of the most dominant species at Elephant Island, *N. rossii*, is given in Fig. 9.3. A strong increase of GSI with body length could be observed with a maximal GSI of up to 29 %. Furthermore, the pattern differs from an earlier survey performed in the second half of March and early April 2012 (Kock and Jones, 2012), as for the large individuals higher GSI, but also few post-spawning individuals could be observed in the present survey. Kock and Jones (2012) proposed a spawning time between May and June for *N. rossii*. Together with the maturity stage analyses our data suggest a significant earlier spawning time starting already mid of April. The huge aggregation of large reproductive individuals of *N. rossii* at the North-Western tip of Elephant Island is in line with

earlier observations by Kock and Jones (2012). Thus, our observations during PS112 suggests this place as an important spawning area for *N. rossii*, which should be protected accordingly to foster the conservation and persistence of the species.

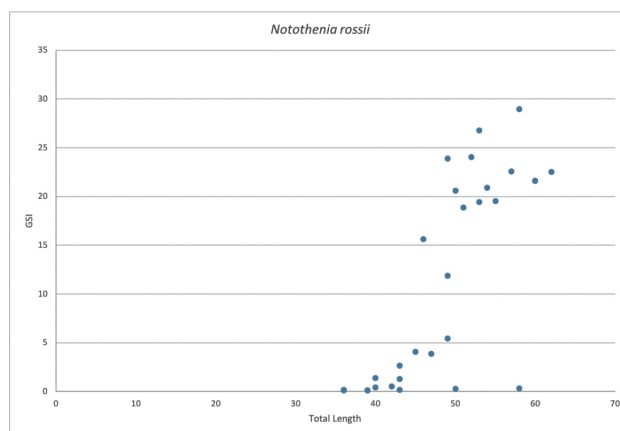


Fig. 9.3: Gonado-somatic index for *N. rossii* ($n = 27$) at Elephant Island (station 64-1) mid of April

Qualitative assessment of the epibenthic macrofauna at the South Shetland Islands and the Antarctic Peninsula:

The epibenthic by-catch of each haul was sorted entirely into 31 operational taxonomic groups (OTU) based on two field guides for the Antarctic nearshore communities (Rauschert and Arntz 2015; Barnes 2007) to the most specific taxonomic level possible. Detailed analyses of the data are still required. From all specimens, photographs were taken for later reanalyses in collaboration with experts of each animal groups. The relative contribution of an OTU to a catch was assigned according to the relative weight and the species richness, respectively. As the used bottom trawl is not designed for quantitative assessment of the sessile macrofauna, only qualitative measures were applied.

Tab. 9.3: Qualitative assessment of the epibenthic macrofauna

The following criteria were used as qualitative marker for each OTU: (+) present; (++) common; (+++) highly abundant. The number of species per OTU is given in brackets.

Operational taxonomic group	Station							
	29-3	30-1	39-1	40-1	63-1	64-1	91-1	92-1
Porifera	++ (1)	+ (2)	++ (7)	+ (2)	++ (4)	++ (7)	+++ (8)	++ (9)
Stauromedusa			+ (1)					+ (1)
Hydrozoa								
Actiniaria			+ (1)			+ (4)	+ (2)	+++ (7)
Scleractinia			+ (1)		+ (1)			
Alcyonaria					+ (1)			
Pennatularia								
Gorgonaria	+ (1)		+ (2)				+ (1)	

Operational taxonomic group	Station							
	29-3	30-1	39-1	40-1	63-1	64-1	91-1	92-1
Brachiopoda								
Bryozoa			+ (1)		+ (1)		+ (3)	
Sipuncula	+ (1)						+ (1)	++ (1)
Gastropoda		+ (1)	+ (2)		+ (2)	+ (3)	+ (2)	+ (1)
Nudibranchia								
Bivalvia			+ (1)				+ (2)	
Cephalopoda	++ (2)	+ (1)	+ (1)	+ (1)	+ (3)	+ (1)		++ (1)
Polychaeta	+ (2)	+ (1)			+ (1)		++ (5)	+ (2)
Echiura								
Pantopoda	+ (1)	+ (1)	+ (1)		+		+ (1)	
Leptostraca								
Amphipoda	+ (1)	+ (1)					+ (2)	++ (4)
Isopoda	+ (2)				+ (1)			
Euphausiacea	+ (1)	+ (1)	+ (1)				+ (1)	
Decapoda								
							++ (2)	++ (2)
Hemichordata								
							++ (5)	
Crinoidea					+ (1)	+ (1)	+ (1)	
Asterioidea	+ (2)	++ (5)	++ (5)		++ (4)	+ (4)	+++ (5)	+++ (8)
Ophiuroidea			+ (1)		+ (3)		+ (1)	+ (2)
Echinoidea			+ (1)		+ (1)	+ (1)	++ (5)	+ (3)
Holothuroidea		+ (1)	+ (1)	+ (1)	+ (3)	+ (1)	++ (4)	++ (3)
Tunicata	+ (1)	+ (1)	++ (1)		+ (1)	+ (1)		
Ascidiacea	+ (1)		++ (6)	+ (1)		++ (5)	+++ (8)	++ (3)
Unclassified								
								+ (3)
Sum of species:	16	15	35	5	28	28	59	50

As can be inferred from Table 9.3 the hauls differ largely in terms of species richness and abundance. Compared to the other stations the hauls North-West of Livingston Island were quite poor in species composition and in agreement with earlier observations (Gutt 2013). The highest species richness was clearly found at the Southern mouth of the Antarctic Sound. At the shallower position (about 430 to 450 m, station 91-1), the typical sponge communities with filter feeders were found. Thus, the sponge community were partially extending to deeper waters possibly due to the complex oceanographic current systems in that area (see Chapter 12). At the deeper position (station 92-1) sponge abundances declined, and a diverse deep-water fauna, typical for the Weddell Sea (Rauschert & Arntz 2015) was found with Actiniaria (sea anemones), Asterioidea and Holothuroidea as the dominating groups, while reasonable amounts of *Notocrangon antarcticus* and amphipods occurred.

Establishment of stable cell lines from Antarctic fish

Primary cell cultures were prepared from *G. gibberifrons*, representing a low-Antarctic species, and *T. bernacchii* and *T. hansonii* as representatives of high-Antarctic species. Typical cells

directly after isolation are shown for *T. hansonii* (Fig. 9.4). For liver round shaped hepatocytes could be obtained, which seemed to contain reasonable numbers of lipid droplets. From spleen mainly erythrocytes and other blood cells were isolated, and only few other cell types became visible. Kidney cells again were mostly round shaped and structured. The head kidney, similar to the spleen mainly involved in blood cell formation and immune response, contained both, round shaped structured cells and erythrocytes. After isolation all cells were kept at 0°C in their respective medium, which was exchanged according to demand (every 2-5 days). Due to the low temperatures, no significant growth of the cultures could be observed. Nevertheless, at the end of this cruise leg all cultures still contained living cells, which will be further cultivated on the next cruise leg (PS113). In case of their survival the cells will be characterized for their specificity and physiological performance at the home institute.

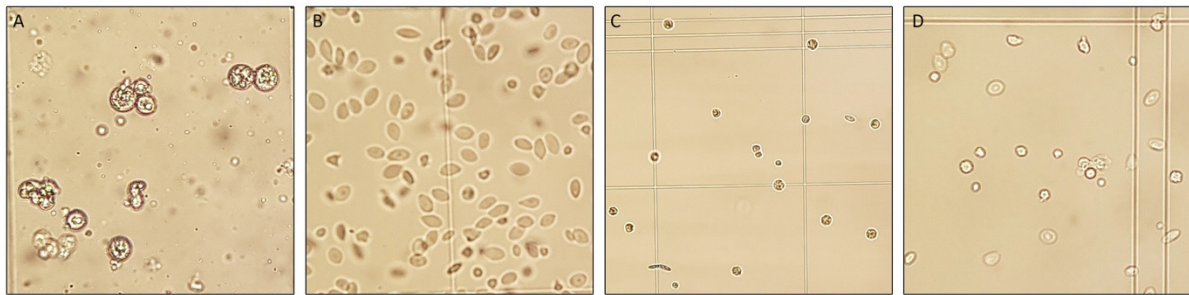


Fig. 9.4: Representative picture(s) of isolated cells. A: liver (400fold); B: spleen (200fold); C: kidney (40fold); D: head kidney (200fold)

Data management

All tissue samples will be stored at the Alfred Wegener Institute (AWI), all samples for population genetics were collected twice and will be stored both at the AWI and at the Biology Department of Padova University. Samples may become available to scientists from other institutions on request. Sponge samples are stored at ICBM, Oldenburg, and may become available on request (Sven Rohde). All data will be made available by publication in scientific journals and subsequent storage in PANGAEA. The molecular data will be submitted to the respective database (NCBI; EMBL).

References

- Agostini C, Patarnello T, Ashford JR, Torres JJ, Zane L, Papetti C (2015) Genetic differentiation in the ice-dependent fish *Pleuragramma antarctica* along the Antarctic Peninsula. *Journal of Biogeography* 42(6), 1103–1113.
- Barnes, DKA (2007). A guide to Antarctic nearshore marine life. British Antarctic Survey, Cambridge, Great Britain.
- Gutt, J (2013): The expedition of the research vessel “Polarstern” to the Antarctic in 2013 (ANT-XXIX/3), Reports on polar and marine research, Bremerhaven, Alfred Wegener Institute for Polar and Marine Research, 665. hdl:10013/epic.41835.
- Holst JC, McDonald A (2000). FISH-LIFT: a device for sampling live fish with trawls. *Fisheries Research* 48, 87-91.

- Kock, K-H, Jones, C D (2012). The composition, abundance and reproductive characteristics of the demersal fish fauna in the Elephant Island–South Shetland Islands region and at the tip of the Antarctic Peninsula (CCAMLR Subarea 48.1). CCAMLR report WG-FSA-12/10.
- Lucassen M (2012): The expedition of the research vessel “Polarstern” to the Antarctic in 2012 (ANT-XXVIII/4), Reports on polar and marine research, Bremerhaven, Alfred Wegener Institute for Polar and Marine Research, 652. hdl:10013/epic.40372
- Mark F C, Hirse T and Pörtner H O (2005). Thermal sensitivity of cellular energy budgets in Antarctic fish hepatocytes. *Polar biology*, 28 (11), pp. 805-814.
- Papetti C, Pujolar JM, Mezzavilla M, La Mesa M, Rock J, Zane L, Patarnello T (2012) Population genetic structure and gene flow patterns between populations of the Antarctic icefish *Chionodraco rastrospinosus*. *J Biogeogr*, 39 (7) 1361-1372.
- Papetti, C., Lucassen, M. and Pörtner, H. O. (2016a). Integrated studies of organismal plasticity through physiological and transcriptomic approaches: examples from marine polar regions. *Briefings in Functional Genomics*, elw024. doi:10.1093/bfpg/elw024.
- Rauschert, M., Arntz, W. (2015). Antarctic Macrobenthos: A field guide of the invertebrates living at the Antarctic seafloor. Arntz and Rauschert Selbstverlag, Wurster Nordseeküste, Germany.
- Stapp, L., Kreiss, C., Pörtner, H.-O., Lannig, G. (2015). Differential impacts of elevated CO₂ and acidosis on the energy budget of gill and liver cells from Atlantic cod, *Gadus morhua*. *Comparative Biochemistry and Physiology, Part A* 187 (2015) 160–167.
- Windisch, H. S., Frickenhaus, S., John, U., Knust, R., Pörtner, H. O. and Lucassen, M. (2014). Stress response or beneficial temperature acclimation: Transcriptomic signatures in Antarctic fish (*Pachycara brachycephalum*). *Molecular Ecology* 23 (14), 3469-3482.

10. FIN WHALE ABUNDANCE

Helena Herr¹, Sacha Viquerat²

¹Uni Hamburg

²TiHo Hannover

Grant-No. AWI_PS112_00

Objectives

Fin whales (*Balaenoptera physalus*) were the most numerous hunted whale species in the Southern Ocean during the era of industrial whaling, reduced to 2 % of their pristine population size (Clapham & Baker 2002). Today, their recovery status is unknown and ecology and habitat use in the Southern Hemisphere are poorly understood (Leaper and Miller 2011; Edwards et al. 2015). Recently, sighting numbers of fin whales in the West Antarctic Peninsula area have been increasing and large feeding aggregations have been observed (Santora et al. 2014; Herr et al. 2016; Viquerat and Herr 2017). Robust information on abundance is required to evaluate these re-occurring aggregations and to relate them to current population estimates. Moreover, drivers of fin whale distribution in the area need to be identified to understand why fin whales have returned to an area from which they have been absent for a long time. Fine-scale spatial data are necessary to relate fin whale densities to environmental parameters in order to identify important habitat and its spatial extent. Dependencies on prey species and relationships between krill distribution and fin whales are essential to evaluate vulnerabilities and threats in the rapidly changing environment of the West Antarctic Peninsula (WAP) for a potentially recovering fin whale population. Therefore, the objectives of this project were to collect data during aerial surveys in order to

- provide a robust minimum abundance estimate of fin whales at the WAP
- produce a model surface of fin whale distribution at the WAP
- identify drivers of fin whale distribution by relating observed densities to static and variable habitat parameters, particularly krill, mapped at the same temporal spatial scale during the expedition.

Work at sea

We used the on-board helicopters for our cetacean survey. The survey flights were conducted following line-transect distance sampling methodology (Buckland et al. 2001) for marine mammal surveys. We planned these transects in an *ad-hoc* manner shortly before the flights. Due to the ship constantly moving and frequently changing weather conditions, decisions if a survey flight could be undertaken, could only be made on short notice. Planning the transects, we aimed at an overall coverage of the area visited by the expedition.

During each flight, we travelled along the transect lines, recording all sightings of cetaceans. Position data was continuously recorded on a laptop computer running customised survey software connected to a gps device, recording sighting events and environmental conditions. Along the transects we continuously noted environmental information (e.g. ice cover) and

sighting conditions. Surveys were flown at 80 - 90 kts at an altitude of 600 ft, covering track lines of app. 110 nm in total per flight in a rectangular shape into the surrounding area of the ship. The survey team of each flight consisted of two observers, seated in the copilots seat and the left seat in the back. This way we ensured full coverage of the left side of the transect. In this set-up, the front observer collects data from the strip below the helicopter, which the observer in the back cannot see.

All sightings of marine mammals were documented including at least species ID, group size, position and distance to the track line (via the declination angle). If the species or group size could not be identified immediately, the survey was halted and the sighting was approached (so called 'closing-mode'; Calambokidis and Barlow 2004). After collection of all important information, the helicopter returned to the track line and the survey was resumed.

Preliminary results

22 survey flights were conducted on 12 days of the expedition. Unfeasible weather conditions prevented flying on all other days. A total of 3,251 km of survey effort were accomplished during 26.3 hours of survey. Survey effort was spread over the whole area of the expedition, roughly covering the ship's cruise track and thereby the tracklines of the acoustic krill survey. Transect placement was aligned along the stations of the CCAMLR grid wherever possible (Fig. 10.1).

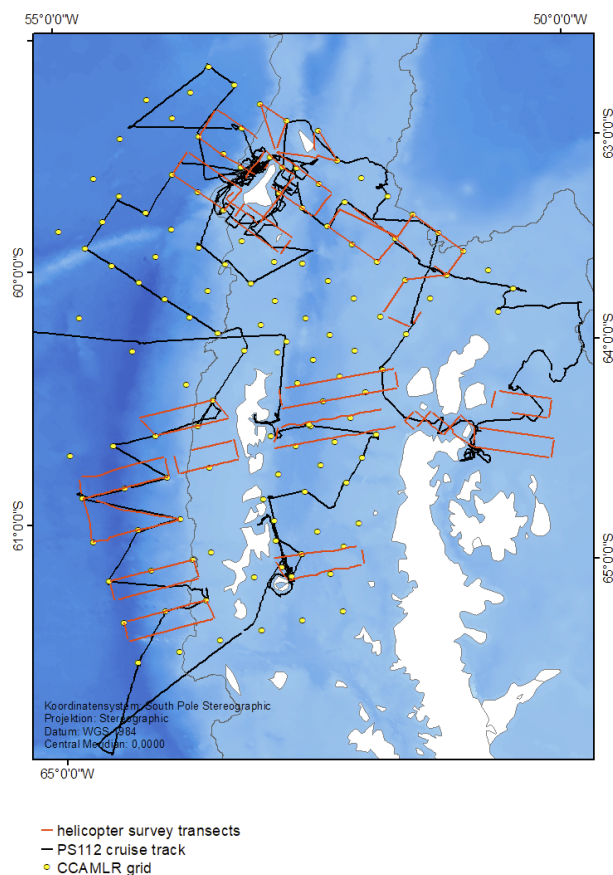


Fig. 10.1: Map showing cruise track (black) and transect lines covered by the helicopter survey

A total of 169 sightings of cetaceans were recorded on effort, comprising 240 individuals. Four baleen whale species, fin whale, humpback whale (*Megaptera novaeangliae*), Southern right whale (*Eubalena australis*) and Antarctic minke whale (*Balaenoptera bonaerensis*), and two toothed whale species, killer whale (*Orcinus orca*) and Southern bottlenose whale (*Hyperoodon planifrons*) were recorded. Fin whales accounted for the majority of sightings with 105 groups and 139 individuals. The second most frequently encountered species were humpback whales with 47 sightings and 73 individuals (Table 10.1). Fin whales were predominantly encountered around Elephant Island, but also north of the South Shetland Islands. Altogether, fin whale sightings were restricted to the outer shelf regions of the study area up to the shelf edge. On the contrary, humpback whales were encountered further away from the shelf edge, closer to the Antarctic Peninsula (Fig. 10.2). This observation is in line with previous findings of Herr et al. (2016) suggesting a horizontal niche separation of the two species.

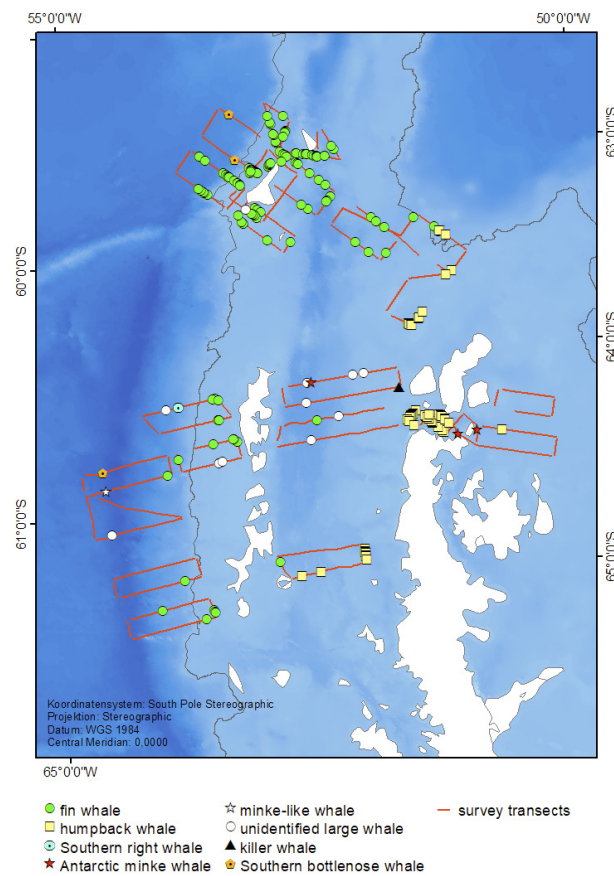


Fig. 9.2: Map representing the covered track lines of the helicopter surveys and positions of all recorded sightings. Species are given in the legend.

Tab. 9.1: List of all cetacean species encountered during the helicopter survey, including number of groups, individuals and average group size.

Species	# groups	# individuals	average group size
Fin whale (<i>Balaenoptera physalus</i>)	105	139	1,3
Humpback whale (<i>Megaptera novaeangliae</i>)	47	73	1,6
Antarctic minke whale (<i>Balaenoptera bonaerensis</i>)	3	3	1
minke-like whale	1	1	1
Southern right whale (<i>Eubalaena australis</i>)	1	1	1
unidentified large whale	9	15	1,7
Killer whale (<i>Orcinus orca</i>)	1	3	3
Southern bottlenose whale (<i>Hyperoodon planifrons</i>)	3	5	1,7

Data management

Survey data will be stored at the University of Hamburg. Upon publication or after 3 years at the latest, all data will be made available on appropriate platforms, such as PANGAEA, GBIF (<http://www.gbif.org>, Global Biodiversity Information Facility) or ANTABIF (<http://www.biodiversity.aq>).

References

- Buckland ST, Anderson DR, Burnham KP, Laake JL, Borchers DL, Thomas L (2001) Introduction to distance sampling: estimating abundance of biological populations. Oxford University Press, Oxford, UK.
- Calambokidis J, Barlow J (2004) Abundance of blue and humpback whales in the eastern North Pacific estimated by capture-recapture and line-transect methods. *Marine Mammal Science*, 20(1), 63-85.
- Clapham PJ, Baker CS (2002) Modern whaling. In: Perrin WF, Würsig B, Thewissen JGM (eds) *Encyclopedia of marine mammals*. Academic Press, New York, NY, p 1328–1332.
- Edwards EF, Hall C, Moore TJ, Sheredy C, Redfern, JV (2015) Global distribution of fin whales *Balaenoptera physalus* in the post-whaling era (1980-2012). *Mammal Review*, 45,197– 214.
- Herr H, Viquerat S, Siegel V, Kock KH and others (2016) Horizontal niche partitioning of humpback and fin whales around the West Antarctic Peninsula: evidence from a concurrent whale and krill survey. *Polar Biology*, 39, 799–818.
- Leeper R, Miller C (2011) Management of Antarctic baleen whales amid past exploitation, current threats and complex marine ecosystems. *Antarctic Science*, 23, 503–529.
- Viquerat S, Herr H (2017) Mid-summer abundance estimates of fin whales (*Balaenoptera physalus*) around the South Orkney Islands and Elephant Island. *Endangered Species Research*, 32, 515–524.

11. TRACE METAL BIOGEOCHEMISTRY

Floria Koch¹, Franziska Pausch², Dorothee
Wilhelms-Dick², Sebastian Böckmann³, Anna
Pagnone², C. Hassler⁴ (not on board), Scarlett
Trimborn^{2,3} (not on board)

¹Hochschule Bremerhaven
²AWI
³Uni Bremen
⁴UNIGE

Grant-No. AWI_PS112_00

Objectives

In 30-50 % of the world's oceans plankton biomass is low even though nutrients and light are plentiful (de Baar et al. 2005). Rather than macronutrients such as nitrate or phosphate, in these high nutrient low chlorophyll (HNLC) regions it is the scarcity of certain trace metals (TM) such as iron (Fe) and/or vitamins, which govern primary production and/or plankton species composition (Martin et al. 1988; de Baar et al. 2005; Bertrand et al. 2007; Koch et al. 2011). The Southern Ocean (SO) is the world's largest HNLC region, and responsible for roughly 40 % of all oceanic uptake of anthropogenic carbon and an area where iron limitation to phytoplankton has been reported (de Baar et al. 2005; Trimborn et al. 2015). In addition, the SO is an important region contributing disproportionately to upwelling of deep water and formation of intermediate and bottom waters linking the Pacific, Indian and Atlantic Oceans and thus being of global importance in climate regulation, biodiversity and biogeochemical cycles (Buesseler 1998; Lumpkin et al. 2007).

In the SO, TMs are present at nmol L⁻¹ concentrations (Boye et al. 2001; Croot et al. 2001; Ibsanmi et al. 2011; Thuroczy et al. 2011). These low concentrations can pose a challenge for the plankton community since many cellular metabolic enzymes require metals (Twining et al. 2013). Especially Fe is required for vital processes such as carbon and nitrogen fixation, nitrate and nitrite reduction, chlorophyll synthesis and essential in the electron transport chain of respiration and photosynthesis (Raven et al. 1999; Behrenfeld et al. 2013; Twining et al. 2013). Zn plays an important role in carbonic anhydrase, the enzyme catalyzing the interconversion of CO₂ and bicarbonate for photosynthesis, and in alkaline phosphatase, an enzyme important in cleaving phosphate from larger organic molecules in times of phosphorus limitation. One challenging oceanographic issues is understanding how the limitation and recycling of trace metals influence the Southern Ocean ecosystem. The availability of trace metals, in particular Fe, is considered the key factor governing SO phytoplankton productivity and community composition. In this context, Fe sources are a key determinant of Fe bioavailability, but the capacity of autotrophic as well as heterotrophic microorganisms to access different chemical forms of Fe is largely unknown. Since phytoplankton are part of a complex food web, their interactions with other trophic levels can have profound effects on the dynamics of the system. This work focused on bacterial-phytoplankton-zooplankton interactions considering biologically excreted organic matter as a control for trace metal chemistry, the bioavailability of these trace metals to the plankton community, their effects on primary productivity and species composition and succession. The objectives of for this cruise were to study the interconnected processes driving the biogeochemical cycles of carbon, trace metals such as Fe and Zn, as well as Vitamin B₁₂.

Work at sea

This study combined station surveys with a targeted experimental approach in order to characterize *in-situ* TM/plankton dynamics and assess how TM sources such as salp/krill fecal pellets and dust sources might alter these.

Trace metal/vitamin dynamics and cycling

At seven stations (Table 11.1) seawater from 25 m depth was obtained using a Teflon - coated 25 L GoFlo bottle deployed on a Dyneema line and processed inside a trace metal clean (TMC) container. At four stations a Teflon membrane pump (Almatec), connected to a polyethylene line was used to pump surface seawater from 25 m depth directly into the trace metal clean van. For all sampling stations, a multifaceted approach was used. To characterize the community composition (virus, bacteria, phytoplankton), samples for light microscopy, size fractionated pigments (HPLC), particulate organic carbon and nitrogen (POC/PON), biogenic silica (BSi) as well as flowcytometry were taken. To shed light on the trace metal requirements of the plankton community, samples for particular trace metals were collected and stored frozen for subsequent analysis by ICP-MS. In addition, concentrations of dissolved TMs, Fe chemical speciation, ligands, humic acid- like substances, macronutrients and dissolved organic carbon were also collected. Removal rates of dissolved trace metals/vitamins by the plankton was measured using triplicate 250 mL polycarbonate (PC) bottles, spiked with either 50 nCi ^{57}Co -B $_{12}$, $^{57}\text{CoCl}$, $^{55}\text{FeCl}$ or $^{65}\text{ZnCl}$ and incubated in an on deck flow through incubator. Bottles were covered with neutral density screening allowing for 50% of light to penetrate, corresponding to light levels at a depth of 20-30 m. In order to determine primary productivity rates, triplicate bottles were spiked with 4 μCi of sodium bicarbonate. Experiments were terminated after 24 hours by filtering each bottle onto 0.2 and 2 μm polycarbonate filters and uptake rates of each isotope was determined by subsequent quantification on a liquid scintillation counter. Bacterial production rates were also estimated using ^3H -Leucine according to Kirchman (2001). Two 2.5 L PC bottles of whole water were allowed to incubate along the spiked bottles, and dissolved vitamin and trace metals concentrations were determined after 24-48 hours as described above. In addition, low TM water was pumped into a 600 L TMC PE tank at PS112_26 and PS112_132 and taken to the AWI to be used for laboratory experiments.

Tab 11.1: Stations sampled on PS112 (ANTXXII/3). P/G denotes the trace metal clean sampling method used with P = membrane pump and G = GoFlo. Fv/Fm refers to the photosynthetic yield as assed using the Rapid Repetition Rate Fluorometer. TM/V denotes stations at which samples for Trace metal/vitamin dynamics and cycling were obtained while FP, Dust and Grazing denote stations at which experiments looking at the impacts of fecal pellets, dust and grazing, respectively were conducted.

Station	Latitude	Longitude	P/G	Fv/Fm	TM/V	FP	Dust	Grazing
PS112_17	62° 44.97'S	59° 00.81'W	G	0.56	X			
PS112_20	63° 00.02'S	60° 00.07'W	G	0.37	X			
PS112_25	62° 53.13'S	60° 13.75'W	G	0.55	X			
PS112_26	62° 14.23'S	64° 33.41'W	P	0.19	X	X	X	X
PS112_31	61° 44.99'S	61° 59.96'W	G	0.32	X			
PS112_55	61° 01.39'S	54° 64.68'W	G	0.32	X			
PS112_61	60° 44.74'S	54° 30.22'W	P	0.35	X	X	X	X
PS112_98	63° 38.56'S	56° 29.54'W	G	0.20	X			
PS112_106	61° 59.73'S	53° 59.81'W	P	0.39	X			X
PS112_120	60° 57.51'S	54° 44.69'W	G	0.41	X			
PS112_132	58° 21.26'S	58° 73.15'W	P	0.12				

Micro- and mesozooplankton grazing impacts on TM/vitamin dynamics

The impacts of micro- and mesozooplankton grazing on trace metal and vitamin cycling rates were measured at three stations (*PS112_26*, *PS112_61*, *PS112_106*). Using a dilution series, the recycling/remineralization rates of trace metals, due to grazing by microzooplankton was determined. For this method, seawater was collected using the membrane pump (as described above) and triplicate 2 L PC bottles were diluted to 15, 30, 50, 75 and 100 % of the whole seawater using 0.2 μm FSW from the same location. The bottles were then incubated at ambient light and temperature. After 62 hours the experiment was terminated by sampling each bottle for pigments, POC/PON and flow cytometry as described above in order to measure the growth rates of the various plankton groups. Concentration changes of trace metals, vitamins and macronutrients were also assed for each dilution allowing calculation of remineralization rates. In addition, mesozooplankton collected using a Bongo net (150 μm) cast to 200 m was collected using a specialized HDPE codend in order to minimize TM contamination. This zooplankton concentrate was then rinsed 6 times with TMC FSW and the use of a 150 μm mesh, taking care to not stress the organisms unnecessarily. From 1 L of concentrated zooplankton 1 mL and 5 mL were added to triplicate 2.5 L PC bottles filled with WSW while an additional treatment consisted of a 1 mL addition to triplicate 2.5 L PC bottles filled with FSW. For each addition, a Mock-bottle received the same treatment but was processed immediately for dissolved TMs, nutrients, POC/PON, pigments and flow cytometry as described above. The experiment was incubated at ambient light and temperature conditions and terminated after 62 hours. Water from each bottle was collected for dissolved TMs, humic-acid like compounds before being prefiltered over a 150 μm mesh, removing the added grazers, and collecting samples for POC/PON, pigments and flowcytometry as described above.

Experiments with salp and krill fecal pellets

To quantify the effect of fecal pellets from krill and salps on the Fe chemistry and bioavailability to phytoplankton, naturally Fe- deplete seawater was collected at 2 stations (*PS112_26* and *PS112_61*) from 25 m depth using a membrane pump as described above. Unfiltered, seawater was collected and transferred into 9 acid- washed 4 L polycarbonate bottles. Triplicate bottles were treated with either salp or krill pellets while three bottles served as the whole seawater (WSW) control. Additionally, filtered seawater (FSW) was produced by using a 0.2 μm acid-cleaned Acropak capsule, removing the plankton community. The previously described treatments were then also applied to the FSW. The amount of fecal material added was normalized to carbon for both salps and krill, adding $\sim 35.7 \mu\text{g L}^{-1}$ of carbon to each bottle for the first and $\sim 57 \mu\text{g L}^{-1}$ of carbon to the second experiment (*PS112_26* and *PS112_61*, respectively). For the salp fecal pellets this constituted a Fe addition of $\sim 81 \text{ pM}$ for the first and $\sim 129 \text{ pM}$ for the second experiment. Unfortunately, no data on Fe content in krill fecal pellets exists at the moment. Fecal pellets for both species were also collected for subsequent carbon and TM stoichiometry analysis back at the AWI. After a 48 hours incubation at ambient light and temperature conditions, samples from each bottle were taken in order to characterize plankton biomass and species composition. Trace metal chemistry, organic ligands and macronutrients were processed as described above. 300 mL from each treatment was 0.2 μm -filtered and a small volume (<5 mL) of concentrated phytoplankton was added, attempting to mimic natural densities. This concentrate was produced from the initial phytoplankton community by gently concentrating 40 L of WSW by gravity filtration onto 0.2 μm polycarbonate filters using a special filtration unit (Millipore, stirred ultrafiltration cells, model Amicon 8400). Primary production and bacterial production rates for each bottle as well as Fe uptake rates were then determine as described above.

The impact of various dust sources on phytoplankton community composition and Fe availability

In addition to recycling processes, aeolian dust constitutes an important source of TMs to HNLC regions of the Southern Ocean. In order to compare the relative importance of TMs from microbial recycling and fecal pellets to dust, two dust addition experiments were conducted at *PS112_26* and *PS112_61*. Dust collected in Patagonia (Argentina) and Australia were added to WSW in triplicate 4 L polycarbonate bottles. The final Fe concentration due to the dust was calculated to be ~ 0.5 nM. While three bottles served as controls, triplicate bottles were also amended with 0.5 nM FeSO_4 , a highly bioavailable Fe source. The bottles were then incubated under ambient light and temperatures for 19 and 12 days (for water collected at *PS112_26* and *PS112_61*, respectively). Experiments were monitored by collecting samples for fluorescence and chlorophyll a concentrations every 48 hours. At the end of the experiment, samples for plankton community composition, biomass, cellular TM stoichiometry and Fe chemistry were collected, as described above. In addition, photosynthesis irradiance curves were conducted using a fast repetition rate fluorometer (FRRf), assessing the photosynthetic fitness of the final phytoplankton community. Lastly, 300 mL of water from each bottle was collected and primary production and bacterial production rates as well as Fe uptake rates were determined as described above.

Preliminary (expected) results

Trace metal/vitamin dynamics and cycling

While most of the samples for plankton community composition and concentrations of nutrients, TM chemistry and vitamins need to be analyzed back at the AWI, preliminary results from the primary and bacterial productivity rates are promising. Primary production rates ranged from 2 to $27 \mu\text{g}_{\text{Carbon}} \text{L}^{-1} \text{d}^{-1}$ with the highest rates observed at *PS112_17*, *PS112_25* and *PS112_120* and the lowest at *PS112_26* (Fig. 12.1a). Bacterial production was also highly variable and ranged from 0.04 to $0.90 \mu\text{g}_{\text{Carbon}} \text{L}^{-1} \text{d}^{-1}$. Highest rates were measured at *PS112_17*, *PS112_20* and *PS112_25* (Fig. 11.1b). Size fractionation reveals a dynamic plankton community, dominated by the $>2 \mu\text{m}$ size fraction at most stations. Preliminary results from the TM and vitamin uptake experiments show that Fe, Zn and vitamin B_{12} are not taken up equally by the two size classes. Vitamin B_{12} is taken up mostly by the picoplankton and Fe mostly by the $>2 \mu\text{m}$ size fraction,

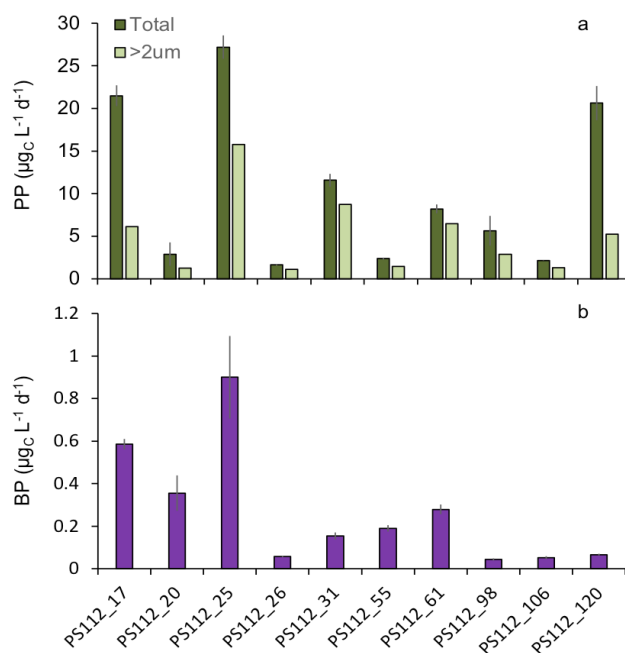
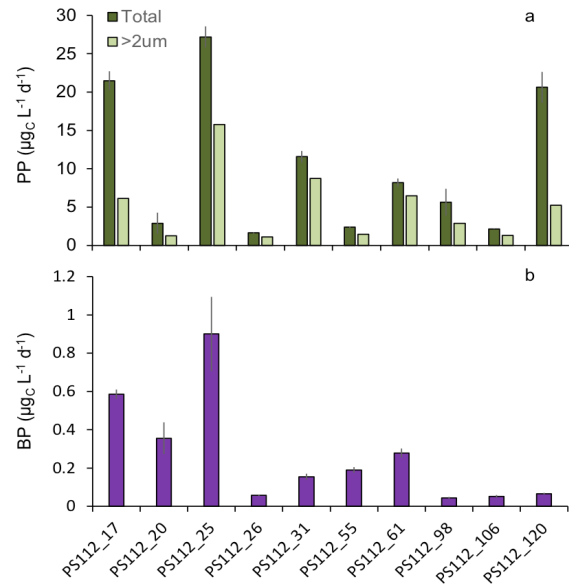


Fig. 11.1: Primary (PP, a) and bacterial (BP, b) production rates measured for PS112. Primary production was size fractionated into total and $>2 \mu\text{m}$ community. Data shown is the mean \pm standard deviation ($n=3$).

while Zn seems to mirror primary production (Fig. 11.2a, b). While the absolute removal rates of TMs and vitamin B₁₂ cannot be determined until precise ambient concentrations are measured back at the AWI, these preliminary results indicate highly complicated TM and vitamin allocation within the various plankton communities.

Fig. 11.2: Relative uptake rate of ⁵⁵Fe (Iron), ⁵⁷Co-B₁₂ (B₁₂), ⁶⁵Zn (Zinc) and primary production (PP) for PS112_26 (a) and PS112_120 (b). The relative percentage of each tracer taken up by the 0.2-2 μm and >2 μm plankton communities are shown.



Micro- and mesozooplankton grazing impacts on TM/vitamin dynamics

None of the samples for these experiments were analyzed on the *Polarstern* and thus no preliminary data is available for this report.

Experiments with salp and krill fecal pellets

The emphasis of these experiments lies with the chemical alterations of the seawater due to the addition of fecal pellets, and samples collected for Fe- and ligand chemistry will be analysed back at the AWI. Preliminary results obtained from the isotope work suggests that only one of the two experiments were successful. The concentrating of phytoplankton for the first experiment failed, resulting in dead cells, as evidenced by subsequent negligible primary and bacterial production rates. Thus, the impact of the treatments on the bioavailability of Fe could not be assessed. For the second experiment, the phytoplankton community was successfully concentrated and added to the treatments as indicated by the relative high primary and bacterial production rates (data not shown). While relative uptake rates of Fe were measured, these results need to be evaluated after robust analysis of the Fe chemistry has been conducted back at the AWI. First results indicate variable treatment effects due to the salp and krill fecal pellet addition for both, WSW and FSW.

The impact of various dust sources on phytoplankton community composition and Fe availability

Preliminary data suggests that both, the addition of various dust sources and FeSO₄, impacted the plankton community composition. The experiment conducted with water collected at PS112_26 exhibited slow growth rates, however, after several days, a separation of the different treatments became apparent. This was seen in both, the biomass as well as the photosynthetic efficiency (Fv/Fm) values. Low Fv/Fm values are indicative of phytoplankton

communities stressed by Fe limitation and thus a good proxy for HNLC conditions (See Table 11.1). The addition of both dust sources and FeSO_4 enhanced the biomass and Fv/Fm values significantly over the control, with the greatest effects occurring in the Australian dust treatment. At the end of the experiment primary production rates mirrored this trend (Fig. 11.3a). In addition, size fractionated primary production suggested a shift in community composition, with the $>2 \mu\text{m}$ size fraction gaining dominance in the Australian dust and FeSO_4 treatments. While phytoplankton biomass and primary production were significantly impacted by the addition of dust and FeSO_4 , significant changes in bacterial production rates occurred only with the Argentinian dust addition. The complete impacts of the treatments on the bioavailability of Fe, Fe chemistry and the phytoplankton community composition can only be assessed after analysis of the samples back at the AWI. Relative changes of $^{55}\text{FeCl}$ taken up by the communities in the different treatments, however, are promising. Even though a majority of the uptake in the control treatment occurred in the $<2 \mu\text{m}$ size fraction, the Australian dust addition resulted in almost all of the Fe being taken up by the larger plankton (Fig. 11.4). The second dust addition experiment conducted with water collected at PS112_61 exhibited large variability within each treatment so that no significant changes in primary-, bacterial production or Fe uptake were observed for the different treatments. A more detailed examination of the Fe chemistry and other parameters including phytoplankton community composition will hopefully shed light on possible treatment effects.

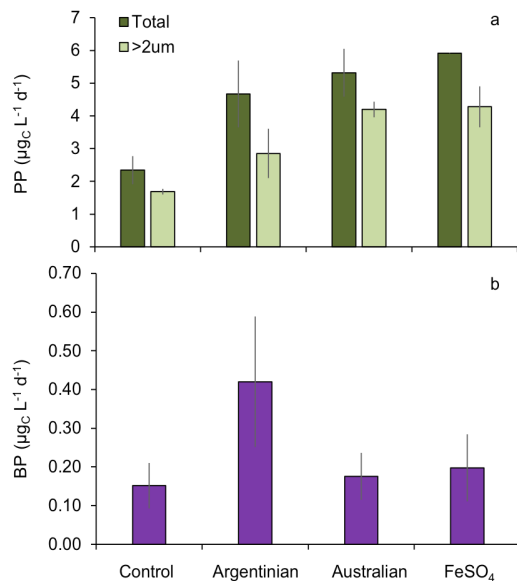


Fig. 11.3: Primary (PP, a) and bacterial (BP, b) production rates measured at the end of the first dust addition experiment conducted with water from PS112_26. Primary production was size fractionated into total and $>2 \mu\text{m}$ community. Data shown is the mean \pm standard deviation ($n=3$).

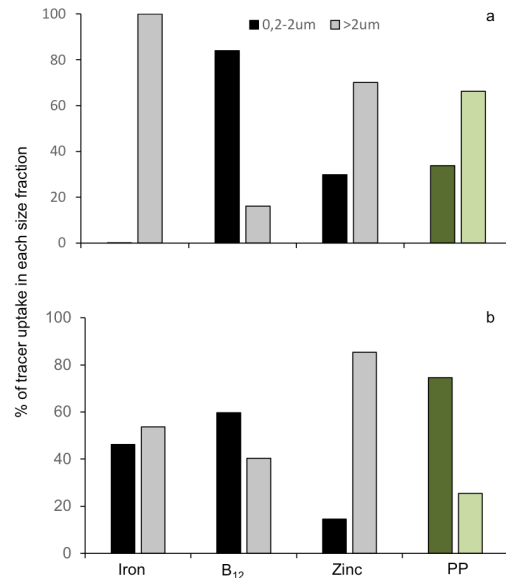


Fig. 11.4: Relative uptake rates of ^{55}Fe for the dust addition experiment conducted with water collected at PS112_26. The relative percentage of tracer taken up by the $0.2\text{-}2 \mu\text{m}$ and $>2 \mu\text{m}$ plankton communities are shown and represent the mean \pm standard deviation ($n=3$).

Data management

All data obtained will be prepared for publication and will be made available via PANGAEA.

References

- Behrenfeld M J and Milligan AJ (2013) Photophysiological Expressions of Iron Stress in Phytoplankton. Annual Review of Marine Science, Vol 5. C. A. Carlson and S. J. Giovannoni. Palo Alto, Annual Reviews, 5, 217-246.
- Bertrand E M et al. (2007) Vitamin B-12 and iron colimitation of phytoplankton growth in the Ross Sea. Limnol. Oceanogr., 52(3), 1079-1093.
- Boye M et al. (2001) Organic complexation of iron in the Southern Ocean. Deep-Sea Res. Part I-Oceanogr. Res. Pap. 48(6), 1477-1497.
- Buesseler K O (1998) The decoupling of production and particulate export in the surface ocean. Glob. Biogeochem. Cycle, 12(2), 297-310.
- Croot PL et al. (2001) Retention of dissolved iron and Fe-II in an iron induced Southern Ocean phytoplankton bloom. Geophys. Res. Lett., 28(18), 3425-3428.
- de Baar HJW et al. (2005) Synthesis of iron fertilization experiments: From the iron age in the age of enlightenment. J. Geophys. Res.-Oceans, 110(C9), 1-24.
- Ibisanmi E et al. (2011) Vertical distributions of iron-(III) complexing ligands in the Southern Ocean. Deep-Sea Res. Part II-Top. Stud. Oceanogr., 58(21-22), 2113-2125.
- Kirchman D. (2001) Measuring bacterial biomass production and growth rates from Leucine incorporation in natural aquatic environments. In: J.H. Paul (ed) Methods in Microbiology Volume 30: Marine Microbiology. Academic Press. pp 227-237.
- Koch F et al. (2011) The effect of vitamin B-12 on phytoplankton growth and community structure in the Gulf of Alaska. Limnol. Oceanogr., 56(3), 1023-1034.
- Lumpkin R and Speer K (2007) Global ocean meridional overturning" J. Phys. Oceanogr., 37(10), 2550-2562.
- Martin JH and Fitzwater SE (1988) Iron deficiency limits phytoplankton growth in the Northeast Pacific Subarctic. Nature, 331(6154), 341-343.
- Raven JA et al. (1999) The role of trace metals in photosynthetic electron transport in O₂-evolving organisms. Photosynth. Res., 60(2-3), 111-149.
- Thuroczy CE et al. (2011) Observation of consistent trends in the organic complexation of dissolved iron in the Atlantic sector of the Southern Ocean. Deep-Sea Res. Part II-Top.
- Trimborn S et al. (2015) Physiological characteristics of open ocean and coastal phytoplankton communities of Western Antarctic Peninsula and Drake Passage waters. Deep-Sea Res. Part I-Oceanogr. Res. Pap., 98, 115-124.
- Twining BS and Baines SB (2013) The Trace Metal Composition of Marine Phytoplankton. Annual Review of Marine Science, Vol 5. C. A. Carlson and S. J. Giovannoni. Palo Alto, Annual Reviews, 5, 191-215.

12. PHYSICAL OCEANOGRAPHY AND BIO-OPTICAL PARAMETERS

Thomas H. Badewien¹, Michael Butter¹,
Anna Friedrichs¹ and Anne-Christin Schulz¹

¹ICBM, Uni Oldenburg

Grant-No. AWI_PS112_00

Objectives

Biological and chemical processes observed during the cruise can be studied in relation to physical oceanography data obtained by profiling and underway systems. Water masses identification and mixing processes can be detected by using parameters such as temperature and salinity as well as current data. The stratification of the water column and circulation patterns are relevant when process studies were conducted. Data derived from underway systems such as the ferry-box allow a more detailed view at the processes occurring at the sea surface.



Fig. 12.1: ICBM-CTD on board Polarstern after a CTD-cast

Work at sea

For the first time we used the custom-built ICBM-CTD-rosette aboard *Polarstern* (Fig. 12.1). The system worked well even under harsh weather conditions such as sea ice cover and water temperature below $-1.8\text{ }^{\circ}\text{C}$. In total, we performed 140 CTD-casts. The sampled water was used for analyses and laboratory experiments with salps and krill.

We used a Sea-Bird Electronics Inc. CTD SBE 911plus probe, SN 09-1266, attached to a SBE 32 Carousel Water Sampler SN 32-1119 containing 24 20-liter Ocean Test Equipment Inc. bottles. The CTD system is equipped with double temperature and conductivity sensors, an oxygen sensor, a pressure sensor, an altimeter, and a combined chlorophyll fluorometer and turbidity sensor. In addition, we attached a deep ocean camera system offered by the Australian Government / Antarctic Division (contact Jim Williams).

Before each measurement, the CTD was adapted to the ambient water at 20 m water depth for 3 minutes. We obtained temperature, conductivity, oxygen, fluorescence, turbidity profiles from the surface down to either 200 m or close to the sea floor. Temperature was determined according to the ITS-90 temperature standard (potential T in $^{\circ}\text{C}$). Absolute salinity (g/kg) was calculated using the TEOS-10 standard (IOC, SCOR and IAPSO, 2010; Millero et al., 2008; McDougall et al. 2012). Within the upper 200 m, the CTD was lowered with 0.5 m/s and below

this depth with 1.0 m/s. In order to obtain high quality footage of the sea life with the camera the lowering speed was reduced to 0.2 m/s at certain depth ranges. Water samples were collected during the up-cast of the CTD at pre-defined depths.

At selected stations the Secchi-disc depth as well as the Fore-Ule number were obtained during daylight.

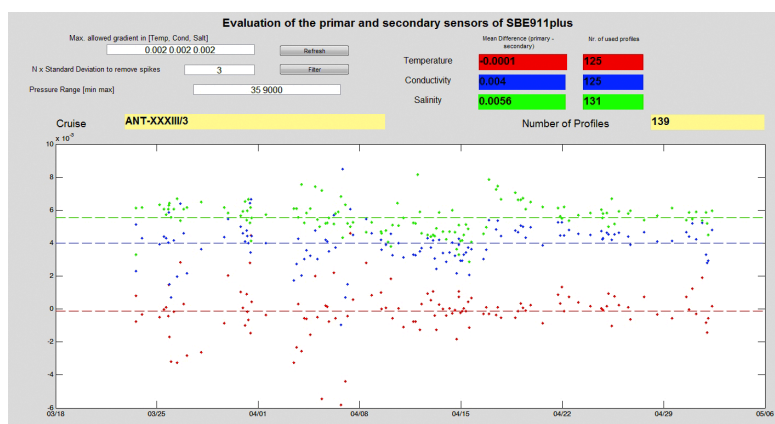


Fig. 12.2: Accuracy check of the temperature and conductivity double sensors based on nearly all CTD-casts during cruise PS112

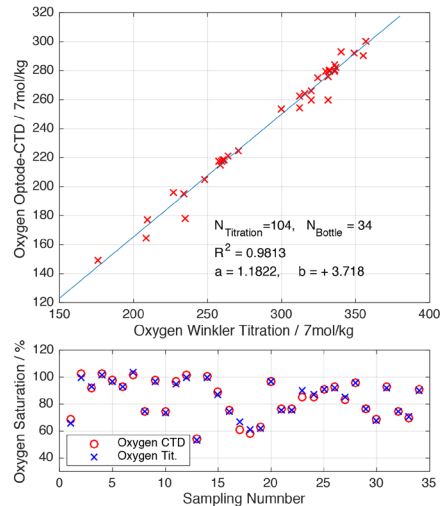
All data were recorded and stored using the standard software Seasave V 7.23.2. The data were processed by means of ManageCTD, loops deleted, and data were added such as the CTD header, and ship position, based on the aboard data system DSHIP. We checked the data for unusual spikes using the despiking-routine of ManageCTD. Finally, data were converted into different formats for subsequent analyses and publication. Other data such as salinometer, Ferrybox, weather recordings, GPS were extracted from the DSHIP-system data for further processing and added as a supplement to the CTD data.

All sensors attached to the frame of the rosette were pre-calibrated by the manufacturers. We compared the data of both temperature and conductivity sensors using data from 125 casts. The temperature sensors had a very high accuracy, with a mean difference of 0.0001 °C. The conductivity sensors had a mean difference of 0.004 mS/cm. There was a small constant offset between both conductivity sensors, see Fig. 12.2. The salinity values show a constant offset of 0.0056. In order to calibrate the salinity data 39 water samples were collected and measured with the aboard salinometer (Optimare precision Salinometer SN 006). The salinity correction was performed by adding a very small constant offset of -0.00003 between the reference and primary sensor 1 as well as a constant offset of 0.0055 between the reference and secondary sensor 2. The salinity data will be corrected with the offsets before publishing.

Oxygen Calibration

For calibration of the Aanderaa oxygen sensor, we used the standard titration technique (Winkler 1888; Grasshoff et al. 1999) to determine the concentration of dissolved oxygen in the seawater. At selected stations we took two to four replicate water samples from different depths. In total, we used 104 water samples for the calibration of the oxygen sensor. The results obtained from the oxygen sensor and the titration measurements match well ($R^2 = 0.9813$, see Fig. 12.3). The correction function has an offset of 3.718 $\mu\text{mol/kg}$; the slope is 1.1822. The oxygen data will be corrected before publishing.

Fig. 12.3: Upper panel - validation of the Aanderaa-type oxygen Optode by using Winkler titration of 104 samples obtained at selected stations during the cruise PS112. Lower panel – comparison of oxygen saturation based on Winkler titration (blue x) and validated CTD data (red circle).



Coloured dissolved organic matter (CDOM)

At nearly all CTD stations samples for colored dissolved organic matter (CDOM) were taken at standard depths (100 m, DCM, surface). In total 270 water samples were taken and filtered through 0.2 μm pore size membrane filter. The absorption of the filtered sample was determined spectrophotometrically (200 nm – 800 nm).

Underway systems

After passing the 200 nm border line three different underway systems were started. Therefore, along the cruise track data of four Ramses radiometers, ADCP (Acoustic Doppler Current Profiler) and ferry-box systems were obtained. An Ocean Surveyor (RD Instruments) vessel mounted phase array ADCP is installed onboard: 150 kHz, SN 3058, bin size of 4 m, max. depth from the surface 340 m, reference method: ship-GPS and ship-gyro). The ADCP data were checked by a volume transport test along a square with a length of each side of one nautical mile.

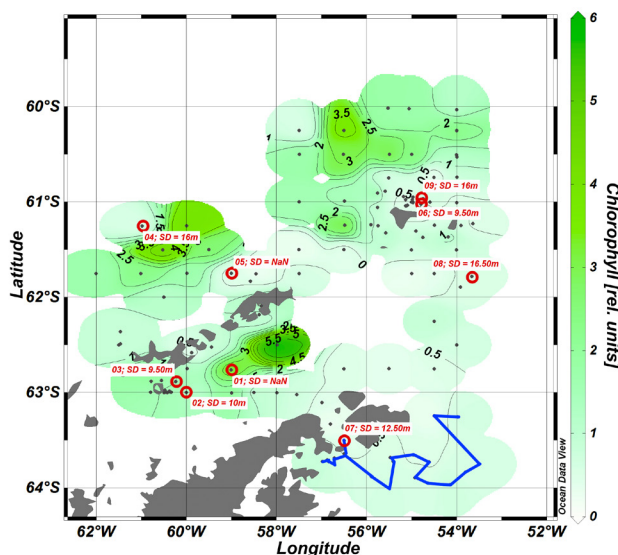


Fig. 12.4: Chlorophyll fluorescence distribution at water depth of 25 m close to the deep chlorophyll maximum (DCM) derived from the CTD-profile data. Dots denote the station, red circle the super-station, SD the Secchi-disc depth and blue line the cruise track used for temperature contour plot, Fig. 12.7.

Preliminary results

To get an overview of the research area the chlorophyll fluorescence distribution is shown in Fig. 12.4. The data were derived at water depths of 25 m close to the deep chlorophyll maximum. The highest concentrations were observed in the center of the Bransfield Strait and

the lowest concentrations in the northwestern part of the Weddell Sea. The observed Secchi-disc depth (Fig. 12.4 SD) varies between 9.5 m and 16.5 m. These depth does not seem to be correlated with the chlorophyll concentration.

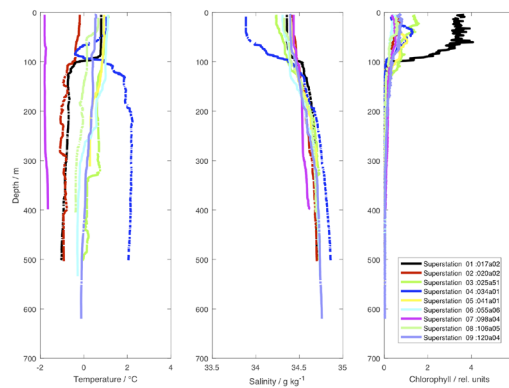


Fig. 12.5: Temperature, salinity and chlorophyll fluorescence profiles data derived at all super-stations, see Fig. 12.4

Nine CTD-stations were selected as super-stations representing the different research areas. Fig. 12.5 shows the profile data of the temperature, salinity and chlorophyll fluorescence derived from those CTD-casts. At all stations except for station 34 and 98 a clear surface mixed layer was observed, represented by all three parameters (temperature, salinity and chlorophyll fluorescence). The profile obtained at station 98 is typical for a shelf sea in ice-covered regions. The detected Weddell Sea Water (WSW) has a temperature below 1.5 °C and a salinity above 34.2 psu. here represented by station 98 (Fig. 12.5). The station 34 is

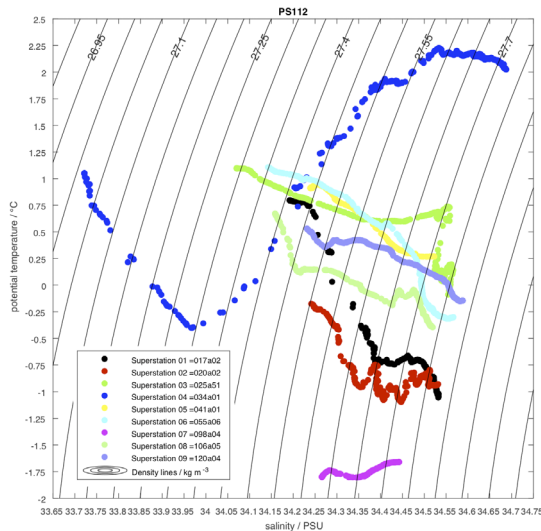


Fig 12.6: TS-diagram with data derived from all super-stations, see Fig. 12.4

off-shore north of the South Shetland Islands. Here, we could distinguish three water masses. These different water masses can be analyzed by using a TS-diagram (Fig. 12.6). The main water masses are Antarctic Surface Water (ASW) with low salinity and a temperature close to 1 °C, the shelf water and the Antarctic Intermediate Water (AAIW) with a temperature above 2 °C and a salinity above 34 psu. Data obtained from all other profiles indicate the occurrence of two water masses highly influenced by mixing processes in upper ocean.

The vertical temperature distribution (Fig. 12.7) shows the typical response to atmospheric cooling processes in the surface layer. In large areas of the transect the water temperature was very close to the freezing point of sea water, sometimes down to 100 m depth. Nevertheless, the water column was clearly stratified except for the stations in the western part of the selected track close to the Antarctic Sound.

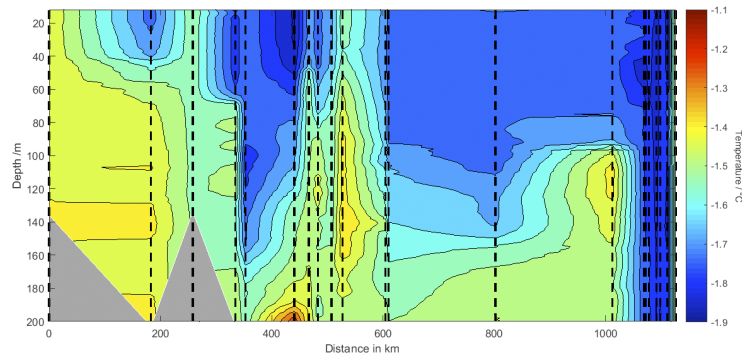


Fig. 12.7: Vertical temperature distribution derived from CTD-profile data (Station 76 to Station 99) along the cruise track, Weddell Sea. The belonging cruise track is shown in Fig. 12.4, blue line.

Figs 12.8 and 12.9 shows preliminary results of the ADCP measurements around Deception Island. The measurement transect started at the inlet of the bay of the island (yellow star) and turned clockwise around the island (duration: 10 h; start at 21:41 UTC (2018-03-30) until 7:44 UTC (2018-03-31)). The near surface currents along the transect are shown in Fig. 12.8. The data were averaged across a water depth ranging from 25 m to 45 m. It can be seen clearly that the currents turned clockwise around the island. Strong currents with values up to 0.4 m s^{-1} were detected near the starting and ending point of the measurement transect. At this position, the current directions differed by nearly 180° (north east and south west). This may be due to tidal forcing as well as due to the influence of the bathymetry in this region. To understand the processes in more detail further investigations are necessary.

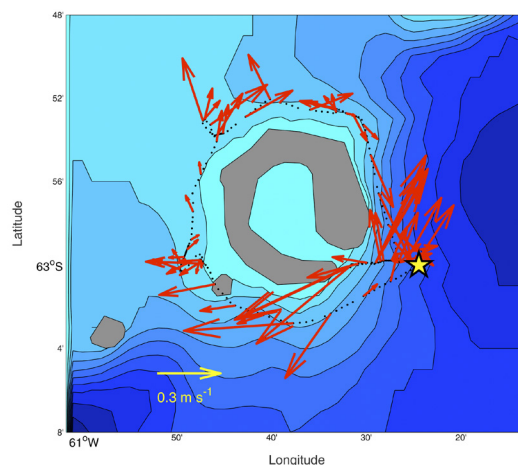


Fig. 12.8: Deception Island – mean surface currents at a water depth from 25 to 45 m. The starting point is marked with a yellow star. Reference velocity vector in yellow with 0.3 m s^{-1} .

The vertical component of the velocity field during this measuring transect is presented in Fig. 12.9. The vertical velocity is shown over the depth along the distance of the transect from the starting point. (see Fig. 12.8 yellow star). Positive values indicate upward directed velocities and negative values downward directed velocities. During the night very high sinking velocities were detected at the eastern part of the island with values up to -0.4 m/s. In this area the bathymetry slope is very steep.

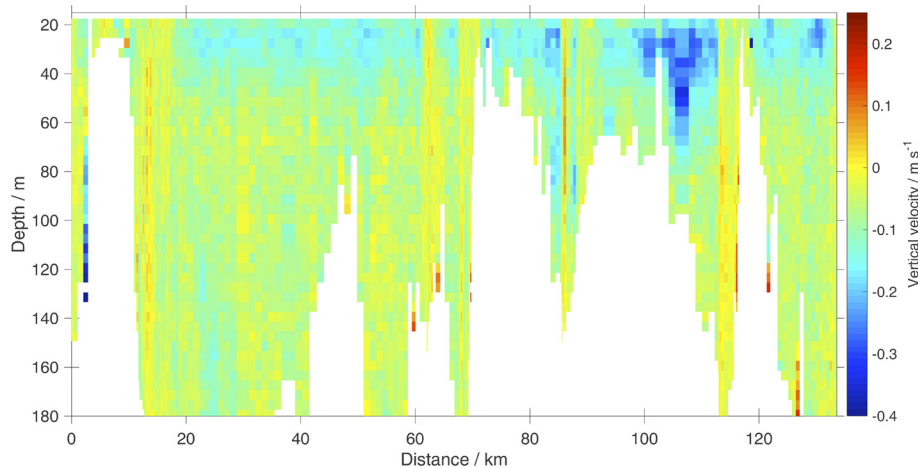


Fig 12.9: Vertical velocity along the transect around deception island (see Fig. 11.8, starting point yellow star); positive values: upward directed velocity and negative values: downward directed velocity

Data management

All CTD-profiles have been checked in terms of quality. Salinity and oxygen data were calibrated with reference methods (Oxygen – Winkler titration, salinity – salinometer). The validated data sets will be available at PANGAEA within 18 months after the cruise at the latest.

References

- Grasshoff K, Kremling K, Ehrhardt M (1999) *Methods of Seawater Analysis*. Wiley-VCH Verlag GmbH; Weinheim.
- IOC, SCOR and IAPSO (2010) *The international thermodynamic equation of seawater – 2010: Calculation and use of thermodynamic properties*. Intergovernmental Oceanographic Commission, Manuals and Guides No. 56, UNESCO (English), 196 pp.
- McDougall TJ, Jackett DR, Millero FJ, Pawlowicz R, Barker PM (2012) A global algorithm for estimating Absolute Salinity. *Ocean Science*, 8, 1123-1134. <http://www.ocean-sci.net/8/1123/2012/os-8-1123-2012.pdf>.
- Millero FJ, Feistel R, Wright DG, McDougall TJ (2008) The composition of Standard Seawater and the definition of the Reference-Composition Salinity Scale. *Deep-Sea Res. I*, 55, 50-72.
- Winkler LW (1888) Die Bestimmung des im Wasser gelösten Sauerstoffes. *Berichte d. deutsch. chem. Gesellschaft*, 21, 2843-2854.

13. SAMPLING AND OBSERVATION OF *SALPA THOMPSONI* AND LARVAL KRILL BY SCIENTIFIC DIVERS

Ulrich Freier¹, Sven Rohde¹, Svenja Julica
Müller¹, Sven Kerwath², Lutz Auerswald²

¹ICBM, Uni Oldenburg
²DAFF

Grant-No. AWI_PS112_00

Objectives

A critical part of the project was to get salps and larval krill in pristine conditions for physiological analysis in general and temperature adaptation experiments on salps in particular. It has been shown on former expeditions that salps collected with nets, even equipped with close cod ends, are not in appropriate conditions for experimental studies onboard. The few existing physiological data on salps were all performed with animals collected by Scuba divers. Therefore, the aim of the scientific dive team was to collect the salp species *S. thompsoni* in particular and when available also larval Krill of the species *Euphausia superba*, under sea ice. In addition, the second aim of the scientific diving group was to film *S. thompsoni* in the natural environment.

Work at sea

The dive operations were performed by using the *Polarstern* rubber boats *Laura* and *Luisa*. *Luisa* is motorised with an 70hp Yamaha outboarder, *Laura* with a 35 hp Diesel outboard motor. Therefore, technical assistance and transportation of the sampling gear was performed with the less powerful rubber boat *Laura*. At the dive site, the boats were connected to each other.

According to AWI safety regulations, prior to the scientific dive operations specific safety operations, were performed. Special attention was given to the appearance of leopard seals. Depending on the weather conditions helicopter flights were carried out within a radius of 5 km around the ship to ensure that no leopard seals were around. Oxygen and first aid was provided on the rubber boats. The hospital on *Polarstern* was on „stand by“ during all dive operations.

Sampling of salps was performed with soup ladles and the modular MASMA PRO -motor pump. The system consists of a motor driven centrifuge pump (0.40 m³ min⁻¹) connected to a plankton filtration system. The filtration was carried out through a zooplankton net (200-1,000 µm mesh size) with a 2 liter cod end located inside the airtight container and placed upstream of the centrifuge pump. It is a modification of the MASMA-Pump, described in Meyer et al. (2009), in the way that the flow rate was adjustable to catch fragile species such as salps. Observation studies of salps in the natural environment, near the surface were performed with a Sony camcorder in a BS Kinetics underwater housing.

Tab 13.1: Total diving operations and helicopter flights for leopard seals observations

Activities PS 112	Helicopter	Zodiac operation	Diving
	Leopard Seal		video/sampling
King George Island	20	180	
Half Moon Island		120	
Deception Island	55	360	90
off Deception Island		175	
Elephant Island	13	240	35
off Elephant Island	16	180	60
Antarctic Sound		190	
Elephant Island	19	260	
total min	123	1705	185

In addition to the successful sampling and filming, listed in Table 13.1. In addition, 15 dive/sampling operations were initiated but cancelled at short notice due to logistical reasons or changing weather conditions.

To maximize the efficiency of the dive operation the following improvements can be suggested:

When dive operations are part of the cruise it has to be considered that station scheduling for other on-board activities needs to be kept flexible, as diving is the operation that is most dependent on weather conditions. A save and effective Antarctic diving operation requires at least 3-4 hours of time in the ship's schedule. Other sampling can continue concurrently, as long as *Polarstern* is on standby and within reach of the divers, to look out for Leopard seals, and to respond to possible emergencies.

A summary of suggestions and examples to optimize the handling of the rubber boats between the decks crew and the scientific dive group during launch and recovery was provided in a written note to the captain and the cruise leader as a kind of SOP.

Data management

The film material will be used for lectures and publications.

References

Meyer B, Fuentes V, Guerra C, Schmidt K, Spahic S, Cisewski B, Freier U, Olariaga A, Bathmann U (2009) Physiology, growth and development of larval krill *Euphausia superba* in autumn and winter in the Lazarev Sea, Antarctica. *Limnology and Oceanography*, 54, 1595-1614.

A.1 TEILNEHMENDE INSTITUTE / PARTICIPATING INSTITUTIONS

Institute	Address
AAD	Australian Antarctic Division 203 Channel Highway Kingston Tasmania 7050 Australia
AWI	Alfred-Wegener-Institut Helmholtz-Zentrum für Polar- und Meeresforschung Postfach 120161 27515 Bremerhaven Germany
BBC	British Broadcasting Corporation Broadcasting House Egton Wing Portland Place London W1A 1AA United Kingdom
DAFF	Department of Agriculture, Forestry and Fisheries Inshore Resources Research Branch: Fisheries Private Bag X2, Rogge Bay 8012 Cape Town, South Africa
DWD	Deutscher Wetterdienst Geschäftsbereich Wettervorhersage Seeschiffahrtsberatung Bernhard Nocht Str. 76 20359 Hamburg Germany
HeliService	Heli Service International GmbH Gorch Fock Strasse 105 26721 Emden Germany
Hochschule Brhv.	Hochschule Bremerhaven An der Karlstadt 8 27568 Bremerhaven Germany

A.1 Teilnehmende Institute / Participating Institutions

Institute	Address
ICBM	Institut für Chemie und Biologie des Meeres Carl-von-Ossietzky-Straße 911 26133 Oldenburg Germany
MARUM	Zentrum für Marine Umweltwissenschaften Leobener Straße 8 28359 Bremen Germany
OGS	Istituto Nazionale di Oceanografia e di Geofisica Sperimentale Via Auguste Piccard 54 34151 Trieste TS Italy
TiHo	Tierärztliche Hochschule Hannover Bünteweg 2 30559 Hannover Germany
UBC	University of British Columbia 2329 West Mall Vancouver, BC V6T 1Z4 Canada
UNIGE	Université de Genève 1205 Genf Switzerland
Uni Bremen	Universität Bremen Bibliothekstraße 1 28359 Bremen Germany
Uni CA	University of California, Santa Cruz 1156 High St Santa Cruz CA 95064 USA
Uni Gdansk	University of Gdansk Jana Bażyńskiego 8 80-309 Gdańsk Poland

Institute	Address
Uni Hamburg	Universität Hamburg Mittelweg 177 20148 Hamburg Germany
Uni Oldenburg	Universität Oldenburg Ammerländer Heerstraße 114 26129 Oldenburg Germany
Uni Padova	Universita di Padova Via 8 Febbraio 1848, 2, 35122 Padova PD Italy
Uni St. Andrews	University of St. Andrews St Andrews KY16 9AJ United Kingdom

A.2 FAHRTTEILNEHMER / CRUISE PARTICIPANTS

Name/ Last name	Vorname/ First name	Institut/ Institute	Beruf/ Profession
Auerswald	Lutz	DAFF	Biologist
Badewien	Thomas	ICBM	Oceanographer
Bahlburg	Dominik	AWI	Student, biology
Bernasconi	Matteo	Uni St. Andrews	Acoustician
Böckmann	Sebastian	Uni Bremen	PhD student, biology
Butter	Michael	ICBM	Student, oceanography
Diociaiuti	Tommaso	OGS	PhD student, biology
Driscoll	Ryan	Uni CA	Biologist
Fernandez	Victor Santos	Heli Service Int.	Mechanic
Flintrop	Clara	MARUM, AWI	PhD student, biology
Freier	Ulrich	ICBM	Biologist
Friedrichs	Anna	ICBM	Oceanographer
Gregory	Bertie	BBC	Camera operator
Halbach	Laura	AWI	Student, biology
Hawthone	Robert	BBC	Camera operator
Heim	Thomas	Heli Service Int.	Mechanic
Hempelt	Juliane	DWD	Technician, meterology
Herr	Helena	Uni Hamburg	Biologist
Iversen	Morten	MARUM, AWI	Biologist
Jager	Harold	Heli Service Int.	Pilot
Kenzia	Jan	Heli Service Int.	Pilot
Kerwath	Sven	DAFF	Biologist
Koch	Florian	Hochschule Brhv., AWI	Biologist
Konrad	Christian	MARUM	Engineer, biology
Koschnick	Nils	AWI	Engineer, biology
Lees	Abigail	BBC	TV Director
Lucassen	Magnus	AWI	Biologist
Meyer	Bettina	AWI, ICBM	Biologist
Monti	Marina	OGS	Biologist
Moorthi	Stefanie	ICBM	Biologist
Müller	Max	DWD	Meteorologist

Name/ Last name	Vorname/ First name	Institut/ Institute	Beruf/ Profession
Müller	Svenja Julica	ICBM	Student, biology
Pagnone	Anna	AWI	PhD student, biology
Pakhomov	Evgeny	UBC	Biologist
Pakhomov	Larysa	UBC	Technician, biology
Panasiuk	Anna	Uni Gdansk	Biologist
Papetti	Chiara	Uni Padua	Biologist
Pauli	Nora	ICBM, AWI	PhD student, biology
Pausch	Franziska	AWI	PhD student, biology
Pitzschler	Lisa	AWI	Student, biology
Plum	Christoph	ICBM	Biologist
Rhode	Sven	ICBM	Biologist
Schulz	Anne-Christin	ICBM	Oceanographer
Viquerat	Sacha	TiHo Hannover	Biologist
Vortkamp	Martina	AWI	Technician, biology
Waller	Natasha	AAD	Technician, biology
Wawrzynek	Justyna	Uni Gdansk	PhD student, biology
Wenta	Philipp	ICBM	PhD student, biology
Wessels	Wiebke	ICBM, AWI	Biologist
Wilhelms-Dick	Dorothee	AWI	Engineer, biology

15. SCHIFFSBESATZUNG / SHIP'S CREW

	Name	Rank
01.	Wunderlich, Thomas	Master
02.	Grundmann, Uwe	Chiefmate
03.	Lauber, Feli	Chiefmate
04.	Fischer, Tibor	2nd Mate
05.	Peine, Lutz	2nd Mate
06.	Farysch, Bernd	Chief
07.	Pohl, Klaus	Ship's Doc.
08.	Schnürch, Helmut	2.Eng.
09.	Buch, Erik-Torsten	2.Eng.
10.	Rusch, Torben 2.	2.Eng.
11.	Brehme, Andreas	E-Eng.
12.	Hofmann, Walter Jörg	Chief ELO
13.	Frank, Gerhard	Electron
14.	Markert, Winfried	Electron.
15.	Winter, Andreas	Electron.
16.	Feiertag, Thomas	Electron.
17.	Sedlak, Andreas	Bosun
18.	Neisner, Winfried	Carpenter
19.	Clasen, Nils	MP Rat
20.	Müller, Steffen	MP Rat
21.	Schröder, Horst	MP Rat
22.	Schröder, Norbert	MP Rat
23.	Fölster, Michael	A.B.
24.	Burzan, Gerd-Ekkehard	A.B.
25.	Brickmann, Peter	A.B.
26.	Köster, Andreas	A.B.
27.	Hartwig-Labahn, Andreas	A.B.
28.	Beth, Detlef	Storekeep.
29.	Plehn, Markus	MP Rat
30.	Waterstradt, Feli	MP Ra
31.	Krösche, Eckard	Mot-man
32.	Dinse, Horst	Mot-man
33.	Watzel, Bernhard	Mot-man
34.	Meißner, Jörg	Cook
35.	Tupy, Mario	Cooksmate
36.	Lohmann, Christian	Cooksmate
37.	Wartenberg, Irina	1. Stwdess
38.	Leue, Andreas Georg	Stwd/KS
39.	Hischke, Peggy	2. Stwdess
40.	Duka, Maribel	2. Stwdess
41.	Krause, Tomasz	2. Steward
42.	Shi, Wubo	2. Steward
43.	Chen, Quan Lun	2. Steward
44.	Sun, Yong Sheng	Laundrym.

A.4 STATIONSLISTE / STATION LIST

Station	Date	Time	Latitude	Longi-tude	Depth [m]	Gear	Action	Comment
PS112_0_Underway-1	2018-03-17	4:00	-53.11588	-70.84446	43	WST	profile start	
PS112_0_Underway-2	2018-03-21	0:38	-57.94454	-61.75469		ADCP_150	profile start	
PS112_0_Underway-2	2018-05-03	2:31	-58.36529	-58.56247	3441	ADCP_150	profile end	
PS112_0_Underway-3	2018-03-21	12:41	-59.73899	-59.61923	3067	FBOX	profile start	
PS112_0_Underway-3	2018-05-03	2:35	-58.36566	-58.56079	3438	FBOX	profile end	
PS112_0_Underway-4	2018-03-21	12:41	-59.73822	-59.62009	3066	PCO2_SUB	profile start	
PS112_0_Underway-4	2018-05-03	2:36	-58.36575	-58.56037	3439	PCO2_SUB	profile end	
PS112_0_Underway-5	2018-03-21	12:41	-59.73764	-59.62077	3065	PCO2_GO	profile start	
PS112_0_Underway-5	2018-05-03	2:35	-58.36571	-58.56056	3440	PCO2_GO	profile end	
PS112_0_Underway-6	2018-03-21	0:39	-57.94721	-61.75146	851	TSG_KEEL	profile start	
PS112_0_Underway-6	2018-04-30	11:00	-60.95663	-54.96953	988	TSG_KEEL	profile end	
PS112_0_Underway-6	2018-04-30	18:00	-61.13834	-54.32693	1240	TSG_KEEL	profile start	
PS112_0_Underway-6	2018-05-03	2:48	-58.34653	-58.60389	3527	TSG_KEEL	profile end	
PS112_0_Underway-7	2018-03-21	0:39	-57.94653	-61.75233	851	TSG_KEEL_2	profile start	
PS112_0_Underway-7	2018-04-30	11:00	-60.95663	-54.96953	988	TSG_KEEL_2	profile end	
PS112_0_Underway-7	2018-04-30	18:00	-61.13834	-54.32693	1240	TSG_KEEL_2	profile start	
PS112_0_Underway-7	2018-05-03	2:47	-58.34701	-58.60258	3517	TSG_KEEL_2	profile end	
PS112_0_Underway-8	2018-03-22	18:00	-62.18810	-58.35451	465	RM	profile start	
PS112_0_Underway-8	2018-04-29	17:01	-60.84824	-55.36696	1540	RM	profile end	
PS112_1-1	2018-03-21	21:45	-61.01159	-58.32920	5224	EK60	profile start	
PS112_1-1	2018-03-23	19:13	-62.08979	-58.33539	69	EK60	station start	
PS112_1-1	2018-03-29	15:48	-62.98684	-60.34951	812	EK60	station start	
PS112_1-1	2018-05-02	21:30	-58.41517	-58.49392	3597	EK60	profile end	

A.4 Stationsliste / Station List

Station	Date	Time	Latitude	Longi-tude	Depth [m]	Gear	Action	Comment
PS112_2-1	2018-03-21	21:08	-61.00377	-58.33374	5221	CTDICBM	station start	
PS112_2-1	2018-03-21	21:23	-61.00648	-58.33227	5223	CTDICBM	at depth	
PS112_2-1	2018-03-21	21:43	-61.01093	-58.32974	5222	CTDICBM	station end	
PS112_2-2	2018-03-21	23:06	-61.01554	-58.32819	5220	TMPUMP	station start	
PS112_2-2	2018-03-21	23:06	-61.01577	-58.32794	5221	TMPUMP	profile start	
PS112_2-2	2018-03-22	1:35	-61.03711	-58.30345	4918	TMPUMP	profile end	
PS112_2-2	2018-03-22	1:36	-61.03923	-58.29787	4950	TMPUMP	station end	
PS112_3-1	2018-03-22	16:57	-62.19170	-58.33646	434	TRAP	at depth	
PS112_4-1	2018-03-22	17:13	-62.18649	-58.34988	457	TRAP	at depth	
PS112_5-1	2018-03-22	20:21	-62.23627	-58.14856	1082	IKMT	station start	
PS112_5-1	2018-03-22	20:28	-62.23165	-58.14393	1031	IKMT	at depth	
PS112_5-1	2018-03-22	20:48	-62.22097	-58.13247	751	IKMT	station end	
PS112_5-2	2018-03-22	21:10	-62.24587	-58.17253	863	IKMT	station start	
PS112_5-2	2018-03-22	21:19	-62.25053	-58.17934	803	IKMT	at depth	
PS112_5-2	2018-03-22	21:41	-62.25841	-58.19078	752	IKMT	station end	
PS112_6-1	2018-03-22	23:06	-62.18471	-58.38640	534	CTDICBM	station start	
PS112_6-1	2018-03-22	23:24	-62.18490	-58.38644	535	CTDICBM	at depth	
PS112_6-1	2018-03-23	0:41	-62.18526	-58.38619	535	CTDICBM	station end	
PS112_7-1	2018-03-23	12:38	-62.09088	-58.33799	74	CTDICBM	station start	
PS112_7-1	2018-03-23	12:53	-62.09080	-58.33593	70	CTDICBM	at depth	
PS112_7-1	2018-03-23	12:59	-62.09081	-58.33626	64	CTDICBM	station end	
PS112_7-2	2018-03-23	13:31	-62.09100	-58.33687	61	SECCI	station start	
PS112_7-2	2018-03-23	13:36	-62.09103	-58.33700	61	SECCI	station end	
PS112_8-1	2018-03-23	17:08	-62.08973	-58.33543	69	BOAT	station start	
PS112_8-2	2018-03-23	23:18	-62.09020	-58.33548	70	BOAT	station start	
PS112_8-2	2018-03-24	0:07	-62.09006	-58.33536	69	BOAT	station end	
PS112_8-3	2018-03-24	2:17	-62.09031	-58.33539	69	MSC	station start	
PS112_8-3	2018-03-24	2:19	-62.09034	-58.33533	69	MSC	at depth	
PS112_8-3	2018-03-24	2:27	-62.09009	-58.33539	69	MSC	station end	
PS112_8-4	2018-03-24	2:44	-62.08980	-58.33516	71	MSC	station start	
PS112_8-4	2018-03-24	2:46	-62.08972	-58.33514	72	MSC	at depth	
PS112_8-4	2018-03-24	2:52	-62.08976	-58.33517	69	MSC	station end	
PS112_8-5	2018-03-24	3:04	-62.09008	-58.33502	69	ISPC	station start	
PS112_8-5	2018-03-24	3:16	-62.08947	-58.33511	75	ISPC	at depth	
PS112_8-5	2018-03-24	3:19	-62.08985	-58.33520	68	ISPC	station end	
PS112_9-1	2018-03-24	20:01	-62.19457	-58.33191	429	TRAP	station start	
PS112_9-1	2018-03-24	20:26	-62.19315	-58.33026	393	TRAP	station end	
PS112_10-1	2018-03-24	20:37	-62.18854	-58.34451	439	TRAP	station start	
PS112_10-1	2018-03-24	21:03	-62.18879	-58.33972	427	TRAP	station end	
PS112_11-1	2018-03-24	22:27	-62.33152	-58.49392	647	CTDICBM	station start	
PS112_11-1	2018-03-24	22:47	-62.33194	-58.49515	648	CTDICBM	at depth	

Station	Date	Time	Latitude	Longi-tude	Depth [m]	Gear	Action	Comment
PS112_11-1	2018-03-24	23:17	-62.33249	-58.49650	651	CTDICBM	station end	
PS112_11-2	2018-03-25	1:08	-62.34836	-58.38963	1471	M-RMT	station start	
PS112_11-2	2018-03-25	1:22	-62.33825	-58.38673	1494	M-RMT	profile start	
PS112_11-2	2018-03-25	1:41	-62.32471	-58.38902	1461	M-RMT	profile end	
PS112_11-2	2018-03-25	1:43	-62.32350	-58.38909	1448	M-RMT	station end	
PS112_12-1	2018-03-25	4:07	-62.50045	-57.98955	1805	CTDICBM	station start	
PS112_12-1	2018-03-25	4:21	-62.49996	-57.98696	1806	CTDICBM	at depth	
PS112_12-1	2018-03-25	4:31	-62.49953	-57.98589	1807	CTDICBM	station end	
PS112_12-2	2018-03-25	4:42	-62.49570	-57.98714	1812	ISPC	station start	
PS112_12-2	2018-03-25	5:19	-62.49413	-57.98271	1810	ISPC	at depth	
PS112_12-2	2018-03-25	5:40	-62.49424	-57.98109	1809	ISPC	station end	
PS112_12-3	2018-03-25	6:04	-62.49021	-57.98699	1814	M-RMT	station start	
PS112_12-3	2018-03-25	6:18	-62.48519	-57.99649	1818	M-RMT	station end	
PS112_12-3	2018-03-25	6:35	-62.48449	-57.99277	1817	M-RMT	station start	
PS112_12-3	2018-03-25	6:38	-62.48301	-57.99622	1820	M-RMT	profile start	
PS112_12-3	2018-03-25	6:52	-62.47762	-58.00949	1834	M-RMT	at depth	
PS112_12-3	2018-03-25	7:33	-62.46834	-58.03100	1850	M-RMT	station end	
PS112_13-1	2018-03-25	11:46	-63.02118	-57.55914	126	CTDICBM	station start	
PS112_13-1	2018-03-25	11:55	-63.02207	-57.55060	118	CTDICBM	at depth	
PS112_13-1	2018-03-25	12:05	-63.02268	-57.54083	122	CTDICBM	station end	
PS112_13-2	2018-03-25	12:13	-63.02201	-57.53605	117	SECCI	station start	
PS112_13-2	2018-03-25	12:16	-63.02177	-57.53480	119	SECCI	station end	
PS112_13-3	2018-03-25	13:14	-62.97598	-57.59013	116	IKMT	at depth	
PS112_13-3	2018-03-25	13:26	-62.96841	-57.59884	119	IKMT	station end	
PS112_14-1	2018-03-25	14:57	-63.00154	-57.99318	430	CTDICBM	station start	
PS112_14-1	2018-03-25	15:09	-63.00248	-57.99148	419	CTDICBM	at depth	
PS112_14-1	2018-03-25	15:22	-63.00278	-57.99079	414	CTDICBM	station end	
PS112_14-2	2018-03-25	15:33	-63.00306	-57.99003	411	SECCI	station start	
PS112_14-2	2018-03-25	15:36	-63.00312	-57.98960	410	SECCI	station end	
PS112_14-3	2018-03-25	15:47	-63.00233	-57.98951	419	IKMT	station start	
PS112_14-3	2018-03-25	15:54	-62.99930	-57.99357	452	IKMT	at depth	
PS112_14-3	2018-03-25	16:14	-62.99281	-58.00237	466	IKMT	station end	
PS112_14-4	2018-03-25	16:35	-63.00125	-57.98664	453	IKMT	station start	
PS112_14-4	2018-03-25	16:38	-63.00041	-57.98728	468	IKMT	at depth	
PS112_14-4	2018-03-25	16:58	-62.99726	-57.98833	456	IKMT	station end	
PS112_15-1	2018-03-25	18:38	-62.99898	-58.50258	382	CTDICBM	station start	
PS112_15-1	2018-03-25	18:51	-62.99974	-58.50042	383	CTDICBM	at depth	
PS112_15-1	2018-03-25	19:05	-62.99866	-58.50501	377	CTDICBM	station end	
PS112_15-2	2018-03-25	19:27	-62.99877	-58.50304	380	CTDICBM	station start	
PS112_15-2	2018-03-25	19:33	-62.99930	-58.50005	383	CTDICBM	at depth	
PS112_15-2	2018-03-25	19:39	-62.99952	-58.49983	383	CTDICBM	station end	

A.4 Stationsliste / Station List

Station	Date	Time	Latitude	Longi-tude	Depth [m]	Gear	Action	Comment
PS112_15-3	2018-03-25	20:37	-62.99943	-58.50142	382	CTDICBM	station start	
PS112_15-3	2018-03-25	20:43	-62.99928	-58.50028	384	CTDICBM	at depth	
PS112_15-3	2018-03-25	20:49	-62.99913	-58.49912	386	CTDICBM	station end	
PS112_15-4	2018-03-25	21:10	-62.99754	-58.49801	393	IKMT	station start	
PS112_15-4	2018-03-25	21:18	-62.99283	-58.50585	390	IKMT	at depth	
PS112_15-4	2018-03-25	21:43	-62.98124	-58.52691	412	IKMT	station end	
PS112_16-1	2018-03-25	23:30	-63.00515	-58.99195	506	CTDICBM	station start	
PS112_16-1	2018-03-25	23:32	-63.00494	-58.99270	508	CTDICBM	at depth	
PS112_16-1	2018-03-25	23:57	-63.00573	-58.99903	512	CTDICBM	station end	
PS112_16-2	2018-03-26	0:38	-63.00152	-59.01112	560	IKMT	station start	
PS112_16-2	2018-03-26	1:11	-62.98707	-59.04200	608	IKMT	station end	
PS112_17-1	2018-03-26	3:00	-62.74959	-59.01345	1446	Goflo	station start	
PS112_17-1	2018-03-26	3:36	-62.75688	-59.00495	1440	Goflo	at depth	
PS112_17-1	2018-03-26	3:49	-62.75836	-59.00727	1439	Goflo	station end	
PS112_17-2	2018-03-26	3:56	-62.75998	-59.00718	1439	CTDICBM	station start	
PS112_17-2	2018-03-26	4:16	-62.76179	-59.00817	1438	CTDICBM	at depth	
PS112_17-2	2018-03-26	4:34	-62.76506	-59.01087	1435	CTDICBM	station end	
PS112_17-3	2018-03-26	4:45	-62.76589	-59.01182	1434	ISPC	station start	
PS112_17-3	2018-03-26	5:24	-62.76958	-59.01179	1430	ISPC	at depth	
PS112_17-3	2018-03-26	5:44	-62.77026	-59.01237	1429	ISPC	station end	
PS112_17-4	2018-03-26	6:02	-62.74798	-59.00076	1445	MSC	station start	
PS112_17-4	2018-03-26	6:10	-62.74601	-58.99701	1446	MSC	at depth	
PS112_17-4	2018-03-26	6:15	-62.74621	-58.99618	1446	MSC	station end	
PS112_17-5	2018-03-26	6:33	-62.74382	-58.99652	1447	IKMT	station start	
PS112_17-5	2018-03-26	6:41	-62.74112	-59.00528	1449	IKMT	at depth	
PS112_17-5	2018-03-26	7:06	-62.73353	-59.02618	1452	IKMT	station end	
PS112_17-6	2018-03-26	7:13	-62.73207	-59.02769	1453	HN	station start	
PS112_17-6	2018-03-26	7:17	-62.73171	-59.02748	1453	HN	station end	
PS112_17-7	2018-03-26	7:17	-62.73168	-59.02746	1453	HN	station start	
PS112_17-7	2018-03-26	7:19	-62.73157	-59.02730	1453	HN	station end	
PS112_17-8	2018-03-26	7:19	-62.73153	-59.02725	1453	HN	station start	
PS112_17-8	2018-03-26	7:21	-62.73139	-59.02721	1453	HN	station end	
PS112_17-9	2018-03-26	7:21	-62.73132	-59.02718	1453	HN	station start	
PS112_17-9	2018-03-26	7:23	-62.73106	-59.02710	1454	HN	station end	
PS112_17-10	2018-03-26	7:23	-62.73100	-59.02708	1454	HN	station start	
PS112_17-10	2018-03-26	7:25	-62.73085	-59.02708	1453	HN	station end	
PS112_17-11	2018-03-26	7:25	-62.73082	-59.02707	1454	HN	station start	
PS112_17-11	2018-03-26	7:27	-62.73065	-59.02714	1453	HN	station end	
PS112_18-1	2018-03-26	9:24	-62.52411	-59.44486	648	CTDICBM	station start	
PS112_18-1	2018-03-26	9:40	-62.52448	-59.44443	653	CTDICBM	at depth	
PS112_18-1	2018-03-26	9:52	-62.52423	-59.44568	649	CTDICBM	station end	

Station	Date	Time	Latitude	Longi-tude	Depth [m]	Gear	Action	Comment
PS112_18-2	2018-03-26	10:13	-62.53681	-59.40499	712	IKMT	station start	
PS112_18-2	2018-03-26	10:22	-62.53224	-59.41005	662	IKMT	at depth	
PS112_18-2	2018-03-26	10:45	-62.52011	-59.42143	628	IKMT	station end	
PS112_18-3	2018-03-26	10:48	-62.51917	-59.42163	627	SECCI	station start	
PS112_18-3	2018-03-26	10:52	-62.51849	-59.42077	626	SECCI	station end	
PS112_18-4	2018-03-26	11:28	-62.54373	-59.38253	754	IKMT	station start	
PS112_18-4	2018-03-26	12:21	-62.52758	-59.41465	633	IKMT	station end	
PS112_19-1	2018-03-26	14:39	-62.75137	-59.98511	899	CTDICBM	station start	
PS112_19-1	2018-03-26	14:53	-62.74975	-59.98112	914	CTDICBM	at depth	
PS112_19-1	2018-03-26	15:06	-62.74905	-59.97576	932	CTDICBM	station end	
PS112_19-2	2018-03-26	15:16	-62.74854	-59.97134	934	IKMT	station start	
PS112_19-2	2018-03-26	15:24	-62.74428	-59.97469	929	IKMT	at depth	
PS112_19-2	2018-03-26	15:45	-62.73652	-59.97989	839	IKMT	station end	
PS112_19-3	2018-03-26	15:49	-62.73614	-59.97883	838	SECCI	station start	
PS112_19-3	2018-03-26	15:52	-62.73609	-59.97765	842	SECCI	station end	
PS112_20-1	2018-03-26	19:03	-63.00040	-60.00111	937	Goflo	station start	
PS112_20-1	2018-03-26	19:17	-63.00027	-59.99993	938	Goflo	at depth	
PS112_20-1	2018-03-26	19:29	-62.99999	-59.99994	938	Goflo	station end	
PS112_20-2	2018-03-26	19:41	-63.00013	-60.00013	938	CTDICBM	station start	
PS112_20-2	2018-03-26	20:00	-63.00093	-59.99988	939	CTDICBM	at depth	
PS112_20-2	2018-03-26	20:26	-63.00043	-59.99955	938	CTDICBM	station end	
PS112_20-3	2018-03-26	20:35	-63.00071	-60.00001	938	SECCI	station start	
PS112_20-3	2018-03-26	20:37	-63.00061	-60.00036	937	SECCI	station end	
PS112_20-4	2018-03-26	20:44	-63.00024	-60.00121	937	ISPC	station start	
PS112_20-4	2018-03-26	21:16	-63.00088	-60.00113	938	ISPC	at depth	
PS112_20-4	2018-03-26	21:35	-63.00084	-60.00108	937	ISPC	station end	
PS112_20-5	2018-03-26	21:50	-63.00022	-60.00022	937	MSC	station start	
PS112_20-5	2018-03-26	21:57	-63.00000	-60.00114	937	MSC	at depth	
PS112_20-5	2018-03-26	22:06	-62.99990	-60.00160	938	MSC	station end	
PS112_20-6	2018-03-26	22:30	-63.00044	-60.00186	937	BONGO	station start	
PS112_20-6	2018-03-26	22:42	-63.00051	-60.00469	940	BONGO	at depth	
PS112_20-6	2018-03-26	22:53	-63.00070	-60.00626	943	BONGO	station end	
PS112_20-7	2018-03-26	23:02	-63.00019	-60.00612	945	IKMT	station start	
PS112_20-7	2018-03-26	23:13	-62.99705	-60.00367	960	IKMT	at depth	
PS112_20-7	2018-03-26	23:32	-62.98925	-59.99561	958	IKMT	station end	
PS112_20-8	2018-03-26	23:40	-62.98915	-59.99464	959	HN	station start	
PS112_20-8	2018-03-26	23:52	-62.98968	-59.99823	956	HN	station end	
PS112_21-1	2018-03-27	1:17	-62.99978	-60.42258	514	CTDICBM	station start	
PS112_21-1	2018-03-27	1:31	-63.00125	-60.42239	522	CTDICBM	at depth	
PS112_21-1	2018-03-27	1:41	-62.99994	-60.42231	516	CTDICBM	station end	
PS112_21-2	2018-03-27	1:53	-62.99854	-60.42122	509	IKMT	station start	

A.4 Stationsliste / Station List

Station	Date	Time	Latitude	Longi-tude	Depth [m]	Gear	Action	Comment
PS112_21-2	2018-03-27	2:01	-62.99467	-60.41648	496	IKMT	at depth	
PS112_21-2	2018-03-27	2:22	-62.98478	-60.40137	677	IKMT	station end	
PS112_22-1	2018-03-27	2:40	-62.97264	-60.38997	729	BONGO	station start	
PS112_22-1	2018-03-27	2:47	-62.97314	-60.39122	728	BONGO	at depth	
PS112_22-1	2018-03-27	3:00	-62.97306	-60.39226	728	BONGO	station end	
PS112_23-1	2018-03-27	6:06	-62.58719	-59.69697	561	IKMT	station start	
PS112_23-1	2018-03-27	6:15	-62.58368	-59.70203	560	IKMT	at depth	
PS112_23-1	2018-03-27	6:34	-62.57701	-59.71405	574	IKMT	station end	
PS112_24-1	2018-03-27	21:47	-62.58343	-59.87896	128	BONGO	station start	
PS112_24-1	2018-03-27	22:28	-62.58205	-59.87994	195	BONGO	station end	
PS112_24-2	2018-03-27	22:38	-62.58228	-59.88077	173	IKMT	station start	
PS112_24-2	2018-03-27	22:49	-62.58244	-59.88048	171	IKMT	station end	
PS112_24-3	2018-03-28	1:02	-62.58214	-59.87750	213	IKMT	station start	
PS112_24-3	2018-03-28	3:48	-62.58187	-59.88151	193	IKMT	station end	
PS112_24-4	2018-03-28	1:20	-62.58124	-59.88120	240	CTDICBM	station start	
PS112_24-4	2018-03-28	1:33	-62.58169	-59.88071	211	CTDICBM	at depth	
PS112_24-4	2018-03-28	2:13	-62.58184	-59.88340	165	CTDICBM	station end	
PS112_24-5	2018-03-28	2:37	-62.58118	-59.88203	229	SECCI	station start	
PS112_24-5	2018-03-28	2:45	-62.58157	-59.88100	217	SECCI	station end	
PS112_24-6	2018-03-28	2:53	-62.58145	-59.88214	210	ISPC	station start	
PS112_24-6	2018-03-28	3:05	-62.58165	-59.88330	180	ISPC	at depth	
PS112_24-6	2018-03-28	3:12	-62.58176	-59.88371	164	ISPC	station end	
PS112_24-7	2018-03-28	3:26	-62.58157	-59.88379	172	MSC	at depth	
PS112_24-7	2018-03-28	3:31	-62.58173	-59.88342	173	MSC	station end	
PS112_24-8	2018-03-28	4:12	-62.58264	-59.88128	149	IKMT	station start	
PS112_24-8	2018-03-28	4:16	-62.58193	-59.88285	172	IKMT	at depth	
PS112_24-8	2018-03-28	4:32	-62.57787	-59.89141	308	IKMT	station end	
PS112_24-9	2018-03-28	4:39	-62.57890	-59.88906	261	IKMT	station start	
PS112_24-9	2018-03-28	4:42	-62.57865	-59.88953	271	IKMT	at depth	
PS112_24-9	2018-03-28	4:58	-62.57314	-59.90202	389	IKMT	station end	
PS112_24-10	2018-03-28	5:03	-62.57326	-59.90219	386	IKMT	station start	
PS112_24-10	2018-03-28	5:07	-62.57240	-59.90435	392	IKMT	at depth	
PS112_24-10	2018-03-28	5:23	-62.56727	-59.91738	372	IKMT	station end	
PS112_24-11	2018-03-28	5:31	-62.56789	-59.91637	367	IKMT	station start	
PS112_24-11	2018-03-28	5:35	-62.56780	-59.91670	368	IKMT	at depth	
PS112_24-11	2018-03-28	5:49	-62.56280	-59.92677	385	IKMT	station end	
PS112_24-12	2018-03-28	5:54	-62.56247	-59.92695	390	IKMT	station start	
PS112_24-12	2018-03-28	5:58	-62.56178	-59.92788	397	IKMT	at depth	
PS112_24-12	2018-03-28	6:15	-62.55662	-59.93930	345	IKMT	station end	
PS112_24-13	2018-03-28	18:29	-62.57940	-59.88340	325	BOAT	station start	
PS112_24-13	2018-03-28	21:17	-62.57860	-59.88977	274	BOAT	station end	

Station	Date	Time	Latitude	Longi-tude	Depth [m]	Gear	Action	Comment
PS112_24-14	2018-03-28	18:40	-62.57977	-59.88327	307	BONGO	station start	
PS112_24-14	2018-03-28	19:02	-62.57935	-59.88401	317	BONGO	at depth	
PS112_24-14	2018-03-28	19:13	-62.57979	-59.88367	300	BONGO	station end	
PS112_24-15	2018-03-28	22:58	-62.57865	-59.88817	309	SECCI	station start	
PS112_24-15	2018-03-28	23:10	-62.57993	-59.88344	299	SECCI	station end	
PS112_24-17	2018-03-28	23:50	-62.57838	-59.87396	413	IKMT	station start	
PS112_24-17	2018-03-28	23:56	-62.57826	-59.87560	410	IKMT	at depth	
PS112_24-17	2018-03-28	23:58	-62.57825	-59.87595	408	IKMT	station end	
PS112_24-18	2018-03-29	0:16	-62.57797	-59.87855	405	ISPC	station start	
PS112_24-18	2018-03-29	0:42	-62.57841	-59.88124	374	ISPC	at depth	
PS112_24-18	2018-03-29	0:58	-62.57919	-59.88162	344	ISPC	station end	
PS112_24-19	2018-03-29	0:40	-62.57832	-59.88117	377	HN	station start	
PS112_24-19	2018-03-29	1:34	-62.58231	-59.88311	148	HN	station end	
PS112_25-1	2018-03-29	10:36	-63.00139	-60.41862	551	IKMT	station start	
PS112_25-1	2018-03-29	10:45	-62.99920	-60.42984	449	IKMT	at depth	
PS112_25-1	2018-03-29	11:06	-62.99377	-60.45802	348	IKMT	station end	
PS112_25-2	2018-03-29	11:35	-63.00172	-60.41924	546	IKMT	station start	
PS112_25-2	2018-03-29	11:42	-63.00039	-60.42354	507	IKMT	at depth	
PS112_25-2	2018-03-29	12:02	-62.99736	-60.43503	387	IKMT	station end	
PS112_25-3	2018-03-29	12:09	-62.99648	-60.43657	372	IKMT	station start	
PS112_25-3	2018-03-29	12:12	-62.99592	-60.43869	366	IKMT	at depth	
PS112_25-3	2018-03-29	12:29	-62.99220	-60.44997	430	IKMT	station end	
PS112_25-4	2018-03-29	13:28	-63.00370	-60.42441	515	IKMT	station start	
PS112_25-4	2018-03-29	13:33	-63.00192	-60.42954	477	IKMT	at depth	
PS112_25-4	2018-03-29	14:02	-62.99269	-60.44775	427	IKMT	station end	
PS112_25-5	2018-03-29	14:51	-62.99743	-60.34949	681	CTDICBM	station start	
PS112_25-5	2018-03-29	15:06	-62.99428	-60.35226	731	CTDICBM	at depth	
PS112_25-5	2018-03-29	15:20	-62.99046	-60.35228	796	CTDICBM	station end	
PS112_25-6	2018-03-29	15:36	-62.98756	-60.35142	810	SECCI	station start	
PS112_25-6	2018-03-29	15:37	-62.98747	-60.35130	811	SECCI	station end	
PS112_25-7	2018-03-29	23:03	-62.97615	-60.48050	113	BOAT	station end	
PS112_25-8	2018-03-29	21:48	-62.97389	-60.47721	144	CTDICBM	at depth	
PS112_25-8	2018-03-29	22:00	-62.97376	-60.47799	140	CTDICBM	station end	
PS112_25-9	2018-03-29	22:14	-62.97368	-60.47846	137	ISPC	station start	
PS112_25-9	2018-03-29	22:26	-62.97383	-60.47897	131	ISPC	at depth	
PS112_25-9	2018-03-29	22:35	-62.97380	-60.47868	134	ISPC	station end	
PS112_25-10	2018-03-30	0:27	-62.97832	-60.46671	268	IKMT	station start	
PS112_25-10	2018-03-30	0:37	-62.97254	-60.46885	237	IKMT	at depth	
PS112_25-10	2018-03-30	1:00	-62.96069	-60.47145	211	IKMT	station end	
PS112_25-11	2018-03-30	3:38	-62.96479	-60.46907	250	IKMT	station start	
PS112_25-11	2018-03-30	3:41	-62.96615	-60.46593	301	IKMT	at depth	

A.4 Stationsliste / Station List

Station	Date	Time	Latitude	Longi-tude	Depth [m]	Gear	Action	Comment
PS112_25-11	2018-03-30	3:57	-62.96971	-60.45201	388	IKMT	station end	
PS112_25-12	2018-03-30	6:30	-62.97218	-60.46194	303	IKMT	station start	
PS112_25-12	2018-03-30	6:32	-62.97158	-60.46256	307	IKMT	at depth	
PS112_25-12	2018-03-30	6:43	-62.96908	-60.46469	319	IKMT	station end	
PS112_25-13	2018-03-30	9:37	-63.01116	-60.47588	362	IKMT	station start	
PS112_25-13	2018-03-30	9:42	-63.00845	-60.47532	337	IKMT	at depth	
PS112_25-13	2018-03-30	9:54	-63.00413	-60.47500	261	IKMT	station end	
PS112_25-14	2018-03-30	11:06	-63.01445	-60.47726	410	IKMT	station start	
PS112_25-14	2018-03-30	11:12	-63.01242	-60.47783	385	IKMT	at depth	
PS112_25-14	2018-03-30	11:35	-63.00182	-60.47671	236	IKMT	station end	
PS112_25-15	2018-03-30	11:58	-63.01452	-60.48683	358	IKMT	station start	
PS112_25-15	2018-03-30	12:06	-63.01223	-60.48405	338	IKMT	at depth	
PS112_25-15	2018-03-30	12:12	-63.01018	-60.48157	332	IKMT	station end	
PS112_25-16	2018-03-30	12:36	-63.01526	-60.49102	357	IKMT	station start	
PS112_25-16	2018-03-30	12:38	-63.01469	-60.49083	352	IKMT	at depth	
PS112_25-16	2018-03-30	12:50	-63.01130	-60.48733	318	IKMT	station end	
PS112_25-17	2018-03-30	13:10	-63.00944	-60.49898	257	IKMT	station start	
PS112_25-17	2018-03-30	13:14	-63.00852	-60.49731	250	IKMT	at depth	
PS112_25-17	2018-03-30	13:30	-63.00504	-60.49120	224	IKMT	station end	
PS112_25-18	2018-03-30	13:39	-63.00430	-60.48733	248	IKMT	station start	
PS112_25-18	2018-03-30	13:49	-63.00100	-60.48266	201	IKMT	at depth	
PS112_25-18	2018-03-30	13:55	-62.99981	-60.48065	195	IKMT	station end	
PS112_25-19	2018-03-30	14:02	-62.99909	-60.47960	194	IKMT	station start	
PS112_25-19	2018-03-30	14:08	-62.99643	-60.47888	184	IKMT	at depth	
PS112_25-19	2018-03-30	14:18	-62.99432	-60.47821	211	IKMT	station end	
PS112_25-20	2018-03-30	14:31	-62.99176	-60.47457	265	IKMT	station start	
PS112_25-20	2018-03-30	14:35	-62.99091	-60.47411	275	IKMT	at depth	
PS112_25-20	2018-03-30	14:51	-62.98731	-60.47232	294	IKMT	station end	
PS112_25-21	2018-03-30	15:37	-62.98826	-60.47592	250	IKMT	station start	
PS112_25-21	2018-03-30	15:44	-62.98504	-60.47587	262	IKMT	at depth	
PS112_25-21	2018-03-30	16:00	-62.97819	-60.47577	186	IKMT	station end	
PS112_25-22	2018-03-30	16:44	-62.99880	-60.52537	31.8	BOAT	station start	
PS112_25-22	2018-03-30	22:55	-63.00183	-60.53063	32.2	BOAT	station end	
PS112_25-23	2018-03-30	17:40	-63.03691	-60.52965	331	ADCP_150	profile start	
PS112_25-23	2018-03-30	19:44	-62.97110	-60.47830	186	ADCP_150	profile end	
PS112_25-24	2018-03-30	18:25	-63.00418	-60.50321	158	CTDICBM	station start	
PS112_25-24	2018-03-30	18:37	-63.00148	-60.49682	141	CTDICBM	at depth	
PS112_25-24	2018-03-30	18:45	-63.00053	-60.49492	147	CTDICBM	station end	
PS112_25-25	2018-03-30	18:54	-62.99867	-60.49245	132	SECCI	station start	
PS112_25-25	2018-03-30	19:00	-62.99723	-60.49023	117	SECCI	station end	
PS112_25-26	2018-03-30	20:14	-62.99795	-60.48946	146	IKMT	station start	

Station	Date	Time	Latitude	Longi-tude	Depth [m]	Gear	Action	Comment
PS112_25-26	2018-03-30	20:18	-62.99459	-60.48801	98	IKMT	at depth	
PS112_25-26	2018-03-30	20:31	-62.98291	-60.48098	205	IKMT	station end	
PS112_25-27	2018-03-30	21:43	-62.99823	-60.48328	187	CTDICBM	station start	
PS112_25-27	2018-03-30	21:58	-62.99847	-60.48334	188	CTDICBM	at depth	
PS112_25-27	2018-03-30	22:11	-62.99842	-60.48362	188	CTDICBM	station end	
PS112_25-28	2018-03-30	23:28	-62.99675	-60.47090	220	IKMT	station start	
PS112_25-28	2018-03-31	0:00	-62.99704	-60.42905	410	IKMT	station end	
PS112_25-29	2018-03-31	1:40	-62.99716	-60.78871	180	CTDICBM	station start	
PS112_25-29	2018-03-31	1:52	-62.99657	-60.79190	177	CTDICBM	at depth	
PS112_25-29	2018-03-31	2:02	-62.99577	-60.79343	172	CTDICBM	station end	
PS112_25-30	2018-03-31	2:04	-62.99577	-60.79339	171	HN	station start	
PS112_25-30	2018-03-31	2:09	-62.99587	-60.79313	172	HN	station end	
PS112_25-31	2018-03-31	2:40	-63.00297	-60.82836	289	IKMT	station start	
PS112_25-31	2018-03-31	2:49	-62.99799	-60.82430	257	IKMT	at depth	
PS112_25-31	2018-03-31	3:14	-62.98442	-60.81296	66	IKMT	station end	
PS112_25-32	2018-03-31	4:06	-62.88422	-60.78663	179	CTDICBM	station start	
PS112_25-32	2018-03-31	4:18	-62.88358	-60.78503	183	CTDICBM	at depth	
PS112_25-32	2018-03-31	4:25	-62.88343	-60.78456	184	CTDICBM	station end	
PS112_25-33	2018-03-31	4:38	-62.89643	-60.76531	130	IKMT	station start	
PS112_25-33	2018-03-31	4:42	-62.89595	-60.76173	126	IKMT	at depth	
PS112_25-33	2018-03-31	4:52	-62.89495	-60.75276	113	IKMT	station end	
PS112_25-34	2018-03-31	5:46	-62.87643	-60.55242	233	CTDICBM	station start	
PS112_25-34	2018-03-31	5:57	-62.87571	-60.55268	246	CTDICBM	at depth	
PS112_25-34	2018-03-31	6:08	-62.87522	-60.55336	248	CTDICBM	station end	
PS112_25-35	2018-03-31	6:18	-62.87920	-60.53414	185	IKMT	station start	
PS112_25-35	2018-03-31	6:23	-62.87994	-60.52721	90	IKMT	at depth	
PS112_25-35	2018-03-31	6:31	-62.88134	-60.51838	52	IKMT	station end	
PS112_25-36	2018-03-31	7:32	-62.99779	-60.44090	382	CTDICBM	station start	
PS112_25-36	2018-03-31	7:48	-62.99773	-60.44153	381	CTDICBM	at depth	
PS112_25-36	2018-03-31	8:13	-62.99796	-60.44606	377	CTDICBM	station end	
PS112_25-37	2018-03-31	8:24	-62.99917	-60.44678	395	IKMT	station start	
PS112_25-37	2018-03-31	8:34	-62.99958	-60.45968	306	IKMT	at depth	
PS112_25-37	2018-03-31	9:02	-63.00243	-60.49513	170	IKMT	station end	
PS112_25-38	2018-03-31	9:45	-62.99636	-60.33662	747	CTDICBM	station start	
PS112_25-38	2018-03-31	10:04	-62.99613	-60.33808	748	CTDICBM	at depth	
PS112_25-38	2018-03-31	10:28	-62.99601	-60.33922	746	CTDICBM	station end	
PS112_25-39	2018-03-31	10:13	-62.99600	-60.33807	749	BOAT	station start	
PS112_25-39	2018-03-31	11:43	-62.99001	-60.37497	711	BOAT	station end	
PS112_25-40	2018-03-31	10:39	-62.99517	-60.34551	718	IKMT	station start	
PS112_25-40	2018-03-31	10:46	-62.99461	-60.35348	701	IKMT	at depth	
PS112_25-40	2018-03-31	11:06	-62.99363	-60.37258	677	IKMT	station end	

A.4 Stationsliste / Station List

Station	Date	Time	Latitude	Longi-tude	Depth [m]	Gear	Action	Comment
PS112_25-41	2018-03-31	11:17	-62.99292	-60.37623	653	CTDICBM	station start	
PS112_25-41	2018-03-31	11:24	-62.99240	-60.37565	689	CTDICBM	at depth	
PS112_25-41	2018-03-31	11:31	-62.99150	-60.37558	696	CTDICBM	station end	
PS112_25-42	2018-03-31	11:56	-62.98869	-60.37513	693	CTDICBM	station start	
PS112_25-42	2018-03-31	12:04	-62.98809	-60.37519	699	CTDICBM	at depth	
PS112_25-42	2018-03-31	12:10	-62.98753	-60.37513	704	CTDICBM	station end	
PS112_25-43	2018-03-31	12:37	-62.98654	-60.37555	721	CTDICBM	station start	
PS112_25-43	2018-03-31	12:43	-62.98617	-60.37518	727	CTDICBM	at depth	
PS112_25-43	2018-03-31	12:52	-62.98521	-60.37456	743	CTDICBM	station end	
PS112_25-44	2018-03-31	13:32	-62.99958	-60.43379	435	DSTRM	station start	
PS112_25-44	2018-04-01	15:07	-62.87005	-60.19192	254	DSTRM	station end	
PS112_25-45	2018-03-31	22:15	-62.95908	-60.35542	834	ISPC	station start	
PS112_25-45	2018-03-31	22:51	-62.95739	-60.35316	850	ISPC	at depth	
PS112_25-45	2018-03-31	23:11	-62.95690	-60.35161	851	ISPC	station end	
PS112_25-46	2018-04-01	2:04	-62.95107	-60.31614	924	MN_M7	station start	
PS112_25-46	2018-04-01	2:23	-62.95070	-60.31702	922	MN_M7	at depth	
PS112_25-46	2018-04-01	3:03	-62.95176	-60.31574	924	MN_M7	station end	
PS112_25-47	2018-04-01	3:20	-62.94992	-60.32822	904	IKMT	at depth	
PS112_25-47	2018-04-01	3:28	-62.94866	-60.33531	885	IKMT	station start	
PS112_25-47	2018-04-01	3:33	-62.94754	-60.34049	871	IKMT	station end	
PS112_25-48	2018-04-01	4:17	-62.96205	-60.46198	301	MN_M7	station start	
PS112_25-48	2018-04-01	4:29	-62.96244	-60.45829	358	MN_M7	at depth	
PS112_25-48	2018-04-01	4:39	-62.96293	-60.45481	409	MN_M7	station end	
PS112_25-49	2018-04-01	4:53	-62.96114	-60.45939	327	IKMT	station start	
PS112_25-49	2018-04-01	5:00	-62.96274	-60.45650	397	IKMT	at depth	
PS112_25-49	2018-04-01	5:15	-62.96872	-60.44872	412	IKMT	station end	
PS112_25-50	2018-04-01	11:17	-62.88551	-60.22919	968	Goflo	station start	
PS112_25-50	2018-04-01	11:26	-62.88463	-60.23052	968	Goflo	at depth	
PS112_25-50	2018-04-01	11:35	-62.88407	-60.23129	961	Goflo	station end	
PS112_25-51	2018-04-01	11:49	-62.88360	-60.23395	947	CTDICBM	station start	
PS112_25-51	2018-04-01	12:09	-62.88477	-60.23720	956	CTDICBM	at depth	
PS112_25-51	2018-04-01	12:25	-62.88601	-60.23894	959	CTDICBM	station end	
PS112_25-52	2018-04-01	12:40	-62.88632	-60.24025	959	ISPC	station start	
PS112_25-52	2018-04-01	13:13	-62.88863	-60.23773	970	ISPC	at depth	
PS112_25-52	2018-04-01	13:32	-62.88861	-60.23663	968	ISPC	station end	
PS112_25-53	2018-04-01	14:35	-62.86976	-60.20180	933	DSTRM	station start	
PS112_25-53	2018-04-01	15:06	-62.87003	-60.19221	968	DSTRM	station end	
PS112_25-54	2018-04-01	15:27	-62.87020	-60.18735	969	MSC	station start	
PS112_25-54	2018-04-01	15:32	-62.87045	-60.18681	969	MSC	at depth	
PS112_25-54	2018-04-01	15:37	-62.87065	-60.18627	969	MSC	station end	
PS112_25-55	2018-04-01	15:44	-62.87100	-60.18491	967	MSC	station start	

Station	Date	Time	Latitude	Longi-tude	Depth [m]	Gear	Action	Comment
PS112_25-55	2018-04-01	15:48	-62.87126	-60.18403	966	MSC	at depth	
PS112_25-55	2018-04-01	15:52	-62.87137	-60.18330	965	MSC	station end	
PS112_25-56	2018-04-01	15:59	-62.87164	-60.18190	963	SECCI	station start	
PS112_25-56	2018-04-01	16:03	-62.87170	-60.18076	961	SECCI	station end	
PS112_25-57	2018-04-01	16:04	-62.87170	-60.18047	961	HN	station start	
PS112_25-57	2018-04-01	16:21	-62.87115	-60.17604	956	HN	station end	
PS112_25-58	2018-04-01	16:26	-62.87073	-60.17468	954	BONGO	station start	
PS112_25-58	2018-04-01	16:39	-62.87083	-60.16815	947	BONGO	at depth	
PS112_25-58	2018-04-01	16:53	-62.87188	-60.16408	942	BONGO	station end	
PS112_25-59	2018-04-01	17:07	-62.86991	-60.16157	943	MN_M7	station start	
PS112_25-59	2018-04-01	17:39	-62.86939	-60.15482	946	MN_M7	at depth	
PS112_25-59	2018-04-01	18:01	-62.86927	-60.15155	948	MN_M7	station end	
PS112_25-60	2018-04-01	18:14	-62.86700	-60.15666	950	IKMT	station start	
PS112_25-60	2018-04-01	18:24	-62.86785	-60.16331	947	IKMT	at depth	
PS112_25-60	2018-04-01	18:43	-62.87003	-60.17542	956	IKMT	station end	
PS112_25-61	2018-04-01	18:49	-62.86955	-60.17124	950	BUCKET	station start	
PS112_25-61	2018-04-01	18:58	-62.87007	-60.17034	949	BUCKET	station end	
PS112_26-1	2018-04-02	8:43	-62.23723	-64.55682	2645	TMPUMP	station start	
PS112_26-1	2018-04-02	9:11	-62.23790	-64.55746	2647	TMPUMP	at depth	
PS112_26-1	2018-04-02	10:08	-62.24156	-64.56254	2665	TMPUMP	station start	
PS112_26-1	2018-04-02	10:14	-62.24231	-64.56293	2673	TMPUMP	at depth	
PS112_26-1	2018-04-02	10:28	-62.24374	-64.56497	2678	TMPUMP	profile start	
PS112_26-1	2018-04-02	18:07	-62.38298	-64.58070	2801	TMPUMP	station end	
PS112_26-2	2018-04-02	18:07	-62.38301	-64.58065	2824	BONGO	station start	
PS112_26-2	2018-04-02	18:41	-62.38752	-64.57362	2672	BONGO	at depth	
PS112_26-2	2018-04-02	18:51	-62.38726	-64.57078	2643	BONGO	station end	
PS112_26-3	2018-04-02	19:01	-62.38888	-64.56555	2605	HN	station start	
PS112_26-3	2018-04-02	19:04	-62.38947	-64.56397	2601	HN	station end	
PS112_26-4	2018-04-02	19:19	-62.38805	-64.56983	2642	BT	station start	
PS112_26-4	2018-04-02	19:39	-62.38218	-64.59254	3055	BT	station end	
PS112_27-1	2018-04-03	3:01	-62.25470	-63.00731	4586	CTDICBM	station start	
PS112_27-1	2018-04-03	3:16	-62.25693	-63.00356	4586	CTDICBM	at depth	
PS112_27-1	2018-04-03	3:27	-62.25878	-63.00179	4587	CTDICBM	station end	
PS112_27-2	2018-04-03	3:34	-62.26042	-63.00153	4587	IKMT	station start	
PS112_27-2	2018-04-03	3:43	-62.26376	-63.00618	4585	IKMT	at depth	
PS112_27-2	2018-04-03	4:04	-62.27112	-63.01675	4449	IKMT	station end	
PS112_28-1	2018-04-03	6:43	-62.24825	-61.98949	1904	CTDICBM	station start	
PS112_28-1	2018-04-03	6:58	-62.24863	-61.98874	1907	CTDICBM	at depth	
PS112_28-1	2018-04-03	7:08	-62.24908	-61.98837	1908	CTDICBM	station end	
PS112_28-2	2018-04-03	7:21	-62.24987	-61.98777	1909	IKMT	station start	
PS112_28-2	2018-04-03	7:28	-62.25047	-61.99542	1861	IKMT	at depth	

A.4 Stationsliste / Station List

Station	Date	Time	Latitude	Longi-tude	Depth [m]	Gear	Action	Comment
PS112_28-2	2018-04-03	7:52	-62.25211	-62.00968	1818	IKMT	station end	
PS112_29-1	2018-04-03	10:18	-62.49964	-61.50068	129	CTDICBM	station start	
PS112_29-1	2018-04-03	10:28	-62.49990	-61.50044	129	CTDICBM	at depth	
PS112_29-1	2018-04-03	10:40	-62.50008	-61.50064	130	CTDICBM	station end	
PS112_29-2	2018-04-03	10:48	-62.50015	-61.50248	129	IKMT	station start	
PS112_29-2	2018-04-03	10:53	-62.50037	-61.50861	130	IKMT	at depth	
PS112_29-2	2018-04-03	11:08	-62.50077	-61.52283	135	IKMT	station end	
PS112_29-3	2018-04-03	13:02	-62.44968	-61.31640	236	BT	station start	
PS112_29-3	2018-04-03	13:31	-62.46935	-61.36523	139	BT	at depth	
PS112_29-3	2018-04-03	13:46	-62.47916	-61.39332	124	BT	profile end	
PS112_29-3	2018-04-03	14:16	-62.48486	-61.42747	120	BT	station end	
PS112_29-4	2018-04-03	14:43	-62.48942	-61.46853	128	CTDICBM	station start	
PS112_29-4	2018-04-03	14:58	-62.49039	-61.46389	124	CTDICBM	at depth	
PS112_29-4	2018-04-03	15:07	-62.49084	-61.46436	124	CTDICBM	station end	
PS112_30-1	2018-04-03	15:56	-62.42364	-61.35996	256	BT	station start	
PS112_30-1	2018-04-03	16:35	-62.38843	-61.41260	350	BT	at depth	
PS112_30-1	2018-04-03	17:30	-62.36181	-61.46214	268	BT	station end	
PS112_30-2	2018-04-03	17:58	-62.36307	-61.46104	270	CTDICBM	station start	
PS112_30-2	2018-04-03	18:08	-62.36302	-61.46308	266	CTDICBM	at depth	
PS112_30-2	2018-04-03	18:16	-62.36275	-61.46415	265	CTDICBM	station end	
PS112_30-3	2018-04-03	18:25	-62.36225	-61.46572	266	SECCI	station start	
PS112_30-3	2018-04-03	18:27	-62.36210	-61.46575	267	SECCI	station end	
PS112_30-4	2018-04-03	18:29	-62.36202	-61.46572	267	HN	station start	
PS112_30-4	2018-04-03	18:33	-62.36183	-61.46550	267	HN	station end	
PS112_31-1	2018-04-03	22:40	-61.74979	-61.99925	4197	Goflo	station start	
PS112_31-1	2018-04-03	22:48	-61.74983	-61.99912	4194	Goflo	at depth	
PS112_31-1	2018-04-03	22:58	-61.74995	-61.99954	4196	Goflo	station end	
PS112_31-2	2018-04-03	23:09	-61.75045	-62.00088	4205	CTDICBM	station start	
PS112_31-2	2018-04-03	23:18	-61.75094	-62.00495	4223	CTDICBM	at depth	
PS112_31-2	2018-04-03	23:27	-61.75134	-62.00793	4229	CTDICBM	station end	
PS112_31-3	2018-04-03	23:38	-61.75150	-62.00863	4230	ISPC	station start	
PS112_31-3	2018-04-03	23:44	-61.75153	-62.00851	4230	ISPC	at depth	
PS112_31-3	2018-04-03	23:48	-61.75155	-62.00850	4230	ISPC	station end	
PS112_31-4	2018-04-04	0:03	-61.75180	-62.01092	4232	IKMT	station start	
PS112_31-4	2018-04-04	0:13	-61.74918	-62.02461	4239	IKMT	at depth	
PS112_31-4	2018-04-04	0:35	-61.74439	-62.05131	4170	IKMT	station end	
PS112_32-1	2018-04-04	4:04	-61.75125	-61.01098	3293	CTDICBM	station start	
PS112_32-1	2018-04-04	4:16	-61.75178	-61.01014	3289	CTDICBM	at depth	
PS112_32-1	2018-04-04	4:24	-61.75205	-61.00937	3285	CTDICBM	station end	
PS112_32-2	2018-04-04	4:35	-61.75264	-61.00834	3282	IKMT	station start	
PS112_32-2	2018-04-04	5:03	-61.75240	-61.03710	3450	IKMT	station end	

Station	Date	Time	Latitude	Longi-tude	Depth [m]	Gear	Action	Comment
PS112_33-1	2018-04-04	7:55	-62.00004	-60.49855	1481	CTDICBM	station start	
PS112_33-1	2018-04-04	8:07	-61.99988	-60.49908	1485	CTDICBM	at depth	
PS112_33-1	2018-04-04	8:21	-62.00002	-60.49818	1479	CTDICBM	station end	
PS112_33-2	2018-04-04	8:32	-61.99891	-60.50099	1502	IKMT	station start	
PS112_33-2	2018-04-04	8:40	-61.99641	-60.50963	1554	IKMT	at depth	
PS112_33-2	2018-04-04	9:03	-61.99138	-60.52884	1520	IKMT	station end	
PS112_34-1	2018-04-04	13:57	-61.25555	-60.99086	3971	CTDICBM	station start	
PS112_34-1	2018-04-04	14:14	-61.25414	-60.98175	3969	CTDICBM	at depth	
PS112_34-1	2018-04-04	14:33	-61.25264	-60.97654	3964	CTDICBM	station end	
PS112_34-2	2018-04-04	14:47	-61.25065	-60.97028	3956	ISPC	station start	
PS112_34-2	2018-04-04	15:23	-61.24696	-60.96157	3933	ISPC	at depth	
PS112_34-2	2018-04-04	15:44	-61.24377	-60.95803	3912	ISPC	station end	
PS112_34-3	2018-04-04	15:44	-61.24368	-60.95801	3913	HN	station start	
PS112_34-3	2018-04-04	15:48	-61.24290	-60.95790	3913	HN	station end	
PS112_34-4	2018-04-04	16:01	-61.24032	-60.95721		MSC	at depth	
PS112_34-4	2018-04-04	16:10	-61.23846	-60.95671	3915	MSC	station end	
PS112_34-5	2018-04-04	16:33	-61.23435	-60.95519	3935	CTDICBM	station start	
PS112_34-5	2018-04-04	16:38	-61.23346	-60.95542	3941	CTDICBM	at depth	
PS112_34-5	2018-04-04	16:39	-61.23326	-60.95553	3940	CTDICBM	station end	
PS112_34-6	2018-04-04	16:54	-61.23058	-60.95656	3998	SECCI	station start	
PS112_34-6	2018-04-04	16:56	-61.23022	-60.95674	3998	SECCI	station end	
PS112_34-7	2018-04-04	17:02	-61.22919	-60.95701	4004	BONGO	station start	
PS112_34-7	2018-04-04	17:16	-61.22657	-60.95434	4005	BONGO	at depth	
PS112_34-7	2018-04-04	17:30	-61.22430	-60.95215	4002	BONGO	station end	
PS112_34-8	2018-04-04	17:34	-61.22288	-60.95100	3994	HN	station start	
PS112_34-8	2018-04-04	17:45	-61.21924	-60.94769	3964	HN	station end	
PS112_34-9	2018-04-04	17:50	-61.21745	-60.94636	3954	MN_M7	station start	
PS112_34-9	2018-04-04	18:28	-61.21078	-60.94416	3889	MN_M7	at depth	
PS112_34-9	2018-04-04	18:48	-61.20800	-60.94472	3883	MN_M7	station end	
PS112_34-10	2018-04-04	19:10	-61.19944	-60.95218	3745	IKMT	station start	
PS112_34-10	2018-04-04	19:17	-61.19579	-60.95922	3904	IKMT	at depth	
PS112_34-10	2018-04-04	19:39	-61.18489	-60.98050	3983	IKMT	station end	
PS112_35-1	2018-04-04	22:27	-61.50432	-60.52433	4077	CTDICBM	station start	
PS112_35-1	2018-04-04	22:39	-61.50421	-60.52402	4077	CTDICBM	at depth	
PS112_35-1	2018-04-04	22:51	-61.50411	-60.52421	4078	CTDICBM	station end	
PS112_35-2	2018-04-04	23:01	-61.50318	-60.52787	4065	IKMT	station start	
PS112_35-2	2018-04-04	23:08	-61.50098	-60.53270	4051	IKMT	at depth	
PS112_35-2	2018-04-04	23:27	-61.49363	-60.54787	4056	IKMT	station end	
PS112_36-1	2018-04-05	1:54	-61.74814	-59.99112	1577	CTDICBM	station start	
PS112_36-1	2018-04-05	2:05	-61.74744	-59.98894	1563	CTDICBM	at depth	
PS112_36-1	2018-04-05	2:20	-61.74665	-59.98646	1548	CTDICBM	station end	

A.4 Stationsliste / Station List

Station	Date	Time	Latitude	Longi-tude	Depth [m]	Gear	Action	Comment
PS112_36-2	2018-04-05	2:24	-61.74517	-59.98693	1547	IKMT	station start	
PS112_36-2	2018-04-05	2:31	-61.74034	-59.98958	1561	IKMT	at depth	
PS112_36-2	2018-04-05	2:51	-61.73064	-59.99155	1684	IKMT	station end	
PS112_37-1	2018-04-05	5:42	-61.24981	-59.99933	4961	CTDICBM	station start	
PS112_37-1	2018-04-05	5:56	-61.25060	-59.99756	4963	CTDICBM	at depth	
PS112_37-1	2018-04-05	6:04	-61.25190	-59.99613	4969	CTDICBM	station end	
PS112_37-2	2018-04-05	6:12	-61.25323	-59.99470	4974	IKMT	station start	
PS112_37-2	2018-04-05	6:21	-61.25010	-59.99397	4958	IKMT	at depth	
PS112_37-2	2018-04-05	6:39	-61.24386	-59.99218	4924	IKMT	station end	
PS112_38-1	2018-04-05	9:00	-61.49971	-59.49904	3061	CTDICBM	station start	
PS112_38-1	2018-04-05	9:13	-61.49985	-59.49887	3061	CTDICBM	at depth	
PS112_38-1	2018-04-05	9:24	-61.49974	-59.49905	3061	CTDICBM	station end	
PS112_38-2	2018-04-05	9:39	-61.49811	-59.50577	3146	IKMT	station start	
PS112_38-2	2018-04-05	9:47	-61.49703	-59.51124	3147	IKMT	at depth	
PS112_38-2	2018-04-05	10:06	-61.49458	-59.52219	3183	IKMT	station end	
PS112_39-1	2018-04-05	13:35	-61.83462	-58.71599	199	BT	station start	
PS112_39-1	2018-04-05	14:01	-61.83306	-58.65166	185	BT	at depth	
PS112_39-1	2018-04-05	14:01	-61.83306	-58.65068	187	BT	profile start	
PS112_39-1	2018-04-05	14:16	-61.83355	-58.61626	185	BT	profile end	
PS112_39-1	2018-04-05	14:43	-61.83528	-58.58516	166	BT	station end	
PS112_39-2	2018-04-05	15:05	-61.83500	-58.57800	167	CTDICBM	station start	
PS112_39-2	2018-04-05	15:22	-61.83363	-58.57943	167	CTDICBM	at depth	
PS112_39-2	2018-04-05	15:42	-61.83214	-58.58421	173	CTDICBM	station end	
PS112_39-3	2018-04-05	15:51	-61.83083	-58.58666	178	SECCI	station start	
PS112_39-3	2018-04-05	15:53	-61.83052	-58.58714	180	SECCI	station end	
PS112_40-1	2018-04-05	16:23	-61.76866	-58.56094	269	BT	station start	
PS112_40-1	2018-04-05	16:47	-61.75448	-58.50872	273	BT	at depth	
PS112_40-1	2018-04-05	16:49	-61.75415	-58.50401	273	BT	profile start	
PS112_40-1	2018-04-05	17:04	-61.75172	-58.47014	274	BT	profile end	
PS112_40-1	2018-04-05	17:35	-61.75202	-58.44704	274	BT	station end	
PS112_40-2	2018-04-05	17:57	-61.75280	-58.44471	274	CTDICBM	station start	
PS112_40-2	2018-04-05	18:19	-61.75308	-58.45293	274	CTDICBM	at depth	
PS112_40-2	2018-04-05	18:32	-61.75364	-58.45769	274	CTDICBM	station end	
PS112_41-1	2018-04-05	20:47	-61.74936	-59.00014	323	CTDICBM	station start	
PS112_41-1	2018-04-05	21:04	-61.74990	-58.99954	322	CTDICBM	at depth	
PS112_41-1	2018-04-05	21:23	-61.74889	-58.99884	325	CTDICBM	station end	
PS112_41-2	2018-04-05	21:40	-61.74943	-59.00068	324	ISPC	station start	
PS112_41-2	2018-04-05	22:01	-61.74965	-59.00331	324	ISPC	at depth	
PS112_41-2	2018-04-05	22:16	-61.74956	-59.00420	325	ISPC	station end	
PS112_41-3	2018-04-05	22:34	-61.74980	-59.00290	324	MSC	station start	
PS112_41-3	2018-04-05	22:37	-61.74981	-59.00268	324	MSC	at depth	

Station	Date	Time	Latitude	Longi-tude	Depth [m]	Gear	Action	Comment
PS112_41-3	2018-04-05	22:47	-61.74954	-59.00312	325	MSC	station end	
PS112_41-4	2018-04-05	22:56	-61.74945	-59.00395	325	BONGO	station start	
PS112_41-4	2018-04-05	23:10	-61.74808	-59.00819	327	BONGO	at depth	
PS112_41-4	2018-04-05	23:17	-61.74758	-59.01109	326	BONGO	station end	
PS112_41-5	2018-04-05	23:22	-61.74732	-59.01313	329	HN	station start	
PS112_41-5	2018-04-05	23:49	-61.74595	-59.02349	333	HN	station end	
PS112_41-6	2018-04-05	23:56	-61.74516	-59.02426	335	IKMT	station start	
PS112_41-6	2018-04-06	0:04	-61.74239	-59.01837	334	IKMT	at depth	
PS112_41-6	2018-04-06	0:25	-61.73485	-59.00355	334	IKMT	station end	
PS112_42-1	2018-04-06	4:40	-61.75073	-57.50041	350	CTDICBM	station start	
PS112_42-1	2018-04-06	4:50	-61.75152	-57.49525	352	CTDICBM	at depth	
PS112_42-1	2018-04-06	4:57	-61.75150	-57.49302	347	CTDICBM	station end	
PS112_42-2	2018-04-06	5:07	-61.75134	-57.48967	345	IKMT	station start	
PS112_42-2	2018-04-06	5:16	-61.75231	-57.47756	349	IKMT	at depth	
PS112_42-2	2018-04-06	5:36	-61.75450	-57.45305	355	IKMT	station end	
PS112_43-1	2018-04-06	8:03	-61.50022	-57.49965	617	CTDICBM	station start	
PS112_43-1	2018-04-06	8:17	-61.50065	-57.49966	612	CTDICBM	at depth	
PS112_43-1	2018-04-06	8:29	-61.50067	-57.49889	610	CTDICBM	station end	
PS112_43-2	2018-04-06	8:39	-61.50174	-57.50443	611	IKMT	station start	
PS112_43-2	2018-04-06	8:47	-61.50263	-57.51208	606	IKMT	at depth	
PS112_43-2	2018-04-06	9:07	-61.50539	-57.52640	581	IKMT	station end	
PS112_44-1	2018-04-06	12:21	-60.99826	-57.49943	3956	CTDICBM	station start	
PS112_44-1	2018-04-06	12:32	-60.99919	-57.49758	3953	CTDICBM	at depth	
PS112_44-1	2018-04-06	12:43	-60.99985	-57.49831	3959	CTDICBM	station end	
PS112_44-2	2018-04-06	12:50	-60.99982	-57.49697	3953	SECCI	station start	
PS112_44-2	2018-04-06	12:50	-60.99981	-57.49694	3953	SECCI	station end	
PS112_44-3	2018-04-06	13:00	-60.99931	-57.49408	3938	HN	station start	
PS112_44-3	2018-04-06	13:11	-60.99884	-57.49001	3920	HN	station end	
PS112_44-4	2018-04-06	13:11	-60.99882	-57.48985	3921	IKMT	station start	
PS112_44-4	2018-04-06	13:25	-60.99477	-57.50278	3939	IKMT	at depth	
PS112_44-4	2018-04-06	13:49	-60.98733	-57.53110	4015	IKMT	station end	
PS112_45-1	2018-04-06	16:53	-60.49983	-57.49460	3575	CTDICBM	station start	
PS112_45-1	2018-04-06	17:04	-60.50057	-57.49201	3574	CTDICBM	at depth	
PS112_45-1	2018-04-06	17:13	-60.50069	-57.49015	3572	CTDICBM	station end	
PS112_45-2	2018-04-06	17:28	-60.50058	-57.48840	3568	SECCI	station start	
PS112_45-2	2018-04-06	17:30	-60.50051	-57.48828	3566	SECCI	station end	
PS112_45-3	2018-04-06	17:34	-60.49937	-57.49014	3562	IKMT	station start	
PS112_45-3	2018-04-06	17:41	-60.49667	-57.49501	3562	IKMT	at depth	
PS112_45-3	2018-04-06	18:03	-60.49085	-57.50182	3574	IKMT	station end	
PS112_46-1	2018-04-06	19:37	-60.24922	-57.49784	2125	CTDICBM	station start	
PS112_46-1	2018-04-06	19:49	-60.24887	-57.49726	2144	CTDICBM	at depth	

A.4 Stationsliste / Station List

Station	Date	Time	Latitude	Longi-tude	Depth [m]	Gear	Action	Comment
PS112_46-1	2018-04-06	20:02	-60.24885	-57.49658	2229	CTDICBM	station end	
PS112_46-2	2018-04-06	20:12	-60.24780	-57.50210	2156	IKMT	station start	
PS112_46-2	2018-04-06	20:21	-60.24597	-57.51192	2075	IKMT	at depth	
PS112_46-2	2018-04-06	20:41	-60.24089	-57.53231	1969	IKMT	station end	
PS112_47-1	2018-04-06	23:48	-60.25165	-56.50679	3723	CTDICBM	station start	
PS112_47-1	2018-04-07	0:06	-60.25091	-56.50228	3727	CTDICBM	at depth	
PS112_47-1	2018-04-07	0:17	-60.24945	-56.50458	3741	CTDICBM	station end	
PS112_47-2	2018-04-07	0:27	-60.24997	-56.50682	3746	ISPC	station start	
PS112_47-2	2018-04-07	0:30	-60.25018	-56.50732	3730	ISPC	station end	
PS112_47-2	2018-04-07	0:31	-60.25028	-56.50752	3730	ISPC	station start	
PS112_47-2	2018-04-07	1:02	-60.25185	-56.51214	3720	ISPC	at depth	
PS112_47-2	2018-04-07	1:24	-60.25412	-56.51620	3715	ISPC	station end	
PS112_47-3	2018-04-07	1:33	-60.25389	-56.51738	3715	IKMT	station start	
PS112_47-3	2018-04-07	1:43	-60.25288	-56.53093	3706	IKMT	at depth	
PS112_47-3	2018-04-07	2:04	-60.24871	-56.56101	3683	IKMT	station end	
PS112_48-1	2018-04-07	3:47	-60.50043	-56.51201	3793	CTDICBM	station start	
PS112_48-1	2018-04-07	3:59	-60.49988	-56.51229	3792	CTDICBM	at depth	
PS112_48-1	2018-04-07	4:10	-60.49955	-56.51260	3791	CTDICBM	station end	
PS112_48-2	2018-04-07	4:19	-60.49963	-56.51348	3793	IKMT	station start	
PS112_48-2	2018-04-07	4:27	-60.50188	-56.51999	3802	IKMT	at depth	
PS112_48-2	2018-04-07	4:44	-60.50793	-56.53672	3826	IKMT	station end	
PS112_49-1	2018-04-07	7:59	-60.49996	-55.49728	3530	CTDICBM	station start	
PS112_49-1	2018-04-07	8:13	-60.49999	-55.49260	3529	CTDICBM	at depth	
PS112_49-1	2018-04-07	8:26	-60.50011	-55.48785	3526	CTDICBM	station end	
PS112_49-2	2018-04-07	8:46	-60.50782	-55.49941	3524	IKMT	station start	
PS112_49-2	2018-04-07	8:56	-60.51133	-55.50273	3515	IKMT	at depth	
PS112_49-2	2018-04-07	9:18	-60.51923	-55.51271	3494	IKMT	station end	
PS112_50-1	2018-04-07	12:42	-61.00144	-55.00442	409	CTDICBM	station start	
PS112_50-1	2018-04-07	12:55	-61.00156	-55.00141	425	CTDICBM	at depth	
PS112_50-1	2018-04-07	13:07	-61.00305	-54.99882	430	CTDICBM	station end	
PS112_50-2	2018-04-07	13:38	-61.01192	-54.99505	312	IKMT	station start	
PS112_50-2	2018-04-07	13:46	-61.01747	-54.99577	240	IKMT	at depth	
PS112_50-2	2018-04-07	14:09	-61.02952	-54.99544	178	IKMT	station end	
PS112_50-3	2018-04-07	14:45	-61.00985	-54.99165	379	IKMT	station start	
PS112_50-3	2018-04-07	14:51	-61.01264	-54.99050	336	IKMT	at depth	
PS112_50-3	2018-04-07	15:01	-61.01647	-54.98895	261	IKMT	station end	
PS112_50-4	2018-04-07	16:00	-61.07831	-54.86667	119	BOAT	station start	
PS112_50-4	2018-04-07	20:34	-61.04908	-55.01446	118	BOAT	station end	
PS112_50-5	2018-04-07	16:19	-61.07793	-54.86500	121	CTDICBM	station start	
PS112_50-5	2018-04-07	16:29	-61.07629	-54.86427	125	CTDICBM	at depth	
PS112_50-5	2018-04-07	16:34	-61.07513	-54.86372	130	CTDICBM	station end	

Station	Date	Time	Latitude	Longi-tude	Depth [m]	Gear	Action	Comment
PS112_50-6	2018-04-07	17:24	-61.02551	-55.00840	170	IKMT	station start	
PS112_50-6	2018-04-07	17:35	-61.02730	-55.00472	173	IKMT	at depth	
PS112_50-6	2018-04-07	17:46	-61.02952	-55.00189	165	IKMT	station end	
PS112_50-7	2018-04-07	17:50	-61.03024	-55.00234	158	IKMT	station start	
PS112_50-7	2018-04-07	17:55	-61.03126	-55.00098	154	IKMT	at depth	
PS112_50-7	2018-04-07	18:03	-61.03166	-54.99864	156	IKMT	station end	
PS112_50-8	2018-04-07	18:09	-61.03154	-54.99767	160	IKMT	station start	
PS112_50-8	2018-04-07	18:11	-61.03149	-54.99702	162	IKMT	at depth	
PS112_50-8	2018-04-07	18:20	-61.03096	-54.99600	169	IKMT	station end	
PS112_50-9	2018-04-07	18:22	-61.03086	-54.99554	171	IKMT	station start	
PS112_50-9	2018-04-07	18:24	-61.03062	-54.99548	173	IKMT	at depth	
PS112_50-9	2018-04-07	18:35	-61.03162	-54.99122	179	IKMT	station end	
PS112_50-10	2018-04-07	18:38	-61.03193	-54.99030	179	IKMT	station start	
PS112_50-10	2018-04-07	18:41	-61.03235	-54.98918	178	IKMT	at depth	
PS112_50-10	2018-04-07	18:50	-61.03364	-54.98654	177	IKMT	station end	
PS112_50-11	2018-04-07	19:16	-61.02657	-55.03358	146	IKMT	station start	
PS112_50-11	2018-04-07	19:24	-61.02928	-55.03105	141	IKMT	station end	
PS112_50-12	2018-04-07	19:30	-61.03077	-55.02963	137	IKMT	at depth	
PS112_50-12	2018-04-07	19:36	-61.03211	-55.02802	136	IKMT	station end	
PS112_50-13	2018-04-07	19:38	-61.03269	-55.02711	134	IKMT	station start	
PS112_50-13	2018-04-07	19:41	-61.03309	-55.02619	132	IKMT	at depth	
PS112_50-13	2018-04-07	19:46	-61.03411	-55.02352	131	IKMT	station end	
PS112_50-14	2018-04-07	19:49	-61.03454	-55.02247	131	IKMT	station start	
PS112_50-14	2018-04-07	19:51	-61.03507	-55.02121	129	IKMT	at depth	
PS112_50-14	2018-04-07	19:59	-61.03637	-55.01796	124	IKMT	station end	
PS112_50-15	2018-04-07	20:20	-61.04893	-55.01116	127	BUCKET	station start	
PS112_50-15	2018-04-07	20:21	-61.04894	-55.01156	126	BUCKET	station end	
PS112_50-16	2018-04-07	20:51	-61.04008	-55.00658	123	BUCKET	station start	
PS112_50-16	2018-04-07	20:55	-61.03936	-55.00754	129	BUCKET	station end	
PS112_50-17	2018-04-07	22:55	-60.94383	-55.25446	407	EK60	profile start	
PS112_50-17	2018-04-08	9:53	-61.05357	-54.69214	468	EK60	profile end	
PS112_51-1	2018-04-08	0:33	-61.00174	-55.22936	221	IKMT	station start	
PS112_51-1	2018-04-08	0:33	-61.00210	-55.22949	216	IKMT	at depth	
PS112_51-1	2018-04-08	0:44	-61.00695	-55.23743	214	IKMT	station end	
PS112_51-2	2018-04-08	2:22	-60.99470	-55.15955	259	IKMT	station start	
PS112_51-2	2018-04-08	2:26	-60.99715	-55.16214	251	IKMT	at depth	
PS112_51-2	2018-04-08	2:35	-61.00029	-55.16423	204	IKMT	station end	
PS112_51-3	2018-04-08	8:07	-61.05309	-54.77098	211	IKMT	station start	
PS112_51-3	2018-04-08	8:11	-61.05504	-54.76883	195	IKMT	at depth	
PS112_51-3	2018-04-08	8:30	-61.06231	-54.76125	172	IKMT	station end	
PS112_51-4	2018-04-08	8:39	-61.06293	-54.75952	171	IKMT	station start	

A.4 Stationsliste / Station List

Station	Date	Time	Latitude	Longi-tude	Depth [m]	Gear	Action	Comment
PS112_51-4	2018-04-08	8:41	-61.06370	-54.75805	168	IKMT	at depth	
PS112_51-4	2018-04-08	8:50	-61.06677	-54.75148	156	IKMT	station end	
PS112_52-1	2018-04-08	10:49	-61.06900	-54.80590	156	CTDICBM	at depth	
PS112_52-1	2018-04-08	10:59	-61.06871	-54.80658	158	CTDICBM	station end	
PS112_52-2	2018-04-08	11:30	-61.06880	-54.80753	156	CTDICBM	station start	
PS112_52-2	2018-04-08	11:37	-61.06861	-54.80830	157	CTDICBM	at depth	
PS112_52-2	2018-04-08	11:37	-61.06860	-54.80833	157	CTDICBM	station end	
PS112_52-3	2018-04-08	12:10	-61.06621	-54.81110	174	BOAT	station start	
PS112_52-3	2018-04-08	13:13	-61.06292	-54.80929	192	BOAT	station end	
PS112_53-1	2018-04-08	12:20	-61.06488	-54.81240	180	CTDICBM	station start	
PS112_53-1	2018-04-08	12:21	-61.06482	-54.81247	180	CTDICBM	at depth	
PS112_53-1	2018-04-08	12:30	-61.06376	-54.81391	190	CTDICBM	station end	
PS112_54-1	2018-04-08	14:06	-61.03553	-54.77261	528	DSTRM	station start	
PS112_54-1	2018-04-08	14:38	-61.03700	-54.76943	520	DSTRM	station end	
PS112_55-1	2018-04-08	14:53	-61.03377	-54.77955	531	ISPC	station start	
PS112_55-1	2018-04-08	15:29	-61.03319	-54.77226	532	ISPC	at depth	
PS112_55-1	2018-04-08	15:48	-61.03294	-54.76964	532	ISPC	station end	
PS112_55-2	2018-04-08	16:13	-61.02977	-54.76565	537	IKMT	station start	
PS112_55-2	2018-04-08	16:21	-61.03182	-54.75704	535	IKMT	at depth	
PS112_55-2	2018-04-08	16:45	-61.03730	-54.73867	526	IKMT	station end	
PS112_55-3	2018-04-08	17:07	-61.02900	-54.76018	537	BOAT	station start	
PS112_55-3	2018-04-08	20:33	-61.02252	-54.80936	543	BOAT	station end	
PS112_55-4	2018-04-08	17:24	-61.02968	-54.76703	537	RMT	station start	
PS112_55-4	2018-04-08	17:41	-61.02269	-54.79318	544	RMT	at depth	
PS112_55-4	2018-04-08	18:15	-61.00787	-54.84492	554	RMT	station end	
PS112_55-5	2018-04-08	18:49	-61.02323	-54.77793	544	Goflo	station start	
PS112_55-5	2018-04-08	18:56	-61.02354	-54.78274	544	Goflo	at depth	
PS112_55-5	2018-04-08	19:07	-61.02287	-54.78470	545	Goflo	station end	
PS112_55-6	2018-04-08	19:15	-61.02242	-54.78616	545	CTDICBM	station start	
PS112_55-6	2018-04-08	19:46	-61.02368	-54.79483	544	CTDICBM	at depth	
PS112_55-6	2018-04-08	20:07	-61.02250	-54.80293	544	CTDICBM	station end	
PS112_55-7	2018-04-08	20:11	-61.02235	-54.80483	543	SECCI	station start	
PS112_55-7	2018-04-08	20:14	-61.02227	-54.80618	543	SECCI	station end	
PS112_55-8	2018-04-08	20:49	-61.01131	-54.80759	555	MSC	station start	
PS112_55-8	2018-04-08	20:52	-61.01132	-54.80842	555	MSC	at depth	
PS112_55-8	2018-04-08	20:57	-61.01143	-54.80982	555	MSC	station end	
PS112_55-9	2018-04-08	21:11	-61.01224	-54.81763	556	BONGO	station start	
PS112_55-9	2018-04-08	21:24	-61.01222	-54.82052	557	BONGO	at depth	
PS112_55-9	2018-04-08	21:34	-61.01286	-54.82326	554	BONGO	station end	
PS112_55-10	2018-04-08	21:36	-61.01295	-54.82368	554	HN	station start	
PS112_55-10	2018-04-08	21:47	-61.01369	-54.82699	554	HN	station end	

Station	Date	Time	Latitude	Longi-tude	Depth [m]	Gear	Action	Comment
PS112_55-11	2018-04-08	21:54	-61.01403	-54.82887	553	ISPC	station start	
PS112_55-11	2018-04-08	22:26	-61.01320	-54.83619	555	ISPC	at depth	
PS112_55-11	2018-04-08	22:49	-61.01263	-54.84045	556	ISPC	station end	
PS112_55-12	2018-04-08	23:07	-61.00856	-54.84059	554	RMT	station start	
PS112_55-12	2018-04-08	23:25	-60.99710	-54.83685	562	RMT	at depth	
PS112_55-12	2018-04-08	23:55	-60.97628	-54.83570	600	RMT	station end	
PS112_55-13	2018-04-09	0:33	-61.00569	-54.83743	555	IKMT	station start	
PS112_55-13	2018-04-09	1:01	-60.98951	-54.83802	570	IKMT	station end	
PS112_55-14	2018-04-09	1:53	-61.04839	-54.82869	278	IKMT	station start	
PS112_55-14	2018-04-09	1:56	-61.04989	-54.83072	276	IKMT	at depth	
PS112_55-14	2018-04-09	2:07	-61.05359	-54.83684	235	IKMT	station end	
PS112_55-15	2018-04-09	2:46	-61.01523	-54.85196	558	ISPC	station start	
PS112_55-15	2018-04-09	3:22	-61.01766	-54.84978	555	ISPC	at depth	
PS112_55-15	2018-04-09	3:42	-61.01935	-54.85228	549	ISPC	station end	
PS112_55-16	2018-04-09	3:52	-61.01986	-54.85196	547	IKMT	station start	
PS112_55-16	2018-04-09	4:01	-61.01810	-54.84368	552	IKMT	at depth	
PS112_55-16	2018-04-09	4:21	-61.01488	-54.82429	553	IKMT	station end	
PS112_55-17	2018-04-09	4:38	-61.01807	-54.85377	555	RMT	station start	
PS112_55-17	2018-04-09	4:56	-61.01632	-54.83349	552	RMT	at depth	
PS112_55-17	2018-04-09	5:27	-61.01378	-54.80081	555	RMT	station end	
PS112_55-18	2018-04-09	8:07	-61.00758	-54.97002	534	ISPC	station start	
PS112_55-18	2018-04-09	8:37	-61.01006	-54.98421	458	ISPC	at depth	
PS112_55-18	2018-04-09	8:57	-61.01099	-54.99350	347	ISPC	station end	
PS112_55-19	2018-04-09	9:16	-60.99853	-54.98695	530	RMT	station start	
PS112_55-19	2018-04-09	9:30	-60.99433	-54.97315	553	RMT	at depth	
PS112_55-19	2018-04-09	9:59	-60.98868	-54.95181	590	RMT	station end	
PS112_55-20	2018-04-09	10:27	-60.99718	-54.98150	542	IKMT	station start	
PS112_55-20	2018-04-09	10:36	-60.99526	-54.97515	550	IKMT	at depth	
PS112_55-20	2018-04-09	10:58	-60.99117	-54.96164	570	IKMT	station end	
PS112_55-21	2018-04-09	11:13	-60.99681	-54.96910	556	CTDICBM	station start	
PS112_55-21	2018-04-09	11:33	-61.00150	-54.96891	561	CTDICBM	at depth	
PS112_55-21	2018-04-09	11:49	-61.00321	-54.96990	560	CTDICBM	station end	
PS112_55-22	2018-04-09	12:23	-61.00806	-54.97098	530	CTDICBM	station start	
PS112_55-22	2018-04-09	12:28	-61.00864	-54.97065	523	CTDICBM	at depth	
PS112_55-22	2018-04-09	12:31	-61.00936	-54.97082	515	CTDICBM	station end	
PS112_55-23	2018-04-09	13:11	-61.03033	-54.92789	338	DSTRM	station start	
PS112_55-23	2018-04-09	13:46	-61.03282	-54.92168	316	DSTRM	station end	
PS112_55-24	2018-04-09	14:38	-61.04903	-54.87942	266	ISPC	station start	
PS112_55-24	2018-04-09	15:02	-61.05335	-54.86662	256	ISPC	at depth	
PS112_55-24	2018-04-09	15:11	-61.05447	-54.86696	235	ISPC	station end	
PS112_55-25	2018-04-09	15:17	-61.05403	-54.86634	240	HN	station start	

A.4 Stationsliste / Station List

Station	Date	Time	Latitude	Longi-tude	Depth [m]	Gear	Action	Comment
PS112_55-25	2018-04-09	15:42	-61.06185	-54.87179	222	HN	station end	
PS112_55-26	2018-04-09	16:09	-61.03113	-54.93161	343	IKMT	station start	
PS112_55-26	2018-04-09	16:22	-61.02185	-54.91726	405	IKMT	at depth	
PS112_55-26	2018-04-09	16:52	-61.00769	-54.89677	571	IKMT	station end	
PS112_56-1	2018-04-09	19:47	-60.74827	-55.50624	3259	CTDICBM	station start	
PS112_56-1	2018-04-09	20:00	-60.74813	-55.50912	3266	CTDICBM	at depth	
PS112_56-1	2018-04-09	20:10	-60.74811	-55.51190	3277	CTDICBM	station end	
PS112_56-2	2018-04-09	20:24	-60.74409	-55.51112	3324	IKMT	station start	
PS112_56-2	2018-04-09	20:32	-60.73942	-55.50840	3371	IKMT	at depth	
PS112_56-2	2018-04-09	20:50	-60.72650	-55.50035	3417	IKMT	station end	
PS112_57-1	2018-04-09	23:09	-60.50153	-54.99885	3334	CTDICBM	station start	
PS112_57-1	2018-04-09	23:23	-60.50157	-54.99780	3335	CTDICBM	at depth	
PS112_57-1	2018-04-09	23:31	-60.50108	-54.99674	3336	CTDICBM	station end	
PS112_57-2	2018-04-09	23:36	-60.50037	-54.99591	3335	HN	station start	
PS112_57-2	2018-04-09	23:48	-60.49972	-54.99416	3337	HN	station end	
PS112_57-3	2018-04-09	23:54	-60.49799	-54.99260	3338	IKMT	station start	
PS112_57-3	2018-04-10	0:04	-60.49072	-54.98720	3351	IKMT	at depth	
PS112_57-3	2018-04-10	0:27	-60.47541	-54.97451	3374	IKMT	station end	
PS112_58-1	2018-04-10	3:26	-60.50476	-54.00478	2951	CTDICBM	station start	
PS112_58-1	2018-04-10	3:42	-60.50720	-54.00635	2952	CTDICBM	at depth	
PS112_58-1	2018-04-10	3:49	-60.50816	-54.00666	2952	CTDICBM	station end	
PS112_58-2	2018-04-10	4:00	-60.50885	-54.00700	2952	IKMT	station start	
PS112_58-2	2018-04-10	4:08	-60.50495	-54.00258	2950	IKMT	at depth	
PS112_58-2	2018-04-10	4:31	-60.49430	-53.98732	2942	IKMT	station end	
PS112_59-1	2018-04-10	6:00	-60.25407	-53.99850	NA	CTDICBM	station start	
PS112_59-1	2018-04-10	6:11	-60.25221	-53.99861	2629	CTDICBM	at depth	
PS112_59-1	2018-04-10	6:20	-60.25142	-53.99919	2619	CTDICBM	station end	
PS112_59-2	2018-04-10	6:29	-60.25001	-53.99919	2610	IKMT	station start	
PS112_59-2	2018-04-10	6:59	-60.23140	-53.98558	2542	IKMT	station end	
PS112_60-1	2018-04-10	12:16	-60.01843	-55.50891	3472	TMPUMP	station start	
PS112_60-1	2018-04-10	14:16	-60.00390	-55.53420	3476	TMPUMP	station end	
PS112_60-2	2018-04-10	14:41	-60.01561	-55.52589	3477	CTDICBM	station start	
PS112_60-2	2018-04-10	14:47	-60.01523	-55.52639	3479	CTDICBM	at depth	
PS112_60-2	2018-04-10	14:52	-60.01439	-55.52695	3477	CTDICBM	station end	
PS112_60-3	2018-04-10	15:40	-60.01734	-55.51411	3475	CTDICBM	station start	
PS112_60-3	2018-04-10	16:52	-60.01427	-55.52269	3477	CTDICBM	at depth	
PS112_60-3	2018-04-10	18:08	-60.01313	-55.53285	3479	CTDICBM	station end	
PS112_60-4	2018-04-10	18:08	-60.01311	-55.53292	3479	HN	station start	
PS112_60-4	2018-04-10	18:15	-60.01276	-55.53341	3479	HN	station end	
PS112_60-5	2018-04-10	18:21	-60.01197	-55.53225	3478	IKMT	station start	
PS112_60-5	2018-04-10	18:30	-60.00937	-55.52446	3477	IKMT	at depth	

Station	Date	Time	Latitude	Longi-tude	Depth [m]	Gear	Action	Comment
PS112_60-5	2018-04-10	18:52	-60.00332	-55.50627	3473	IKMT	station end	
PS112_61-1	2018-04-11	0:30	-60.74630	-54.50299	2927	CTDICBM	station start	
PS112_61-1	2018-04-11	0:42	-60.74424	-54.50512	2936	CTDICBM	at depth	
PS112_61-1	2018-04-11	0:54	-60.74211	-54.50706	2938	CTDICBM	station end	
PS112_61-2	2018-04-11	1:05	-60.73923	-54.50727	2944	IKMT	station start	
PS112_61-2	2018-04-11	1:13	-60.73437	-54.49838	2949	IKMT	at depth	
PS112_61-2	2018-04-11	1:37	-60.72332	-54.47777	2939	IKMT	station end	
PS112_61-3	2018-04-11	2:16	-60.74566	-54.50368	2932	TMPUMP	station start	
PS112_61-3	2018-04-11	2:17	-60.74557	-54.50377	2933	TMPUMP	at depth	
PS112_61-3	2018-04-11	7:47	-60.67428	-54.55755	2973	TMPUMP	station end	
PS112_61-4	2018-04-11	8:11	-60.67115	-54.55082	2978	BONGO	station start	
PS112_61-4	2018-04-11	8:30	-60.66760	-54.54594	2975	BONGO	at depth	
PS112_61-4	2018-04-11	8:45	-60.66464	-54.54194	2976	BONGO	station end	
PS112_62-1	2018-04-11	11:51	-61.04501	-54.84398	274	BT	station start	
PS112_62-1	2018-04-11	12:27	-61.03659	-54.88472	276	BT	at depth	
PS112_62-1	2018-04-11	12:28	-61.03629	-54.88739	276	BT	profile start	
PS112_62-1	2018-04-11	12:44	-61.03380	-54.92314	321	BT	profile end	
PS112_62-1	2018-04-11	13:29	-61.03914	-54.95046	286	BT	station end	
PS112_63-1	2018-04-11	14:29	-60.95880	-55.08078	391	BT	station start	
PS112_63-1	2018-04-11	15:07	-60.97247	-55.10223	300	BT	at depth	
PS112_63-1	2018-04-11	15:10	-60.97326	-55.10729	297	BT	profile start	
PS112_63-1	2018-04-11	15:25	-60.97827	-55.13847	278	BT	profile end	
PS112_63-1	2018-04-11	16:08	-60.97344	-55.14442	271	BT	station end	
PS112_63-2	2018-04-11	16:28	-60.97577	-55.13475	281	CTDICBM	station start	
PS112_63-2	2018-04-11	16:44	-60.97700	-55.13347	282	CTDICBM	at depth	
PS112_63-2	2018-04-11	16:53	-60.97792	-55.13386	281	CTDICBM	station end	
PS112_64-1	2018-04-11	18:20	-60.88123	-55.56412	182	BT	station start	
PS112_64-1	2018-04-11	18:39	-60.88710	-55.61140	159	BT	at depth	
PS112_64-1	2018-04-11	18:40	-60.88737	-55.61331	143	BT	profile start	
PS112_64-1	2018-04-11	18:55	-60.89281	-55.64699	154	BT	profile end	
PS112_64-1	2018-04-11	19:32	-60.90690	-55.63393	126	BT	station end	
PS112_64-2	2018-04-11	20:37	-60.89020	-55.58402	154	CTDICBM	station start	
PS112_64-2	2018-04-11	20:47	-60.88868	-55.58376	172	CTDICBM	at depth	
PS112_64-2	2018-04-11	20:52	-60.88843	-55.58398	174	CTDICBM	station end	
PS112_65-1	2018-04-11	23:58	-60.99603	-56.49382	2094	CTDICBM	station start	
PS112_65-1	2018-04-12	0:11	-60.99197	-56.49022	2097	CTDICBM	at depth	
PS112_65-1	2018-04-12	0:20	-60.99002	-56.48942	2102	CTDICBM	station end	
PS112_65-2	2018-04-12	0:53	-60.98392	-56.48841	2115	IKMT	station start	
PS112_65-2	2018-04-12	1:03	-60.97786	-56.47622	2042	IKMT	at depth	
PS112_65-2	2018-04-12	1:24	-60.96685	-56.45023	2045	IKMT	station end	
PS112_66-1	2018-04-12	3:21	-61.24751	-56.49439	361	CTDICBM	station start	

A.4 Stationsliste / Station List

Station	Date	Time	Latitude	Longi-tude	Depth [m]	Gear	Action	Comment
PS112_66-1	2018-04-12	3:32	-61.24519	-56.48700	360	CTDICBM	at depth	
PS112_66-1	2018-04-12	3:45	-61.24276	-56.48258	341	CTDICBM	station end	
PS112_66-2	2018-04-12	3:51	-61.24156	-56.47817	357	IKMT	station start	
PS112_66-2	2018-04-12	4:01	-61.24017	-56.46302	417	IKMT	at depth	
PS112_66-2	2018-04-12	4:23	-61.23714	-56.42870	413	IKMT	station end	
PS112_67-1	2018-04-12	6:05	-61.50079	-56.50495	486	CTDICBM	station start	
PS112_67-1	2018-04-12	6:17	-61.50081	-56.50418	486	CTDICBM	at depth	
PS112_67-1	2018-04-12	6:25	-61.50093	-56.50300	486	CTDICBM	station end	
PS112_67-2	2018-04-12	6:32	-61.50094	-56.50222	486	IKMT	station start	
PS112_67-2	2018-04-12	6:42	-61.50418	-56.48942	498	IKMT	at depth	
PS112_67-2	2018-04-12	7:06	-61.51094	-56.45886	514	IKMT	station end	
PS112_67-3	2018-04-12	7:51	-61.50129	-56.49376	489	RMT	station start	
PS112_67-3	2018-04-12	8:10	-61.50953	-56.46951	513	RMT	at depth	
PS112_67-3	2018-04-12	8:51	-61.51920	-56.43596	510	RMT	station end	
PS112_68-1	2018-04-12	12:29	-61.74934	-55.50466	1943	IKMT	station start	
PS112_68-1	2018-04-12	12:59	-61.75280	-55.49477	2029	IKMT	at depth	
PS112_68-1	2018-04-12	13:21	-61.75870	-55.47786	2259	IKMT	station end	
PS112_69-1	2018-04-12	16:56	-61.25196	-55.74386	122	CTDICBM	station start	
PS112_69-1	2018-04-12	17:04	-61.25123	-55.74328	124	CTDICBM	at depth	
PS112_69-1	2018-04-12	17:10	-61.25033	-55.74342	121	CTDICBM	station end	
PS112_69-2	2018-04-12	17:21	-61.25038	-55.74197	120	IKMT	station start	
PS112_69-2	2018-04-12	17:27	-61.25397	-55.73623	122	IKMT	at depth	
PS112_69-2	2018-04-12	17:43	-61.26112	-55.72397	122	IKMT	station end	
PS112_70-1	2018-04-12	21:29	-61.24723	-54.49734	533	CTDICBM	station start	
PS112_70-1	2018-04-12	21:44	-61.24501	-54.49431	557	CTDICBM	at depth	
PS112_70-1	2018-04-12	21:56	-61.24330	-54.49178	587	CTDICBM	station end	
PS112_70-2	2018-04-12	22:08	-61.23949	-54.48515	634	IKMT	station start	
PS112_70-2	2018-04-12	22:17	-61.23412	-54.47450	678	IKMT	at depth	
PS112_70-2	2018-04-12	22:40	-61.22174	-54.45194	833	IKMT	station end	
PS112_71-1	2018-04-13	1:26	-61.50317	-54.99918	632	CTDICBM	station start	
PS112_71-1	2018-04-13	1:37	-61.50328	-55.00144	633	CTDICBM	at depth	
PS112_71-1	2018-04-13	1:47	-61.50326	-55.00331	634	CTDICBM	station end	
PS112_71-2	2018-04-13	2:00	-61.50433	-55.00744	640	IKMT	station start	
PS112_71-2	2018-04-13	2:11	-61.51119	-55.01421	696	IKMT	at depth	
PS112_71-2	2018-04-13	2:40	-61.52873	-55.03442	901	IKMT	station end	
PS112_72-1	2018-04-13	4:22	-61.75056	-54.99840	2033	CTDICBM	station start	
PS112_72-1	2018-04-13	4:32	-61.75179	-54.99749	2036	CTDICBM	at depth	
PS112_72-1	2018-04-13	4:40	-61.75112	-54.99684	2038	CTDICBM	station end	
PS112_72-2	2018-04-13	4:49	-61.75005	-54.99634	2038	IKMT	station start	
PS112_72-2	2018-04-13	4:58	-61.75572	-54.99976	2025	IKMT	at depth	
PS112_72-2	2018-04-13	5:18	-61.76380	-55.00523	1982	IKMT	station end	

Station	Date	Time	Latitude	Longi-tude	Depth [m]	Gear	Action	Comment
PS112_73-1	2018-04-13	7:05	-61.75102	-54.50077	680	CTDICBM	station start	
PS112_73-1	2018-04-13	7:20	-61.75103	-54.50083	680	CTDICBM	at depth	
PS112_73-1	2018-04-13	7:31	-61.75085	-54.50043	681	CTDICBM	station end	
PS112_73-2	2018-04-13	7:52	-61.75528	-54.49089	703	IKMT	station start	
PS112_73-2	2018-04-13	8:02	-61.76114	-54.48532	741	IKMT	at depth	
PS112_73-2	2018-04-13	8:27	-61.77485	-54.47270	771	IKMT	station end	
PS112_74-1	2018-04-13	11:26	-62.25320	-54.49937	783	CTDICBM	station start	
PS112_74-1	2018-04-13	11:39	-62.25389	-54.50022	787	CTDICBM	at depth	
PS112_74-1	2018-04-13	11:46	-62.25421	-54.50250	786	CTDICBM	station end	
PS112_74-2	2018-04-13	11:57	-62.25429	-54.51014	773	IKMT	station start	
PS112_74-2	2018-04-13	12:03	-62.25374	-54.51597	758	IKMT	at depth	
PS112_74-2	2018-04-13	12:20	-62.25051	-54.53614	696	IKMT	station end	
PS112_75-1	2018-04-13	15:47	-62.61409	-54.57291	278	RMT	station start	
PS112_75-1	2018-04-13	16:09	-62.60785	-54.57282	282	RMT	at depth	
PS112_75-1	2018-04-13	16:20	-62.60419	-54.57231	276	RMT	station end	
PS112_76-1	2018-04-13	17:41	-62.75087	-54.50337	144	CTDICBM	station start	
PS112_76-1	2018-04-13	17:50	-62.75267	-54.49844	144	CTDICBM	at depth	
PS112_76-1	2018-04-13	17:57	-62.75416	-54.49425	144	CTDICBM	station end	
PS112_76-2	2018-04-13	18:06	-62.75543	-54.49047	145	SECCI	station start	
PS112_76-2	2018-04-13	18:09	-62.75562	-54.49007	145	SECCI	station end	
PS112_76-3	2018-04-13	18:09	-62.75564	-54.49004	145	HN	station start	
PS112_76-3	2018-04-13	18:28	-62.75669	-54.49095	145	HN	station end	
PS112_76-4	2018-04-13	18:35	-62.75642	-54.49124	145	IKMT	station start	
PS112_76-4	2018-04-13	18:42	-62.75354	-54.49095	145	IKMT	at depth	
PS112_76-4	2018-04-13	18:56	-62.74668	-54.48859	142	IKMT	station end	
PS112_77-1	2018-04-13	23:05	-63.25646	-53.97262	254	CTDICBM	station start	
PS112_77-1	2018-04-13	23:21	-63.25609	-53.97285	254	CTDICBM	at depth	
PS112_77-1	2018-04-13	23:30	-63.25613	-53.97339	255	CTDICBM	station end	
PS112_77-2	2018-04-13	23:42	-63.25811	-53.97251	254	HN	station start	
PS112_77-2	2018-04-14	0:32	-63.26391	-53.96790	254	HN	station end	
PS112_77-3	2018-04-14	1:25	-63.34031	-53.91906	254	IKMT	station start	
PS112_77-3	2018-04-14	1:34	-63.33660	-53.92403	255	IKMT	at depth	
PS112_77-3	2018-04-14	1:52	-63.32739	-53.93289	260	IKMT	station end	
PS112_78-1	2018-04-14	4:39	-63.24492	-54.49794	141	CTDICBM	at depth	
PS112_78-1	2018-04-14	4:45	-63.24553	-54.49619	141	CTDICBM	station end	
PS112_78-2	2018-04-14	4:55	-63.24728	-54.49199	139	IKMT	station start	
PS112_78-2	2018-04-14	5:02	-63.24296	-54.49348	138	IKMT	at depth	
PS112_78-2	2018-04-14	5:18	-63.23443	-54.49629	135	IKMT	station end	
PS112_79-1	2018-04-14	9:41	-63.75063	-53.50055	441	CTDICBM	station start	
PS112_79-1	2018-04-14	9:55	-63.75001	-53.50121	440	CTDICBM	at depth	
PS112_79-1	2018-04-14	10:14	-63.74959	-53.50056	440	CTDICBM	station end	

A.4 Stationsliste / Station List

Station	Date	Time	Latitude	Longi-tude	Depth [m]	Gear	Action	Comment
PS112_79-2	2018-04-14	10:25	-63.74680	-53.50350	439	IKMT	station start	
PS112_79-2	2018-04-14	10:35	-63.74109	-53.51152	433	IKMT	at depth	
PS112_79-2	2018-04-14	10:57	-63.72889	-53.52671	417	IKMT	station end	
PS112_80-1	2018-04-14	13:02	-63.85669	-53.78657	513	IKMT	station start	
PS112_80-1	2018-04-14	13:13	-63.85064	-53.79046	505	IKMT	at depth	
PS112_80-1	2018-04-14	13:35	-63.83516	-53.80055	481	IKMT	station end	
PS112_80-2	2018-04-14	13:50	-63.83379	-53.79959	479	CTDICBM	station start	
PS112_80-2	2018-04-14	14:09	-63.83591	-53.80547	482	CTDICBM	at depth	
PS112_80-2	2018-04-14	14:23	-63.83821	-53.81271	483	CTDICBM	station end	
PS112_80-3	2018-04-14	14:29	-63.83839	-53.81547	484	HN	station start	
PS112_80-3	2018-04-14	14:59	-63.84171	-53.82505	488	HN	station end	
PS112_81-1	2018-04-14	16:20	-63.97751	-54.11767	411	IKMT	station start	
PS112_81-1	2018-04-14	16:28	-63.97342	-54.12230	397	IKMT	at depth	
PS112_81-1	2018-04-14	16:51	-63.96278	-54.13728	386	IKMT	station end	
PS112_81-2	2018-04-14	16:59	-63.96331	-54.13971	385	CTDICBM	station start	
PS112_81-2	2018-04-14	17:13	-63.96616	-54.14131	386	CTDICBM	at depth	
PS112_81-2	2018-04-14	17:31	-63.97016	-54.14509	388	CTDICBM	station end	
PS112_82-1	2018-04-14	19:12	-63.96359	-54.63324	346	IKMT	station start	
PS112_82-1	2018-04-14	19:19	-63.95940	-54.63671	347	IKMT	at depth	
PS112_82-1	2018-04-14	19:39	-63.95064	-54.64447	342	IKMT	station end	
PS112_82-2	2018-04-14	19:50	-63.95099	-54.64487	342	CTDICBM	station start	
PS112_82-2	2018-04-14	20:06	-63.95124	-54.64472	344	CTDICBM	at depth	
PS112_82-2	2018-04-14	20:18	-63.95254	-54.64334	339	CTDICBM	station end	
PS112_83-1	2018-04-14	22:02	-63.91743	-54.94232	391	IKMT	station start	
PS112_83-1	2018-04-14	22:11	-63.91090	-54.93996	390	IKMT	at depth	
PS112_83-1	2018-04-14	22:34	-63.89668	-54.93286	380	IKMT	station end	
PS112_83-2	2018-04-14	22:49	-63.89485	-54.93015	377	CTDICBM	station start	
PS112_83-2	2018-04-14	23:09	-63.89460	-54.92662	377	CTDICBM	at depth	
PS112_83-2	2018-04-14	23:29	-63.89412	-54.92302	377	CTDICBM	station end	
PS112_84-1	2018-04-15	1:11	-63.75106	-54.63647	195	IKMT	station start	
PS112_84-1	2018-04-15	1:23	-63.74260	-54.63527	201	IKMT	at depth	
PS112_84-1	2018-04-15	1:50	-63.72733	-54.61856	205	IKMT	station end	
PS112_84-2	2018-04-15	2:00	-63.72743	-54.61359	208	CTDICBM	station start	
PS112_84-2	2018-04-15	2:13	-63.72896	-54.60963	209	CTDICBM	at depth	
PS112_84-2	2018-04-15	2:20	-63.73010	-54.60837	210	CTDICBM	station end	
PS112_85-1	2018-04-15	4:04	-63.66513	-54.95398	271	IKMT	station start	
PS112_85-1	2018-04-15	4:11	-63.66160	-54.95772	280	IKMT	at depth	
PS112_85-1	2018-04-15	4:30	-63.65337	-54.96880	300	IKMT	station end	
PS112_85-2	2018-04-15	4:39	-63.65288	-54.96943	299	CTDICBM	station start	
PS112_85-2	2018-04-15	4:52	-63.65462	-54.96339	294	CTDICBM	at depth	
PS112_85-2	2018-04-15	5:07	-63.65400	-54.96647	297	CTDICBM	station end	

Station	Date	Time	Latitude	Longi-tude	Depth [m]	Gear	Action	Comment
PS112_86-1	2018-04-15	7:02	-63.69639	-55.47527	436	IKMT	station start	
PS112_86-1	2018-04-15	7:11	-63.69066	-55.47367	444	IKMT	at depth	
PS112_86-1	2018-04-15	7:34	-63.67595	-55.46984	463	IKMT	station end	
PS112_86-2	2018-04-15	7:48	-63.68220	-55.47638	448	CTDICBM	station start	
PS112_86-2	2018-04-15	8:03	-63.68123	-55.47436	454	CTDICBM	at depth	
PS112_86-2	2018-04-15	8:18	-63.68071	-55.47311	456	CTDICBM	station end	
PS112_86-3	2018-04-15	8:45	-63.69792	-55.47164	441	RMT	station start	
PS112_86-3	2018-04-15	9:01	-63.68612	-55.46922	456	RMT	at depth	
PS112_86-3	2018-04-15	9:34	-63.66541	-55.45684	474	RMT	station end	
PS112_87-1	2018-04-15	10:36	-63.73610	-55.42059	485	IKMT	station start	
PS112_87-1	2018-04-15	10:45	-63.73043	-55.41792	491	IKMT	at depth	
PS112_87-1	2018-04-15	11:09	-63.71819	-55.41248	495	IKMT	station end	
PS112_87-2	2018-04-15	11:20	-63.72305	-55.41031	494	CTDICBM	station start	
PS112_87-2	2018-04-15	11:34	-63.72460	-55.40761	494	CTDICBM	at depth	
PS112_87-2	2018-04-15	11:41	-63.72528	-55.40360	494	CTDICBM	station end	
PS112_88-1	2018-04-15	13:47	-63.99849	-55.50940	311	CTDICBM	station start	
PS112_88-1	2018-04-15	14:04	-64.00046	-55.51026	311	CTDICBM	at depth	
PS112_88-1	2018-04-15	14:12	-64.00092	-55.51044	310	CTDICBM	station end	
PS112_89-1	2018-04-15	17:00	-63.88392	-55.88415	411	CTDICBM	station start	
PS112_89-1	2018-04-15	17:14	-63.88361	-55.88861	411	CTDICBM	at depth	
PS112_89-1	2018-04-15	17:31	-63.88386	-55.88976	411	CTDICBM	station end	
PS112_89-2	2018-04-15	17:41	-63.88294	-55.89150	411	SECCI	station start	
PS112_89-2	2018-04-15	17:43	-63.88273	-55.89182	411	SECCI	station end	
PS112_93-1	2018-04-16	0:06	-63.65304	-56.53511	396	IKMT	station start	
PS112_93-1	2018-04-17	0:08	-63.67483	-56.92184	402	IKMT	at depth	
PS112_93-1	2018-04-17	0:22	-63.67112	-56.90360	348	IKMT	station end	
PS112_90-1	2018-04-16	11:44	-63.73532	-56.84866	649	ISPC	station start	
PS112_90-1	2018-04-16	12:15	-63.73303	-56.84025	618	ISPC	at depth	
PS112_90-1	2018-04-16	12:37	-63.72990	-56.83962	587	ISPC	station end	
PS112_90-2	2018-04-16	12:52	-63.72853	-56.83965	564	CTDICBM	station start	
PS112_90-2	2018-04-16	13:13	-63.72683	-56.83832	521	CTDICBM	at depth	
PS112_90-2	2018-04-16	13:42	-63.72205	-56.83769	264	CTDICBM	station end	
PS112_90-3	2018-04-16	14:21	-63.73585	-56.84880	653	DSTRM	station start	
PS112_90-3	2018-04-16	15:01	-63.73295	-56.84468	621	DSTRM	station end	
PS112_91-1	2018-04-16	16:10	-63.67503	-56.97094	315	BT	station start	
PS112_91-1	2018-04-16	16:32	-63.68171	-56.92658	441	BT	at depth	
PS112_91-1	2018-04-16	16:36	-63.68379	-56.92033	446	BT	profile start	
PS112_91-1	2018-04-16	16:51	-63.69335	-56.89841	436	BT	profile end	
PS112_91-1	2018-04-16	17:30	-63.70736	-56.87304	441	BT	station end	
PS112_91-2	2018-04-16	17:46	-63.70664	-56.86517	432	CTDICBM	station start	

A.4 Stationsliste / Station List

Station	Date	Time	Latitude	Longi-tude	Depth [m]	Gear	Action	Comment
PS112_91-2	2018-04-16	18:06	-63.70634	-56.87122	435	CTDICBM	at depth	
PS112_91-2	2018-04-16	18:22	-63.70611	-56.87524	445	CTDICBM	station end	
PS112_91-3	2018-04-16	18:25	-63.70609	-56.87577	448	SECCI	station start	
PS112_91-3	2018-04-16	18:30	-63.70602	-56.87700	456	SECCI	station end	
PS112_92-1	2018-04-16	19:31	-63.67263	-57.09777	636	BT	station start	
PS112_92-1	2018-04-16	20:05	-63.70074	-57.03362	641	BT	at depth	
PS112_92-1	2018-04-16	20:10	-63.70446	-57.02600	626	BT	profile start	
PS112_92-1	2018-04-16	20:25	-63.71272	-57.00684	664	BT	profile end	
PS112_92-1	2018-04-16	21:01	-63.72342	-56.98296	667	BT	station end	
PS112_92-2	2018-04-16	21:57	-63.72507	-56.98239	648	CTDICBM	station start	
PS112_92-2	2018-04-16	22:22	-63.72550	-56.98079	640	CTDICBM	at depth	
PS112_92-2	2018-04-16	22:38	-63.72579	-56.97908	637	CTDICBM	station end	
PS112_93-2	2018-04-17	2:05	-63.71788	-56.76153	169	IKMT	station start	
PS112_93-2	2018-04-17	2:09	-63.71702	-56.76397	169	IKMT	at depth	
PS112_93-2	2018-04-17	2:18	-63.71232	-56.77206	193	IKMT	station end	
PS112_94-1	2018-04-17	3:50	-63.73270	-56.73117	581	IKMT	station start	
PS112_94-1	2018-04-17	3:56	-63.73082	-56.73786	548	IKMT	at depth	
PS112_94-1	2018-04-17	4:10	-63.72651	-56.75254	457	IKMT	station end	
PS112_95-1	2018-04-17	6:03	-63.86743	-56.78029	372	IKMT	station start	
PS112_95-1	2018-04-17	6:08	-63.86545	-56.78709	361	IKMT	at depth	
PS112_95-1	2018-04-17	6:20	-63.86191	-56.79969	262	IKMT	station end	
PS112_96-1	2018-04-17	8:39	-63.75583	-56.74342	603	IKMT	station start	
PS112_96-1	2018-04-17	8:45	-63.75346	-56.74731	597	IKMT	at depth	
PS112_96-1	2018-04-17	8:59	-63.74721	-56.75817	630	IKMT	station end	
PS112_96-2	2018-04-17	9:35	-63.74773	-56.74326	614	CTDICBM	station start	
PS112_96-2	2018-04-17	9:55	-63.74790	-56.73362	600	CTDICBM	at depth	
PS112_96-2	2018-04-17	10:25	-63.74759	-56.72077	587	CTDICBM	station end	
PS112_97-1	2018-04-17	11:42	-63.70456	-56.75075	270	DSTRM	station start	
PS112_97-1	2018-04-17	12:13	-63.70365	-56.74438	272	DSTRM	station end	
PS112_97-2	2018-04-17	12:54	-63.68738	-56.72009	278	CTDICBM	station start	
PS112_97-2	2018-04-17	13:07	-63.68735	-56.71529	285	CTDICBM	at depth	
PS112_97-2	2018-04-17	13:20	-63.68844	-56.71218	291	CTDICBM	station end	
PS112_97-3	2018-04-17	13:33	-63.68950	-56.71186	290	ISPC	station start	
PS112_97-3	2018-04-17	13:53	-63.69140	-56.71550	283	ISPC	at depth	
PS112_97-3	2018-04-17	14:09	-63.69430	-56.71534	269	ISPC	station end	
PS112_98-1	2018-04-17	15:35	-63.64654	-56.47975	491	DSTRM	station start	
PS112_98-1	2018-04-17	16:05	-63.64674	-56.48374	471	DSTRM	station end	
PS112_98-2	2018-04-17	16:20	-63.64960	-56.48741	447	ISPC	station start	
PS112_98-2	2018-04-17	16:49	-63.65164	-56.48945	432	ISPC	at depth	
PS112_98-2	2018-04-17	17:05	-63.65164	-56.49044	426	ISPC	station end	
PS112_98-3	2018-04-17	17:33	-63.64263	-56.49235	391	Goflo	station start	

Station	Date	Time	Latitude	Longi-tude	Depth [m]	Gear	Action	Comment
PS112_98-3	2018-04-17	17:39	-63.64380	-56.49109	416	Goflo	at depth	
PS112_98-3	2018-04-17	17:54	-63.64671	-56.48963	424	Goflo	station end	
PS112_98-4	2018-04-17	18:09	-63.64626	-56.49299	412	CTDICBM	station start	
PS112_98-4	2018-04-17	18:28	-63.64447	-56.49467	383	CTDICBM	at depth	
PS112_98-4	2018-04-17	18:45	-63.64399	-56.49806	358	CTDICBM	station end	
PS112_98-5	2018-04-17	18:57	-63.64493	-56.49822	362	SECCI	station start	
PS112_98-5	2018-04-17	19:00	-63.64506	-56.49830	362	SECCI	station end	
PS112_98-6	2018-04-17	19:15	-63.64466	-56.50104	353	BONGO	station start	
PS112_98-6	2018-04-17	19:35	-63.64595	-56.50445	356	BONGO	at depth	
PS112_98-6	2018-04-17	19:48	-63.64585	-56.50914	353	BONGO	station end	
PS112_98-7	2018-04-17	19:51	-63.64619	-56.50978	351	BONGO	station start	
PS112_98-7	2018-04-17	20:04	-63.64741	-56.51198	359	BONGO	at depth	
PS112_98-7	2018-04-17	20:14	-63.64753	-56.51520	359	BONGO	station end	
PS112_98-8	2018-04-17	20:19	-63.64798	-56.51531	360	HN	station start	
PS112_98-8	2018-04-17	20:28	-63.64930	-56.51428	361	HN	station end	
PS112_98-9	2018-04-17	20:39	-63.65319	-56.50708	367	IKMT	station start	
PS112_98-9	2018-04-17	20:46	-63.64945	-56.50929	349	IKMT	at depth	
PS112_98-9	2018-04-17	21:14	-63.64335	-56.49897	357	IKMT	station end	
PS112_98-10	2018-04-17	21:35	-63.65334	-56.48509	465	ISPC	station start	
PS112_98-10	2018-04-17	22:09	-63.65637	-56.47924	570	ISPC	at depth	
PS112_98-10	2018-04-17	22:28	-63.65653	-56.47464	600	ISPC	station end	
PS112_98-11	2018-04-18	3:03	-63.64316	-56.42223	591	ISPC	station start	
PS112_98-11	2018-04-18	3:37	-63.64593	-56.43395	590	ISPC	at depth	
PS112_98-11	2018-04-18	3:56	-63.65001	-56.43597	592	ISPC	station end	
PS112_98-12	2018-04-18	9:05	-63.67288	-56.46201	602	ISPC	station start	
PS112_98-12	2018-04-18	9:38	-63.67078	-56.46131	600	ISPC	at depth	
PS112_98-12	2018-04-18	9:59	-63.66895	-56.46185	602	ISPC	station end	
PS112_98-13	2018-04-18	11:20	-63.65166	-56.45671	605	ICE-BUCKET	station end	
PS112_98-14	2018-04-18	14:53	-63.61373	-56.42747	566	BOAT	station end	
PS112_98-15	2018-04-18	14:22	-63.61636	-56.42381	578	DSTRM	station start	
PS112_98-15	2018-04-18	14:45	-63.61453	-56.42841	552	DSTRM	station end	
PS112_98-16	2018-04-18	15:15	-63.61236	-56.42165	612	ISPC	station start	
PS112_98-16	2018-04-18	15:48	-63.61308	-56.42478	595	ISPC	at depth	
PS112_98-16	2018-04-18	16:08	-63.61214	-56.42936	567	ISPC	station end	
PS112_99-1	2018-04-18	17:46	-63.50363	-56.49509	808	CTDICBM	at depth	
PS112_99-1	2018-04-18	18:09	-63.50532	-56.49388	796	CTDICBM	station end	
PS112_99-2	2018-04-18	18:22	-63.50655	-56.49189	789	IKMT	station start	
PS112_99-2	2018-04-18	18:32	-63.50242	-56.48996	829	IKMT	at depth	
PS112_99-2	2018-04-18	18:52	-63.49537	-56.48335	892	IKMT	station end	
PS112_100-1	2018-04-18	20:29	-63.39971	-56.90000	167	ADCP_150	profile start	
PS112_100-1	2018-04-18	21:35	-63.36814	-56.59987	359	ADCP_150	profile end	

A.4 Stationsliste / Station List

Station	Date	Time	Latitude	Longi-tude	Depth [m]	Gear	Action	Comment
PS112_101-1	2018-04-18	22:26	-63.32965	-56.80812	252	CTDICBM	station start	
PS112_101-1	2018-04-18	22:44	-63.33058	-56.80532	256	CTDICBM	at depth	
PS112_101-1	2018-04-18	23:03	-63.32831	-56.80918	251	CTDICBM	station start	
PS112_101-1	2018-04-18	23:03	-63.32825	-56.80925	251	CTDICBM	station end	
PS112_101-2	2018-04-18	23:16	-63.32606	-56.81156	245	BONGO	station start	
PS112_101-2	2018-04-18	23:33	-63.32416	-56.81298	242	BONGO	at depth	
PS112_101-2	2018-04-18	23:43	-63.32219	-56.81571	241	BONGO	station end	
PS112_101-3	2018-04-18	23:54	-63.31866	-56.81797	238	IKMT	station start	
PS112_101-3	2018-04-18	23:58	-63.31753	-56.81757	237	IKMT	at depth	
PS112_101-3	2018-04-19	0:11	-63.31029	-56.81247	218	IKMT	station end	
PS112_101-4	2018-04-19	0:18	-63.30823	-56.81182	214	IKMT	station start	
PS112_101-4	2018-04-19	0:28	-63.30240	-56.80847	202	IKMT	at depth	
PS112_101-4	2018-04-19	0:34	-63.29868	-56.80636	184	IKMT	station end	
PS112_102-1	2018-04-19	2:13	-63.10627	-56.98172	560	CTDICBM	station start	
PS112_102-1	2018-04-19	2:40	-63.10671	-56.99018	546	CTDICBM	at depth	
PS112_102-1	2018-04-19	3:07	-63.10738	-56.99774	527	CTDICBM	station end	
PS112_102-2	2018-04-19	3:18	-63.10653	-56.99539	543	IKMT	station start	
PS112_102-2	2018-04-19	3:25	-63.10309	-56.98949	531	IKMT	at depth	
PS112_102-2	2018-04-19	3:47	-63.09414	-56.96927	338	IKMT	station end	
PS112_103-1	2018-04-19	6:57	-62.75118	-56.50167	198	CTDICBM	station start	
PS112_103-1	2018-04-19	7:11	-62.75160	-56.50012	198	CTDICBM	at depth	
PS112_103-1	2018-04-19	7:23	-62.75009	-56.50207	202	CTDICBM	station end	
PS112_103-2	2018-04-19	7:35	-62.74671	-56.50280	209	IKMT	station start	
PS112_103-2	2018-04-19	7:44	-62.74025	-56.50550	214	IKMT	at depth	
PS112_103-2	2018-04-19	8:08	-62.72558	-56.51285	213	IKMT	station end	
PS112_104-1	2018-04-19	11:07	-62.74884	-55.50262	121	CTDICBM	station start	
PS112_104-1	2018-04-19	11:11	-62.74870	-55.50449	119	CTDICBM	at depth	
PS112_104-1	2018-04-19	11:26	-62.74816	-55.51168	122	CTDICBM	station end	
PS112_104-2	2018-04-19	11:35	-62.74660	-55.51962	129	IKMT	station start	
PS112_104-2	2018-04-19	11:41	-62.74372	-55.52826	128	IKMT	at depth	
PS112_104-2	2018-04-19	11:54	-62.73642	-55.54812	143	IKMT	station end	
PS112_105-1	2018-04-19	19:08	-62.50100	-53.99747	773	CTDICBM	station start	
PS112_105-1	2018-04-19	19:18	-62.50161	-53.99577	774	CTDICBM	at depth	
PS112_105-1	2018-04-19	19:31	-62.50183	-53.99512	774	CTDICBM	station end	
PS112_105-2	2018-04-19	19:38	-62.50220	-53.99338	776	SECCI	station start	
PS112_105-2	2018-04-19	19:43	-62.50255	-53.99170	778	SECCI	station end	
PS112_105-3	2018-04-19	19:46	-62.50166	-53.99282	779	IKMT	station start	
PS112_105-3	2018-04-19	19:54	-62.49854	-53.99888	779	IKMT	at depth	
PS112_105-3	2018-04-19	20:10	-62.49278	-54.00738	782	IKMT	station end	
PS112_106-1	2018-04-20	9:07	-61.99605	-53.99682	547	TMPUMP	station start	
PS112_106-1	2018-04-20	12:27	-61.94355	-53.94263	530	TMPUMP	station end	

Station	Date	Time	Latitude	Longi-tude	Depth [m]	Gear	Action	Comment
PS112_106-2	2018-04-20	12:48	-61.93557	-53.93661	542	BONGO	station start	
PS112_106-2	2018-04-20	13:03	-61.93170	-53.93294	560	BONGO	at depth	
PS112_106-2	2018-04-20	13:10	-61.92949	-53.93089	568	BONGO	station end	
PS112_106-3	2018-04-20	13:31	-61.92335	-53.92638	577	DSTRM	station start	
PS112_106-3	2018-04-20	13:51	-61.91800	-53.92362	582	DSTRM	station end	
PS112_106-4	2018-04-20	14:22	-61.91266	-53.91267	631	ISPC	station start	
PS112_106-4	2018-04-20	14:48	-61.90648	-53.90989	637	ISPC	at depth	
PS112_106-4	2018-04-20	15:10	-61.90226	-53.90830	544	ISPC	station end	
PS112_106-5	2018-04-20	15:21	-61.89892	-53.90996	465	CTDICBM	station start	
PS112_106-5	2018-04-20	15:37	-61.89398	-53.91412	424	CTDICBM	at depth	
PS112_106-5	2018-04-20	15:52	-61.89089	-53.91852	413	CTDICBM	station end	
PS112_106-6	2018-04-20	16:03	-61.88900	-53.92053	409	IKMT	station start	
PS112_106-6	2018-04-20	16:14	-61.89426	-53.92765	410	IKMT	at depth	
PS112_106-6	2018-04-20	16:40	-61.90620	-53.94183	423	IKMT	station end	
PS112_106-7	2018-04-20	18:31	-61.88639	-53.99483	370	BONGO	station start	
PS112_106-7	2018-04-20	18:56	-61.88987	-53.99800	373	BONGO	at depth	
PS112_106-7	2018-04-20	19:08	-61.89117	-53.99729	374	BONGO	station end	
PS112_106-8	2018-04-20	19:11	-61.89178	-53.99778	376	BONGO	station start	
PS112_106-8	2018-04-20	19:37	-61.89411	-54.00002	374	BONGO	at depth	
PS112_106-8	2018-04-20	19:54	-61.89511	-53.99895	376	BONGO	station end	
PS112_106-9	2018-04-20	19:56	-61.89513	-53.99858	376	HN	station start	
PS112_106-9	2018-04-20	20:00	-61.89519	-53.99775	378	HN	station end	
PS112_106-10	2018-04-20	20:09	-61.89556	-53.99571	378	ISPC	station start	
PS112_106-10	2018-04-20	20:35	-61.89635	-53.99371	377	ISPC	at depth	
PS112_106-10	2018-04-20	20:53	-61.89826	-53.98672	371	ISPC	station end	
PS112_106-11	2018-04-21	2:04	-61.91362	-53.91938	568	ISPC	station start	
PS112_106-11	2018-04-21	2:39	-61.90967	-53.90568	709	ISPC	at depth	
PS112_106-11	2018-04-21	3:00	-61.90914	-53.89786	750	ISPC	station end	
PS112_106-12	2018-04-21	8:00	-61.91018	-53.76655	790	ISPC	station start	
PS112_106-12	2018-04-21	8:36	-61.90606	-53.75235	794	ISPC	at depth	
PS112_106-12	2018-04-21	8:57	-61.90222	-53.74459	789	ISPC	station end	
PS112_106-13	2018-04-21	14:16	-61.81282	-53.64635	566	DSTRM	station start	
PS112_106-13	2018-04-21	14:37	-61.80679	-53.64968	558	DSTRM	station end	
PS112_106-14	2018-04-21	15:10	-61.80710	-53.65339	556	ISPC	station start	
PS112_106-14	2018-04-21	15:45	-61.79831	-53.65589	554	ISPC	at depth	
PS112_106-14	2018-04-21	16:06	-61.79298	-53.65747	585	ISPC	station end	
PS112_106-15	2018-04-21	16:16	-61.78998	-53.65874	610	CTDICBM	station start	
PS112_106-15	2018-04-21	16:39	-61.78270	-53.66476	690	CTDICBM	at depth	
PS112_106-15	2018-04-21	17:03	-61.77801	-53.67388	742	CTDICBM	station end	
PS112_106-16	2018-04-21	17:13	-61.77642	-53.67811	710	SECCI	station start	
PS112_106-16	2018-04-21	17:15	-61.77607	-53.67911	697	SECCI	station end	

A.4 Stationsliste / Station List

Station	Date	Time	Latitude	Longi-tude	Depth [m]	Gear	Action	Comment
PS112_106-17	2018-04-21	17:29	-61.76478	-53.67953	453	IKMT	station start	
PS112_106-17	2018-04-21	17:39	-61.75545	-53.68032	375	IKMT	at depth	
PS112_106-17	2018-04-21	18:02	-61.73975	-53.68583	337	IKMT	station end	
PS112_107-1	2018-04-21	20:19	-61.50049	-54.00065	733	CTDICBM	station start	
PS112_107-1	2018-04-21	20:30	-61.50222	-54.00293	736	CTDICBM	at depth	
PS112_107-1	2018-04-21	20:43	-61.50415	-54.00482	740	CTDICBM	station end	
PS112_107-2	2018-04-21	21:25	-61.50384	-53.99564	728	IKMT	station start	
PS112_107-2	2018-04-21	21:33	-61.50116	-53.98873	721	IKMT	at depth	
PS112_107-2	2018-04-21	21:54	-61.49607	-53.97552	719	IKMT	station end	
PS112_108-1	2018-04-21	23:30	-61.24931	-53.90004	1239	CTDICBM	station start	
PS112_108-1	2018-04-21	23:43	-61.24827	-53.90345	1234	CTDICBM	at depth	
PS112_108-1	2018-04-21	23:51	-61.24777	-53.90614	1227	CTDICBM	station end	
PS112_108-2	2018-04-22	0:01	-61.24837	-53.91028	1214	IKMT	station start	
PS112_108-2	2018-04-22	0:09	-61.24454	-53.90915	1219	IKMT	at depth	
PS112_108-2	2018-04-22	0:30	-61.23524	-53.90489	1243	IKMT	station end	
PS112_109-1	2018-04-22	2:28	-61.00370	-53.99855	1128	CTDICBM	station start	
PS112_109-1	2018-04-22	2:39	-61.00722	-53.99583	1175	CTDICBM	at depth	
PS112_109-1	2018-04-22	2:49	-61.01011	-53.99513	1181	CTDICBM	station end	
PS112_109-2	2018-04-22	2:58	-61.01256	-53.99942	1146	IKMT	station start	
PS112_109-2	2018-04-22	3:05	-61.01409	-54.01038	1063	IKMT	at depth	
PS112_109-2	2018-04-22	3:25	-61.01741	-54.03099	877	IKMT	station end	
PS112_110-1	2018-04-22	11:21	-61.30463	-54.90625	522	CTDICBM	at depth	
PS112_110-1	2018-04-22	11:36	-61.30314	-54.90620	481	CTDICBM	station end	
PS112_110-2	2018-04-22	13:58	-61.35097	-54.85871	843	M-RMT	station start	
PS112_110-2	2018-04-22	14:31	-61.33521	-54.87236	807	M-RMT	at depth	
PS112_110-2	2018-04-22	15:22	-61.30477	-54.90037	518	M-RMT	profile end	
PS112_110-2	2018-04-22	15:31	-61.29991	-54.90400	393	M-RMT	station end	
PS112_110-3	2018-04-22	17:42	-61.27619	-54.90033	183	IKMT	station start	
PS112_110-3	2018-04-22	17:49	-61.27415	-54.90421	183	IKMT	station end	
PS112_110-4	2018-04-22	18:01	-61.26873	-54.91084	168	IKMT	station start	
PS112_110-4	2018-04-22	18:10	-61.26472	-54.91316	155	IKMT	station end	
PS112_110-5	2018-04-22	18:26	-61.25953	-54.90510	136	IKMT	station start	
PS112_110-5	2018-04-22	18:41	-61.25359	-54.91185	127	IKMT	station end	
PS112_110-6	2018-04-22	20:36	-61.31660	-55.35085	77	EK60	profile start	
PS112_110-6	2018-04-23	8:53	-61.36778	-54.19317	443	EK60	profile end	
PS112_110-7	2018-04-23	1:10	-61.37564	-54.86578	897	IKMT	station start	
PS112_110-7	2018-04-23	1:24	-61.38083	-54.85933	885	IKMT	at depth	
PS112_110-7	2018-04-23	1:44	-61.39202	-54.84566	929	IKMT	station end	
PS112_110-8	2018-04-23	2:28	-61.37392	-54.75633	367	CTDICBM	station start	
PS112_110-8	2018-04-23	2:44	-61.37193	-54.75285	363	CTDICBM	at depth	
PS112_110-8	2018-04-23	2:53	-61.37145	-54.74839	360	CTDICBM	station end	

Station	Date	Time	Latitude	Longi-tude	Depth [m]	Gear	Action	Comment
PS112_110-9	2018-04-23	7:54	-61.34628	-54.30808	743	IKMT	station start	
PS112_110-9	2018-04-23	8:03	-61.34771	-54.31724	911	IKMT	at depth	
PS112_110-9	2018-04-23	8:22	-61.35435	-54.32614	932	IKMT	station end	
PS112_111-1	2018-04-23	12:42	-61.07095	-54.75680	130	IKMT	station start	
PS112_111-1	2018-04-23	12:48	-61.07184	-54.76117	123	IKMT	at depth	
PS112_111-1	2018-04-23	13:02	-61.07291	-54.76570	119	IKMT	station end	
PS112_111-2	2018-04-23	14:17	-61.00860	-54.83220	554	IKMT	station start	
PS112_111-2	2018-04-23	14:20	-61.00936	-54.83611	554	IKMT	at depth	
PS112_111-2	2018-04-23	14:32	-61.01159	-54.84583	556	IKMT	station end	
PS112_111-3	2018-04-23	14:38	-61.01278	-54.85009	557	IKMT	station start	
PS112_111-3	2018-04-23	14:41	-61.01345	-54.85352	559	IKMT	at depth	
PS112_111-3	2018-04-23	14:52	-61.01524	-54.86000	563	IKMT	station end	
PS112_111-4	2018-04-23	15:16	-61.01490	-54.85406	559	RMT	station start	
PS112_111-4	2018-04-23	15:20	-61.01555	-54.86027	562	RMT	at depth	
PS112_111-4	2018-04-23	15:33	-61.01597	-54.87043	556	RMT	station end	
PS112_111-5	2018-04-23	21:59	-61.02144	-54.78959	548	CTDICBM	station start	
PS112_111-5	2018-04-23	22:19	-61.02297	-54.79316	544	CTDICBM	at depth	
PS112_111-5	2018-04-23	22:41	-61.02198	-54.80164	544	CTDICBM	station end	
PS112_111-6	2018-04-23	23:00	-61.02369	-54.80953	543	EPNET	station start	
PS112_111-6	2018-04-23	23:05	-61.02317	-54.81221	544	EPNET	at depth	
PS112_111-6	2018-04-23	23:14	-61.02244	-54.81582	545	EPNET	station end	
PS112_111-7	2018-04-23	23:27	-61.02118	-54.82167	544	EPNET	station start	
PS112_111-7	2018-04-23	23:30	-61.02075	-54.82315	544	EPNET	at depth	
PS112_111-7	2018-04-23	23:34	-61.02017	-54.82465	545	EPNET	station end	
PS112_111-8	2018-04-23	23:38	-61.01938	-54.82692	546	EPNET	station start	
PS112_111-8	2018-04-23	23:42	-61.01901	-54.82835	547	EPNET	at depth	
PS112_111-8	2018-04-23	23:46	-61.01846	-54.83021	548	EPNET	station end	
PS112_111-9	2018-04-23	23:46	-61.01838	-54.83043	548	EPNET	station start	
PS112_111-9	2018-04-23	23:51	-61.01781	-54.83263	549	EPNET	at depth	
PS112_111-9	2018-04-23	23:54	-61.01728	-54.83424	550	EPNET	station end	
PS112_111-10	2018-04-24	0:01	-61.01598	-54.83754	552	EPNET	station start	
PS112_111-10	2018-04-24	0:06	-61.01514	-54.83999	553	EPNET	at depth	
PS112_111-10	2018-04-24	0:10	-61.01445	-54.84199	555	EPNET	station end	
PS112_111-11	2018-04-24	0:20	-61.01428	-54.84661	556	IKMT	station start	
PS112_111-11	2018-04-24	0:27	-61.01806	-54.85097	554	IKMT	at depth	
PS112_111-11	2018-04-24	0:34	-61.02101	-54.85509	522	IKMT	station end	
PS112_111-12	2018-04-24	1:54	-60.91294	-54.85059	742	IKMT	station start	
PS112_111-12	2018-04-24	1:55	-60.91342	-54.85144	742	IKMT	at depth	
PS112_111-12	2018-04-24	2:00	-60.91483	-54.85422	742	IKMT	station end	
PS112_111-13	2018-04-24	2:08	-60.91632	-54.85689	741	IKMT	station start	
PS112_111-13	2018-04-24	2:10	-60.91687	-54.85795	740	IKMT	at depth	

A.4 Stationsliste / Station List

Station	Date	Time	Latitude	Longi-tude	Depth [m]	Gear	Action	Comment
PS112_111-13	2018-04-24	2:13	-60.91733	-54.85888	740	IKMT	station end	
PS112_111-14	2018-04-24	2:18	-60.91811	-54.86012	739	IKMT	station start	
PS112_111-14	2018-04-24	2:21	-60.91912	-54.86233	739	IKMT	at depth	
PS112_111-14	2018-04-24	2:30	-60.92055	-54.86547	738	IKMT	station end	
PS112_111-15	2018-04-24	2:38	-60.92207	-54.86896	739	IKMT	station start	
PS112_111-15	2018-04-24	2:39	-60.92223	-54.86937	738	IKMT	at depth	
PS112_111-15	2018-04-24	2:39	-60.92228	-54.86951	737	IKMT	station end	
PS112_111-16	2018-04-24	3:43	-60.92890	-55.02863	1100	IKMT	at depth	
PS112_111-16	2018-04-24	3:52	-60.93208	-55.03537	847	IKMT	station end	
PS112_111-17	2018-04-24	3:58	-60.93450	-55.03950	687	IKMT	station start	
PS112_111-17	2018-04-24	4:00	-60.93648	-55.04189	619	IKMT	at depth	
PS112_111-17	2018-04-24	4:09	-60.93970	-55.04916	530	IKMT	station end	
PS112_111-18	2018-04-24	4:13	-60.94103	-55.05188	520	IKMT	station start	
PS112_111-18	2018-04-24	4:15	-60.94216	-55.05387	512	IKMT	at depth	
PS112_111-18	2018-04-24	4:22	-60.94475	-55.06086	488	IKMT	station end	
PS112_111-19	2018-04-24	4:26	-60.94593	-55.06530	480	IKMT	station start	
PS112_111-19	2018-04-24	4:29	-60.94734	-55.06730	472	IKMT	at depth	
PS112_111-19	2018-04-24	4:37	-60.94976	-55.07122	469	IKMT	station end	
PS112_111-20	2018-04-24	5:50	-61.04058	-55.16854	66	IKMT	station start	
PS112_111-20	2018-04-24	5:53	-61.04124	-55.17334	64	IKMT	at depth	
PS112_111-20	2018-04-24	6:00	-61.04189	-55.18193	60	IKMT	station end	
PS112_111-21	2018-04-24	6:02	-61.04179	-55.18391	58	IKMT	station start	
PS112_111-21	2018-04-24	6:06	-61.04142	-55.18997	53	IKMT	at depth	
PS112_111-21	2018-04-24	6:13	-61.04080	-55.19705	52	IKMT	station end	
PS112_111-22	2018-04-24	6:16	-61.03938	-55.19936	52	IKMT	station start	
PS112_111-22	2018-04-24	6:19	-61.03785	-55.20035	54	IKMT	at depth	
PS112_111-22	2018-04-24	6:31	-61.03362	-55.20471	72	IKMT	station end	
PS112_111-23	2018-04-24	7:10	-60.98758	-55.20720	260	IKMT	station start	
PS112_111-23	2018-04-24	7:15	-60.99043	-55.21044	258	IKMT	at depth	
PS112_111-23	2018-04-24	7:29	-60.99815	-55.22005	204	IKMT	station end	
PS112_111-24	2018-04-24	7:55	-60.98974	-55.20775	256	IKMT	station start	
PS112_111-24	2018-04-24	7:59	-60.99170	-55.20946	248	IKMT	at depth	
PS112_111-24	2018-04-24	8:08	-60.99669	-55.21614	211	IKMT	station end	
PS112_111-25	2018-04-24	8:33	-60.98830	-55.21016	277	IKMT	station start	
PS112_111-25	2018-04-24	8:36	-60.99004	-55.21196	263	IKMT	at depth	
PS112_111-25	2018-04-24	8:45	-60.99499	-55.21861	221	IKMT	station end	
PS112_111-26	2018-04-24	13:29	-61.03770	-55.17092	71	BOAT	station start	
PS112_111-26	2018-04-24	17:40	-61.04117	-55.12221	86	BOAT	station end	
PS112_111-27	2018-04-24	13:58	-61.03756	-55.16311	72	IKMT	station start	
PS112_111-27	2018-04-24	14:00	-61.03695	-55.16028	71	IKMT	at depth	
PS112_111-27	2018-04-24	14:08	-61.03517	-55.15185	77	IKMT	station end	

Station	Date	Time	Latitude	Longi-tude	Depth [m]	Gear	Action	Comment
PS112_111-28	2018-04-24	16:38	-61.04147	-55.13261	92	CTDICBM	station start	
PS112_111-28	2018-04-24	16:42	-61.04162	-55.13219	92	CTDICBM	at depth	
PS112_111-28	2018-04-24	16:47	-61.04183	-55.13146	91	CTDICBM	station end	
PS112_111-29	2018-04-24	17:15	-61.04118	-55.12863	90	CTDICBM	station start	
PS112_111-29	2018-04-24	17:20	-61.04110	-55.12820	89	CTDICBM	at depth	
PS112_111-29	2018-04-24	17:21	-61.04110	-55.12801	89	CTDICBM	station end	
PS112_111-30	2018-04-24	18:08	-61.04233	-55.11595	92	CTDICBM	station start	
PS112_111-30	2018-04-24	18:13	-61.04224	-55.11421	93	CTDICBM	at depth	
PS112_111-30	2018-04-24	18:18	-61.04186	-55.11215	93	CTDICBM	station end	
PS112_111-31	2018-04-24	18:41	-61.03563	-55.09776	101	SECCI	station start	
PS112_111-31	2018-04-24	18:43	-61.03561	-55.09717	102	SECCI	station end	
PS112_111-32	2018-04-24	19:02	-61.03573	-55.09389	103	CTDICBM	station start	
PS112_111-32	2018-04-24	19:10	-61.03581	-55.09272	104	CTDICBM	at depth	
PS112_111-32	2018-04-24	19:27	-61.03583	-55.09162	105	CTDICBM	station end	
PS112_112-1	2018-04-25	0:11	-61.32102	-55.35003	78	ADCP_150	profile start	
PS112_112-1	2018-04-25	14:57	-60.91591	-55.71585	161	ADCP_150	station end	
PS112_113-1	2018-04-25	1:56	-61.32659	-55.57139	89	CTDICBM	station start	
PS112_113-1	2018-04-25	2:04	-61.32612	-55.57173	102	CTDICBM	at depth	
PS112_113-1	2018-04-25	2:11	-61.32571	-55.57076	118	CTDICBM	station end	
PS112_113-2	2018-04-25	2:03	-61.32617	-55.57188	100	HN	station start	
PS112_113-2	2018-04-25	2:46	-61.32553	-55.56199	137	HN	station end	
PS112_114-1	2018-04-25	4:28	-61.23872	-55.90328	148	CTDICBM	station start	
PS112_114-1	2018-04-25	4:40	-61.23828	-55.90315	148	CTDICBM	at depth	
PS112_114-1	2018-04-25	4:43	-61.23832	-55.90314	148	CTDICBM	station end	
PS112_114-2	2018-04-25	5:02	-61.24025	-55.89832	148	IKMT	station start	
PS112_114-2	2018-04-25	5:10	-61.24290	-55.88893	149	IKMT	at depth	
PS112_114-2	2018-04-25	5:27	-61.24667	-55.87222	151	IKMT	station end	
PS112_115-1	2018-04-25	7:59	-61.14595	-55.75505	90	IKMT	station start	
PS112_115-1	2018-04-25	8:03	-61.14771	-55.75237	90	IKMT	at depth	
PS112_115-1	2018-04-25	8:14	-61.15137	-55.74774	90	IKMT	station end	
PS112_116-1	2018-04-25	10:06	-61.05887	-55.75574	104	CTDICBM	station start	
PS112_116-1	2018-04-25	10:15	-61.05873	-55.75859	105	CTDICBM	at depth	
PS112_116-1	2018-04-25	10:21	-61.05866	-55.76081	105	CTDICBM	station end	
PS112_116-2	2018-04-25	10:31	-61.05871	-55.76539	105	IKMT	station start	
PS112_116-2	2018-04-25	10:35	-61.06096	-55.76512	104	IKMT	at depth	
PS112_116-2	2018-04-25	10:46	-61.06597	-55.76595	102	IKMT	station end	
PS112_117-2	2018-04-25	13:52	-60.90733	-55.75874	224	CTDICBM	station start	
PS112_117-2	2018-04-25	14:04	-60.90716	-55.75820	225	CTDICBM	at depth	
PS112_117-2	2018-04-25	14:18	-60.90815	-55.75411	223	CTDICBM	station end	
PS112_117-3	2018-04-25	14:22	-60.90840	-55.75303	222	HN	station start	
PS112_117-3	2018-04-25	14:48	-60.90910	-55.74646	218	HN	station end	

A.4 Stationsliste / Station List

Station	Date	Time	Latitude	Longi-tude	Depth [m]	Gear	Action	Comment
PS112_118-1	2018-04-25	18:53	-60.98690	-54.95697	592	DSTRM	station start	
PS112_118-1	2018-04-25	19:11	-60.98661	-54.95795	592	DSTRM	station end	
PS112_118-2	2018-04-25	19:47	-60.98050	-54.96205	634	ISPC	station start	
PS112_118-2	2018-04-25	20:19	-60.98031	-54.96646	615	ISPC	at depth	
PS112_118-2	2018-04-25	20:42	-60.98008	-54.96932	605	ISPC	station end	
PS112_118-3	2018-04-25	21:35	-60.97629	-54.98202	601	CTDICBM	station start	
PS112_118-3	2018-04-25	21:58	-60.97621	-54.98461	584	CTDICBM	at depth	
PS112_118-3	2018-04-25	22:24	-60.97528	-54.99016	568	CTDICBM	station end	
PS112_118-4	2018-04-26	0:06	-60.97822	-55.02454	488	ISPC	station start	
PS112_118-4	2018-04-26	0:33	-60.98073	-55.02933	467	ISPC	at depth	
PS112_118-4	2018-04-26	0:52	-60.98227	-55.03368	437	ISPC	station end	
PS112_118-5	2018-04-26	2:02	-60.98855	-55.02070	448	ISPC	station start	
PS112_118-5	2018-04-26	2:50	-60.99389	-55.01819	413	ISPC	station end	
PS112_118-6	2018-04-26	4:03	-60.98252	-55.02125	475	ISPC	station start	
PS112_118-6	2018-04-26	4:35	-60.98207	-55.01973	481	ISPC	at depth	
PS112_118-6	2018-04-26	4:54	-60.98255	-55.01839	482	ISPC	station end	
PS112_118-7	2018-04-26	8:03	-60.93919	-55.07079	487	ISPC	station start	
PS112_118-7	2018-04-26	8:33	-60.93700	-55.08370	485	ISPC	at depth	
PS112_118-7	2018-04-26	8:53	-60.93585	-55.09179	480	ISPC	station end	
PS112_118-8	2018-04-26	11:08	-60.92760	-55.15595	343	DSTRM	station start	
PS112_118-8	2018-04-26	11:27	-60.93025	-55.16166	345	DSTRM	station end	
PS112_118-9	2018-04-26	11:41	-60.93120	-55.16190	348	ISPC	station start	
PS112_118-9	2018-04-26	12:05	-60.93462	-55.16666	364	ISPC	at depth	
PS112_118-9	2018-04-26	12:19	-60.93704	-55.17006	362	ISPC	station end	
PS112_118-10	2018-04-26	12:34	-60.93986	-55.17365	354	CTDICBM	station start	
PS112_118-10	2018-04-26	12:51	-60.94311	-55.17933	377	CTDICBM	at depth	
PS112_118-10	2018-04-26	13:05	-60.94591	-55.18196	380	CTDICBM	station end	
PS112_119-1	2018-04-26	14:58	-60.99614	-54.63037	572	DSTRM	station start	
PS112_119-1	2018-04-26	15:21	-60.99710	-54.62287	570	DSTRM	station end	
PS112_119-2	2018-04-26	15:37	-60.99743	-54.60871	572	ISPC	station start	
PS112_119-2	2018-04-26	16:12	-60.99914	-54.60291	571	ISPC	at depth	
PS112_119-2	2018-04-26	16:34	-60.99959	-54.59665	573	ISPC	station end	
PS112_119-3	2018-04-26	16:45	-60.99996	-54.59491	573	CTDICBM	station start	
PS112_119-3	2018-04-26	17:09	-61.00082	-54.59018	576	CTDICBM	at depth	
PS112_119-3	2018-04-26	17:28	-61.00088	-54.58563	577	CTDICBM	station end	
PS112_119-4	2018-04-26	17:38	-60.99923	-54.58427	575	SECCI	station start	
PS112_119-4	2018-04-26	17:40	-60.99858	-54.58414	576	SECCI	station end	
PS112_119-5	2018-04-26	19:10	-60.98952	-54.55830	578	ISPC	station start	
PS112_119-5	2018-04-26	19:40	-60.98410	-54.55281	582	ISPC	at depth	
PS112_119-5	2018-04-26	20:01	-60.98126	-54.55381	588	ISPC	station end	
PS112_119-6	2018-04-26	22:04	-60.96481	-54.55782	623	ISPC	station start	

Station	Date	Time	Latitude	Longi-tude	Depth [m]	Gear	Action	Comment
PS112_119-6	2018-04-26	22:38	-60.96125	-54.56432	626	ISPC	at depth	
PS112_119-6	2018-04-26	22:59	-60.96008	-54.57170	621	ISPC	station end	
PS112_119-7	2018-04-26	23:12	-60.96041	-54.59311	634	IKMT	station start	
PS112_119-7	2018-04-26	23:21	-60.96049	-54.60640	639	IKMT	at depth	
PS112_119-7	2018-04-26	23:42	-60.96122	-54.63926	641	IKMT	station end	
PS112_119-8	2018-04-27	0:21	-60.95037	-54.63718	648	ISPC	station start	
PS112_119-8	2018-04-27	1:33	-60.96478	-54.62288	636	ISPC	at depth	
PS112_119-8	2018-04-27	1:40	-60.96636	-54.62225	633	ISPC	station end	
PS112_119-9	2018-04-27	3:02	-60.97033	-54.61267	614	ISPC	station start	
PS112_119-9	2018-04-27	3:34	-60.96930	-54.61472	619	ISPC	at depth	
PS112_119-9	2018-04-27	3:52	-60.97005	-54.61677	616	ISPC	station end	
PS112_119-10	2018-04-27	4:56	-60.96529	-54.61716	636	IKMT	station start	
PS112_119-10	2018-04-27	5:06	-60.96353	-54.62846	638	IKMT	at depth	
PS112_119-10	2018-04-27	5:27	-60.95882	-54.65021	639	IKMT	station end	
PS112_119-11	2018-04-27	6:02	-60.95277	-54.63149	650	ISPC	station start	
PS112_119-11	2018-04-27	6:36	-60.95005	-54.62720	651	ISPC	at depth	
PS112_119-11	2018-04-27	6:55	-60.94961	-54.62986	651	ISPC	station end	
PS112_119-12	2018-04-27	8:00	-60.93874	-54.65441	653	ISPC	station start	
PS112_119-12	2018-04-27	8:31	-60.93637	-54.65946	652	ISPC	at depth	
PS112_119-12	2018-04-27	8:52	-60.93649	-54.66882	655	ISPC	station end	
PS112_119-13	2018-04-27	10:01	-60.93376	-54.68274	656	ISPC	station start	
PS112_119-13	2018-04-27	10:34	-60.93383	-54.69396	657	ISPC	at depth	
PS112_119-13	2018-04-27	10:55	-60.93478	-54.70171	653	ISPC	station end	
PS112_119-14	2018-04-27	11:04	-60.93585	-54.71278	654	IKMT	station start	
PS112_119-14	2018-04-27	11:12	-60.93676	-54.72736	650	IKMT	at depth	
PS112_119-14	2018-04-27	11:34	-60.93787	-54.76153	658	IKMT	station end	
PS112_119-15	2018-04-27	12:04	-60.93171	-54.73178	669	DSTRM	station start	
PS112_119-15	2018-04-27	12:27	-60.93312	-54.73977	667	DSTRM	station end	
PS112_119-16	2018-04-27	12:42	-60.93500	-54.74395	663	ISPC	station start	
PS112_119-16	2018-04-27	13:13	-60.94169	-54.74668	649	ISPC	at depth	
PS112_119-16	2018-04-27	13:33	-60.94395	-54.75265	647	ISPC	station end	
PS112_120-1	2018-04-27	13:43	-60.94698	-54.75601	644	DSTRM	station start	
PS112_120-1	2018-04-27	13:58	-60.95137	-54.75695	645	DSTRM	station end	
PS112_120-2	2018-04-27	14:24	-60.95284	-54.74112	639	MSC	station start	
PS112_120-2	2018-04-27	14:31	-60.95393	-54.74135	638	MSC	at depth	
PS112_120-2	2018-04-27	14:37	-60.95513	-54.74121	640	MSC	station end	
PS112_120-3	2018-04-27	14:58	-60.95853	-54.74478	641	Goflo	station start	
PS112_120-3	2018-04-27	15:05	-60.95925	-54.74383	639	Goflo	at depth	
PS112_120-3	2018-04-27	15:18	-60.96001	-54.74379	640	Goflo	station end	
PS112_120-4	2018-04-27	15:30	-60.96124	-54.74522	635	CTDICBM	station start	
PS112_120-4	2018-04-27	15:54	-60.96480	-54.74612	629	CTDICBM	at depth	

A.4 Stationsliste / Station List

Station	Date	Time	Latitude	Longi-tude	Depth [m]	Gear	Action	Comment
PS112_120-4	2018-04-27	16:19	-60.96781	-54.74399	621	CTDICBM	station end	
PS112_120-5	2018-04-27	16:31	-60.96917	-54.74388	620	SECCI	station start	
PS112_120-5	2018-04-27	16:35	-60.96951	-54.74379	616	SECCI	station end	
PS112_120-6	2018-04-27	16:47	-60.97061	-54.74202	613	BONGO	station start	
PS112_120-6	2018-04-27	17:09	-60.97257	-54.73877	608	BONGO	at depth	
PS112_120-6	2018-04-27	17:21	-60.97348	-54.73902	605	BONGO	station end	
PS112_120-7	2018-04-27	17:27	-60.97353	-54.73634	605	BONGO	station start	
PS112_120-7	2018-04-27	17:45	-60.97410	-54.73406	603	BONGO	at depth	
PS112_120-7	2018-04-27	17:58	-60.97491	-54.73004	600	BONGO	station end	
PS112_120-8	2018-04-27	18:11	-60.96976	-54.73473	613	HN	station start	
PS112_120-8	2018-04-27	18:15	-60.96960	-54.73415	614	HN	station end	
PS112_120-9	2018-04-27	18:22	-60.96992	-54.73577	613	IKMT	station start	
PS112_120-9	2018-04-27	18:30	-60.97007	-54.74625	620	IKMT	at depth	
PS112_120-9	2018-04-27	18:52	-60.97161	-54.76552	619	IKMT	station end	
PS112_120-10	2018-04-27	19:08	-60.96482	-54.74739	630	HN	station start	
PS112_120-10	2018-04-27	19:15	-60.96401	-54.74634	633	HN	station end	
PS112_120-11	2018-04-27	20:05	-60.96071	-54.74904	641	ISPC	station start	
PS112_120-11	2018-04-27	20:39	-60.95863	-54.75440	641	ISPC	at depth	
PS112_120-11	2018-04-27	20:58	-60.95548	-54.75527	640	ISPC	station end	
PS112_120-12	2018-04-28	0:04	-60.93447	-54.76810	659	ISPC	station start	
PS112_120-12	2018-04-28	0:36	-60.93716	-54.77265	656	ISPC	at depth	
PS112_120-12	2018-04-28	0:57	-60.93936	-54.77593	651	ISPC	station end	
PS112_120-13	2018-04-28	1:59	-60.94235	-54.77992	648	ISPC	station start	
PS112_120-13	2018-04-28	2:31	-60.94809	-54.78041	648	ISPC	at depth	
PS112_120-13	2018-04-28	2:54	-60.95200	-54.78002	645	ISPC	station end	
PS112_120-14	2018-04-28	4:05	-60.96172	-54.76682	636	ISPC	station start	
PS112_120-14	2018-04-28	4:36	-60.96226	-54.75387	638	ISPC	at depth	
PS112_120-14	2018-04-28	4:56	-60.96263	-54.74402	634	ISPC	station end	
PS112_120-15	2018-04-28	5:57	-60.96076	-54.76725	636	ISPC	station start	
PS112_120-15	2018-04-28	6:29	-60.95714	-54.75943	639	ISPC	at depth	
PS112_120-15	2018-04-28	6:48	-60.95513	-54.75955	641	ISPC	station end	
PS112_120-16	2018-04-28	7:57	-60.96118	-54.81769	635	ISPC	station start	
PS112_120-16	2018-04-28	8:32	-60.95913	-54.82065	640	ISPC	at depth	
PS112_120-16	2018-04-28	8:52	-60.95843	-54.82491	642	ISPC	station end	
PS112_120-17	2018-04-28	9:51	-60.95743	-54.84067	641	ISPC	station start	
PS112_120-17	2018-04-28	10:23	-60.95725	-54.85285	642	ISPC	at depth	
PS112_120-17	2018-04-28	10:45	-60.95716	-54.85852	643	ISPC	station end	
PS112_120-18	2018-04-28	11:00	-60.95747	-54.86780	642	DSTRM	station start	
PS112_120-18	2018-04-28	11:23	-60.96033	-54.87477	640	DSTRM	station end	
PS112_120-19	2018-04-28	11:33	-60.96173	-54.87595	641	ISPC	station start	
PS112_120-19	2018-04-28	12:06	-60.96579	-54.88014	640	ISPC	at depth	

Station	Date	Time	Latitude	Longi-tude	Depth [m]	Gear	Action	Comment
PS112_120-19	2018-04-28	12:26	-60.96794	-54.88228	636	ISPC	station end	
PS112_121-1	2018-04-28	12:38	-60.96930	-54.88374	633	DSTRM	station start	
PS112_121-1	2018-04-28	12:54	-60.97022	-54.88484	632	DSTRM	station end	
PS112_121-2	2018-04-28	13:20	-60.96838	-54.87091	632	CTDICBM	station start	
PS112_121-2	2018-04-28	13:46	-60.96865	-54.87238	631	CTDICBM	at depth	
PS112_121-2	2018-04-28	14:07	-60.96888	-54.87685	631	CTDICBM	station end	
PS112_121-3	2018-04-28	14:18	-60.96939	-54.88127	632	SECCI	station start	
PS112_121-3	2018-04-28	14:25	-60.96915	-54.88206	633	SECCI	station end	
PS112_121-4	2018-04-28	14:55	-60.96613	-54.91534	621	M-RMT	station start	
PS112_121-4	2018-04-28	15:19	-60.96362	-54.94955	876	M-RMT	at depth	
PS112_121-4	2018-04-28	15:20	-60.96355	-54.95075	881	M-RMT	profile start	
PS112_121-4	2018-04-28	16:04	-60.96462	-55.02269	521	M-RMT	profile end	
PS112_121-4	2018-04-28	16:12	-60.96645	-55.02483	502	M-RMT	station end	
PS112_121-5	2018-04-28	16:44	-60.97458	-54.90317	622	ISPC	station start	
PS112_121-5	2018-04-28	17:22	-60.97560	-54.90117	619	ISPC	at depth	
PS112_121-5	2018-04-28	17:45	-60.97603	-54.90254	616	ISPC	station end	
PS112_121-6	2018-04-28	21:58	-60.97845	-54.90450	600	ISPC	station start	
PS112_121-6	2018-04-28	22:30	-60.97854	-54.90561	599	ISPC	at depth	
PS112_121-6	2018-04-28	22:51	-60.98027	-54.90707	593	ISPC	station end	
PS112_121-7	2018-04-29	0:01	-60.98100	-54.91503	596	ISPC	station start	
PS112_121-7	2018-04-29	0:34	-60.98605	-54.91891	598	ISPC	at depth	
PS112_121-7	2018-04-29	0:53	-60.98878	-54.91992	594	ISPC	station end	
PS112_121-8	2018-04-29	1:24	-60.99192	-54.94008	584	M-RMT	station start	
PS112_121-8	2018-04-29	1:39	-60.99106	-54.95568	577	M-RMT	at depth	
PS112_121-8	2018-04-29	2:11	-60.99034	-54.99498	514	M-RMT	station end	
PS112_121-9	2018-04-29	3:00	-60.98286	-54.92299	600	ISPC	station start	
PS112_121-9	2018-04-29	3:31	-60.98422	-54.91716	597	ISPC	at depth	
PS112_121-9	2018-04-29	3:52	-60.98558	-54.91179	594	ISPC	station end	
PS112_121-10	2018-04-29	4:58	-60.98502	-54.90304	591	ISPC	station start	
PS112_121-10	2018-04-29	5:28	-60.98647	-54.90465	592	ISPC	at depth	
PS112_121-10	2018-04-29	5:48	-60.98930	-54.90296	588	ISPC	at depth	
PS112_121-11	2018-04-29	7:00	-60.98819	-54.88409	585	ISPC	station start	
PS112_121-11	2018-04-29	7:30	-60.99118	-54.87777	581	ISPC	at depth	
PS112_121-11	2018-04-29	7:53	-60.99221	-54.87252	578	ISPC	station end	
PS112_121-12	2018-04-29	9:02	-60.98003	-54.90877	594	ISPC	station start	
PS112_121-12	2018-04-29	9:35	-60.98199	-54.90641	593	ISPC	at depth	
PS112_121-12	2018-04-29	9:54	-60.98333	-54.90551	594	ISPC	station end	
PS112_121-13	2018-04-29	11:03	-60.98247	-54.93137	607	DSTRM	station start	
PS112_121-13	2018-04-29	11:26	-60.98235	-54.93551	609	DSTRM	station end	
PS112_121-14	2018-04-29	11:38	-60.98414	-54.93747	609	ISPC	station start	
PS112_121-14	2018-04-29	12:10	-60.98680	-54.93738	604	ISPC	at depth	

A.4 Stationsliste / Station List

Station	Date	Time	Latitude	Longi-tude	Depth [m]	Gear	Action	Comment
PS112_121-14	2018-04-29	12:30	-60.98725	-54.93680	603	ISPC	station end	
PS112_122-1	2018-04-29	12:40	-60.98771	-54.93593	601	DSTRM	station start	
PS112_122-1	2018-04-29	13:01	-60.98859	-54.93439	598	DSTRM	station end	
PS112_122-2	2018-04-29	13:29	-60.98274	-54.92788	604	CTDICBM	station start	
PS112_122-2	2018-04-29	13:50	-60.98278	-54.92655	603	CTDICBM	at depth	
PS112_122-2	2018-04-29	14:11	-60.98330	-54.92726	603	CTDICBM	station end	
PS112_122-3	2018-04-29	14:18	-60.98338	-54.92759	603	SECCI	station start	
PS112_122-3	2018-04-29	14:22	-60.98348	-54.92759	603	SECCI	station end	
PS112_122-4	2018-04-29	14:25	-60.98353	-54.92769	603	HN	station start	
PS112_122-4	2018-04-29	14:32	-60.98359	-54.92782	603	HN	station end	
PS112_122-5	2018-04-29	21:02	-60.96768	-54.96100	834	ISPC	station start	
PS112_122-5	2018-04-29	21:37	-60.96473	-54.95931	878	ISPC	at depth	
PS112_122-5	2018-04-29	21:58	-60.96596	-54.96009	860	ISPC	station end	
PS112_122-6	2018-04-29	23:04	-60.96770	-54.98725	653	ISPC	station start	
PS112_122-6	2018-04-29	23:38	-60.96569	-55.00161	569	ISPC	at depth	
PS112_122-6	2018-04-29	23:58	-60.96517	-55.00918	558	ISPC	station end	
PS112_122-7	2018-04-30	1:01	-60.97307	-55.01301	511	ISPC	station start	
PS112_122-7	2018-04-30	1:31	-60.97272	-55.02029	500	ISPC	at depth	
PS112_122-7	2018-04-30	1:48	-60.97289	-55.02323	498	ISPC	station end	
PS112_122-8	2018-04-30	3:00	-60.97272	-55.02835	499	ISPC	station start	
PS112_122-8	2018-04-30	3:33	-60.96818	-55.02783	496	ISPC	at depth	
PS112_122-8	2018-04-30	3:52	-60.96849	-55.02667	497	ISPC	station end	
PS112_122-9	2018-04-30	4:59	-60.97402	-55.00658	521	ISPC	station start	
PS112_122-9	2018-04-30	5:31	-60.97505	-54.99211	559	ISPC	at depth	
PS112_122-9	2018-04-30	5:52	-60.97325	-54.98405	623	ISPC	station end	
PS112_122-10	2018-04-30	7:09	-60.96270	-54.99128	620	ISPC	station start	
PS112_122-10	2018-04-30	7:44	-60.96419	-54.98769	655	ISPC	at depth	
PS112_122-10	2018-04-30	8:06	-60.96453	-54.98327	712	ISPC	station end	
PS112_122-11	2018-04-30	9:03	-60.96418	-54.97048	861	ISPC	station start	
PS112_122-11	2018-04-30	9:33	-60.96473	-54.96686	875	ISPC	at depth	
PS112_122-11	2018-04-30	9:53	-60.96590	-54.96594	860	ISPC	station end	
PS112_122-12	2018-04-30	11:02	-60.95659	-54.96912	989	DSTRM	station start	
PS112_122-12	2018-04-30	11:25	-60.95784	-54.97128	965	DSTRM	station end	
PS112_122-13	2018-04-30	11:41	-60.95764	-54.97155	969	ISPC	station start	
PS112_122-13	2018-04-30	12:11	-60.95600	-54.97007	995	ISPC	at depth	
PS112_122-13	2018-04-30	12:31	-60.95469	-54.97013	1009	ISPC	station end	
PS112_122-14	2018-04-30	12:54	-60.95169	-54.96973	1034	CTDICBM	station start	
PS112_122-14	2018-04-30	13:14	-60.94976	-54.97119	1049	CTDICBM	at depth	
PS112_122-14	2018-04-30	13:32	-60.94869	-54.97463	1065	CTDICBM	station end	
PS112_122-15	2018-04-30	13:49	-60.94756	-54.97732	1081	SECCI	station start	
PS112_122-15	2018-04-30	13:53	-60.94738	-54.97823	1085	SECCI	station end	

Station	Date	Time	Latitude	Longi-tude	Depth [m]	Gear	Action	Comment
PS112_123-1	2018-04-29	16:32	-60.80266	-55.33174	2433	ADCP_150	profile start	
PS112_123-1	2018-04-29	18:17	-60.90031	-55.33143	278	ADCP_150	profile end	
PS112_124-1	2018-04-30	17:21	-61.13492	-54.33155	202	CTDICBM	station start	
PS112_124-1	2018-04-30	17:54	-61.13818	-54.32669	1241	CTDICBM	at depth	
PS112_124-1	2018-04-30	18:23	-61.13846	-54.33024	1221	CTDICBM	station end	
PS112_125-1	2018-04-30	23:03	-61.36926	-54.18581	542	CTDICBM	station start	
PS112_125-1	2018-04-30	23:19	-61.36729	-54.18415	482	CTDICBM	at depth	
PS112_125-1	2018-04-30	23:32	-61.36666	-54.18625	455	CTDICBM	station end	
PS112_126-1	2018-05-01	5:03	-61.22798	-53.64581	1305	CTDICBM	station start	
PS112_126-1	2018-05-01	5:36	-61.22736	-53.63742	1300	CTDICBM	at depth	
PS112_126-1	2018-05-01	6:06	-61.22575	-53.64099	1315	CTDICBM	station end	
PS112_127-1	2018-05-01	16:07	-60.74003	-53.98957	2339	CTDICBM	station start	
PS112_127-1	2018-05-01	16:21	-60.74043	-53.99130	2312	CTDICBM	at depth	
PS112_127-1	2018-05-01	16:33	-60.74077	-53.99204	2285	CTDICBM	station end	
PS112_128-1	2018-05-01	21:47	-60.52528	-53.99468	2940	CTDICBM	station start	
PS112_128-1	2018-05-01	21:59	-60.52865	-53.99404	2941	CTDICBM	at depth	
PS112_128-1	2018-05-01	22:12	-60.53192	-53.99335	2918	CTDICBM	station end	
PS112_129-1	2018-05-02	0:07	-60.24925	-53.99962	2606	CTDICBM	station start	
PS112_129-1	2018-05-02	0:18	-60.24861	-53.99575	2606	CTDICBM	at depth	
PS112_129-1	2018-05-02	0:27	-60.24862	-53.99267	2612	CTDICBM	station end	
PS112_130-1	2018-05-02	1:58	-60.03378	-53.99912	2978	CTDICBM	station start	
PS112_130-1	2018-05-02	2:11	-60.03175	-53.99717	2991	CTDICBM	at depth	
PS112_130-1	2018-05-02	2:21	-60.03000	-53.99618	2998	CTDICBM	station end	
PS112_130-2	2018-05-02	2:39	-60.02761	-53.99196	3018	IKMT	station start	
PS112_130-2	2018-05-02	2:48	-60.02116	-53.99953	3018	IKMT	at depth	
PS112_130-2	2018-05-02	3:07	-60.01089	-54.00876	3010	IKMT	station end	
PS112_131-1	2018-05-02	6:21	-60.03404	-55.00481	3477	IKMT	station start	
PS112_131-1	2018-05-02	6:29	-60.03008	-55.01528	3479	IKMT	at depth	
PS112_131-1	2018-05-02	6:50	-60.02129	-55.03848	3482	IKMT	station end	
PS112_131-2	2018-05-02	7:08	-60.01705	-55.05074	3428	CTDICBM	station start	
PS112_131-2	2018-05-02	8:30	-60.02024	-55.05847	3463	CTDICBM	at depth	
PS112_131-2	2018-05-02	10:15	-60.02338	-55.07894	3494	CTDICBM	station end	
PS112_132-1	2018-05-02	21:58	-58.35662	-58.61630	3502	BUCKET	station start	
PS112_132-1	2018-05-02	21:59	-58.35654	-58.61581	3483	BUCKET	station end	
PS112_132-2	2018-05-02	22:06	-58.35637	-58.61381	3497	CTDICBM	station start	
PS112_132-2	2018-05-02	22:14	-58.35629	-58.61128	3492	CTDICBM	at depth	
PS112_132-2	2018-05-02	22:21	-58.35634	-58.60808	3487	CTDICBM	station end	
PS112_132-3	2018-05-02	22:38	-58.35427	-58.61924	3505	TMPUMP	station start	
PS112_132-3	2018-05-02	22:51	-58.35469	-58.61506	3498	TMPUMP	at depth	
PS112_132-3	2018-05-03	2:31	-58.36533	-58.56226	3440	TMPUMP	station end	

Gear abbreviations	Gear
ADCP_150	ADCP 150kHz
BOAT	Boat
BONGO	Bongo Net
BT	Bottom Trawl
BUCKET	Bucket Water Sampling
CTDICBM	CTD ICBM
DSTRM	Drifting Sediment-Trap Mooring
EK60	Fish Finder Echosounder EK60
EPNET	EP_NET
FBOX	FerryBox
Goflo	Trace Metal Clean Bottle Cast
HN	Hand Net
ICEBUCKET	Ice fishing
IKMT	Isaak-Kidd Midwater Trawl
ISPC	In-Situ Particle Camera
M-RMT	Multiple Rectangular Midwater Trawl
MN_M7	Multinet Medium 7 Nets
MSC	Marine Snow Catcher
PCO2_GO	pCO2 GO
PCO2_SUB	pCO2 Subctech
RM	Radiation Measurements
RMT	Rectangular Midwater Trawl
SECCI	Seccidisk ICBM
TMPUMP	Trace Metal Sea Water Pump
TRAP	Fish Trap
TSG_KEEL	Thermosalinograph Keel
TSG_KEEL_2	Thermosalinograph Keel 2
WST	Weatherstation

Die **Berichte zur Polar- und Meeresforschung** (ISSN 1866-3192) werden beginnend mit dem Band 569 (2008) als Open-Access-Publikation herausgegeben. Ein Verzeichnis aller Bände einschließlich der Druckausgaben (ISSN 1618-3193, Band 377-568, von 2000 bis 2008) sowie der früheren **Berichte zur Polarforschung** (ISSN 0176-5027, Band 1-376, von 1981 bis 2000) befindet sich im electronic Publication Information Center (**ePIC**) des Alfred-Wegener-Instituts, Helmholtz-Zentrum für Polar- und Meeresforschung (AWI); see <http://epic.awi.de>. Durch Auswahl "Reports on Polar- and Marine Research" (via "browse"/"type") wird eine Liste der Publikationen, sortiert nach Bandnummer, innerhalb der absteigenden chronologischen Reihenfolge der Jahrgänge mit Verweis auf das jeweilige pdf-Symbol zum Herunterladen angezeigt.

The **Reports on Polar and Marine Research** (ISSN 1866-3192) are available as open access publications since 2008. A table of all volumes including the printed issues (ISSN 1618-3193, Vol. 377-568, from 2000 until 2008), as well as the earlier **Reports on Polar Research** (ISSN 0176-5027, Vol. 1-376, from 1981 until 2000) is provided by the electronic Publication Information Center (**ePIC**) of the Alfred Wegener Institute, Helmholtz Centre for Polar and Marine Research (AWI); see URL <http://epic.awi.de>. To generate a list of all Reports, use the URL <http://epic.awi.de> and select "browse"/ "type" to browse "Reports on Polar and Marine Research". A chronological list in declining order will be presented, and pdf icons displayed for downloading.

Zuletzt erschienene Ausgaben:

Recently published issues:

722 (2018) The Expedition PS112 of the Research Vessel POLARSTERN to the Antarctic Peninsula Region in 2018, edited by Bettina Meyer and Wiebke Weßels

721 (2018) Alfred Wegener im 1. Weltkrieg. Ein Polarforscher und die „Urkatastrophe des 20. Jahrhunderts“, by Christian R. Salewski

720 (2018) The Expedition PS98 of the Research Vessel POLARSTERN to the Atlantic Ocean in 2016, edited by Bernhard Pospichal

719 (2018) The Expeditions PS106/1 and 2 of the Research Vessel POLARSTERN to the Arctic Ocean in 2017, edited by Andreas Macke and Hauke Flores

718 (2018) The Expedition PS111 of the Research Vessel POLARSTERN to the southern Weddell Sea in 2018, edited by Michael Schröder

717 (2018) The Expedition PS107 of the Research Vessel POLARSTERN to the Fram Strait and the AWI-HAUSGARTEN in 2017, edited by Ingo Schewe

716 (2018) Polar Systems under Pressure, 27th International Polar Conference, Rostock, 25 - 29 March 2018, German Society for Polar Research, edited by H. Kassens, D. Damaske, B. Diekmann, D. Fütterer, G. Heinemann, U. Karsten, E.M. Pfeiffer, J. Regnery, M. Scheinert, J. Thiede, R. Tiedemann & D. Wagner

715 (2018) The Expedition PS109 of the Research Vessel POLARSTERN to the Nordic Seas in 2017, edited by Torsten Kanzow

714 (2017) The Expedition SO258/2 of the Research Vessel SONNE to the central Indian Ocean in 2017, edited by Wolfram Geissler

713 (2017) The Expedition PS102 of the Research Vessel POLARSTERN to the Atlantic Ocean in 2016, edited by Karen Wiltshire, Eva-Maria Brodte, Annette Wilson and Peter Lemke

712 (2017) The Expedition PS104 of the Research Vessel POLARSTERN to the Amundsen Sea in 2017, edited by Karsten Gohl



ALFRED-WEGENER-INSTITUT
HELMHOLTZ-ZENTRUM FÜR POLAR-
UND MEERESFORSCHUNG

BREMERHAVEN

Am Handelshafen 12
27570 Bremerhaven
Telefon 0471 4831-0
Telefax 0471 4831-1149
www.awi.de

